

## INFORMATION TO USERS

This was produced from a copy of a document sent to us for microfilming. While the most advanced technological means to photograph and reproduce this document have been used, the quality is heavily dependent upon the quality of the material submitted.

The following explanation of techniques is provided to help you understand markings or notations which may appear on this reproduction.

1. The sign or "target" for pages apparently lacking from the document photographed is "Missing Page(s)". If it was possible to obtain the missing page(s) or section, they are spliced into the film along with adjacent pages. This may have necessitated cutting through an image and duplicating adjacent pages to assure you of complete continuity.
2. When an image on the film is obliterated with a round black mark it is an indication that the film inspector noticed either blurred copy because of movement during exposure, or duplicate copy. Unless we meant to delete copyrighted materials that should not have been filmed, you will find a good image of the page in the adjacent frame.
3. When a map, drawing or chart, etc., is part of the material being photographed the photographer has followed a definite method in "sectioning" the material. It is customary to begin filming at the upper left hand corner of a large sheet and to continue from left to right in equal sections with small overlaps. If necessary, sectioning is continued again—beginning below the first row and continuing on until complete.
4. For any illustrations that cannot be reproduced satisfactorily by xerography, photographic prints can be purchased at additional cost and tipped into your xerographic copy. Requests can be made to our Dissertations Customer Services Department.
5. Some pages in any document may have indistinct print. In all cases we have filmed the best available copy.

University  
Microfilms  
International

300 N. ZEEB ROAD, ANN ARBOR, MI 48106  
18 BEDFORD ROW, LONDON WC1R 4EJ, ENGLAND

8014992

TRICAMO, STEPHEN J.

FORCE BALANCING MACHINES AND OPTIMIZATION OF DYNAMIC  
REACTIONS FOR PLANAR MECHANISMS

*City University of New York*

PH.D.

1980

University  
Microfilms  
International

300 N. Zeeb Road, Ann Arbor, MI 48106

18 Bedford Row, London WC1R 4EJ, England

Copyright 1980

by

Tricamo, Stephen J.

All Rights Reserved

PLEASE NOTE:

In all cases this material has been filmed in the best possible way from the available copy. Problems encountered with this document have been identified here with a check mark .

1. Glossy photographs \_\_\_\_\_
2. Colored illustrations \_\_\_\_\_
3. Photographs with dark background  \_\_\_\_\_
4. Illustrations are poor copy \_\_\_\_\_
5. Print shows through as there is text on both sides of page \_\_\_\_\_
6. Indistinct, broken or small print on several pages  \_\_\_\_\_ throughout
7. Tightly bound copy with print lost in spine \_\_\_\_\_
8. Computer printout pages with indistinct print  \_\_\_\_\_
9. Page(s) \_\_\_\_\_ lacking when material received, and not available from school or author \_\_\_\_\_
10. Page(s) \_\_\_\_\_ seem to be missing in numbering only as text follows \_\_\_\_\_
11. Poor carbon copy \_\_\_\_\_
12. Not original copy, several pages with blurred type \_\_\_\_\_
13. Appendix pages are poor copy \_\_\_\_\_
14. Original copy with light type \_\_\_\_\_
15. Curling and wrinkled pages \_\_\_\_\_
16. Other \_\_\_\_\_

FORCE BALANCING MACHINES AND OPTIMIZATION  
OF DYNAMIC REACTIONS FOR PLANAR MECHANISMS

by

STEPHEN J. TRICAMO

A dissertation submitted to the  
Graduate Faculty in Engineering  
in partial fulfillment of the  
requirements for the degree of  
Doctor of Philosophy, The City  
University of New York.

1980

© COPYRIGHT BY  
STEPHEN J. TRICAMO  
1980

This manuscript has been read and accepted for the Graduate Faculty in Engineering in satisfaction of the dissertation requirement for the degree of Doctor of Philosophy.

1-17-80  
date

Gerard G. Lowen  
Chairman of Examining Committee

1-18-80  
date

FE Tran  
Executive Officer

Prof. G. G. Lowen (Chairman)

Prof. F. Freudenstein

Prof. D. Goldfarb

Prof. M. Levitsky

Prof. S. B. Menkes

Prof. M. L. Pei

Supervisory Committee

To my wife, Elaine, and our  
daughters, Leigh, Nancy and  
Jennifer, whose love made  
it all possible.

**ABSTRACT**

The results of certain theoretical and experimental investigations in the field of force balancing of planar mechanisms, which introduce novel computer-aided design methods, are presented.

Experimentation showed that a mechanism designed to be fully force balanced exhibits a residual imbalance, brought about by unavoidable manufacturing tolerances and material nonhomogeneities. A new theory for a group of devices which allow the complete removal of these residual shaking forces of a four-bar linkage and other balanceable mechanisms, is shown.

This theory was subsequently applied to the actual design of a balancing device for a four-bar linkage. It was found that the goal of complete elimination of the residual shaking forces was not attainable and that it was necessary to modify the theory such that the best possible reduction in these forces could be obtained. Subsequent experiments, which use minimax as well as least squares approaches and had most successful outcomes, are described.

Further, a new two-counterweight method of partial

force balancing which makes it possible, by way of what has been called the equipollent circle constraint equation, to prescribe the maximum shaking force of a constant input speed four-bar linkage by way of a wide range of practical counterweight configurations, is given.

Finally, a novel nonlinear optimization formulation which makes it possible to simultaneously minimize the maximum values of the various dynamic reactions of a four-bar linkage while maintaining the ability to prescribe the maximum shaking force, is introduced. This computer-aided design technique, which employs counterweights on all links, was applied to both partial as well as full force balancing and produced gratifying results.

## ACKNOWLEDGEMENTS

It has been my honor and privilege to have been guided in my studies by one of the foremost scholars in the field of machine design, Professor Gerard G. Lowen. I will always be grateful for the assistance, encouragement and counsel he so generously provided. His dedication, ability and personal warmth exemplify the highest standards of professional conduct.

I would like to express my sincere thanks to Professor Donald Goldfarb, of the Computer Science Department, for his invaluable help and advice.

I would also like to thank the remaining members of my supervisory committee for their time and interest.

The technical expertise and assistance of Mr. Sorin Davidovici, of the Electrical Engineering Department, is warmly acknowledged.

My gratitude extends to Mr. Alfred Galente for his assistance in the construction of early experimental prototypes and to Mr. Bernard Roiss both for his technical help as well as his general encouragement and good cheer.

Finally, the financial support received from the National Science Foundation under Grant No. ENG76-21924 is gratefully acknowledged.

## TABLE OF CONTENTS

	<u>Page</u>
ABSTRACT	v
LIST OF TABLES	xiv
LIST OF FIGURES	xv
NOMENCLATURE	xvii
I. INTRODUCTION	1
A. Background	5
B. Results Of Investigation	9
II. THEORY OF FULL FORCE BALANCING MACHINES FOR RECIPROCATING MECHANISMS	15
A. Introduction	15
B. Theory Of Four-Bar Linkage Balancing Machine	17
C. Generalization Of Theory Of Full Force Balancing Machines	23
1. Generalization For Mechanisms Containing Revolutes Only	24
2. Generalization For Mechanisms Containing Both Revolutes And Sliders	31
III. A PRACTICAL BALANCING MACHINE FOR FOUR-BAR LINKAGES	34
A. Introduction	34
B. Adaptation Of Balancing Machine Theory	36
1. Minimax Balancing Optimization	37
2. Least Squares Balancing Optimization	40
C. Balancing Machine Design And Instrumentation	41
1. Basic Configuration Of Balancing Machine	41
2. Instrumentation And Data Evaluation	48
a. Shaking Force Components	48
b. Input Link Angle	48
c. Instantaneous Input Link Angular Velocity	49
d. Instantaneous Input Link Angular Acceleration	52

	<u>Page</u>
D. Experiment And Application Of Balancing Optimization Techniques	53
1. Experience With Unbalanced Mechanism: Motor Vibrations And Speed Variations	53
2. Theoretically Balanced Mechanism	56
3. Results Of Minimax Balancing Optimization	59
4. Results Of Least Squares Balancing Optimization	63
E. Discussion Of Results	66
1. Sources Of Experimental Inaccuracies	66
a. Motor Vibration	66
b. Cross Talk In Force Platforms	67
c. Ground Bearing Force Addition	69
2. Influence Of Cross Talk And Addition Errors On Magnitudes Of Experimental Shaking Force Readouts	71
3. Comparison Of Optimization Methods	74
IV. A NEW METHOD FOR PRESCRIBING THE MAXIMUM SHAKING FORCE OF A FOUR-BAR LINKAGE WITH FLEXIBILITY IN COUNTERWEIGHT DESIGN	78
A. Introduction	78
B. Hodograph And Statement Of Problem	82
C. Special Case Of General Solution: Simple Reduction Of Hodograph	88
1. Design Of Output Link Counterweight	90
2. Design Of Input Link Counterweight	92
3. Relationship To Full Force Balancing	94
D. General Solution: Equipollent Circle Constraint Equation And Flexibility In Counterweight Design	96
1. Equipollent Circle Constraint Equation And Resulting Hodograph	96
2. Adaptation To Output Link Counterweight Design	98
a. Determination Of Theoretical Design Range	98
b. Determination Of Output Link Counterweight Angles $\theta_3^*$	102
3. Design Of Input Link Counterweight	103

	<u>Page</u>
E. Examples	106
1. Parameters Of Unbalanced Mechanism	106
2. Determination Of Radius And Location Of Center Of Smallest Circumscribing Circle To Rotated Shaking Force Hodograph. Maximum Shaking Force	109
3. Determination Of Counterweights For Simple 50 Percent Reduction	111
a. Output Link Counterweight	111
b. Input Link Counterweight	112
4. Determination Of Counterweights For 50 Percent Reduction Of Maximum Shaking Force By General Solution	113
a. Theoretical Design Range	113
b. Counterweight Design For Arbitrary Point Within Theoretical Design Range	115
i. Output Link Counterweights	115
ii. Input Link Counterweights	116
c. Counterweight Design Flexibility And Its Influence On Various Mechanism Reactions	118
5. Results For 75 Percent Reduction In Maximum Shaking Force By General Solution	122
V. SIMULTANEOUS OPTIMIZATION OF DYNAMIC REACTIONS OF A FOUR-BAR LINKAGE WITH PRESCRIBED MAXIMUM SHAKING FORCE	124
A. Introduction	124
B. General Equipollent Circle Constraint Equation	127
C. Formulation Of Optimization Problem	129
D. Computational Sequence Of Optimization Procedure	132
1. Determination Of Counterweight Parameters For Partial Force Balancing	132
2. Determination Of Counterweight Parameters For Full Force Balancing	138
3. Determination Of Optimum Mechanism Reactions	141

	<u>Page</u>
E. Examples	142
1. Reduction Of 50 And 75 Percent In The Maximum Shaking Force	142
2. Full Force Balance	144
3. Input Moment Optimization For A Fully Force Balanced Mechanism	144
4. Results Of Optimizations And Conclusions	144
VI. APPENDICES	150
APPENDIX A. SHAKING FORCE EXPRESSIONS FOR A FOUR-BAR LINKAGE WITH GENERAL LINK MASS DISTRIBUTION	150
1. Shaking Force Expression In Terms Of $\phi_1$ , $\phi_2$ And $\phi_3$	150
a. Exponential Form	150
b. Cartesian Component Form	152
2. Shaking Force Expression In Terms of $\phi_1$ And $\phi_3$	153
a. Exponential Form	153
b. Cartesian Component Form	155
3. Notation Allowing Distinction Between Balanced And Unbalanced Mechanisms	155
APPENDIX B. ON THE NUMBER OF MASS-DISTANCE PARAMETERS OF A FOUR-BAR LINKAGE WHICH MAY BE DETERMINED WITH THE HELP OF THE SHAKING FORCE COMPONENTS	160
1. Proof Of Singularity Of Matrix Originally Proposed For Solution Of Individual Link Mass-Distance Products	161
2. Proof Of Nonsingularity Of Balancing Equation Matrix Used To Solve For General Mass-Distance Products	163

	<u>Page</u>
APPENDIX C. DESCRIPTION OF AUGMENTED LAGRANGIAN OPTIMIZATION PROGRAM AND APPLICATION TO MINIMAX BALANCING OPTIMIZATION	165
1. Theory Of Optimization Method	165
2. Description Of Computer Program	166
a. Main Program	167
b. Subroutine VF01BD	170
3. Example: Minimax Solution Of Overdetermined System Of Balancing Equations	171
a. Main Program	172
b. Subroutine VF01BD	175
c. Augmented Lagrangian Subroutines	189
d. Essential Elements Of Program Output	209
i. First Outer Iteration	209
ii. Fourth (Last) Outer Iteration	211
APPENDIX D. APPLICATION OF AUGMENTED LAGRANGIAN OPTIMIZATION PROGRAM TO LEAST SQUARES BALANCING OPTIMIZATION	212
1. Main Program	212
2. Subroutine VF01BD	216
3. Essential Elements Of Program Output	224
APPENDIX E. REVIEW OF A CHEBYSHEV-TYPE SINGLE COUNTERWEIGHT SHAKING FORCE OPTIMIZATION OF CONSTANT SPEED PLANAR LINKAGES	226
APPENDIX F. COMPUTER PROGRAMS CIRCLE AND FMAX	231
1. Program CIRCLE: Determination Of Smallest Circumscribing Circle To A Given Shaking Force Hodograph	231
a. Main Program	231
b. Subroutine VF01BD	235
c. Essential Elements Of Program Output	239
2. Program FMAX: Determination Of Maximum Bearing Forces, Shaking And Input Moments Of A Given Mechanism	241

	<u>Page</u>
APPENDIX G. COMPUTER PROGRAM OPTIMIZE	248
1. Main Program	248
2. Subroutine VF01BD	253
3. Essential Elements Of Program Output	274
APPENDIX H. COMPUTER PROGRAM OPTM41	277
1. Main Program	277
2. Subroutine VF01BD	281
3. Essential Elements Of Program Output	288
APPENDIX I. KINEMATIC EQUATIONS OF A FOUR-BAR LINKAGE	290
1. Link Angles	290
2. Link Angular Velocities	291
3. Link Angular Accelerations	291
VII. REFERENCES	292

## LIST OF TABLES

<u>Table</u>	<u>Title</u>	<u>Page</u>
3.1	Equipment Used In Experiment	44
3.2	Experimental Mechanism Data	47
3.3	Experimental Data For Theoretically Balanced Mechanism	58
4.1	Parameters of Unbalanced Linkage	108
4.2	Influence of Partial Balancing ( $\eta=0.5$ ) on Various Forces and Moments	121
4.3	Maximum Dynamic Reactions for Extrema of Design Ranges Corresponding to 50 and 75 Percent Reductions of Maximum Shaking Force	123
5.1	Comparison of Maximum Dynamic Reactions of Unbalanced, Balanced and Optimized Example Mechanism	145

## LIST OF FIGURES

<u>Figure</u>	<u>Title</u>	<u>Page</u>
2.1	General Four-Bar Linkage	18
2.2	Balanceable N-Linked Mechanism	25
3.1	Comparison of Typical Computed and Experimental Residual Shaking Force Components for a Four-Bar Linkage	38
3.2	Schematic View of Balancing Setup	42
3.3	Photographs of Balancing Setup	43
3.4	Link Dimensions	46
3.5	Determination of Instantaneous Angular Velocity	51
3.6	Comparison of Experimental and Computed Values of Shaking Force Components of Unbalanced Mechanism (Average Input Speed: 120 RPM)	54
3.7	Shaking Force Components and Angular Velocity of Theoretically Balanced Mechanism (Average Input Speed: 120 RPM)	57
3.8	Photograph of Minimax Fine-Balanced Experimental Mechanism Showing Correction Masses Installed	61
3.9	Comparison of Filtered Shaking Force Components Before and After Fine Balancing By Minimax Optimization Method (Average Input Speed: 120 RPM)	62
3.10	Comparison of Filtered Shaking Force Components Before and After Fine Balancing By Least Squares Optimization Method (Average Input Speed: 120 RPM)	65

<u>Figure</u>	<u>Title</u>	<u>Page</u>
3.11	Comparison of Minimax and Least Squares Optimized Shaking Force Components with Corresponding Experimental Curves	75
4.1	Shaking Force Hodograph of Constant Input Speed Four-Bar Linkage with All Vectors Rotated By Negative of Input Angle	84
4.2	Original and Simply Reduced Shaking Force Hodograph	89
4.3	Original and Reduced Shaking Force Hodograph Resulting from the Flexible Design Method	99
4.4	Example Four-Bar Linkage	107
4.5	Range of Output Link Counterweight Parameters and Certain Corresponding Input Link Counterweight Parameters for a 50 Percent Reduction in Maximum Shaking Force (Counterweight Thickness = 0.625 in.)	119
5.1	Original and Reduced Shaking Force Hodograph Resulting from Three-Counterweight Optimization Method	134
5.2	Example Four-Bar Linkage with Three Counterweights	143
A.1	General Four-Bar Linkage	151
A.2	Nomenclature Associated with Links and Counterweights	157
E.1	Shaking Force Hodograph of Constant Input Speed Mechanism Rotated by Negative of Input Angle	227
E.2	Shaking Force Hodograph of Fig. E.1 Modified by Addition of Input Link Counterweight	229
E.3	Smallest Circumscribing Circle to Hodograph Shown in Fig. E.1	230

## NOMENCLATURE

$a_j$  = pivot-to-pivot dimension of link  $j$

$a_j'(t)$  =  $j^{\text{th}}$  time dependent link-to-link length

$A, A^0$  = magnitude of equivalent mass-distance product of input and coupler link for counterweighted and original mechanism, respectively

$B, B^0$  = magnitude of equivalent mass-distance product of output and coupler link for counterweighted and original mechanism, respectively

$C, C_1, C_2$  = center of smallest circumscribing circle to shaking force hodograph of four-bar mechanism using simple reduction method, two-counterweight reduction method and three-counterweight reduction method, respectively

$C_{Sx}, C_{Sy}$  = x and y components of center of smallest circumscribing circle to shaking force hodograph of four-bar mechanism with input counterweight only

$c_i(\bar{x})$  =  $i^{\text{th}}$  constraint of optimization problem

$\bar{d}$  = constant vector

$d_j$  = width of link  $j$

$F_{M/GX}$ ,  $F_{M/GY}$  = x and y components of shaking force

$F_{12}$  = bearing force between input link and coupler link

$F_{23}$  = bearing force between coupler link and output link

$F_{34}$  = bearing force between output link and ground link

$F_{41}$  = bearing force between ground link and input link

$F_{CX_i}$ ,  $F_{CY_i}$  =  $i^{\text{th}}$  computed value of x and y components of shaking force

$F_{EX_i}$ ,  $F_{EY_i}$  =  $i^{\text{th}}$  experimental value of x and y components of shaking force

$F_{X_i}$ ,  $F_{Y_i}$  =  $i^{\text{th}}$  difference of computed and experimental shaking force components

$F_{LX}$ ,  $F_{LY}$  = x and y components of output of left force platform

$F_{RX}$ ,  $F_{RY}$  = x and y components of output of right force platform

$F_{TOT}$  = experimental reading of sum of bearing force components in x or y direction

$h_j$  = thickness of link j

$h_j^*$  = thickness of counterweight on link j

$h_{rj}, h_{kj}$  = fixed pivot-to-pivot dimension of link  $j$

$K$  = percentage error of individual bearing force component readings

$K_j$  = kinematic variable relating to link  $j$

$m_j, m_j^o, m_j^*$  = masses of total link, existing link and counterweight, respectively

$m_{jp}^c, m_{jq}^c$  = correction masses required to fine balance a mechanism

$m_j p_j, m_j q_j$  = mass-distance product of link  $j$  along  $x$  and  $y$  axis, respectively

$M$  = total mass of moving links of a mechanism

$M_{M/G}$  = shaking moment

$M_{41}$  = input moment

$p_j, q_j$  = body-fixed coordinates of the position of the center of mass of link  $j$

$p_j^c, q_j^c$  = location of balancing holes on link  $j$  along  $x$  and  $y$  axis, respectively

$P_j, Q_j$  = general mass-distance terms

$r_j$  = body-fixed link dimension locating center of mass of link j

$R$  = radius of smallest circumscribing circle to shaking force hodograph of four-bar mechanism with multiple counterweights

$R_E$  = radius of equipollent circle

$R_j^*$  = radius of counterweight attached to link j

$R_S$  = radius of smallest circumscribing circle to shaking force hodograph of four-bar mechanism with input counterweight only

$W_j$  = weighting factors for reactions used in nonlinear optimization procedure

$z$  = objective function used in certain nonlinear optimization procedures

$\alpha, \alpha^0$  = angle of equivalent mass-distance product of input and coupler link for counterweighted and original mechanism, respectively

$\beta, \beta^0$  = angle of equivalent mass-distance product of output and coupler link for counterweighted and original mechanism, respectively

$\gamma_j$  = kinematic variable

$\delta_s, \delta, \delta_1$  = angles of inclination with respect to x axis of  
circumscribing circles to hodograph with centers  
 $C_s, C$  and  $C_1$ , respectively

$\zeta$  = angular position of center of circumscribing circle

$\eta$  = factor expressing reduction in unbalanced maximum shaking  
force

$\theta_j$  = angle of inclination of center of mass of link j with  
respect to body-fixed x axis

$\theta_j^*$  = angle to center of counterweight on link j as measured  
from x axis

$\mu$  = proportionality factor relating R to  $R_s$

$\rho_j^*$  = density of counterweight on link j

$\phi_j$  = angular position of link j taken with respect to x axis

$\dot{\phi}_j, \ddot{\phi}_j$  = angular velocity and angular acceleration of link j,  
respectively

$\psi$  = angle of rotation of shaking force hodograph

## I. INTRODUCTION

The elimination or reduction of disturbances transmitted by high speed or heavy duty machinery to their surroundings is of great importance. These disturbances are objectionable because of their negative effects on the productivity of these machines. The resulting vibration, wear and fatigue problems limit their speeds and, with that, their full potential. In addition, the associated noise may represent a serious threat to the health of the operator.

The present work represents an attempt to answer some of the unresolved questions in this field.

Experimentation had shown that if a mechanism was designed to be fully force balanced, it did not necessarily imply that all the shaking forces were removed. This residual imbalance is due to unavoidable manufacturing tolerances and the unpredictable nonhomogeneity of the materials used. Thus, clearly there was a need to devise some procedure by which this residual imbalance could be totally removed or, at least, considerably reduced. To this end, a theory for a group of devices which would allow the complete removal of the residual shaking forces of a four-bar linkage and other balanceable mechanisms, was

developed.

When this theory was applied to a specific design of a balancing device for a four-bar linkage, it was found that this goal of complete elimination of the residual shaking forces was not attainable and that it was necessary to modify the theory such that the best possible reduction in these forces could be achieved. An experiment which uses this new approximating method was most successful and a reduction of as much as 65 percent of the residual shaking force could be obtained.

Secondly, since at the time of the inception of this work G. G. Lowen and F. R. Tepper had just completed a single counterweight method of prescribing the RMS shaking force of a four-bar linkage [80], it was felt that it would be desirable to develop a technique of partial force balancing which allows the limitation of the maximum shaking force of such a mechanism. This goal was realized by the adaptation of a Chebyshev-type partial balancing procedure devised by Ya. L. Gheronimus [25]. The resulting new two-counterweight method makes it possible, with the help of what has been called the equipollent circle constraint equation, to attain the identical prescribed maximum shaking force by way of a considerable range of practical counterweight configurations.

While this work proceeded, and with some insights provided by previous work of G. G. Lowen, F. R. Tepper and R. S. Berkof [ 51], it became clear that if one extends the above approach by introducing an additional coupler counterweight, it becomes possible to obtain significant reductions in such dynamic reactions as the maximum bearing forces, the maximum input moment and the maximum shaking moment of a four-bar linkage, while maintaining the ability to prescribe the maximum shaking force. Professor Donald Goldfarb, of the Computer Science Department of the City College of New York, suggested that a simultaneous optimization of these reactions may be obtained by the use of an optimization method previously used to solve linear minimax problems. In this formulation, the increases in the dynamic reactions, due to balancing, are controlled by a common minimization parameter which represents the objective function of the problem. This new approach was incorporated into the Harwell Augmented Lagrangian optimization code<sup>1</sup> and it was found that it led to most gratifying

---

<sup>1</sup> It was found that this code could also be used to excellent advantage in connection with the balancing machine as well as the method for prescribing the maximum shaking force of a mechanism. Appendix C serves as a guide for the use of this program.

results. It was possible to keep the increases in the various dynamic reactions of both partially and fully force balanced mechanisms, when compared to those of the unbalanced linkage, to values that previously had not been attained.

## A. Background

Since the mechanism balancing literature was reviewed by G. G. Lowen and R. S. Berkof in 1968 [49] and again by the same authors, together with F. R. Tepper, in 1977 [10], only those references which are of importance to the present work, and which have not been mentioned in the previous section, will be briefly discussed.

The Method of Linearly Independent Vectors, first given by R. S. Berkof and G. G. Lowen [8], represents the point of departure for the investigation of a four-bar linkage balancing device. This method was later generalized by F. R. Tepper and G. G. Lowen [76]. The latter work also gave a balanceability criterion which is used to good advantage in the generalization of the theory of full force balancing machines.

In the field of mechanism optimization, J. P. Sadler and R. W. Mayne [63] introduced the use of nonlinear programming techniques for the minimization of the maximum values of certain reactions in a constant input speed general four-bar linkage. They minimized the maximum shaking force while limiting the magnitude of the shaking moment. This optimization was repeated with an additional constraint on the maximum value of the largest bearing force. All

solutions are represented by trade-off charts. These optimizations were accomplished with point mass counterweights which are attached to the input and output links. (While the neglect of the counterweight moments of inertia is of no consequence as far as the shaking force is concerned, it matters to varying degrees when it comes to the shaking moment, the input moment and the various bearing forces.) The mathematical technique consisted of converting constrained optimization problems to unconstrained ones by using the exterior penalty function approach. The subsequent optima were then determined with the help of a variable metric procedure.

J. P. Sadler [64] applied the above optimization procedure to six-bar linkages and individually minimized the maximum values of the shaking force, the shaking moment, the input torque fluctuation as well as a bearing force by both one and two point masses of prescribed magnitude. A trade-off between maximum shaking force and input torque fluctuation was also undertaken, using either two or three balancing masses. For the two balancing mass case, this was accomplished both with and without an additional bearing force constraint. Finally, a 40 percent reduction in both maximum shaking force and shaking moment was accomplished

for a six-bar stone crusher mechanism with the help of a composite objective function. The efficiency of nonlinear programming, when applied to linkage balancing, was demonstrated by duplicating the analytically obtainable full force balance results for both four-bar and six-bar linkages.

In a unique study, combining kinematic synthesis and the dynamic design of four-bar linkages, F. L. Conte, G. R. George, R. W. Mayne and J. P. Sadler [14] showed that nonlinear programming can be successfully applied for the determination of that linkage which not only satisfies the kinematic objectives, but also provides optimum dynamic characteristics.

B. Porter and D. J. Sanger [59] also showed the application of nonlinear programming techniques to the optimization of certain dynamic reactions of an inline four-bar linkage with links of constant cross-section. To this end, an objective function consisting of the sum of the weighted mean square values of the shaking force, the shaking moment, the input torque and the bearing forces was introduced. The minimization of this function is subject to constraints on the two design variables which are represented by the inline location as well as the magnitude of the radius of a circular counterweight attached to the input link. (The

input link counterweight was designed according to the Method of Linearly Independent Vectors and was chosen to have a minimum moment of inertia.) The authors selected the weighting factors in such a way that they only performed the simultaneous optimization of two reactions. Their success was greater for forces than for moments.

S. Schonfeld [65] reported on a computer program which combines the ability to generate the various reactions of planar linkages together with their optimization by means of nonlinear programming techniques. A successful example of a weighted optimization of the shaking moment and the input torque of a six-bar linkage is shown. The same author together with H. Dresig [66] discussed, without example, the simultaneous optimization of all linkage reactions by the application of the usual techniques of linear analysis.

## B. Results Of Investigation

The present section reports briefly on the results of the investigation which consists of the following parts:

1. Theory Of Full Force Balancing Machines For Reciprocating Mechanisms
2. A Practical Balancing Machine For Four-Bar Linkages
3. A New Method For Prescribing The Maximum Shaking Force Of A Four-Bar Linkage With Flexibility In Counterweight Design
4. Simultaneous Optimization Of Dynamic Reactions Of A Four-Bar Linkage With Prescribed Maximum Shaking Force

1. Theory Of Full Force Balancing Machines For Reciprocating Mechanisms

The theoretical basis for new balancing fixtures capable of removing the unavoidable residual shaking force found in theoretically balanced mechanisms is presented. This new approach is first applied to a four-bar linkage with a general mass distribution. Subsequently, it is generalized to include all balanceable planar mechanisms.

In both instances, sets of shaking force component

equations are solved for certain general mass-distance products. To obtain these parameters, which form the basis for the design of the required correction masses, the values of the residual shaking force components and of all kinematic properties must be known from experimentation for certain positions of the mechanism.

## 2. A Practical Balancing Machine For Four-Bar Linkages

The development of an actual force balancing machine along the lines of the new theory and capable of removing a large portion of the residual shaking force found in a theoretically fully force balanced four-bar linkage, is described.

While it was not possible, because of experimental error, to obtain unique answers for the desired correction masses from various sets of balancing equations, a method was devised which makes use of many sets of such expressions. The problem was interpreted as one of finding the best possible solution to an overdetermined system of balancing equations. Both a least squares and a minimax approach were developed.

Although it was not possible to remove all residual imbalance, both methods furnished considerable reductions

of the shaking force components. The minimax method was found to give a somewhat greater reduction than the least squares approach.

3. A New Method For Prescribing The Maximum Shaking Force Of A Four-Bar Linkage With Flexibility In Counterweight Design

This novel two-counterweight method of partial force balancing of a four-bar linkage, which forms the basis for a comprehensive optimization method discussed later, allows the designer to realize a prescribed value for the maximum shaking force anywhere between zero and an inherent upper limit. In addition, by taking advantage of a certain mathematical property, which has been called the equipollent circle constraint equation, it becomes possible to attain the identical prescribed maximum shaking force for a wide range of output and associated input link counterweight configurations.

This technique, which is generally only applicable to constant speed mechanisms, builds upon a Chebyshev-type partial balancing method, first given by Ya. L. Gheronimus, which only uses an input link counterweight. The equipollent circle constraint equation, which allows flexibility in

counterweight design for a prescribed maximum shaking force, represents an adaptation of a parallel concept, used by G. G. Lowen and F. R. Tepper to prescribe the RMS shaking force.

Examples involving both a 50 and a 75 percent reduction in the maximum shaking force are given and the associated ranges of possible counterweight designs are determined. The magnitudes of such maximum dynamic reactions as bearing forces, input moment and shaking moment have been computed for each of the above reductions in the maximum shaking force for a full range of counterweight designs. These reactions show little variation in magnitude over a substantial portion of this range. In light of the above, this flexibility in counterweight configuration offers advantages when certain space limitations have to be observed.

#### 4. Simultaneous Optimization Of Dynamic Reactions Of A Four-Bar Linkage With Prescribed Maximum Shaking Force

This extension of the previously described new partial balancing method makes it possible to simultaneously minimize the maximum dynamic reactions of a constant speed four-bar linkage while maintaining the ability to prescribe the

maximum shaking force. The general reduction of the values of these reactions, when compared to those obtained by the previous method, is based on the introduction of a coupler counterweight in addition to those located on the input and output links. The resulting increase in the number of design variables is reflected in what has now been called the general equipollent circle constraint equation. The simultaneous optimum reduction of the maximum bearing forces, the maximum input moment and the maximum shaking moment now becomes a function of the proper combination of the coupler and output link counterweight parameters.

To this end, an optimization procedure was devised which allows for the determination of these counterweight parameters. This procedure satisfies the general equipollent circle constraint equation while it imposes constraints on the maximum dynamic reactions. The latter inequality constraints are controlled by a minimization parameter  $z$  which serves as the objective function of the optimization.

The above optimization procedure was incorporated into the Harwell Augmented Lagrangian optimization code which was used to obtain optimum counterweight designs for a 50 and a 75 percent reduction in the maximum shaking force. It was found that the benefits of this optimization were most

pronounced for the larger reduction in the maximum shaking force.

This three-counterweight method was also adapted to a fully force balanced mechanism. The associated reductions in the dynamic reactions, when compared to those associated with the two-counterweight Method of Linearly Independent Vectors, was found to be especially gratifying.

Finally, the optimization procedure was modified for an input moment minimization of a fully force balanced mechanism. Again, a comparison of the resulting maximum input moment with that associated with the above two-counterweight method shows a considerable reduction.

## II. THEORY OF FULL FORCE BALANCING MACHINES FOR RECIPROCATING MECHANISMS

### A. Introduction

While it is theoretically possible to design linkages which are fully force balanced, there are practical difficulties in attaining this aim. Due to unavoidable manufacturing tolerances and the unpredictable nonhomogeneity of the materials used, the shaking force of an actual mechanism, built to be theoretically force balanced, generally does not vanish completely. Furthermore, this residual imbalance may be amplified by any variation in the input velocity.

The following describes the first theoretical approach to full force balancing machines for reciprocating mechanisms. It is felt to be unique because it represents the first attempt at such machines for mechanisms in which the counterweights do not all rotate at the speed of a single shaft, as is the case in automotive engines.

The new theory is first applied to a four-bar linkage with a general mass distribution. Subsequently, it is generalized to include all balanceable planar mechanisms [76].

In both instances, sets of shaking force component equations are solved for certain general mass-distance products. To obtain these parameters, which form the basis for the design of the required correction masses, the values of the residual shaking force components and of all kinematic properties must be known from experimentation for certain positions of the mechanism.

## B. Theory Of Four-Bar Linkage Balancing Machine

To understand the concept<sup>1</sup> of the balancing machine for a four-bar linkage with a general mass distribution, as shown in Figure 2.1, consider first the following compact form of the shaking force expression, as given by equation (A.7) of Appendix A:

$$\bar{F}_{M/G} = (P_1 + iQ_1)K_1e^{i\gamma_1} + (P_3 + iQ_3)K_3e^{i\gamma_3} \quad (2.1)$$

where  $P_1 = m_1p_1 + m_2a_1 - \frac{a_1}{a_2} m_2p_2$

$$Q_1 = m_1q_1 - \frac{a_1}{a_2} m_2q_2$$

$$P_3 = m_3p_3 + \frac{a_3}{a_2} m_2p_2$$

$$Q_3 = m_3q_3 + \frac{a_3}{a_2} m_2q_2$$

$$\left. \begin{aligned} K_j &= \sqrt{\dot{\phi}_j^4 + \ddot{\phi}_j^2} \\ \gamma_j &= \phi_j - \phi_j' \\ \phi_j' &= \tan^{-1} \frac{\ddot{\phi}_j}{\dot{\phi}_j^2} \end{aligned} \right\} j = 1, 3$$

---

<sup>1</sup>In the search for a force balancing machine for four-bar linkages, it became evident that the present approach represents the only feasible one. Appendix B.1 proves this by showing that one may not uniquely determine the individual link mass-distance products  $m_j p_j$  and  $m_j q_j$  ( $j=1,2,3$ ) which could possibly be modified by suitable correction masses.

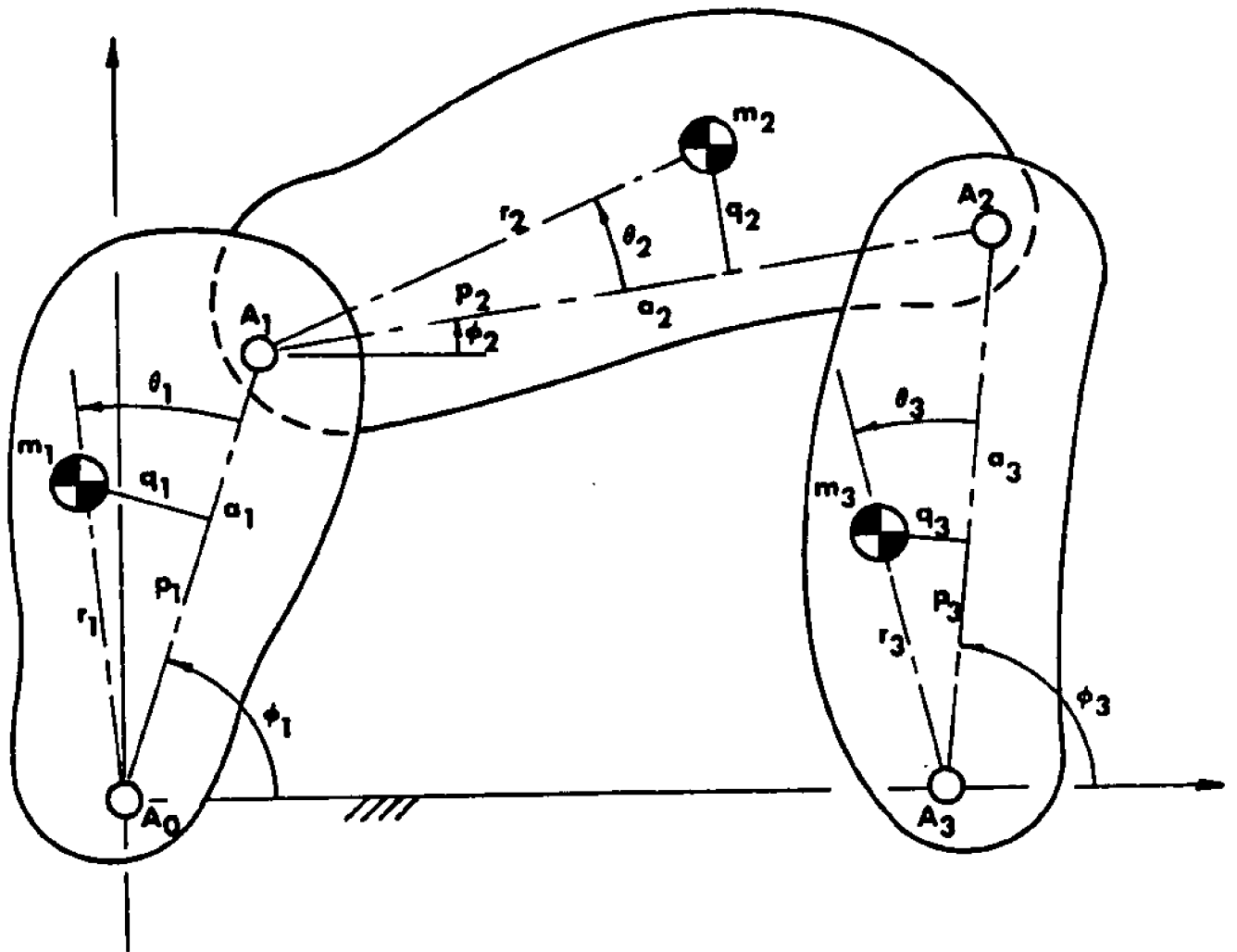


FIG. 2.1 GENERAL FOUR-BAR LINKAGE

For a fully force balanced mechanism, the shaking force  $\bar{F}_{M/G}$  vanishes because the general mass-distance terms  $P_j$  and  $Q_j$  have been made to vanish. For the almost balanced mechanism, these factors are not equal to zero because of the various previously mentioned uncertainties. If their actual magnitudes for a given mechanism can be found experimentally, they can be made to vanish by a suitable adjustment of the mass distribution of the links involved.

For example, with

$$P_1 \neq 0,$$

one may then find a correction quantity defined as

$$\Delta P_1 = m_1 p_1^c P_1^c$$

such that

$$P_1 + \Delta P_1 = 0. \quad (2.2)$$

This corrective mass-distance product  $\Delta P_1$  may be positive or negative, depending on the sign of  $P_1$ . It can be physically realized by adding or subtracting a correction mass  $m_1 p_1^c$  at a distance  $p_1^c$  along the body-fixed x-axis of link 1. Similar corrections to the remaining mass-distance

products can be defined as follows:

$$\Delta Q_1 = -Q_1 = m_{1q}^c q_1^c \quad (2.3)$$

$$\Delta P_3 = -P_3 = m_{3p}^c P_3^c \quad (2.4)$$

$$\Delta Q_3 = -Q_3 = m_{3q}^c q_3^c \quad (2.5)$$

Appendix B.2 proves that if one applies the component forms (A.17) and (A.18) of the shaking force equation (2.1) at two mechanism positions for which all kinematic values and shaking force components are known from experimentation, one may solve uniquely for the four general mass-distance products  $P_j$  and  $Q_j$  ( $j=1,3$ ). When given in matrix form, this set of expressions becomes (see equation (B.9)):

$$\begin{bmatrix}
 K_{11} \cos \gamma_{11} & -K_{11} \sin \gamma_{11} & K_{31} \cos \gamma_{31} & -K_{31} \sin \gamma_{31} \\
 K_{11} \sin \gamma_{11} & K_{11} \cos \gamma_{11} & K_{31} \sin \gamma_{31} & K_{31} \cos \gamma_{31} \\
 K_{12} \cos \gamma_{12} & -K_{12} \sin \gamma_{12} & K_{32} \cos \gamma_{32} & -K_{32} \sin \gamma_{32} \\
 K_{12} \sin \gamma_{12} & K_{12} \cos \gamma_{12} & K_{32} \sin \gamma_{32} & K_{32} \cos \gamma_{32}
 \end{bmatrix}
 \begin{bmatrix}
 P_1 \\
 Q_1 \\
 P_3 \\
 Q_3
 \end{bmatrix}
 =
 \begin{bmatrix}
 F_M/G_{X1} \\
 F_M/G_{Y1} \\
 F_M/G_{X2} \\
 F_M/G_{Y2}
 \end{bmatrix}
 \quad (2.6)$$

$$\left. \begin{aligned}
 \text{where}^1 \quad K_{ij} &= \sqrt{\dot{\phi}_{ij}^4 + \ddot{\phi}_{ij}^2} \quad (\text{These terms are always positive.}) \\
 \gamma_{ij} &= \phi_{ij} - \phi_{ij}' \\
 \phi_{ij}' &= \tan^{-1} \frac{\ddot{\phi}_{ij}}{\dot{\phi}_{ij}^2}
 \end{aligned} \right\} \begin{array}{l} i = 1, 3 \\ j = 1, 2 \end{array}$$

(The second subscript in these terms indicate at which position the quantity is evaluated.)

This procedure furnishes the identical results whether or not friction in the joints is considered. This may be shown by the following reasoning: Whenever there is a residual shaking force, the force equal and opposite to it has, according to Newton's law for systems of rigid bodies,

---

<sup>1</sup>The required kinematic relationships are reproduced in Appendix I.

the same magnitude as the vector which represents the product of the total mass of the mechanism and the vectorial acceleration of its total center of mass. This net force of the ground on the mechanism remains the same whether or not friction is present. (Of course, the individual ground pivot forces are changed when cognizance is taken of bearing friction in a mechanism.)

### C. Generalization Of Theory Of Full Force Balancing Machines

The following shows that the principle of the four-bar linkage balancing machine may be extended to all planar single degree of freedom linkages in which no group of links produce identical kinematic terms at all times and which meet the balancing criterion given by F. R. Tepper and G. G. Lowen [76]. This criterion states that "A planar mechanism without axisymmetric link groupings can be fully force balanced by internal mass redistribution if, and only if, from each link there is a contour to the ground by way of revolutes only".

The following generalization will follow the same line of reasoning as used in Appendix B where it was shown that the general mass-distance products  $P_j$  and  $Q_j$  can be found from the repeated application of shaking force component equations which are made up of linearly independent terms. This linear independence is again assured by the use of constraint equations which have their origin in the double differentiation of the applicable mechanism loop equations. As before, the values of the kinematic terms and the shaking force components must be known from experimentation at the applicable mechanism positions.

The generalization of balancing machines will first be shown for linkages which contain only revolute. Subsequently, it is extended to mechanisms which also contain sliders.

### 1. Generalization For Mechanisms Containing Revolutes Only

In order to derive the shaking force equation for an n-linked mechanism containing revolutes only (for a typical case, see loop  $O_1ABO_2$  of Figure 2.2), F. R. Tepper and G. G. Lowen [76] showed that the mass-distance product associated with its center of mass is given by:

$$M\bar{r}_s = \sum_{j=1}^{n-1} \left[ m_j r_j e^{i\theta_j} + \sum_{k=1}^{k^*} (m h e^{i\alpha})_{kj} \right] e^{i\phi_j} + \bar{d} \quad (2.7)$$

In the foregoing, there will always be  $n-1$  terms of the type  $m_j r_j e^{i\theta_j}$ , which refer to the mass-distance products of the individual link centers of mass with respect to their body-fixed origins. The  $k^*$  terms containing the constant coefficients  $(m h e^{i\alpha})_{kj}$  represent the  $k^*$  mass-distance products which involve the fixed pivot-to-pivot vectors  $h e^{i\alpha}$  (such as  $b_2 e^{i\alpha_2}$  in Figure 2.2). They occur only when the description of the center of mass trajectory of a specific link includes the fixed pivot-to-pivot distances of another link (for example, when the center

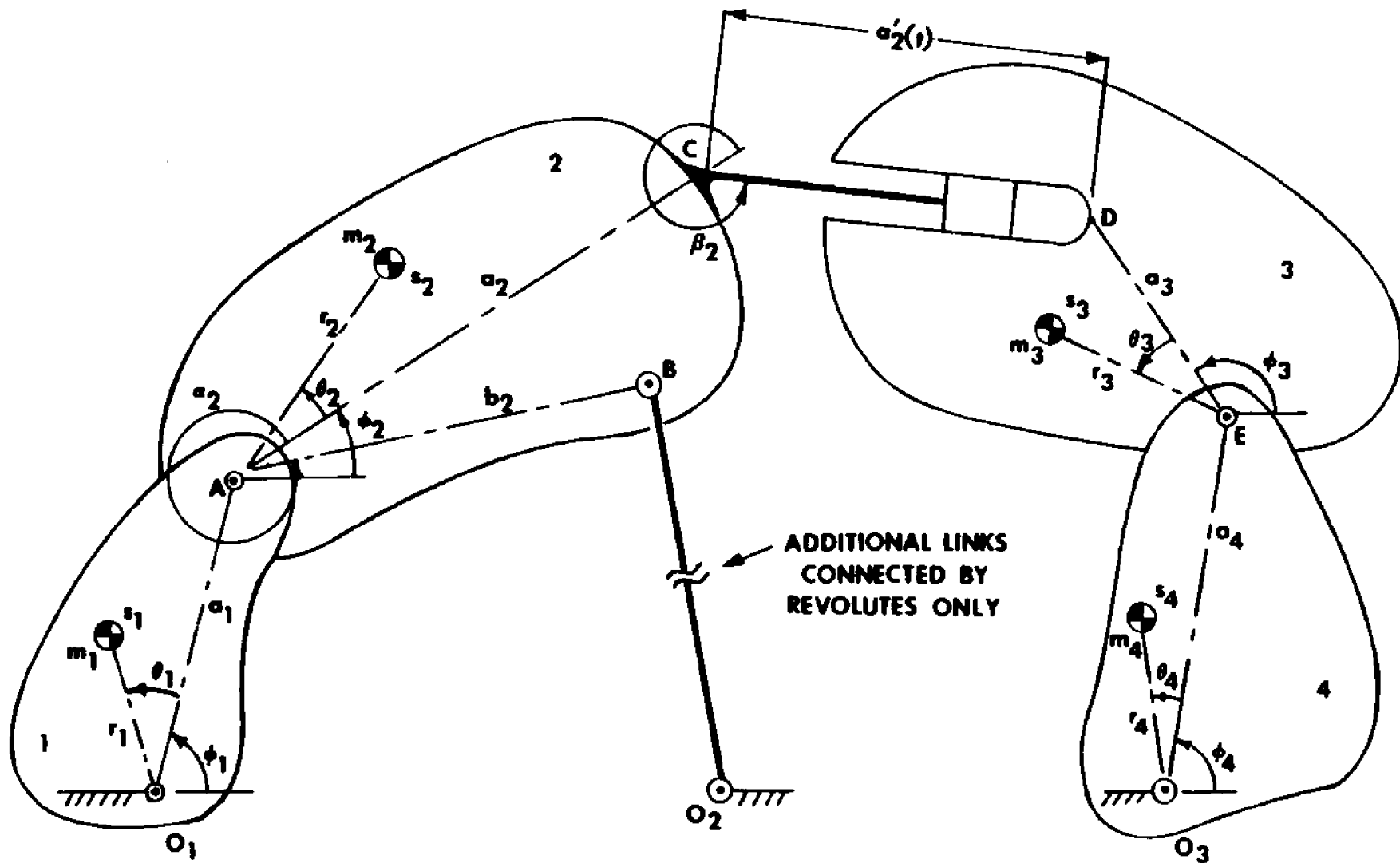


FIGURE 3.4 BALANCEABLE N-LINKED MECHANISM

of mass trajectory  $\bar{r}_{s_2}$  is defined by way of the contour  $O_2BAS_2$ ). Finally,  $\bar{d}$  is a constant mass-distance vector.

Double differentiation, change of sign and rearrangement of the above furnishes, according to Newton's law, the following shaking force component equations<sup>1</sup>:

$$\sum_{j=1}^{n-1} [(K_j \cos \gamma_j) A_j - (K_j \sin \gamma_j) B_j] = -M \ddot{r}_{sx_j} = F_{M/G_{X_j}} \quad (2.8)$$

and

$$\sum_{j=1}^{n-1} [(K_j \sin \gamma_j) A_j + (K_j \cos \gamma_j) B_j] = -M \ddot{r}_{sy_j} = F_{M/G_{Y_j}} \quad (2.9)$$

where

$$A_j = m_j r_j \cos \theta_j + \sum_{k=1}^{k^*} (mh)_{kj} \cos \alpha_{kj}$$

$$B_j = m_j r_j \sin \theta_j + \sum_{k=1}^{k^*} (mh)_{kj} \sin \alpha_{kj}$$

$$K_j = \sqrt{\dot{\phi}_j^4 + \ddot{\phi}_j^2}$$

$$\gamma_j = \phi_j - \phi_j'$$

$$\phi_j' = \tan^{-1} \frac{\ddot{\phi}_j}{\dot{\phi}_j^2}$$

---

<sup>1</sup> Equations (2.8) and (2.9) hold regardless of whether or not friction in the various bearings is taken into account. See page 21.

Each of the component equations consists of a sum of  $2(n - 1)$  terms with constant mass-distance products. Many of these terms are proportional to each other. It will now be shown that this proportionality can be eliminated by making use of the doubly differentiated component forms of the  $\frac{n}{2} - 1$  independent loop equations associated with an  $n$ -linked mechanism [57].

The  $r^{\text{th}}$  independent loop equation of such a mechanism containing revolute only may be resolved into the following component form:

$$\sum_{j=1}^n h_{rj} \cos(\alpha_{rj} + \phi_j) = 0 \quad (2.10)$$

and

$$\sum_{j=1}^n h_{rj} \sin(\alpha_{rj} + \phi_j) = 0, \quad (r=1, 2, \dots, \frac{n}{2} - 1) \quad (2.11)$$

Double differentiation of the above results in the following component form:

$$- \sum_{j=1}^{n-1} h_{rj} K_j \cos(\alpha_{rj} + \gamma_j) = 0 \quad (2.12)$$

and

$$- \sum_{j=1}^{n-1} h_{rj} K_j \sin(\alpha_{rj} + \gamma_j) = 0 \quad (2.13)$$

With  $(\frac{n}{2} - 1)$  loop equations there will be  $2(\frac{n}{2} - 1)$  constraint equations of the above type. The simultaneous application of these constraint equations to each of the shaking force component expressions reduces the number of terms in these expressions to  $n$ , i.e.

$$n = 2(n - 1) - 2(\frac{n}{2} - 1) \quad (2.14)$$

The resulting expressions are:

$$\sum_{j=1}^{n/2} [(K_j \cos \gamma_j) P_j - (K_j \sin \gamma_j) Q_j] = F_{M/G_{Xj}} \quad (2.15)$$

and

$$\sum_{j=1}^{n/2} [(K_j \sin \gamma_j) P_j + (K_j \cos \gamma_j) Q_j] = F_{M/G_{Yj}} \quad (2.16)$$

In the above, the general mass-distance products  $P_j$  and  $Q_j$ , which again must be determined to obtain the corrective mass-distance products  $\Delta P_j$  and  $\Delta Q_j$ , are of the following form:

$$\begin{aligned}
P_j = m_j p_j + \sum_{w=\frac{n}{2}+1}^{n-1} f_{wj} m_w r_w \cos(\sigma_{wj} + \theta_w) \\
+ \sum_{k=1}^{k^*} \left[ (mh \cos \alpha)_{kj} + \sum_{w=\frac{n}{2}+1}^{n-1} f_{wj} (mh)_{kw} \cos(\sigma_{wj} + \alpha_{kw}) \right]
\end{aligned} \tag{2.17}$$

and

$$\begin{aligned}
Q_j = m_j q_j + \sum_{w=\frac{n}{2}+1}^{n-1} f_{wj} m_w r_w \sin(\sigma_{wj} + \theta_w) \\
+ \sum_{k=1}^{k^*} \left[ (mh \sin \alpha)_{kj} + \sum_{w=\frac{n}{2}+1}^{n-1} f_{wj} (mh)_{kw} \sin(\sigma_{wj} + \alpha_{kw}) \right]
\end{aligned} \tag{2.18}$$

The  $f_{wj}$  and  $\sigma_{wj}$  terms represent constants which result from the elimination of the linear dependence.

Because of the use of constraint equations, each of the above force component expressions is made up of a sum of  $n$  linearly independent terms. Both expressions are linearly independent of each other since they represent the orthogonal components of a single vector.

In order to solve for the  $n$  corrective mass-distance products, it is necessary to use  $\frac{n}{2}$  pairs of shaking force component equations, of the form of equations (2.15) and (2.16), for  $\frac{n}{2}$  mechanism positions for which all kinematic and

shaking force component values are known from experimentation. The resulting set of simultaneous equations takes the following matrix form:

$$\begin{bmatrix}
 K_{11} \cos \gamma_{11} & -K_{11} \sin \gamma_{11} & \cdot & \cdot & \cdot & K_{\frac{n1}{2}} \cos \gamma_{\frac{n1}{2}} & -K_{\frac{n1}{2}} \sin \gamma_{\frac{n1}{2}} \\
 K_{11} \sin \gamma_{11} & K_{11} \cos \gamma_{11} & \cdot & \cdot & \cdot & K_{\frac{n1}{2}} \sin \gamma_{\frac{n1}{2}} & K_{\frac{n1}{2}} \cos \gamma_{\frac{n1}{2}} \\
 \cdot & \cdot & & & & \cdot & \cdot \\
 \cdot & \cdot & & & & \cdot & \cdot \\
 \cdot & \cdot & & & & \cdot & \cdot \\
 K_{\frac{1n}{2}} \cos \gamma_{\frac{1n}{2}} & -K_{\frac{1n}{2}} \sin \gamma_{\frac{1n}{2}} & \cdot & \cdot & \cdot & K_{\frac{nn}{22}} \cos \gamma_{\frac{nn}{22}} & -K_{\frac{nn}{22}} \sin \gamma_{\frac{nn}{22}} \\
 K_{\frac{1n}{2}} \sin \gamma_{\frac{1n}{2}} & K_{\frac{1n}{2}} \cos \gamma_{\frac{1n}{2}} & \cdot & \cdot & \cdot & K_{\frac{nn}{22}} \sin \gamma_{\frac{nn}{22}} & K_{\frac{nn}{22}} \cos \gamma_{\frac{nn}{22}}
 \end{bmatrix}
 \begin{bmatrix}
 P_1 \\
 Q_1 \\
 \cdot \\
 \cdot \\
 \cdot \\
 P_{\frac{n}{2}} \\
 Q_{\frac{n}{2}}
 \end{bmatrix}
 =
 \begin{bmatrix}
 F_{M/G_{X1}} \\
 F_{M/G_{Y1}} \\
 \cdot \\
 \cdot \\
 \cdot \\
 F_{M/G_{X\frac{n}{2}}} \\
 F_{M/G_{Y\frac{n}{2}}}
 \end{bmatrix}$$

(2.19)

The second subscript in the above expression refers to the  $\frac{n}{2}$  mechanism positions.

Each of the resulting  $n$  row vectors of the coefficient matrix is linearly independent as long as no groups of the  $\frac{n}{2}$  links produce identical kinematic terms for all  $\frac{n}{2}$  positions of the mechanism. Thus, the matrix has rank  $n$  and may be solved uniquely for the  $n$  general mass-distance products  $P_j$  and  $Q_j$ .

With the  $P_j$  and  $Q_j$  terms now available, the corrective mass-distance products  $\Delta P_j$  and  $\Delta Q_j$  (and therefore the corrective masses  $m_j^C$ ) required to eliminate the residual imbalance are found from:

$$P_j + \Delta P_j = 0 \quad (2.20)$$

$$\text{and } Q_j + \Delta Q_j = 0 \quad (2.21)$$

$$j = 1, 2, \dots, \frac{n}{2}$$

## 2. Generalization For Mechanisms Containing Both Revolutes And Sliders

For an  $n$ -linked mechanism which contains  $s$  sliders in addition to revolutes (see Figure 2.2), the mass-distance product associated with its center of mass is given by:

$$M\bar{r}_s = \sum_{j=1}^{n-1-s} \left[ (m_j r_j e^{i\theta_j} + \sum_{k=1}^{k^*} (m h e^{i\alpha})_{kj} e^{i\phi_j} + \sum_{u=1}^s (m a'(t) e^{i\beta})_{uj} e^{i\phi_j} \right] + \bar{d} \quad (2.22)$$

The  $s$  time dependent mass-distance products  $(m a'(t) e^{i\beta})_{uj}$  are due to the variable "link lengths" associated with the  $s$  sliders (for example, see  $a_2'(t) e^{i\beta_2}$  in Figure 2.2). All other terms are identical to those given in equation (2.7).

For each of the  $s$  sliders in a balanceable mechanism there is a loop equation which contains only one time dependent term, i.e.:

$$a_r'(t)e^{i(\beta_r + \phi_r)} + \sum_{j=1}^n h_{rj} e^{i(\alpha_{rj} + \phi_j)} = 0, \quad (r=1,2,\dots,s) \quad (2.23)$$

These  $s$  loop equations are now used to eliminate the time dependent mass-distance products in equation (2.22). This results in an expression similar to equation (2.7) containing  $(n - 1 - s)$  terms with constant mass-distance products in addition to the constant:

$$M\bar{F}_s = \sum_{j=1}^{n-1-s} \left[ m_j r_j e^{i\theta_j} + \sum_{k=1}^{k'} (m h e^{i\alpha})_{kj} \right] e^{i\phi_j} + \bar{d} \quad (2.24)$$

(Note that the use of the loop equations leads to a greater number of terms of the type  $m h e^{i\alpha}$  .)

Again, following the procedure outlined in the previous section, the above expression is doubly differentiated and put into component form. Each of these component expressions now consists of a sum of  $2(n - 1 - s)$  linearly dependent terms. These are made linearly independent with the help of  $2(\frac{n}{2} - 1 - s)$  component constraint equations of the type

of equations (2.12) - (2.13) which are obtained from the remaining  $(\frac{n}{2} - 1 - s)$  independent loop equations. The resulting number of linearly independent terms in the shaking force component equations will again be  $n$ , since

$$n = 2(n - 1 - s) - 2(\frac{n}{2} - 1 - s)$$

These final expressions are identical with equations (2.15) and (2.16) and the  $n$  corrective mass-distance products may again be obtained with the help of equation (2.19) with its associated matrix of rank  $n$ .

### III. A PRACTICAL BALANCING MACHINE FOR FOUR-BAR LINKAGES

#### A. Introduction

The following reports on the development of an actual force balancing machine capable of fine balancing a four-bar linkage.

Because of the experimental errors inherent in the determination of the shaking force components and the various necessary kinematic quantities, it was not possible to proceed completely along the lines of the theory given in Section II-B. Whenever the general mass-distance products  $P_j$  and  $Q_j$  ( $j=1,3$ ) were evaluated for a given set of two angular positions, according to equations (2.6), the results differed from those obtained for any other set of two angular positions. Thus, it became clear that a method for determining these quantities, which makes use of many sets of observations, had to be developed.

Section B shows that this problem may be interpreted as one of finding the best possible solution to an overdetermined system of balancing equations. It further outlines how solutions may be obtained by both a minimax and a least squares approach<sup>1</sup>.

---

<sup>1</sup>This was accomplished for both cases with the help of an existing Augmented Lagrangian optimization program (Harwell Subroutine Library, VF01AD). While more conventional programs could have been used for these solutions, it was found most convenient to formulate these problems for the above program since it was used in other parts of this dissertation.

Section C gives a description of the experimental apparatus and explains the methods by which data are obtained.

Section D shows examples of both minimax and least squares fine balancing procedures. While both approaches furnished considerable reductions of the shaking force components of a theoretically fully force balanced mechanism, the minimax method led to the greater reduction of these components.

Section E gives a detailed discussion of the sources of the experimental errors and concludes that there is good reason why the minimax method furnishes the more desirable results.

Appendix C shows the use of the Harwell code as well as its adaptation to the minimax approach of finding the best possible solution to the overdetermined system of balancing equations.

Appendix D shows the adaptation of the same program to the least squares approach.

## B. Adaptation Of Balancing Machine Theory

Since, as stated earlier, due to experimental errors, more than two sets of data must be employed for the determination of the general mass-distance products  $P_j$  and  $Q_j$  ( $j=1,3$ ), the following overdetermined system of balancing equations, based on equation (2.6), results:

$$\begin{bmatrix}
 K_{11}\cos\gamma_{11} & -K_{11}\sin\gamma_{11} & K_{31}\cos\gamma_{31} & -K_{31}\sin\gamma_{31} \\
 K_{11}\sin\gamma_{11} & K_{11}\cos\gamma_{11} & K_{31}\sin\gamma_{31} & K_{31}\cos\gamma_{31} \\
 \cdot & \cdot & \cdot & \cdot \\
 \cdot & \cdot & \cdot & \cdot \\
 \cdot & \cdot & \cdot & \cdot \\
 \cdot & \cdot & \cdot & \cdot \\
 K_{1m}\cos\gamma_{1m} & -K_{1m}\sin\gamma_{1m} & K_{3m}\cos\gamma_{3m} & -K_{3m}\sin\gamma_{3m} \\
 K_{1m}\sin\gamma_{1m} & K_{1m}\cos\gamma_{1m} & K_{3m}\sin\gamma_{3m} & K_{3m}\cos\gamma_{3m}
 \end{bmatrix}
 \begin{bmatrix}
 P_1 \\
 Q_1 \\
 P_3 \\
 Q_3
 \end{bmatrix}
 =
 \begin{bmatrix}
 F_M/G_{X1} \\
 F_M/G_{Y1} \\
 \cdot \\
 \cdot \\
 \cdot \\
 \cdot \\
 F_M/G_{Xm} \\
 F_M/G_{Ym}
 \end{bmatrix}
 \quad (3.1)$$

where  $m$  represents the total number of pairs (i.e. angular positions) of data chosen.

The solutions of the above system will furnish values for the  $P_j$  and  $Q_j$  terms such that the left hand side of the matrix equations approximates the right hand side either in a minimax or a least squares sense at all chosen positions.

Figure 3.1 shows the above from a different point of view. The solid curves represent purely experimental values of the shaking force components  $F_{M/G_X}$  and  $F_{M/G_Y}$  as plotted against the crank angle  $\phi_1$ . The dashed curves stand for computed values of these forces. They are obtained with the help of experimentally determined angles, angular velocities and accelerations of the input link. The  $P_j$  and  $Q_j$  terms in these expressions are chosen such that the differences  $\Delta F_x$  and  $\Delta F_y$  between the two sets of curves are minimized according to a minimax or a least squares criterion.

Both of these approaches will now be discussed. The results of their actual implementation are shown in Section D. (The use of the Harwell program for this purpose is shown in Appendices C and D.)

### 1. Minimax Balancing Optimization

The maximum value of the differences  $\Delta F_x$  and  $\Delta F_y$  between the sets of shaking force curves is minimized in this approach.

To accomplish this by way of the Augmented Lagrangian

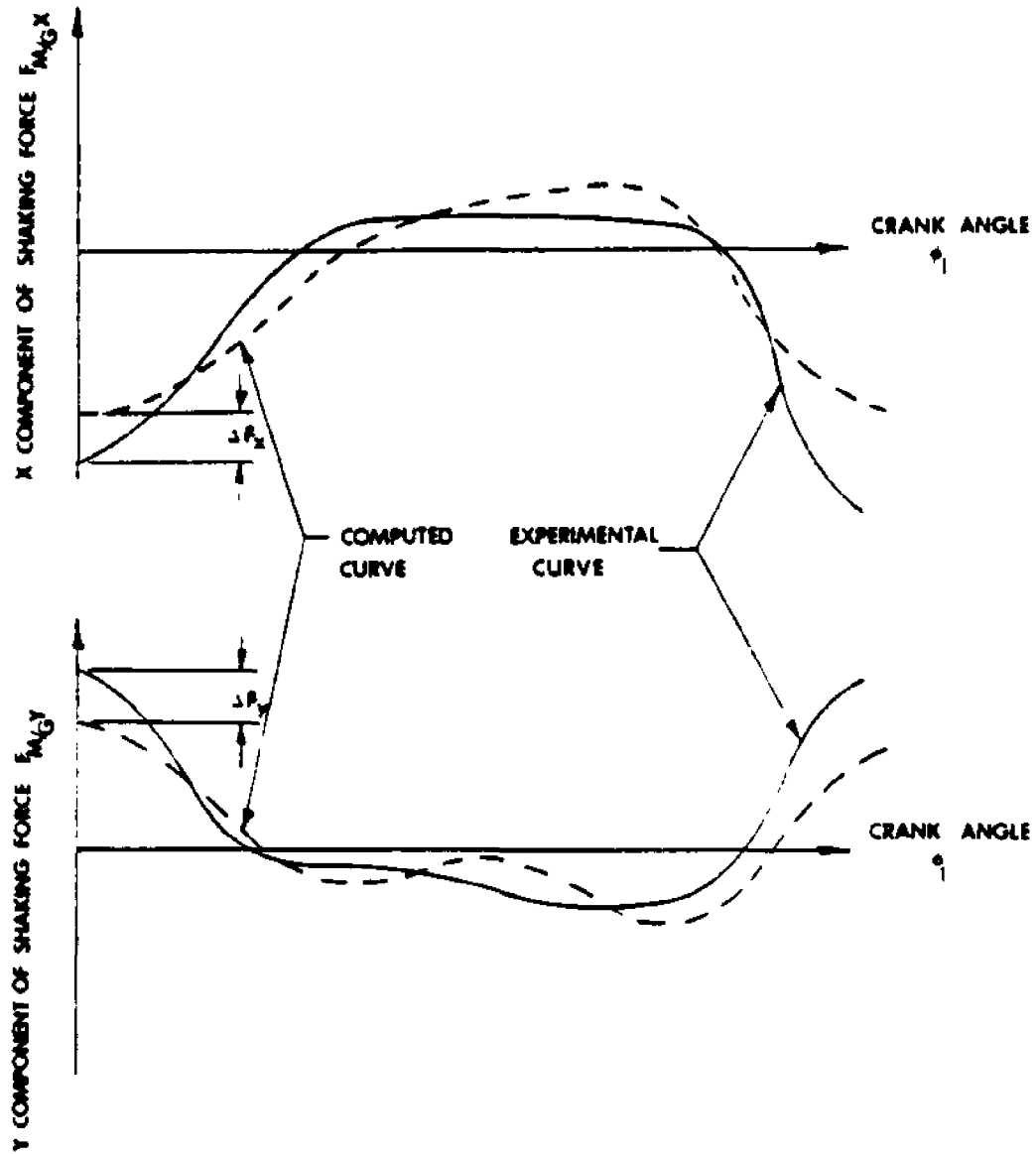


FIGURE 3.1: COMPARISON OF TYPICAL COMPUTED AND EXPERIMENTAL RESIDUAL SHAKING FORCE COMPONENTS FOR A FOUR-BAR LINKAGE

program, the square of the differences<sup>1</sup>  $\Delta F_x$  and  $\Delta F_y$  are constrained at  $m$  values of the input angle  $\phi_1$  to be less than or equal to a new variable  $z$ . This variable represents the objective function which is to be minimized.

In equation form, the above becomes

$$\text{minimize } z \quad (3.2)$$

by the optimal choice of  $P_1$ ,  $Q_1$ ,  $P_3$  and  $Q_3$ , subject to the following inequality constraints:

$$\left. \begin{aligned} (\Delta F_{x_i})^2 &\leq z \\ (\Delta F_{y_i})^2 &\leq z \end{aligned} \right\} \quad (i=1, 2, \dots, m) \quad (3.3)$$

where

$$\Delta F_{x_i} = F_{CX_i} - F_{EX_i}$$

$$\Delta F_{y_i} = F_{CY_i} - F_{EY_i}$$

and

$F_{CX_i}$  =  $i^{\text{th}}$  computed value of shaking force component  $F_{M/G_x}$

$F_{CY_i}$  =  $i^{\text{th}}$  computed value of shaking force component  $F_{M/G_y}$

---

<sup>1</sup>The reason for constraining the squares of these differences between the curves, rather than the actual differences or the absolute values of the differences directly, lies in the nature of the optimization program. In essence, the absolute values of the differences are constrained.

$F_{EX_i}$  =  $i^{\text{th}}$  experimental value of shaking force component  $F_{M/G_x}$

$F_{EY_i}$  =  $i^{\text{th}}$  experimental value of shaking force component  $F_{M/G_y}$

The subscript  $i$  indicates that the constraints are evaluated at the  $m$  mechanism positions.

## 2. Least Squares Balancing Optimization

In the least squares approach, the sum of the squares of the differences  $\Delta F_x$  and  $\Delta F_y$  are minimized at the  $m$  mechanism positions. This sum also represents the objective function. Thus formally,

$$\text{minimize } \sum_{i=1}^m \left[ (\Delta F_{X_i})^2 + (\Delta F_{Y_i})^2 \right] \quad (3.4)$$

### C. Balancing Machine Design And Instrumentation

The following describes the design of the experimental balancing machine as well as the manner in which the required test data are obtained.

#### 1. Basic Configuration Of Balancing Machine

Figure 3.2 shows an overall view as well as a schematic of the experimental balancing setup while Figure 3.3 gives photographs of the final configuration. All components are listed in Table 3.1.

The variable speed DC motor, whose armature becomes part of the input link of the mechanism, is mounted on one of the force platforms while the output link ground bearing support is mounted on the other. The coupler link is attached to the flywheel portion of the input link. Both input and output links carry circular counterweights which are designed according to the Method of Linearly Independent Vectors [ 8 ]. In addition, each of these links contains four symmetrical balancing holes at known distances from their axes of revolution. These serve, depending on need, to receive the correction masses associated with the mass-distance products  $\Delta P_j$  and  $\Delta Q_j$  ( $j=1,3$ ).

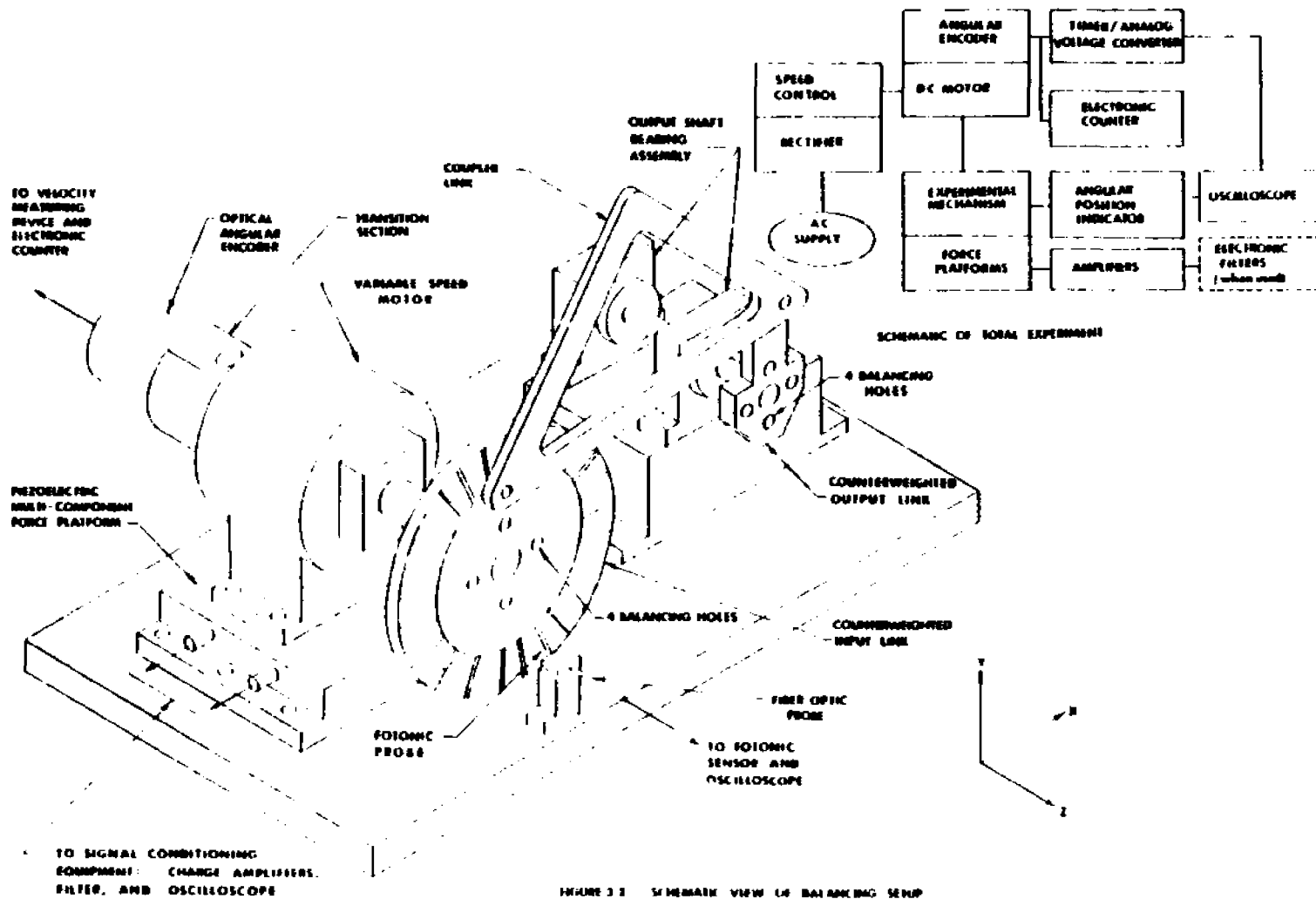


FIGURE 3-3 SCHEMATIC VIEW OF BALANCING SETUP

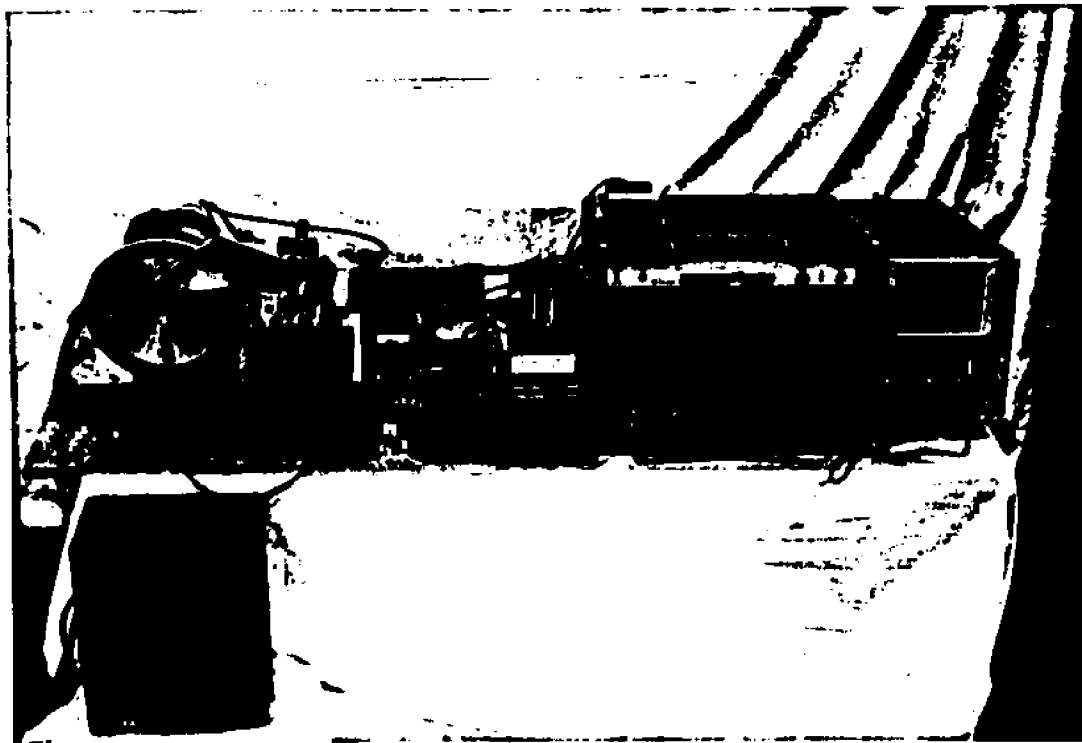
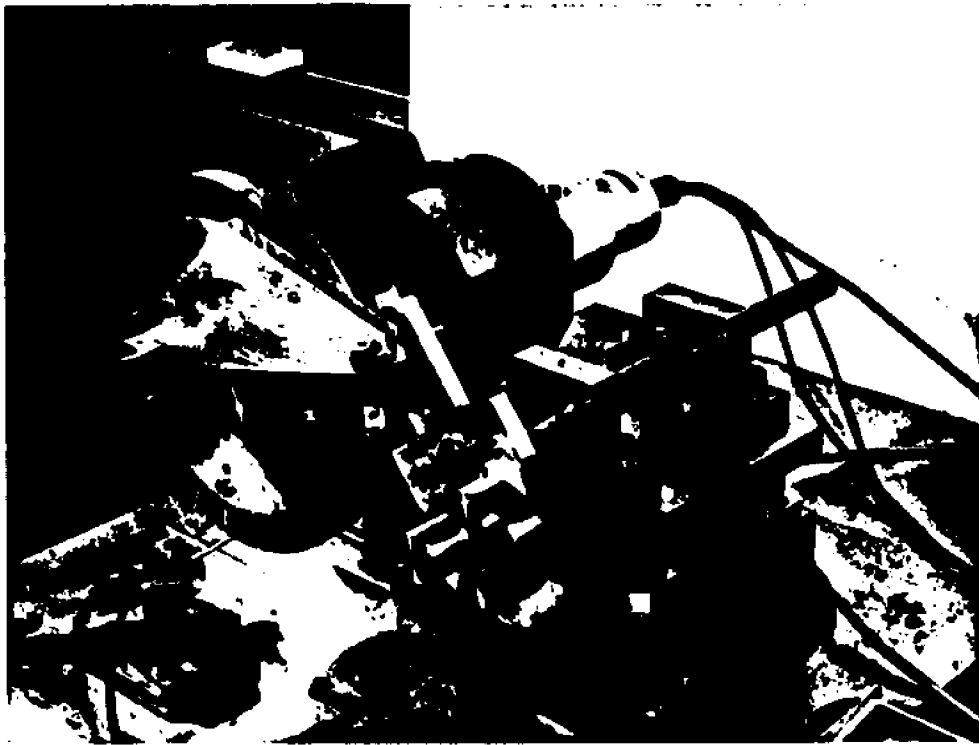


Figure 3.3: Photographs of Balancing Setup

Motor	Westinghouse DC Type FK, 1/6 HP
Motor Speed Control	Boston Gear Radiotrol 1/3 HP Motor Speed Control
Force Platforms	Kistler Instrumente, A.G. Three Component Measuring Platform Type 9257A
Amplifiers	Kistler Instrumente, A.G. Charge Amplifier, Type 5001
Fiber Optic Probe	MTI Instruments Division Fotonic Sensor Model KD-38
Angular Encoder	Theta Instruments Optical Incremental Shaft Encoder Model 05-720-3
Electronic Counter	Hewlett-Packard Timer-Counter Model 5326 A
Electronic Filters	Krohn-Hite Corporation Electronic Filter Model 3750
Oscilloscope	Tektronix Dual Trace Storage Display Model 5103N/D11

Table 3.1: Equipment Used In Experiment

The piezoelectric force platforms furnish the X and Y components of the ground bearing forces of the input and output links.

The fiber optic probe together with the reflecting strips on the flywheel are used for the determination of the angular position of the input link.

The angular encoder, which is driven directly by the armature shaft of the motor, supplies the signal for the instantaneous angular velocity measurement of the input link. It is also used in conjunction with an electronic counter to obtain the average angular velocity for one mechanism cycle.

Figure 3.4 shows the important dimensions of the linkage, including the locations of the balancing holes and of the centers of the circular counterweights. In addition, it indicates the position of the edge of the "zero-degree" reflecting strip with respect to the axis  $A_0A_1$  (see Section 2b below). Table 3.2 lists all link mass parameters before and after the theoretical full force balance.

In order to solve for the correction masses, it is necessary to know, in addition to link dimensions, the magnitudes of the shaking force components together with the corresponding values of the input link angular velocity



Table 3.2: Experimental Mechanism Data

Before Theoretical Balance			After Theoretical Balance			
Link 1	Link 2	Link 3	Link 1		Link 3	
$p_1^0 = .046 \text{ in}$	$p_2^0 = p_2 = 4.950 \text{ in}$	$p_3^0 = .142 \text{ in}$	$p_1^* = -2.702 \text{ in}$	$p_1 = -.105 \text{ in}$	$p_3^* = -1.813 \text{ in}$	$p_3 = -.545 \text{ in}$
$q_1^0 = 0.0 \text{ in}$	$q_2^0 = q_2 = 0.647 \text{ in}$	$q_3^0 = .001 \text{ in}$	$q_1^* = 0.346 \text{ in}$	$q_1 = 0.019 \text{ in}$	$q_3^* = -0.204 \text{ in}$	$q_3 = -.071 \text{ in}$
$m_1^0 =$ 274.041x10 <sup>-4</sup> lb-sec <sup>2</sup> /in	$m_2^0 = m_2 =$ 36.503x10 <sup>-4</sup> lb-sec <sup>2</sup> /in	$m_3^0 =$ 75.855x10 <sup>-4</sup> lb-sec <sup>2</sup> /in	$m_1^* =$ 15.933x10 <sup>-4</sup> lb-sec <sup>2</sup> /in	$m_1 =$ 289.964x10 <sup>-4</sup> lb-sec <sup>2</sup> /in	$m_3^* =$ 41.088x10 <sup>-4</sup> lb-sec <sup>2</sup> /in	$m_3 =$ 116.943x10 <sup>-4</sup> lb-sec <sup>2</sup> /in

and acceleration as functions of the input link angle.

The method of measuring these quantities will now be discussed.

## 2. Instrumentation And Data Evaluation

### a. Shaking Force Components

The shaking force components  $F_{M/G_x}$  and  $F_{M/G_y}$  are obtained by adding the respective X and Y components of the ground bearing forces. These signals, once processed through charge amplifiers, are fed directly into the dual trace oscilloscope. When filtered traces are desired, a low pass electronic filter, adjusted to eliminate signals above 30 Hz, is used. (For typical unfiltered and filtered traces, see Figure 3.7.)

### b. Input Link Angle

The flywheel carries 72 equally spaced reflecting strips which return the light of the photonic sensor. The light beam is of sufficiently small diameter so that the probe is capable of furnishing a clearly defined signal on the oscilloscope as soon as the leading edge of the reflecting tape crosses the beam. (See the spiked signals on the bottom of the photographs in Figures 3.6a and 3.6b.) The

alignment of the reflecting strips was guided by radially engraved lines on the flywheel. The first of these accurately placed 5 degree lines coincides with the axis  $A_0A_1$  which is used to define the input angle  $\phi_1$ .

When  $\phi_1$  equals zero, the leading edge of the "zero-degree" reflecting strip coincides with a vertical line through the center point  $A_0$ . Figure 3.4 shows this reflecting strip located to the left of this line which is at 90 degrees to the axis  $A_0A_1$ . This configuration is necessitated by the counterclockwise rotation of the link. In order to make sure that the signal indicating the zero position is initiated at the correct point, the probe is adjusted while the mechanism is clamped to make line  $A_0A_1$  horizontal.

The angular encoder could not be used for this purpose since no simple alignment for the zero position could be devised.

### c. Instantaneous Input Link Angular Velocity

The instantaneous input link angular velocity is obtained by determining the time intervals between the one-half degree signals from the angular encoder with the help of a digital counter. Subsequently, this count is converted to an analog voltage. Thus, the shorter the time,

the lower the voltage. Because of the nature of the counter and the digital-to-analog converter, it was necessary to correlate the voltage range to a given interval of angular velocities. Since the mechanism was run at speeds between 100 and 150 RPM, the 10 volt range had to correspond to time intervals of between  $1/1200$  to  $1/1800$  of a second<sup>1</sup>. Figure 3.5 illustrates the appearance of the velocity-voltage trace on the oscilloscope screen in relation to the input link angular position signals. The zero voltage line corresponding to 150 RPM is on top of the figure, while, due to an inverted voltage scale, lower speeds, as expressed by higher voltages, appear further down.

The determination of the angular velocity at point A of the above figure now serves as an example of the conversion of voltage to angular velocity:

- a. Measure the voltage  $V_A$  with the help of the oscilloscope scale.
- b. Convert this voltage to time:

$$t = \frac{1}{1800} + \left(\frac{V_A}{10}\right) \left(\frac{1}{1200} - \frac{1}{1800}\right) \quad (3.5)$$

---

<sup>1</sup>The time for each of the 720 one-half degree intervals is given by  $t = \frac{1}{12 \times \text{RPM}}$  (sec) .

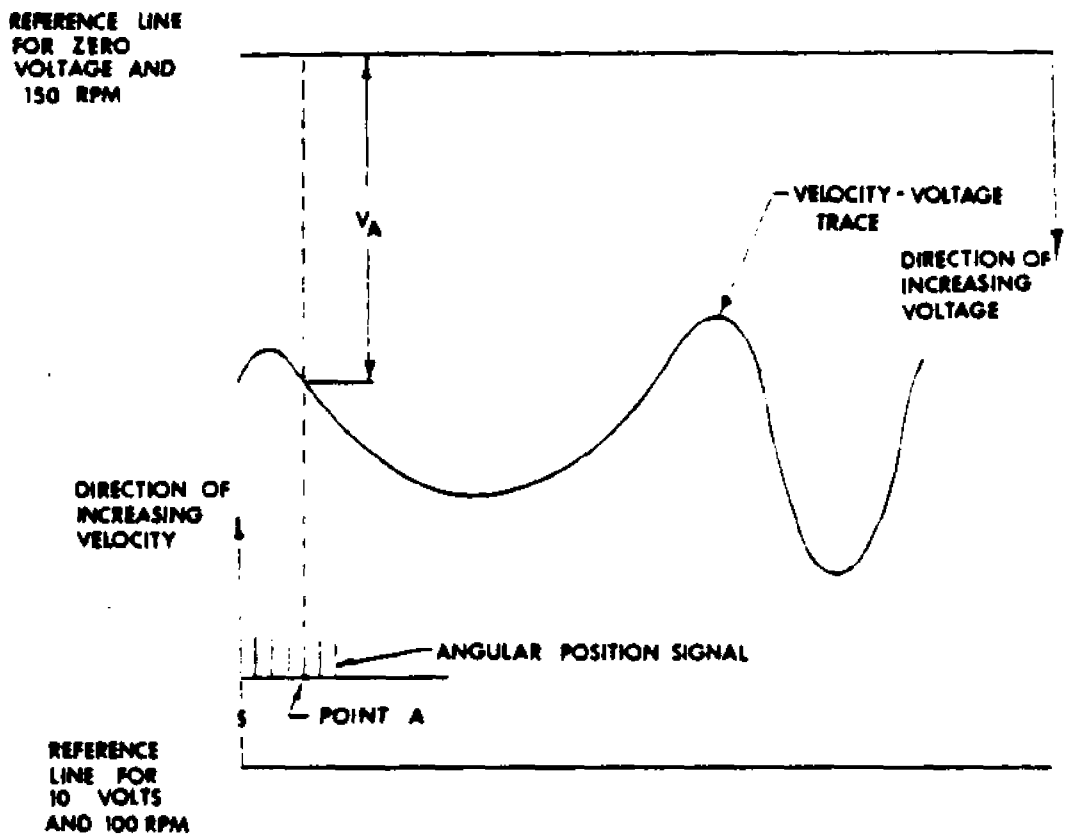


FIGURE 3.5: DETERMINATION OF INSTANTANEOUS ANGULAR VELOCITY

- c. The angular velocity corresponding to this time interval between one-half degree signals is given by:

$$\text{RPM} = \frac{60}{720t}$$

or 
$$\dot{\phi}_1 = \frac{2\pi}{720t} \quad (\text{rad/sec}) \quad (3.6)$$

d. Instantaneous Input Link Angular Acceleration

Once the instantaneous angular velocity  $\dot{\phi}_1$  of the input link has been determined experimentally for all of the 72 five degree positions  $\phi_1$ , it is expressed in the form of the Fourier series  $\dot{\phi}_1 = f(\phi_1)$ . This series is differentiated with respect to time to obtain the instantaneous input link angular acceleration  $\ddot{\phi}_1$ , i.e.

$$\ddot{\phi}_1 = \frac{df(\phi_1)}{d\phi_1} \cdot \dot{\phi}_1 \quad (3.7)$$

The value for  $\dot{\phi}_1$  is taken from the experimental data.

This is accomplished by computer program FOURIE which is reproduced in Appendix C along with the Augmented Lagrangian package.

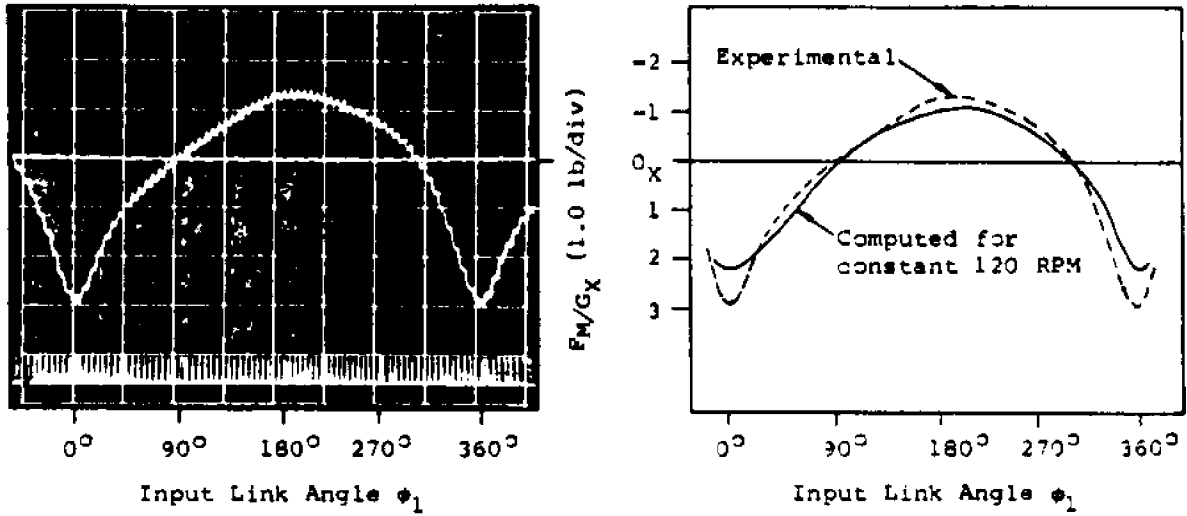
#### D. Experiment And Application Of Balancing Optimization Techniques

The following section shows how the experimental data, obtained from the theoretically balanced mechanism, are used in both the minimax and least squares fine balancing approaches. It further illustrates that the results of both methods lead to considerable shaking force reductions by way of the associated correction masses. The computational details of the minimax optimization are described in Appendix C. (This appendix also serves as an example of the use of the Augmented Lagrangian optimization program.) Appendix D shows the details of the program modifications for the least squares balancing optimization.

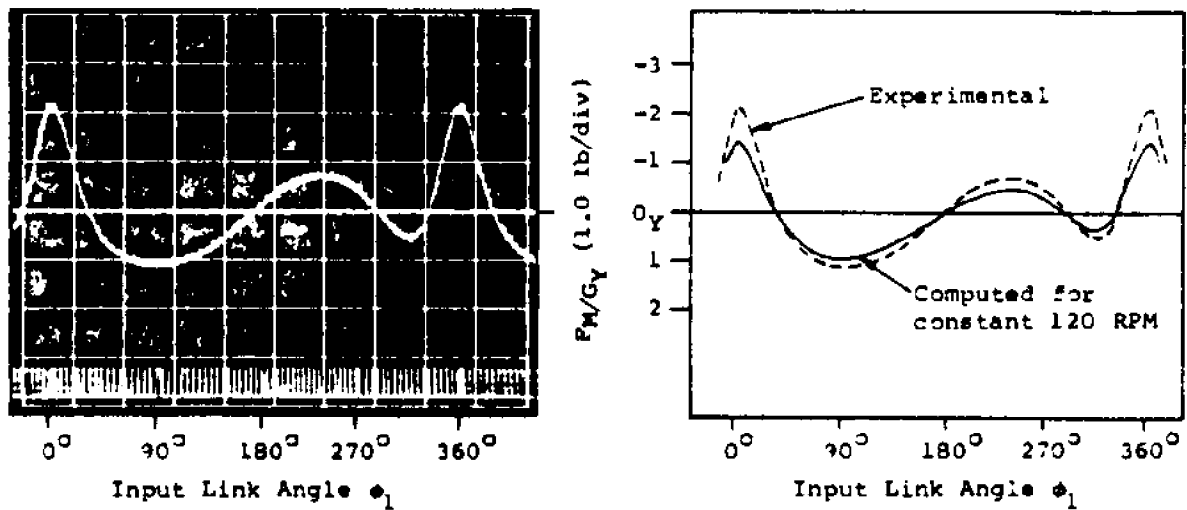
To put certain experimental procedures into proper perspective, the experience gained in connection with the unbalanced mechanism is discussed first.

##### 1. Experience With Unbalanced Mechanism: Motor Vibrations And Speed Variations

Figure 3.6 shows oscillograms of the shaking force components of the unbalanced mechanism running at an average speed of 120 RPM, together with the associated angular



a. X-Component of Shaking Force ( $F_M/G_X$ )



b. Y-Component of Shaking Force ( $F_M/G_Y$ )

Figure 3.6: Comparison of Experimental and Computed Values of Shaking Force Components of Unbalanced Mechanism (Average Input Speed: 120 RPM)

position signals of the input link. (Note that in all shaking force oscillograms, the downward direction is positive.)

The superposed 120 cps wave is due to the vibrations of the DC motor which runs on a rectified 60 cps AC current. This effect, which is due to the magnetic contraction of the motor housing, becomes more pronounced as the force signals require greater amplification with improved force balance. Since this "noise" could not be excluded without totally changing the experimental setup and since electrical filtering distorts the output, it was decided to use graphically faired versions of these experimental curves for computational purposes.

Figures 3.6a and 3.6b also show comparisons of such faired experimental and computed force component curves of the unbalanced mechanism. (The computations were made with the parameters of Table 3.2 for a constant speed of 120 RPM.) These comparisons indicate that the experimental values of the forces exceed the computed ones by as much as 25 and 34 percent for the X and Y components, respectively. Investigation showed that a good part of this difference may be attributed to the variation of angular velocity during one mechanism cycle. This variation is even more pronounced for the

theoretically balanced mechanism, and it became clear early in the investigation that this change in angular velocity had to be determined and included in the computations.

(See Section C-2-c for the actual experimental determination of the instantaneous velocity.)

## 2. Theoretically Balanced Mechanism

Figure 3.7 shows original, filtered as well as faired traces of the theoretically balanced mechanism when run at an average velocity of 120 RPM. (See Table 3.2 and Figure 3.4 for design data.)

The maximum shaking forces are 0.480 pounds and -0.590 pounds in the X and Y direction, respectively. These surprisingly large residual shaking force components furnish the justification for the present investigation. In addition to the shaking force components, Figure 3.7 gives simultaneous five degree angular position signals of the input link as well as the associated voltage-velocity trace. (Note the intentional enlargements of the angular position signals at 0, 90, 180 and 270 degrees.)

Table 3.3 lists force, angular velocity and angular acceleration values for each five degree interval of the input link angle  $\phi_1$ . The values for angular velocity

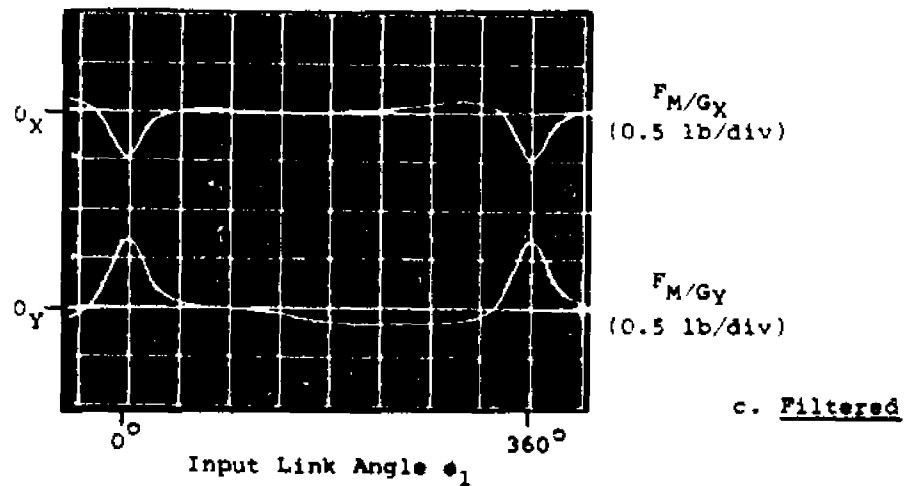
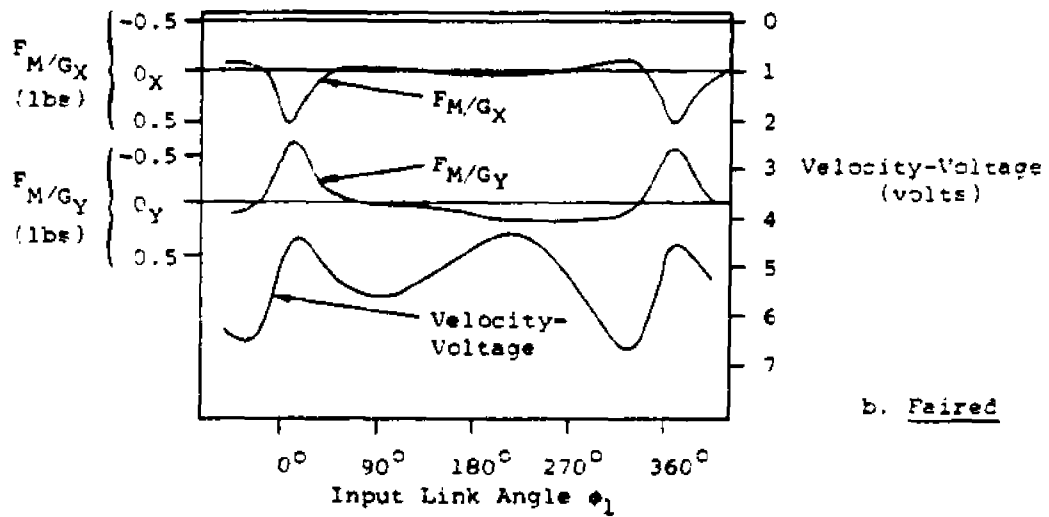
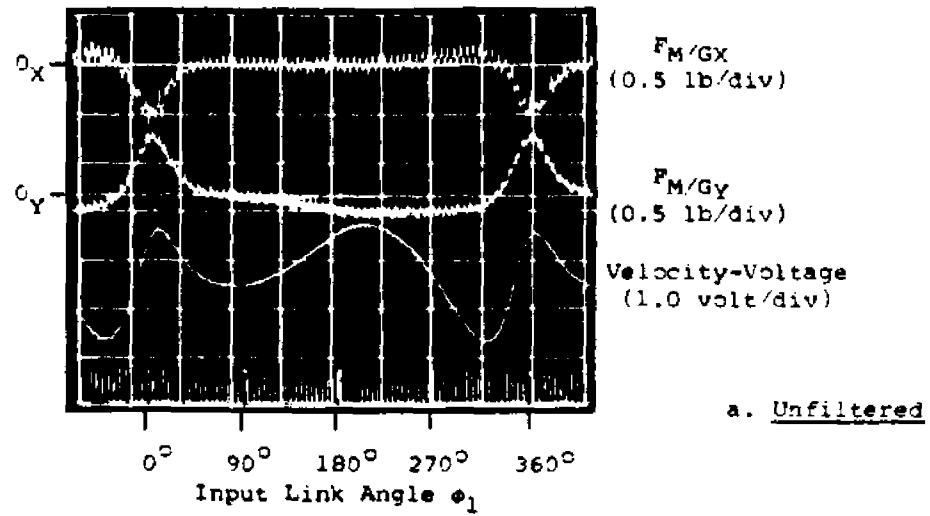


Figure 3.7: Shaking Force Components and Angular Velocity of Theoretically Balanced Mechanism (Average Input Speed: 120 RPM)

INPUT LINK ANGLE $\phi_1$ (DEG.)	INPUT LINK ANGULAR VELOCITY $\dot{\phi}_1$ (RAD/SEC)	INPUT LINK ANGULAR ACCELERATION $\ddot{\phi}_1$ (RAD/SEC <sup>2</sup> )	X COMPONENT OF SHAKING FORCE $F_M/GX$ (lbs.)	Y COMPONENT OF SHAKING FORCE $F_M/GY$ (lbs.)
0	12.751	27.136	.479	-.570
5	12.940	19.551	.480	-.590
10	12.965	-7.477	.449	-.551
15	12.911	-8.293	.384	-.468
20	12.832	-14.269	.259	-.374
25	12.746	-10.480	.202	-.282
30	12.670	-11.865	.195	-.218
35	12.597	-9.863	.060	-.173
40	12.537	-9.254	.030	-.120
45	12.476	-7.376	.009	-.097
50	12.433	-5.382	-.003	-.066
55	12.398	-4.339	-.015	-.054
60	12.372	-3.152	-.026	-.039
65	12.352	-2.554	-.029	-.029
70	12.337	-1.754	-.031	-.024
75	12.327	-1.060	-.034	-.018
80	12.321	-0.684	-.035	-.012
85	12.317	-0.190	-.034	-.009
90	12.320	0.763	-.031	-.006
95	12.325	0.603	-.029	0.0
100	12.331	1.368	-.029	.006
105	12.341	1.403	-.027	.009
110	12.355	2.357	-.024	.015
115	12.371	2.120	-.023	.023
120	12.390	3.726	-.020	.026
125	12.418	3.589	-.015	.030
130	12.442	3.952	-.012	.039
135	12.474	4.908	-.012	.048
140	12.511	5.396	-.015	.058
145	12.552	6.182	-.017	.065
150	12.600	7.747	-.019	.075
155	12.654	7.408	-.021	.083
160	12.706	3.631	-.024	.093
165	12.770	3.968	-.027	.099
170	12.826	7.990	-.030	.116
175	12.891	7.770	-.031	.122
180	12.928	6.303	-.032	.129
185	12.968	5.399	-.033	.132
190	12.997	3.569	-.037	.141
195	13.019	2.973	-.038	.144
200	13.034	1.683	-.038	.150
205	13.043	0.905	-.038	.153
210	13.047	0.435	-.039	.155
215	13.049	0.092	-.041	.156
220	13.046	-1.036	-.046	.158
225	13.038	-1.417	-.051	.159
230	13.025	-2.434	-.053	.150
235	13.006	-3.212	-.056	.160
240	12.990	-5.312	-.061	.161
245	12.939	-6.305	-.063	.161
250	12.891	-7.551	-.072	.161
255	12.835	-9.277	-.077	.160
260	12.763	-11.500	-.084	.150
265	12.682	-12.006	-.091	.159
270	12.598	-12.382	-.096	.155
275	12.512	-12.186	-.101	.156
280	12.425	-12.324	-.113	.155
285	12.338	-11.257	-.119	.153
290	12.261	-11.568	-.126	.150
295	12.175	-11.209	-.134	.147
300	12.106	-0.992	-.143	.144
305	12.037	-9.197	-.147	.134
310	11.977	-8.367	-.150	.129
315	11.913	-7.419	-.144	.116
320	11.890	0.395	-.123	.076
325	11.896	1.444	-.119	.074
330	11.930	7.646	-.081	.044
335	11.989	8.636	-.032	-.023
340	12.077	15.597	.036	-.111
345	12.199	19.400	.122	-.206
350	12.390	31.705	.253	-.345
355	12.600	22.634	.254	-.439
360	12.751	27.136	.479	-.570

TABLE 3.3: EXPERIMENTAL DATA FOR THEORETICALLY BALANCED MECHANISM

and acceleration were determined by the methods of Section C-2-c and C-2-d, respectively. (See also program FOURIE in Appendix C-3-b.) This table furnishes the data for the minimax as well as the least squares balancing optimizations.

### 3. Results Of Minimax Balancing Optimization

This section gives the results of the minimax balancing optimization. Equations (C.9) in Section 3-d of Appendix C gives the following values for the "minimax" mass-distance products  $P_j$  and  $Q_j$  ( $j=1,3$ ):

$$\begin{aligned}
 P_1 &= -50.85 \times 10^{-5} \quad \text{lb-sec}^2 \\
 Q_1 &= -57.56 \times 10^{-5} \quad \text{lb-sec}^2 \\
 P_3 &= 181.98 \times 10^{-5} \quad \text{lb-sec}^2 \\
 Q_3 &= 21.95 \times 10^{-5} \quad \text{lb-sec}^2
 \end{aligned}
 \tag{3.8}$$

According to equations (2.2) - (2.5), the mass-distance products of the correction masses then become:

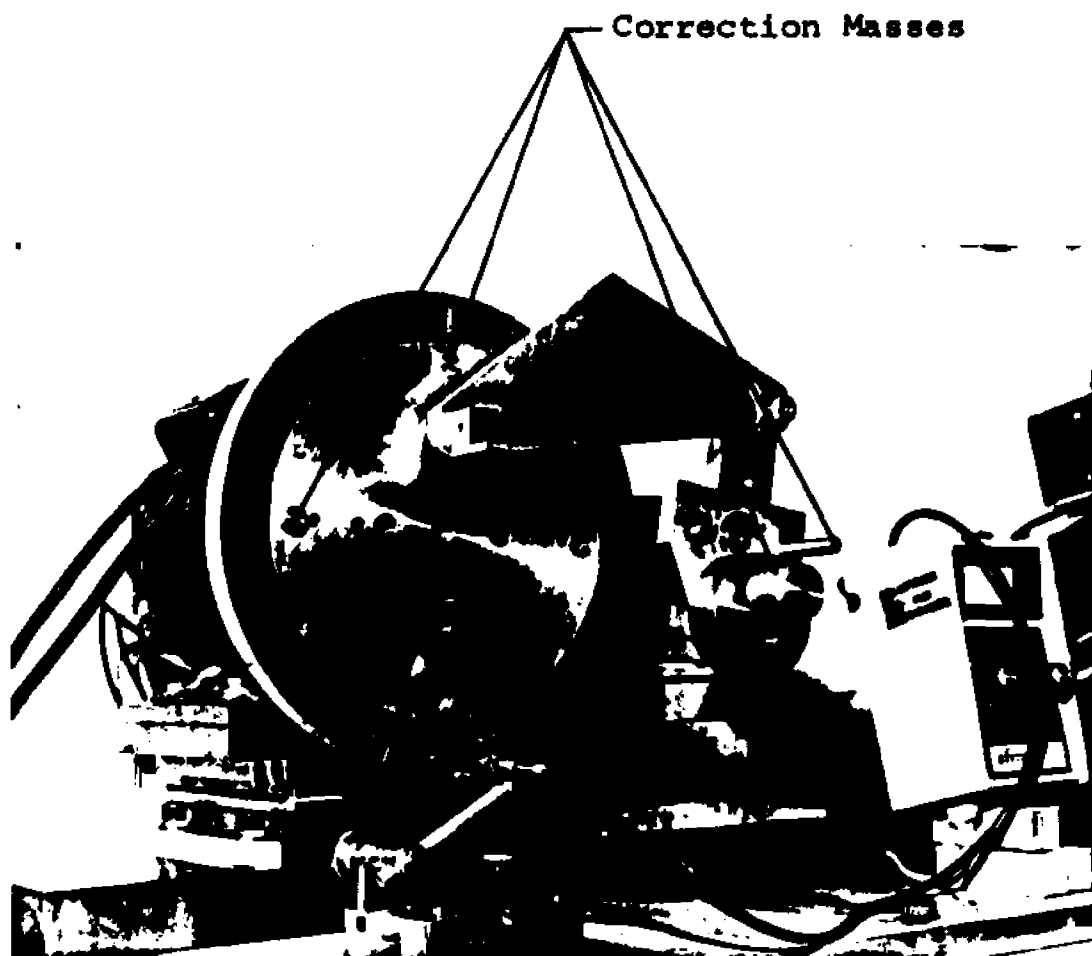
$$\begin{aligned}
 \Delta P_1 &= m_{1p}^c (p_1^c) = 50.85 \times 10^{-5} \quad \text{lb-sec}^2 \\
 \Delta Q_1 &= m_{1q}^c (q_1^c) = 57.56 \times 10^{-5} \quad \text{lb-sec}^2 \\
 \Delta P_3 &= m_{3p}^c (p_3^c) = -181.98 \times 10^{-5} \quad \text{lb-sec}^2 \\
 \Delta Q_3 &= m_{3q}^c (q_3^c) = -21.95 \times 10^{-5} \quad \text{lb-sec}^2
 \end{aligned}
 \tag{3.9}$$

With the values for  $p_i^c$  and  $q_i^c$  ( $i=1,3$ ) as given in Figure 3.4 the four correction masses are computed to be:

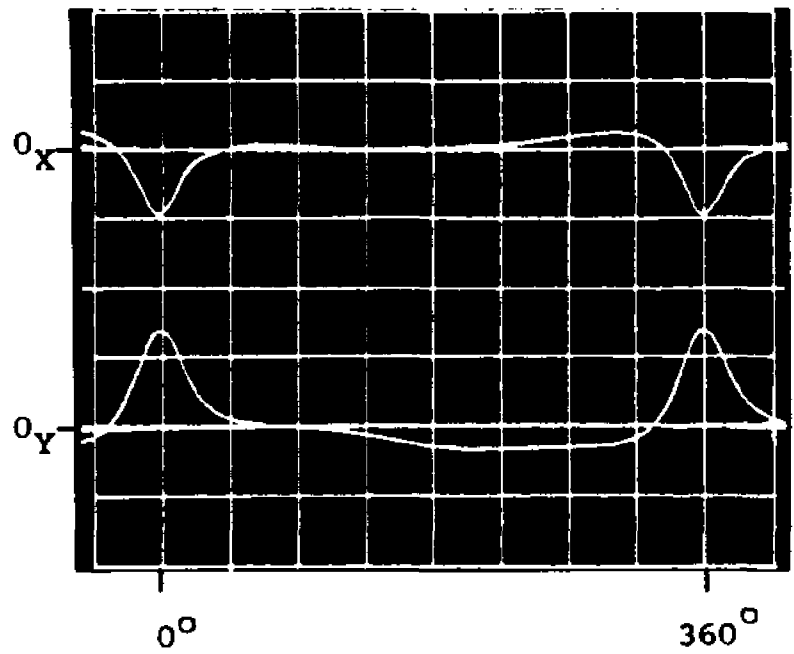
$$\begin{aligned}
 m_{1p}^c &= \frac{\Delta P_1}{p_1^c} = \frac{50.85 \times 10^{-5}}{3.500} = 14.53 \times 10^{-5} \left( \frac{\text{lb-sec}^2}{\text{in}} \right) \\
 &\text{at the positive } p_1^c \text{ location} \\
 m_{1q}^c &= \frac{\Delta Q_1}{q_1^c} = \frac{57.56 \times 10^{-5}}{3.500} = 16.45 \times 10^{-5} \left( \frac{\text{lb-sec}^2}{\text{in}} \right) \\
 &\text{at the positive } q_1^c \text{ location} \\
 m_{3p}^c &= \frac{\Delta P_3}{p_3^c} = \frac{-181.98 \times 10^{-5}}{1.375} = 132.35 \times 10^{-5} \left( \frac{\text{lb-sec}^2}{\text{in}} \right) \\
 &\text{at the negative } p_3^c \text{ location} \\
 m_{3q}^c &= \frac{\Delta Q_3}{q_3^c} = \frac{-21.95 \times 10^{-5}}{1.375} = 15.96 \times 10^{-5} \left( \frac{\text{lb-sec}^2}{\text{in}} \right) \\
 &\text{at the negative } q_3^c \text{ location}
 \end{aligned} \tag{3.10}$$

Figure 3.8 shows a photograph of the installed correction masses as they appear in both the input and output links. Figure 3.9 gives a comparison of the filtered shaking force components before and after minimax fine balancing at the same average input velocity of 120 RPM.

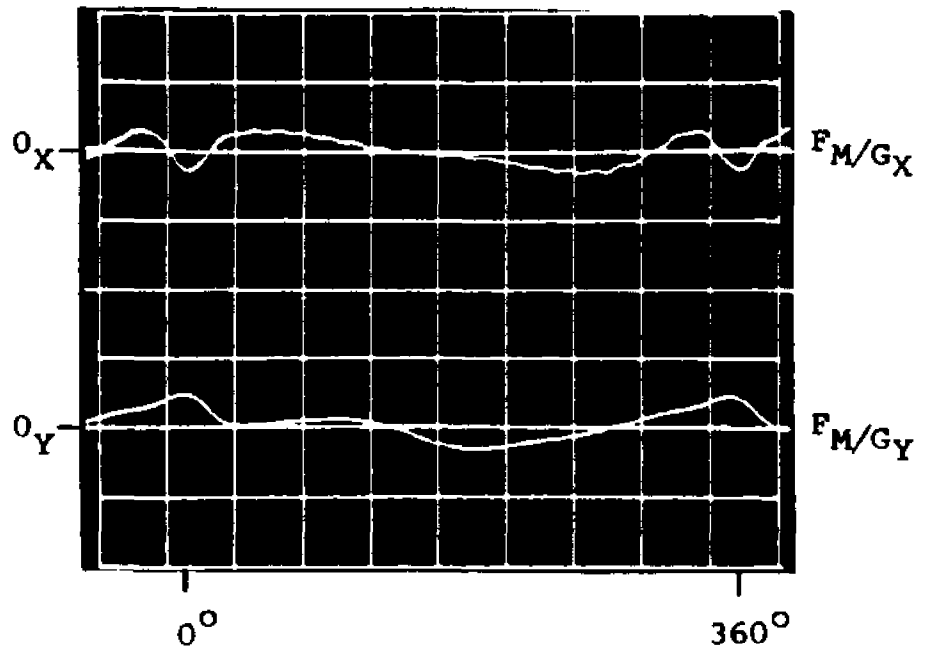
The maximum shaking force components are now  $F_{M/G_x} = .174$  lb and  $F_{M/G_y} = -.215$  lb. This represents a reduction of approximately 65 percent for each of the components when compared to the theoretically force balanced case. (See Section 2 above.)



**Figure 3.8: Photograph of Minimax Fine-Balanced  
Experimental Mechanism Showing Correction  
Masses Installed**



a. Theoretically Balanced Mechanism



b. Minimax Fine-Balanced Mechanism

(All Force Scales: 0.5 lb/div)

Figure 3.9: Comparison of Filtered Shaking Force Components Before and After Fine Balancing By Minimax Optimization Method (Average Input Speed: 120 RPM)

#### 4. Results Of Least Squares Balancing Optimization

This section reports on the results of the least squares balancing optimization. Equations (D.6) in Section 3 of Appendix D give the following values for the "least squares" mass-distance products  $P_j$  and  $Q_j$  ( $j=1,3$ ):

$$\begin{aligned}
 P_1 &= -56.25 \times 10^{-5} && \text{lb-sec}^2 \\
 Q_1 &= -51.81 \times 10^{-5} && \text{lb-sec}^2 \\
 P_3 &= 158.42 \times 10^{-5} && \text{lb-sec}^2 \\
 Q_3 &= 0.36 \times 10^{-5} && \text{lb-sec}^2
 \end{aligned}
 \tag{3.11}$$

According to equations (2.2)-(2.5), the mass-distance products of the correction masses then become:

$$\begin{aligned}
 \Delta P_1 &= m_{1p}^c (p_1^c) = 56.25 \times 10^{-5} && \text{lb-sec}^2 \\
 \Delta Q_1 &= m_{1q}^c (q_1^c) = 51.81 \times 10^{-5} && \text{lb-sec}^2 \\
 \Delta P_3 &= m_{3p}^c (p_3^c) = -158.42 \times 10^{-5} && \text{lb-sec}^2 \\
 \Delta Q_3 &= m_{3q}^c (q_3^c) = -0.36 \times 10^{-5} && \text{lb-sec}^2
 \end{aligned}
 \tag{3.12}$$

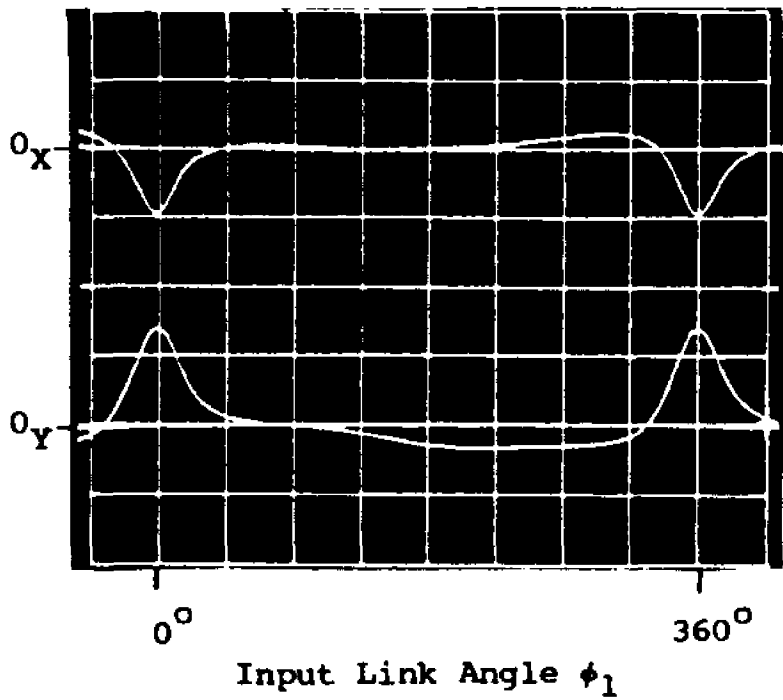
With the values for  $p_i^c$  and  $q_i^c$  ( $i=1,3$ ) as given in Figure 3.4, the four correction masses are computed to be:

$$\begin{aligned}
 m_{1p}^c &= \frac{\Delta P_1}{P_1^c} = \frac{56.25 \times 10^{-5}}{3.500} = 16.07 \times 10^{-5} \left( \frac{\text{lb-sec}^2}{\text{in}} \right) \\
 &\quad \text{at the positive } p_1^c \text{ location} \\
 m_{1q}^c &= \frac{\Delta Q_1}{q_1^c} = \frac{51.81 \times 10^{-5}}{3.500} = 14.80 \times 10^{-5} \left( \frac{\text{lb-sec}^2}{\text{in}} \right) \\
 &\quad \text{at the positive } q_1^c \text{ location} \\
 m_{3p}^c &= \frac{\Delta P_3}{P_3^c} = \frac{-158.42 \times 10^{-5}}{1.375} = 115.21 \times 10^{-5} \left( \frac{\text{lb-sec}^2}{\text{in}} \right) \\
 &\quad \text{at the negative } p_3^c \text{ location} \\
 m_{3q}^c &= \frac{\Delta Q_3}{q_3^c} = \frac{-0.36 \times 10^{-5}}{1.375} = 0.26 \times 10^{-5} \left( \frac{\text{lb-sec}^2}{\text{in}} \right) \\
 &\quad \text{at the negative } q_3^c \text{ location}
 \end{aligned} \tag{3.13}$$

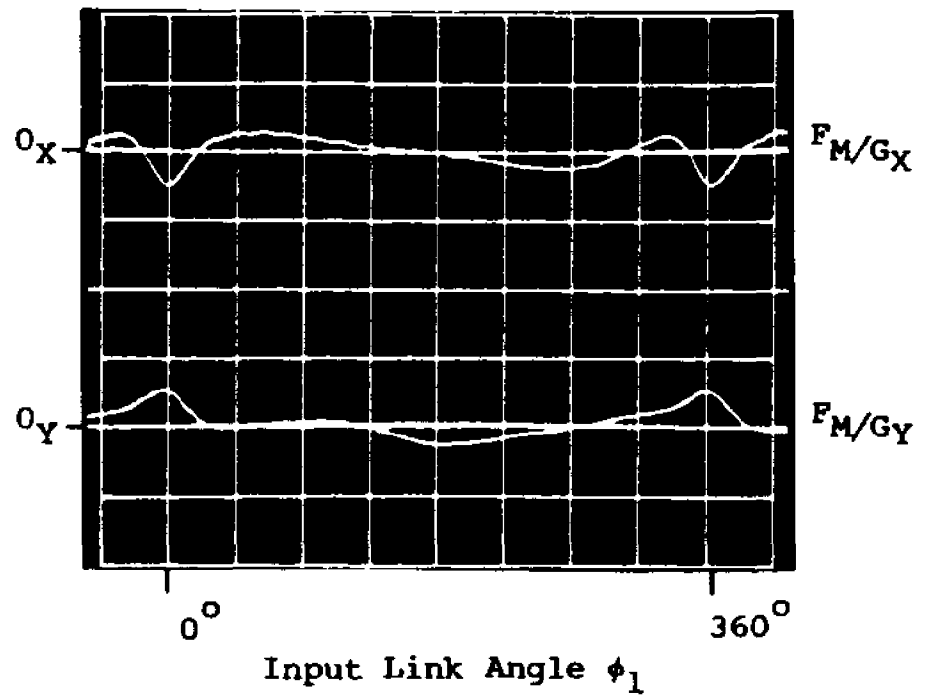
Figure 3.10 gives a comparison of the filtered shaking force components before and after least squares fine balancing at the same average input velocity of 120 RPM.

The maximum shaking force components are now

$F_{M/G_x} = .241 \text{ lb}$  and  $F_{M/G_y} = -.243 \text{ lb}$ . This represents a reduction of approximately 50 and 60 percent, respectively, for each of the components when compared to the theoretically force balanced case.



a. Theoretically Balanced Mechanism



b. Least Squares Fine-Balanced Mechanism

(All Force Scales: 0.5 lb/div)

Figure 3.10: Comparison of Filtered Shaking Force Components Before and After Fine Balancing By Least Squares Optimization Method (Average Input Speed: 120 RPM)

## E. Discussion Of Results

The following sections first discuss the sources of a number of experimental inaccuracies as well as their influence on the magnitudes of the shaking force readouts. Subsequently, the two optimization approaches are compared in the light of these experimental inaccuracies and it is concluded that the minimax method is to be preferred since it furnishes the lowest residual shaking forces after fine balancing.

### 1. Sources Of Experimental Inaccuracies

#### a. Motor Vibration

As discussed in Section D-1, a 120 cps vibration of the motor was responsible for the superposed wave of approximately 0.1 lb. in amplitude in the shaking force readouts<sup>1</sup>. The necessary use of faired shaking force component curves clearly represents a source of inaccuracy.

The direct mounting of the motor on one of the force platforms is the result of a design compromise. In an earlier version of the setup, the motor was mounted separately and its moment was transmitted to the input shaft of the

---

<sup>1</sup>This motor vibration due to the rectified AC current was also found in another motor of higher horsepower.

mechanism by way of two universal joints. The input shaft bearing assembly was mounted on the force platform in the manner of the present output shaft bearing assembly (see Figure 3.2). Because of the inaccuracies of the universal joints, certain forces, in addition to the moment, were transmitted. These forces, which were then picked up by force platform, were sufficiently large to obliterate the shaking force component readings.

An improved signal-to-noise ratio might have been obtained if one could have run the mechanism at higher speeds. The clearance in the motor bearings made speeds much above 120 RPM impossible since the resulting impacts at the crank reversal points distorted the force traces even more than the motor vibrations.

In order to exclude the motor vibration as well as the unwanted force transmission from the motor, it would be best to redesign the setup such that the motor is mounted off the force platform and that it is uncoupled from the mechanism while the force readings are taken.

#### b. Cross Talk In Force Platforms

According to the manufacturer, the component charge outputs of the individual force platforms are subject to

cross talk, i.e. the output due to the force in one direction is influenced by that in the other. The specification sheet shows the following relationships:

$$F_{LX} = F_{14X} - .003F_{14Y} \quad (3.14)$$

$$F_{LY} = F_{14Y} - .002F_{14X} \quad (3.15)$$

$$F_{RX} = F_{34X} + .002F_{34Y} \quad (3.16)$$

$$F_{RY} = F_{34Y} + .009F_{34X} \quad (3.17)$$

where

$F_{LX}$  = X component output of left force platform

$F_{LY}$  = Y component output of left force platform

$F_{RX}$  = X component output of right force platform

$F_{RY}$  = Y component output of right force platform

This type of error may become significant with the present two-platform design since, at certain points in the cycle, the bearing force components become quite large. It might be reduced by mounting the entire mechanism on a single force platform. In such an arrangement, the sums of the bearing force components would be measured directly.

Since these sums are much smaller than the individual components, the effect of the cross talk will also be considerably reduced.

c. Ground Bearing Force Addition

The shaking force components were obtained by the addition of the appropriate individual force platform charge outputs. Because only two charge amplifiers were available, it was necessary to add the respective component signals before they entered these amplifiers. Since each component force pickup of a given platform requires a unique predetermined charge amplifier setting, the addition of the signals makes it impossible to obtain the correct setting for both force gauges simultaneously. On the suggestion of the manufacturer, an average setting was chosen, even though this causes the component outputs of the left (input link) platform to read somewhat higher than the actual value. The opposite effect occurs for the output of the right (output link) platform.

It will now be shown that this condition leads to an error which is proportional to the sum of the absolute values of the individual ground bearing force components.

For this purpose, let

$F_L$  = output of left force platform (X or Y  
component force)

$F_R$  = output of right force platform (X or Y  
component force)

and  $K$  = percentage error of individual bearing force  
component readings, assumed to be common to  
both platforms.

The resulting reading,  $F_{TOT}$ , of the sum of the bearing  
force components in a given direction is then given by:

$$F_{TOT} = (1 + K)F_L + (1 - K)F_R \quad (3.18)$$

If the actual shaking force component is  
represented by

$$R = F_L + F_R \quad (3.19)$$

equation (3.18) becomes:

$$F_{TOT} = R + K(F_L - F_R) \quad (3.20)$$

Since, near or at full force balance,  $F_L$  will always  
have a sign opposite to that of  $F_R$ , the above clearly shows

that the absolute magnitude of the error term  $K(F_L - F_R)$  becomes largest when the magnitudes of the bearing force components are at their maxima. Thus, the reading at  $\phi_1 = 0$  degrees becomes more distorted than at all other positions.

To avoid this distortion, it would again be best to use only a single force platform.

## 2. Influence Of Cross Talk And Addition Errors On Magnitudes Of Experimental Shaking Force Readouts

Evidence (not shown here) from certain computer runs, in which the judicious variations of mass-distance products were made, indicates that the experimental results near  $\phi_1 = 0$  degrees are more exaggerated than at all other positions. (See Figure 3.6 for unbalanced mechanism and Figure 3.11, which is used in conjunction with the fine balancing optimizations.) It will now be shown how a combination of cross talk and addition errors contributes to this exaggeration.

The approximate magnitudes of the ground bearing force components of the theoretically balanced mechanism, at  $\phi_1 = 0$  degrees, are:

$$F_{14X} \approx 10.2 \text{ lb} \quad F_{34X} \approx -9.8 \text{ lb} \quad \text{so that} \quad F_{M/G_X} \approx 0.4 \text{ lb}$$

$$F_{14Y} \approx 2.0 \text{ lb} \quad F_{34Y} \approx -2.5 \text{ lb} \quad \text{and} \quad F_{M/G_Y} \approx -0.5 \text{ lb}$$

The absolute values of the above components represent maxima for the cycle.

Due to cross talk alone one obtains, according to equations (3.14)-(3.17):

$$F_{LX} = 10.2 - .003(2.0) = 10.194 \text{ lb} \quad (3.21)$$

$$F_{LY} = 2.0 - .002(10.2) = 1.980 \text{ lb} \quad (3.22)$$

$$F_{RX} = -9.8 + .002(-2.5) = -9.805 \text{ lb} \quad (3.23)$$

$$F_{RY} = -2.5 + .009(-9.8) = -2.588 \text{ lb} \quad (3.24)$$

With these values, the cross error components,  $C_X$  and  $C_Y$ , become:

$$\begin{aligned} C_X &= (F_{LX} + F_{RX}) - F_{M/G_X} \\ &= (10.194 - 9.805) - .400 = -.011 \text{ lb} \end{aligned} \quad (3.25)$$

$$\begin{aligned} \text{and } C_Y &= (F_{LY} + F_{RY}) - F_{M/G_Y} \\ &= (1.980 - 2.588) + .500 = -.108 \text{ lb} \end{aligned} \quad (3.26)$$

Thus, the cross talk error is larger for the Y component of the shaking force than for the X component.

Now consider how the addition error further influences the magnitudes of the final shaking force components. With the assumption that the percentage error of the individual bearing force component readings is represented by  $K=.005$ , substitution of the results shown in equations (3.21)-(3.24) into equation (3.18) yields the following values for the shaking force component readings:

$$F_{TOTX} = 1.005(10.194) + .995(-9.805) = .489 \text{ lb}$$

$$F_{TOTY} = 1.005(1.980) + .995(-2.588) = -.585 \text{ lb}$$

Thus, the X component reads too high by .089 lb (.489 lb vs. .400 lb) while the Y component is too negative by .085 lb (-.585 lb vs. -.500 lb)<sup>1</sup>.

Investigation, using equation (3.20), showed that after the addition of correction masses, i.e. at or very near to full force balance, there will be a reading error of essentially the same magnitude as long as the same instrumentation is used (i.e.  $K$  remains unchanged).

---

<sup>1</sup> For comparison with the oscillograms, recall that the direction of the positive axes is downward.

### 3. Comparison Of Optimization Methods

In order to compare the relative advantages of the minimax and least squares methods, it is necessary to consider how well the curves associated with each of these methods, and which are used to determine the correction masses, approximate those obtained from experimentation. Further, it must be kept in mind that the experimental values are most exaggerated at  $\phi_1 = 0$  degrees, as has been discussed in the previous section. Figure 3.11 shows such comparisons for both methods.

The minimax method, as might be expected, makes the differences between the experimental and optimized curves essentially equal. For the least squares approach, these differences in each of the shaking force components are largest near  $\phi_1 = 0$  degrees. In addition, when compared to the minimax case, the absolute magnitudes of these differences are greater near  $\phi_1 = 0$  degrees and somewhat smaller near  $\phi_1 = 90$  and  $180$  degrees.

These results are consistent with the fact that the exaggeration of the experimental readings are most pronounced near  $\phi_1 = 0$  degrees. The minimax approach would give equal weight to all the data and attempt to equalize the differences

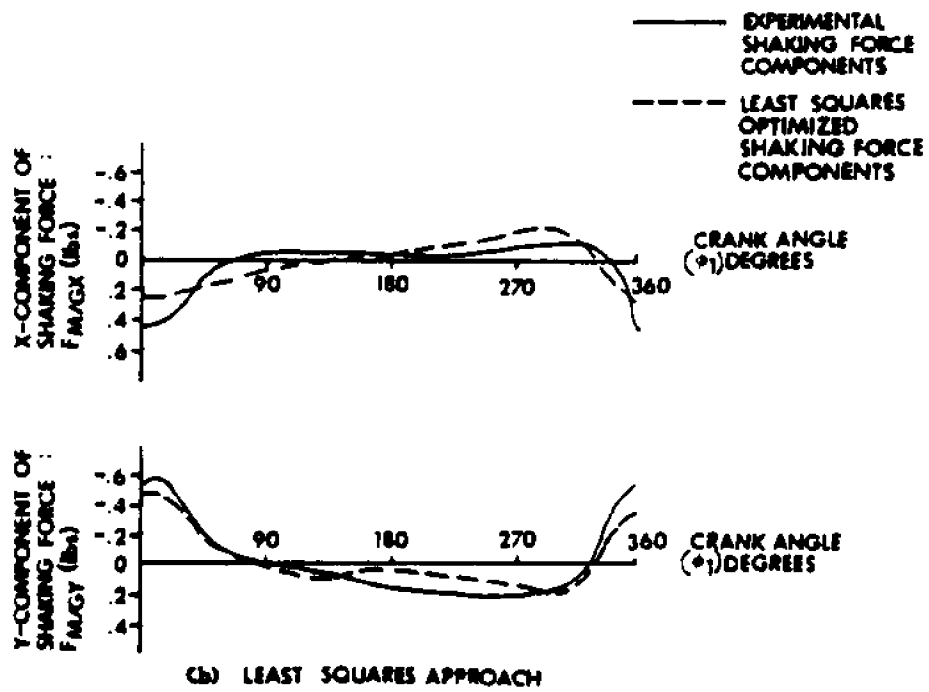
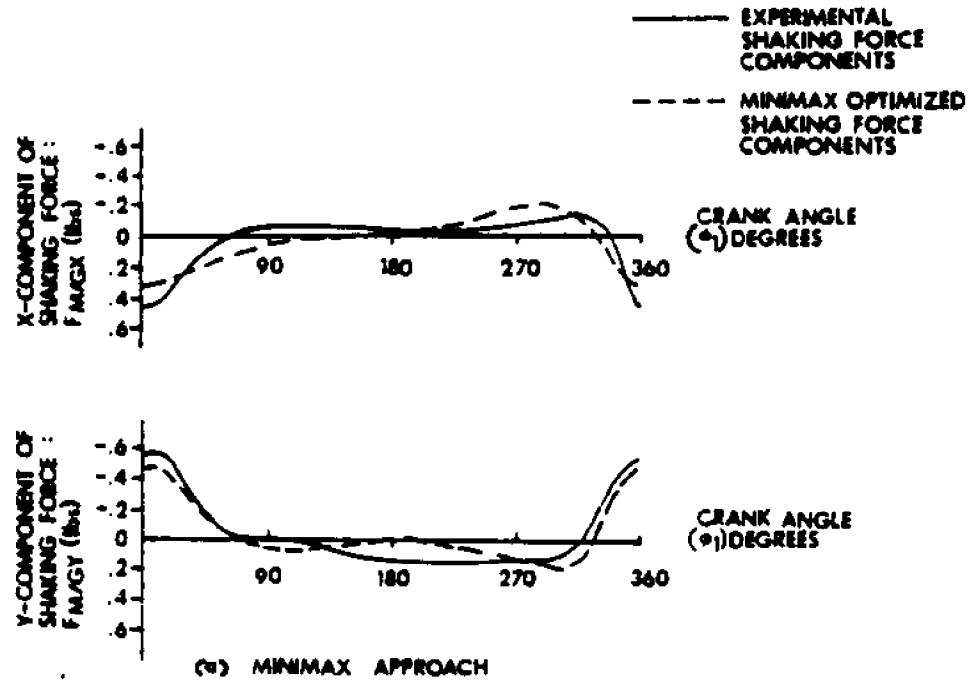


FIGURE 2.11: COMPARISON OF MINIMAX AND LEAST SQUARES OPTIMIZED SHAKING FORCE COMPONENTS WITH CORRESPONDING EXPERIMENTAL CURVES

between the curves. The least squares approach puts less weight on a single area of exaggerated readings and thus furnishes a somewhat better match at the remaining portions of the curves<sup>1</sup>.

Even though the minimax method may somewhat overcompensate at  $\phi_1 = 0$  degrees due to the greater exaggeration of the experimental values associated with this position of maximum shaking force components, it nevertheless reduces the magnitude of the shaking force components more than the least squares method. In view of the fact that these desirable decreases in the maximum values are not accompanied by substantial increases in the shaking force components at other locations during the cycle, one may conclude that the minimax method is to be preferred. This latter point especially holds in comparison with the mid-cycle results of the least squares method. (The above may best be seen by comparing the oscillograms of Figures 3.9 and 3.10.)

Finally, it should be noted that, because of the various experimental errors, no improvement could be obtained by a second fine balancing run.

Notwithstanding all of the above limitations, the

---

<sup>1</sup> Computations which attempted to compensate for the errors at  $\phi_1 = 0$  degrees alone resulted in a small improvement in the matching of these curves.

reductions in the maximum shaking force as obtained by both methods are most gratifying.

#### IV. A NEW METHOD FOR PRESCRIBING THE MAXIMUM SHAKING FORCE OF A FOUR-BAR LINKAGE WITH FLEXIBILITY IN COUNTERWEIGHT DESIGN

##### A. Introduction

This section presents a new two-counterweight method of partial force balancing of a four-bar linkage which allows the designer to realize a prescribed value for the maximum shaking force anywhere between zero and an inherent upper limit. By taking advantage of a certain mathematical property, which has been called the equipollent circle constraint equation, it is possible to attain the identical prescribed maximum shaking force for a wide range of output and associated input link counterweight configurations.

This technique, which is generally only applicable to constant speed mechanisms, builds upon a Chebyshev-type partial balancing method, first given by Ya. L. Gheronimus [25], which only uses an input link counterweight. (For a brief review of this work of Gheronimus, see Appendix E.) The equipollent circle constraint equation, which allows flexibility in counterweight design for a prescribed maximum shaking force, represents an adaptation of a parallel concept, used by G. G. Lowen and F. R. Tepper [52]

to prescribe the RMS shaking force.

In the method of Gheronimus, the shaking force expression is divided by the instantaneous input angle, which has the effect of projecting the shaking force hodograph onto the input link. The resulting hodograph now consists of a constant vector which represents the shaking force contributions proportional to the square of the input link speed, while the contributions of the coupler and output links are represented by a rotating vector of variable length. In order to reduce the maximum shaking force, a counterweight is added to the input link which is proportional to the distance from the origin to the "center" of the hodograph. To this end, the smallest circumscribing circle to the hodograph is determined. Its center represents the Chebyshev, or best uniform, approximation to the given hodograph by a polynomial of degree zero, i.e. a constant. The resulting maximum shaking force is proportional to the radius of the smallest circumscribing circle.

The present extension of this method addresses itself to that portion of the original hodograph which is due to the contributions of the coupler and the output links. It is reasoned that if the inclusion of an output link counterweight can reduce the size of the smallest circumscribing

circle, the resulting shaking force can also be decreased and, with that, limited in magnitude to a prescribed value.

Such a limiting procedure, which gives unique input and output link counterweights by the direct reduction of the circumscribing circle, is first shown.

Subsequently, the equipollent circle constraint equation is introduced. By offering an invariant relationship between the parameters of the output link counterweight, it presents the possibility of accomplishing the identical reduction in the maximum shaking force by a whole range of counterweight designs.

The determination of the smallest circumscribing circle as well as the coordinates of its center have been mechanized with the help of the Harwell Augmented Lagrangian optimization routine. Other computer programs which are based on the appropriate design equations furnish the counterweight dimensions for both of the aforementioned methods.

Examples involving both a 50 and a 75 percent reduction in the maximum shaking force are given and the associated ranges of possible counterweight designs are determined. The magnitudes of such maximum dynamic reactions as bearing forces, input moment and shaking moment have been computed for each of the above reductions in maximum shaking force for a

full range of counterweight designs. While it is clear that for some of the counterweight designs there are unreasonable increases in these dynamic reactions, there is a substantial range of counterweight configurations for which the variation in these reactions is not very large. In light of the above, this flexibility in counterweight configuration offers advantages when certain space limitations have to be observed.

The present work furnishes the basis for the effort in the next section where, in addition to prescribing the maximum shaking force, a simultaneous optimization of the maximum dynamic reactions is accomplished.

## B. Hodograph And Statement Of Problem

Equation (A.26) in Appendix A, when modified for a constant input speed, gives the following expression for the shaking force of an unbalanced four-bar linkage (see Figure 2.1)<sup>1</sup>:

$$\bar{F}_{M/G} = A^{\circ} K_1 e^{i(\phi_1 + \alpha^{\circ})} + B^{\circ} K_3 e^{i(\gamma_3 + \beta^{\circ})} \quad (4.1)$$

where

$$A^{\circ} = \sqrt{(P_1^{\circ})^2 + (Q_1^{\circ})^2} \quad (\text{See equation (A.27).})$$

$$B^{\circ} = \sqrt{(P_3^{\circ})^2 + (Q_3^{\circ})^2} \quad (\text{See equation (A.29).})$$

where the mass-distance products  $P_j^{\circ}$  and  $Q_j^{\circ}$  ( $j=1,3$ ) are given by equations (A.31)-(A.34) and

$$K_1 = \dot{\phi}_1^2 \quad (\text{See equation (A.3).}) \quad (4.2)$$

$$K_3 = \sqrt{\dot{\phi}_3^4 + \ddot{\phi}_3^2} \quad (\text{See equation (A.3).})$$

$$\gamma_3 = \phi_3 - \tan^{-1} \frac{\ddot{\phi}_3}{\dot{\phi}_3^2} \quad (\text{See equation (A.3).})$$

$$\alpha^{\circ} = \tan^{-1} \frac{Q_1^{\circ}}{P_1^{\circ}} \quad (\text{See equation (A.28).})$$

$$\beta^{\circ} = \tan^{-1} \frac{Q_3^{\circ}}{P_3^{\circ}} \quad (\text{See equation (A.30).})$$

---

<sup>1</sup>The notation for parameters of balanced and unbalanced linkages, as given in Appendix A-3, is used.

The vector associated with the first term of the above expression is of constant magnitude and rotates with the constant angular velocity  $\dot{\phi}_1$ . The vector corresponding to the second term has a time-dependent magnitude and rotates with a time-dependent angular velocity.

If one now divides both terms of equation (4.1) by the unit vector  $e^{i\phi_1}$  associated with the input link, one obtains:

$$\bar{F}_{M/G} e^{-i\phi_1} = A^O K_1 e^{i\alpha^O} + B^O K_3 e^{i(\gamma_3 + \beta^O - \phi_1)} \quad (4.3)$$

This operation leaves the magnitude of the shaking force vector corresponding to any mechanism position intact, while its instantaneous direction is rotated through the angle  $-\phi_1$ . (See also Appendix E.)

Figure 4.1 shows a hodograph corresponding to equation (4.3). The constant vector  $\overline{OD}^O$  represents the first term on the right hand side of equation (4.3), while vector  $\overline{D^O E^O}$  stands for the second term. The magnitude of the maximum shaking force of the unbalanced mechanism is given by  $R^O_{MAX}$ .  $R_S$  is the radius of the smallest circumscribing circle to the hodograph. Its center is located by the vector  $\overline{OC}_S$  at angle  $\delta_S$  with respect to the X-axis. As shown in Appendix E, the radius  $R_S$  represents the maximum shaking force which

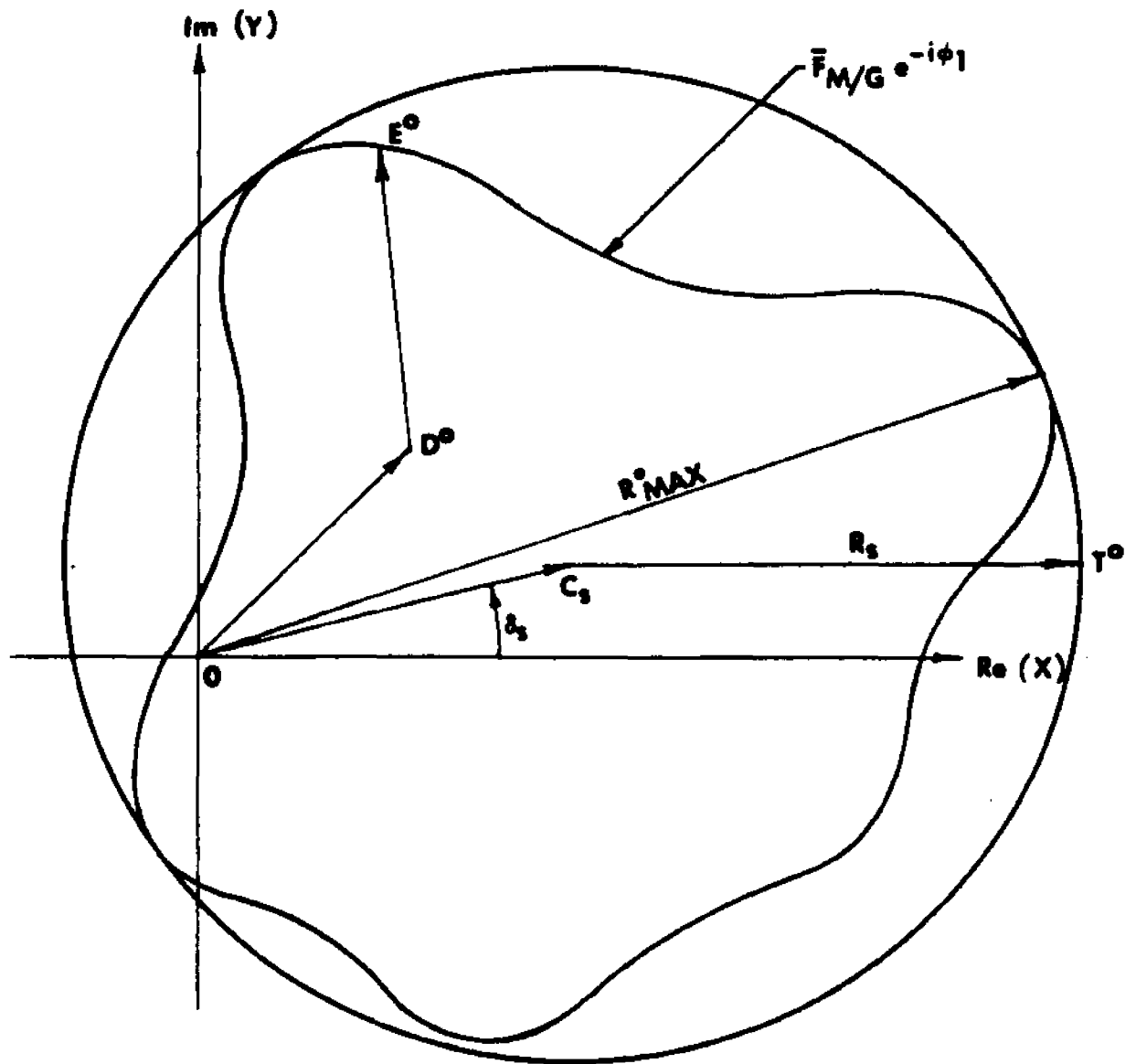


FIG. 4.1 SHAKING FORCE HODOGRAPH OF CONSTANT INPUT SPEED FOUR-BAR LINKAGE WITH ALL VECTORS ROTATED BY NEGATIVE OF INPUT ANGLE

results from a Chebyshev-type optimization involving a single counterweight attached to the input link<sup>1</sup>.

If one now introduces an additional output link counterweight, one may reduce the maximum resulting shaking force further to a value corresponding to a radius  $R$ , which is smaller than  $R_S$ . Such a reduction may be related to the maximum unbalanced shaking force by way of reduction factor  $\eta$ , i.e.

$$\eta = \frac{R}{R^{\circ}_{MAX}} \quad (4.4)$$

The following sections show the realization of this goal. For the sake of clarity, a special case of the more general approach will be discussed first. It involves a proportional reduction of the hodograph which leads to unique counterweight parameters.

The more general approach shows that a whole range of counterweight parameters will satisfy the identical prescribed maximum shaking force. This method involves a rotation of the hodograph, in addition to its proportional reduction.

In either case, the radius  $R_S$  of the smallest circumscribing circle to the hodograph of the unbalanced

---

<sup>1</sup> This single counterweight method alone causes an approximate 35 percent reduction in maximum shaking force when applied to a four-bar linkage.

mechanism, according to equation (4.3), together with the location of the center  $C_S$  of this circle must first be found.

The required Chebyshev criterion is satisfied by the solution of the following minimization problem with inequality constraints:

$$\text{minimize } R_S' \quad (4.5)$$

subject to the inequality constraints

$$(F_{X_i} - C'_S S_x)^2 + (F_{Y_i} - C'_S S_y)^2 \leq (R_S')^2 \quad (4.6)$$

where  $R_S'$  = the "trial radius" during the optimization  
(with units of force)

$F_{X_i}$  = X coordinate of equation (4.3)

$F_{Y_i}$  = Y coordinate of equation (4.3)

$C'_S S_x, C'_S S_y$  = coordinates of point  $C_S'$ , i.e. center of  
circumscribing circle of radius  $R_S'$ .

$i = 1, 2, \dots, 360$ , which corresponds to the  
angles  $\phi_1 = 0, 1, \dots, 359$  degrees.

Appendix F shows how this optimization, which uses the parameters  $R_S'$ ,  $C'_S S_x$  and  $C'_S S_y$  as variables, may be

accomplished for an example linkage with the help of the Harwell Augmented Lagrangian optimization program. (For program details, refer to Appendix C.)

When this optimization is completed, the objective function  $R_S'$  equals the desired radius  $R_S$  and the associated point  $C_S'$  becomes the final center  $C_S$ . The angle  $\delta_S$  may be obtained from

$$\delta_S = \tan^{-1} \frac{C_{Sy}}{C_{Sx}} \quad (4.7)$$

C. Special Case Of General Solution: Simple Reduction  
Of Hodograph

The prescribed maximum shaking force corresponding to radius  $R$  is obtained by proportionally reducing the hodograph in such a way that  $R$  becomes the radius of the resulting circumscribing circle. Figure 4.2 shows the reduced hodograph which is traced out by vector

$$\overline{D^{\circ}E} = \mu \overline{D^{\circ}E^{\circ}} . \quad (4.8)$$

The proportionality factor  $\mu$  relates the radius  $R$  of the reduced circumscribing circle to the radius  $R_S$  of the original smallest circumscribing circle, i.e.

$$\mu = \frac{R}{R_S} , \quad (\mu < 1) \quad (4.9)$$

where  $\mu$  may be obtained with the help of equation (4.4):

$$\mu = \eta \frac{R^{\circ}_{MAX}}{R_S} \quad (4.10)$$

After the reduction, the sides of the quadrilateral  $D^{\circ}ETC$  of the smaller hodograph have the proportionality  $\mu$  with respect to the sides of the quadrilateral  $D^{\circ}E^{\circ}T^{\circ}C_S$  of

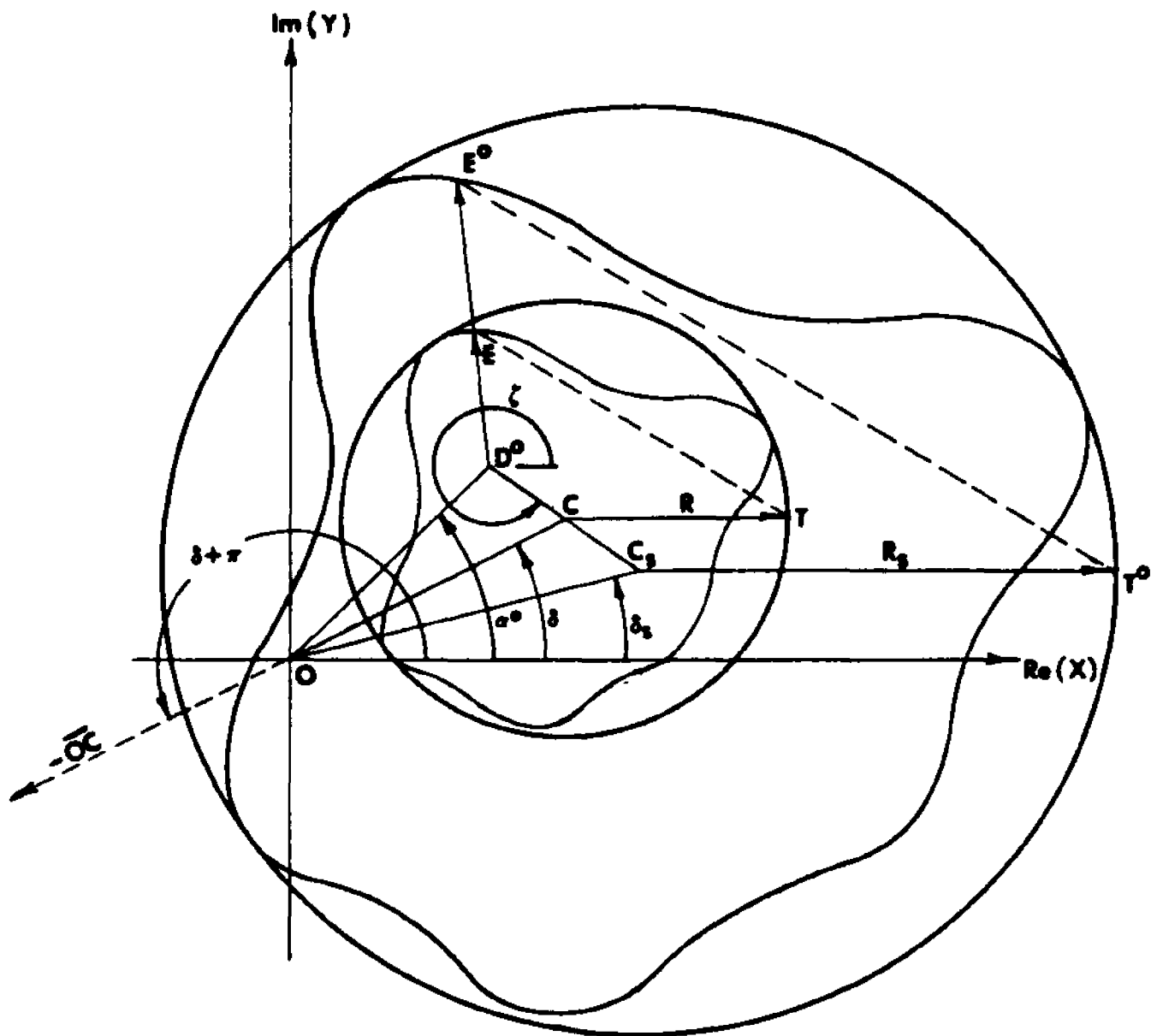


FIG. 4.2 ORIGINAL AND SIMPLY REDUCED SHAKING FORCE HODOGRAPH

the original hodograph. Therefore, the center of the reduced circumscribing circle of radius  $R$  is moved along line  $D^{\circ}C_S$  and may be found by:

$$\overline{D^{\circ}C} = \mu \overline{D^{\circ}C_S} \quad (4.11)$$

In order to realize the prescribed maximum shaking force, both output as well as input link counterweights must be designed. The output link counterweight must be such that the force corresponding to vector  $\overline{D^{\circ}E^{\circ}}$  is reduced to one corresponding to vector  $\overline{D^{\circ}E}$ . The input link counterweight must be proportional to the vector  $-\overline{OC}$ .

#### 1. Design Of Output Link Counterweight

The proportional reduction of the magnitude of the vector  $\overline{D^{\circ}E^{\circ}}$  to  $\overline{D^{\circ}E}$  is accomplished with the help of an output link counterweight. Accordingly, the second term in equation (4.3) becomes:

$$\overline{D^{\circ}E} = BK_3 e^{i(\gamma_3 + \beta - \phi_1)} \quad (4.12)$$

where

$$B = \mu B^{\circ} = \sqrt{(P_3)^2 + (Q_3)^2} \quad (4.13)$$

(See equation (A.15).)

When the counterweight parameters  $m_3^* p_3^*$  and  $m_3^* q_3^*$  are included, as shown in equations (A.37) and (A.38), one obtains:

$$P_3 = m_3^* p_3^* + P_3^0 \quad (4.14)$$

and 
$$Q_3 = m_3^* q_3^* + Q_3^0 \quad (4.15)$$

Further, angle  $\beta$  becomes, according to equation (A.16),

$$\beta = \tan^{-1} \frac{Q_3}{P_3} \quad (4.16)$$

The simple reduction method satisfies the requirement of equation (4.13) by letting

$$P_3 = \mu P_3^0 \quad (4.17)$$

and 
$$Q_3 = \mu Q_3^0 \quad (4.18)$$

The output link counterweight parameters can now be obtained by substituting equations (4.17) and (4.18) into equations (4.14) and (4.15). This results in:

$$m_3^* p_3^* = -(1 - \mu) P_3^0 \quad (4.19)$$

and 
$$m_3^* q_3^* = -(1 - \mu) Q_3^0 \quad (4.20)$$

The above may be reduced, with the help of equations (A.21) and (A.29), to give

$$m_3^* r_3^* = (1 - \mu) B^0 \quad (4.21)$$

Use of equations (A.22) and (A.30) leads to the counterweight angle

$$\theta_3^* = \tan^{-1} \frac{q_3^*}{p_3^*} = \beta^0 + \pi \quad (4.22)$$

(See Figure A.2)

The fact that the reduced hodograph has the same relative position as the original one also reflects itself in the angle  $\beta$ . When equation (4.16) is applied to the present case, one obtains:

$$\beta = \tan^{-1} \frac{\mu Q_3^0}{\mu P_3^0} = \beta^0 \quad (4.23)$$

## 2. Design Of Input Link Counterweight

The force due to the required input link counterweight is represented by vector  $-\overline{OC}$  at angle  $\delta + \pi$ . The following, which shows how the vector  $\overline{OC} = OCe^{i\delta}$  is obtained, forms the basis for the design of the counterweight:

- a. The optimization routine supplies the force components  $C_{S_x}$  and  $C_{S_y}$ , associated with the center point  $C_S$ . Thus, the vector  $\overline{OC_S}$  is given by:

$$\overline{OC_S} e^{i\delta_S} = \sqrt{(C_{S_x})^2 + (C_{S_y})^2} e^{i\delta_S} \quad (4.24)$$

where  $\delta_S = \tan^{-1} \frac{C_{S_y}}{C_{S_x}}$

- b. The vector  $\overline{OD^0}$  is known from equation (4.3), i.e.

$$\overline{OD^0} = A^0 K_1 e^{i\alpha^0} \quad (4.25)$$

- c. To obtain the vector  $\overline{OC_S} e^{i\delta}$  it is further necessary to define the vector  $\overline{D^0 C_S}$  by way of

$$\overline{D^0 C_S} = \overline{OC_S} - \overline{OD^0} \quad (4.26)$$

This becomes, with the help of equations (4.24) and (4.25):

$$\overline{D^0 C_S} e^{i\zeta} = \sqrt{(C_{S_x})^2 + (C_{S_y})^2} e^{i\delta_S} - A^0 K_1 e^{i\alpha^0} \quad (4.27)$$

where  $\zeta = \tan^{-1} \frac{D^0 C_{S_y}}{D^0 C_{S_x}}$

d. The vector  $\overline{OC}$  may now be found with the help of equation (4.11) in addition to equations (4.25) and (4.27). Thus,

$$\overline{OC} = OC e^{i\delta} = A^o K_1 e^{i\alpha^o} + \mu D^o C_s e^{i\zeta} \quad (4.28)$$

$$\text{where } \delta = \tan^{-1} \frac{OC_Y}{OC_X}$$

e. As stated earlier, the force supplied by the input link counterweight must equal

$$-OC e^{i\delta} = OC e^{i(\delta + \pi)} \quad (4.29)$$

This suggests the following design equations:

$$m_1^* r_1^* = \frac{|\overline{OC}|}{\phi_1^2} \quad (4.30)$$

$$\text{and } \theta_1^* = \delta + \pi \quad (4.31)$$

### 3. Relationship To Full Force Balancing

The full force balancing results associated with the Method of Linearly Independent Vectors [ 8 ] are obtained by first letting  $\mu = 0$ . Substitution of this value into equation (4.21) and use of equation (4.22) furnishes the

output link counterweight parameters. The radius of the reduced circumscribing circle is now zero and its center  $C$  is coincident with point  $D^0$  (see Figure 4.2 and equation (4.11)). Therefore, the input link counterweight parameters are found by substituting  $\overline{OC} = \overline{OD^0}$  and  $\delta = \alpha^0$  into equations (4.30) and (4.31), respectively.

D. General Solution: Equipollent Circle Constraint Equation And Flexibility In Counterweight Design

The following shows that the prescribed maximum shaking force which the mechanism exerts on the ground remains constant as long as the mass-distance products associated with the center of mass of the output link lie on certain circles. This invariance phenomenon gives the opportunity for flexibility in counterweight design since a whole range of counterweight radii and angles produce the identical maximum shaking force.

1. Equipollent Circle Constraint Equation And Resulting Hodograph

When equation (4.13) is rewritten with the help of equations (A.10) and (A.11), one obtains, after squaring both sides of the resulting expression:

$$\left(m_3 p_3 + \frac{a_3}{a_2} m_2 p_2\right)^2 + \left(m_3 q_3 + \frac{a_3}{a_2} m_2 q_2\right)^2 = (\mu B^O)^2 \quad (4.32)$$

This form implies that the magnitude of  $\mu B^O$ , as well as the absolute magnitude of a force vector analogous to vector  $\overline{D^O E} = \mu \overline{D^O E^O}$  in Figure 4.2, remains the same as

long as the mass-distance product terms  $m_3 p_3$  and  $m_3 q_3$ , associated with the center of mass of the balanced output link, lie on a circle of radius

$$R_E = \mu B^0 \quad . \quad (4.33)$$

Thus, a range of output link counterweight configurations will lead to the identical prescribed maximum shaking force. Because of this invariance, the circles represented by equation (4.32) have been termed equipollent circles while the expression itself is called the equipollent circle constraint equation. (This terminology was first used in [52].)

For the purpose of counterweight design, one must consider how the above influences the angular position of the reduced hodograph and, with that, the location of the center  $C_1$  of its smallest circumscribing circle.

Equations (4.14)-(4.16) show that a given choice of output link parameters  $m_3^* p_3^*$  and  $m_3^* q_3^*$  decides the magnitude of the general mass-distance terms  $P_3$  and  $Q_3$  and, with that, the angle  $\beta$ . Consequently, whenever the angle  $\beta$  is not equal to

$$\beta^0 = \tan^{-1} \frac{Q_3^0}{P_3^0} \quad ,$$

the reduced shaking force component

$$BK_3 e^{i(\gamma_3 + \beta - \phi_1)}$$

leads the original term

$$B^0 K_3 e^{i(\gamma_3 + \beta^0 - \phi_1)}$$

by the constant phase angle

$$\psi = \beta - \beta^0 . \quad (4.34)$$

Figure 4.3 represents this reduced force component by the vector  $\overline{D^0 E_1}$ . It is shown to lead the vector  $\overline{D^0 E^0}$  by the angle  $\psi$ . As a consequence, the center of the circumscribing circle is rotated into the new position  $C_1$  (with magnitude  $D^0 C_1 = D^0 C$ ) and is located by way of the angle  $\delta_1$  with respect to the X-axis. The input link counterweight must therefore provide a force proportional to vector  $-\overline{OC_1}$  at the angle  $\delta_1 + \pi$ .

## 2. Adaptation To Output Link Counterweight Design

### a. Determination Of Theoretical Design Range

In order to explore the range of counterweight designs which produce the identical prescribed maximum shaking force,

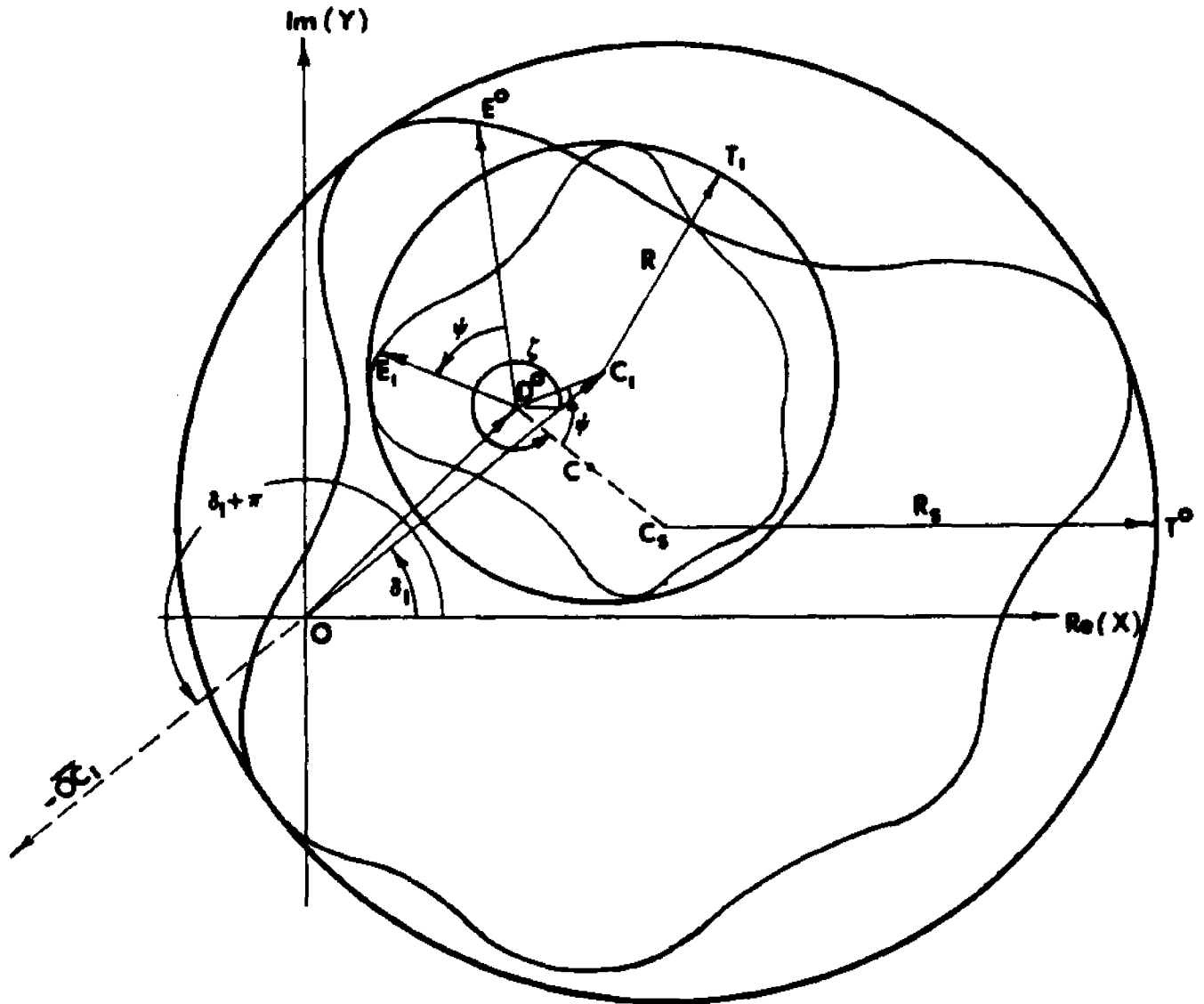


FIG. 4.3 ORIGINAL AND REDUCED SHAKING FORCE HODOGRAPH RESULTING FROM THE FLEXIBLE DESIGN METHOD

equation (4.32) is rewritten in terms of output link counterweight parameters (see equations (4.14), (4.15)):

$$(m_3^* p_3^* + P_3^0)^2 + (m_3^* q_3^* + Q_3^0)^2 = (\mu B^0)^2 \quad (4.35)$$

For convenience, the above is transformed to the following using equations (A.21), (A.22) and (A.29):

$$(m_3^* r_3^*)^2 + 2(P_3^0 \cos \theta_3^* + Q_3^0 \sin \theta_3^*) m_3^* r_3^* + (1 - \mu^2)(B^0)^2 = 0 \quad (4.36)$$

All combinations of  $m_3^* r_3^*$  and  $\theta_3^*$  which satisfy the above expression represent theoretically possible designs for a given maximum shaking force. To determine the limits of  $m_3^* r_3^* = m_3^* r_3^*(\theta_3^*)$  within which this flexibility exists, equation (4.36) is first implicitly differentiated with respect to  $\theta_3^*$  and then  $\frac{d(m_3^* r_3^*)}{d\theta_3^*}$  is set equal to zero. Thus,

$$\left[ 2m_3^* r_3^* + 2(P_3^0 \cos \theta_3^* + Q_3^0 \sin \theta_3^*) \right] \frac{d(m_3^* r_3^*)}{d\theta_3^*} = 2(P_3^0 \sin \theta_3^* - Q_3^0 \cos \theta_3^*) m_3^* r_3^* \quad (4.37)$$

For  $\frac{d(m_3^* r_3^*)}{d\theta_3^*} = 0$ , one obtains the two extremum conditions:

$$(\theta_3^*)_{EX_{1,2}} = \tan^{-1} \frac{Q_3^0}{P_3^0} \quad (4.38)$$

These two possible solutions for the extreme counterweight angles correspond to angles  $\beta^0$  and  $\beta^0 + \pi$  (see equation (A.30)).

Solution of equation (4.36) for the associated mass-distance products  $(m_3^* r_3^*)_{EX}$  shows that the necessary positive values of these parameters can only be obtained for

$$\theta_3^* = \beta^0 + \pi \quad (4.39)$$

This requires substitution of the following into equation (4.36):

$$\sin(\theta_3^*)_{EX} = \frac{-Q_3^0}{B^0} \quad (4.40)$$

and

$$\cos(\theta_3^*)_{EX} = \frac{-P_3^0}{B^0} \quad (4.41)$$

where

$$B^0 = \sqrt{(P_3^0)^2 + (Q_3^0)^2}$$

The resulting solution of the quadratic equation furnishes the minimum and maximum counterweight parameters

of the theoretical design range:

$$(m_3^* r_3^*)_{\text{MIN}} = (1 - \mu) B^{\circ} \quad (4.42)$$

and 
$$(m_3^* r_3^*)_{\text{MAX}} = (1 + \mu) B^{\circ} \quad (4.43)$$

Note that the minimum case is identical to that obtained by the simple reduction of the hodograph (see equations (4.21) and (4.22)).

b. Determination Of Output Link Counterweight Angles  $\theta_3^*$

To determine the values of the angles  $\theta_3^*$  corresponding to any mass-distance product  $m_3^* r_3^*$  within the theoretical design range, the desired  $m_3^* r_3^*$  is substituted into the following modification of equation (4.36):

$$K_4 + K_5 \cos \theta_3^* = -K_6 \sin \theta_3^* \quad (4.44)$$

where 
$$K_4 = (m_3^* r_3^*)^2 + (1 - \mu^2) (B^{\circ})^2$$

$$K_5 = 2P_3^{\circ} m_3^* r_3^*$$

$$K_6 = 2Q_3^{\circ} m_3^* r_3^*$$

Squaring, simplification and subsequent rearrangement leads to the following quadratic equation:

$$\left[ (K_5)^2 + (K_6)^2 \right] \cos^2 \theta_3^* + 2K_4 K_5 \cos \theta_3^* + (K_4)^2 - (K_6)^2 = 0 \quad (4.45)$$

Solving for  $\cos \theta_3^*$  yields:

$$\cos \theta_3^* = \frac{-K_4 K_5 \pm K_6 \sqrt{(K_5)^2 + (K_6)^2 - (K_4)^2}}{(K_5)^2 + (K_6)^2} \quad (4.45)$$

Because of the squaring of equation (4.44), there will be four possible solutions. The two valid ones must satisfy equation (4.44).

It is to be noted that for any given mass-distance product  $m_3^* r_3^*$  within the theoretical design range, there are two possible angular locations  $\theta_3^*$ .

### 3. Design Of Input Link Counterweight

Since there are two possible angles  $\theta_3^*$  for a given  $m_3^* r_3^*$  within the theoretical design range, there must also be two corresponding input link counterweight designs<sup>1</sup>.

For a given choice of angle  $\theta_3^*$ , there will be a vector

$$-\overline{OC}_1 = OC_1 e^{i(\delta_1 + \pi)}$$

---

<sup>1</sup> Recall that for each of the extrema, there is only one input link counterweight.

which forms the basis of the input link counterweight design (see Figure 4.3). This design is accomplished by the following steps:

- a. Angle  $\beta$  is found with the help of a modification of equation (4.16), i.e.

$$\beta = \tan^{-1} \frac{Q_3^O + m_3^* r_3^* \sin \theta_3^*}{P_3^O + m_3^* r_3^* \cos \theta_3^*} \quad (4.47)$$

- b. The angle of rotation  $\psi$  is then obtained by way of equation (4.34):

$$\psi = \beta - \beta^O \quad (4.48)$$

where  $\beta^O = \tan^{-1} \frac{Q_3^O}{P_3^O}$  (See equation (4.2).)

- c. The vector  $\overline{D^O C_1}$ , as shown in Figure 4.3, is found by the rotation of vector  $\overline{D^O C}$ . Thus, with the help of equation (4.27):

$$\overline{D^O C_1} = \mu \overline{D^O C} e^{i(\zeta + \psi)} \quad (4.49)$$

- d. With the above, the vector  $\overline{OC_1}$  may be determined

from:

$$OC_1 e^{i\delta_1} = OD^0 e^{i\alpha^0} + \mu D^0 C_S e^{i(\zeta + \psi)} \quad (4.50)$$

where 
$$\delta_1 = \tan^{-1} \frac{OC_{1Y}}{OC_{1X}}$$

e. Finally, the force of the counterweight must equal

$$-OC_1 e^{i\delta_1} = OC_1 e^{i(\delta_1 + \pi)} \quad (4.51)$$

This leads to the design equations

$$m_1^* r_1^* = \frac{|\overline{OC_1}|}{\phi_1^2} \quad (4.52)$$

and 
$$\theta_1^* = \delta_1 + \pi . \quad (4.53)$$

## E. Examples

The following sample calculations apply the previously developed techniques to the four-bar linkage shown in Figure 4.4, which is assumed to run at a constant speed of 500 rpm. While a 50 percent reduction in the maximum shaking force is shown in detail, only the results of a 75 percent reduction are given. The influence of the design flexibility on the dynamic reactions is considered for both cases.

The counterweights are assumed to be circular as well as tangent to the pivots  $A_0$  and  $A_3$ , respectively.

### 1. Parameters Of Unbalanced Mechanism

Table 4.1 lists the parameters of the unbalanced mechanism. All links and counterweights are made of steel (density =  $0.283 \text{ lb/in}^3$ ).

The general mass-distance terms of the unbalanced mechanism are, according to equations (A.31)-(A.34):

$$P_1^0 = 18.777 \times 10^{-4} \text{ lb-sec}^2 \quad (4.54)$$

$$Q_1^0 = -1.836 \times 10^{-4} \text{ lb-sec}^2 \quad (4.55)$$

$$P_3^0 = 30.913 \times 10^{-4} \text{ lb-sec}^2 \quad (4.56)$$

$$Q_3^0 = 2.755 \times 10^{-4} \text{ lb-sec}^2 \quad (4.57)$$

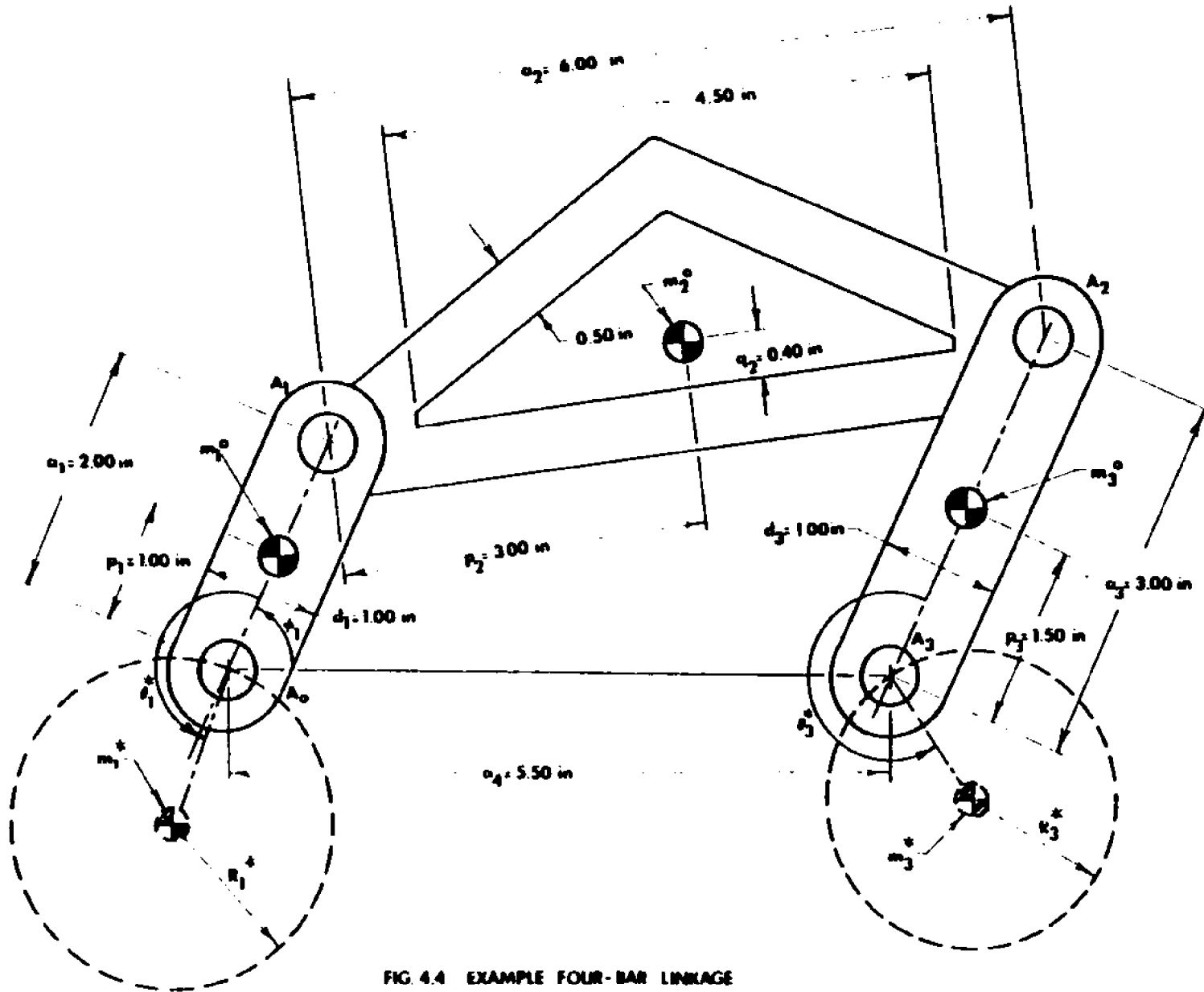


FIG. 4.4 EXAMPLE FOUR-BAR LINKAGE

Table 4.1: Parameters of Unbalanced Linkage

Link j	1	2	3	4
Link length, $a_j$ (in)	2.000	6.000	3.000	5.500
Link width, $d_j$ (in)	1.000	As shown in Figure 4.4	1.000	-
Link thickness, $h_j$ (in)	0.250	0.250	0.250	-
Link mass, $m_j^o$ (lb-sec <sup>2</sup> /in)	$5.1062 \times 10^{-4}$	$13.6710 \times 10^{-4}$	$6.9378 \times 10^{-4}$	-
Center of mass location, $p_j^o$ (in)	1.000	3.000	1.500	-
Center of mass location, $q_j^o$ (in)	0.0	0.403	0.0	-
Radius of gyration, $k_j^o$ (in)	Not required	2.0970	1.6747	-

Substitution of the above into equations (A.27)-(A.30) leads to the following coefficients and angles associated with equation (4.3):

$$A^{\circ} = 18.867 \times 10^{-4} \text{ lb-sec}^2 \quad (4.58)$$

$$\alpha^{\circ} = -5.585 \text{ deg} = -.09747 \text{ rad} \quad (4.59)$$

$$B^{\circ} = 31.036 \times 10^{-4} \text{ lb-sec}^2 \quad (4.60)$$

$$\beta^{\circ} = 5.093 \text{ deg} = .08889 \text{ rad} \quad (4.61)$$

$$K_1 = 2741.557 \text{ rad/sec}^2 \quad (4.62)$$

2. Determination Of Radius And Location Of Center Of Smallest Circumscribing Circle To Rotated Shaking Force Hodograph. Maximum Shaking Force.

Appendix F.1 shows the essential parts as well as the output of program CIRCLE which is used for the determination of the radius and the coordinates of the center of the smallest circumscribing circle to the rotated shaking force hodograph. This program is an adaptation of the Harwell optimization routine and is based on the formulation given by equations (4.5) and (4.6).

Equations (F.7)-(F.9) give the following results:

$$R_S = 15.734 \quad (\text{lbs}) \quad (4.63)$$

$$C_{Sx} = 8.987 \quad (\text{lbs}) \quad (4.64)$$

$$C_{Sy} = -3.464 \quad (\text{lbs}) \quad (4.65)$$

It is to be noted that all "geometric" results are now given in the units of pounds.

From the above, according to equation (4.7):

$$\delta_S = -21.079 \text{ deg} = -.36790 \text{ rad} \quad (4.66)$$

The maximum shaking force is obtained by way of program FMAX. This program, which is given in Appendix F.2, evaluates the absolute magnitude of the shaking force at one degree intervals of the input angle  $\phi_1$  and chooses the largest value. Equation (F.16) shows the final result:

$$R_{MAX}^{\circ} = 25.004 \quad (\text{lbs}) \quad (4.67)$$

With  $\eta = 0.5$ , the proportionality factor  $\mu$ , as given by equation (4.10), and with equations (4.63) and (4.67), becomes:

$$\mu = \eta \frac{R_{MAX}^{\circ}}{R_S} = .795 \quad (4.68)$$

### 3. Determination Of Counterweights For Simple 50 Percent Reduction

#### a. Output Link Counterweight

When the simple reduction method of Section C is used, the mass-distance product of the output link counterweight is determined according to equation (4.21). With equations (4.60) and (4.68), one obtains:

$$m_3^* r_3^* = (1 - \mu) B^0 = 6.362 \times 10^{-4} \text{ lb-sec}^2 \quad (4.69)$$

The counterweight radius,  $R_j^*$ , is then found with the help of the following general design equation for circular and tangent counterweights as shown in Figure 4.4:

$$R_j^* = \left[ \frac{m_j^* r_j^*}{\rho_j^* \pi h_j^*} \right]^{\frac{1}{3}}, \quad j = 1, 3 \quad (4.70)$$

where

$R_j^*$  = counterweight radius

$\rho_j^*$  = density of counterweight

$h_j^*$  = thickness of counterweight

With equation (4.69) and letting  $h_j^* = 0.625 \text{ in.}$ , one

obtains from the above:

$$R_3^* = .762 \text{ in} \quad (4.71)$$

Further, with equations (4.22) and (4.61), the counterweight angle is given by

$$\theta_3^* = \beta^0 + \pi = 185.093 \text{ deg} \quad (4.72)$$

b. Input Link Counterweight (See Section C.2)

The vector  $\overline{OC}_S$  is obtained with the help of equations (4.24), (4.64) and (4.65):

$$\overline{OC}_S e^{i\delta_S} = 9.631 e^{-.36790 i} \quad (4.73)$$

The vector  $\overline{OD}^0$  is determined according to equations (4.25), (4.58), (4.62) and (4.59):

$$\overline{OD}^0 = 5.172 e^{-.09747 i} \quad (4.74)$$

Equation (4.27) gives the vector  $\overline{D}^0 C_S$  with the help of equations (4.73) and (4.74):

$$D^0 C_S = 4.848 \quad (4.75)$$

and  $\zeta = -37.638 \text{ deg} = -.65690 \text{ rad} \quad (4.76)$

The vector  $\overline{OC}$  is found with the help of equations (4.28), (4.74), (4.75) and (4.68):

$$OC = 8.683 \quad (4.77)$$

with  $\delta = -19.210 \text{ deg} = -.33527 \text{ rad} \quad (4.78)$

The input counterweight parameters become, according to equations (4.30) and (4.31):

$$m_1^* r_1^* = 31.672 \times 10^{-4} \text{ lb-sec}^2 \quad (4.79)$$

and  $\theta_1^* = 160.790 \text{ deg} \quad (4.80)$

The associated circular counterweight is again obtained by way of equation (4.70) with  $h_1^* = 0.625$  inches. Thus,

$$R_1^* = 1.301 \text{ in} \quad (4.81)$$

#### 4. Determination Of Counterweights For 50 Percent Reduction Of Maximum Shaking Force By General Solution

##### a. Theoretical Design Range

The theoretical range of possible output link counterweight parameters associated with the general solution is found with the help of equations (4.42) and (4.43).

Accordingly, the minimum mass-distance product is given by

$$(m_3^* r_3^*)_{\text{MIN}} = (1 - \mu) B^{\circ} = 6.362 \times 10^{-4} \text{ lb-sec}^2, \quad (4.82)$$

while the maximum mass-distance product is represented by

$$(m_3^* r_3^*)_{\text{MAX}} = (1 + \mu) B^{\circ} = 55.710 \times 10^{-4} \text{ lb-sec}^2. \quad (4.83)$$

(For  $B^{\circ}$  and  $\mu$ , see equations (4.60) and (4.68), respectively.)

Equation (4.39) indicates the counterweight angle for both extrema as

$$\theta_3^* = \beta^{\circ} + \pi = 185.093 \text{ deg} \quad (4.84)$$

(See also equation (4.61).)

The associated output link counterweight radii, with  $h_3^* = 0.625$  inches, are, according to equation (4.70):

$$(R_3^*)_{\text{MIN}} = 0.762 \text{ in} \quad (4.85)$$

and  $(R_3^*)_{\text{MAX}} = 1.570 \text{ in}$ , respectively. (4.86)

Note again that the minimum mass-distance solution is identical to that obtained by the simple reduction.

b. Counterweight Design For Arbitrary Point  
Within Theoretical Design Range

To show the determination of output as well as input counterweights within the theoretical design range, the following example uses the output link parameter

$$m_3^* r_3^* = 24.880 \times 10^{-4} \text{ lb-sec}^2 \quad (4.87)$$

which is approximately in the center of the design range.

i. Output Link Counterweights

The angles associated with the above value (which also must satisfy equation (4.44)) are given by

$$\theta_{31}^* = 134.168 \text{ deg} \quad (4.88)$$

and  $\theta_{32}^* = 236.017 \text{ deg} \quad (4.89)$

The corresponding counterweight radius as found with the help of equation (4.70) and with  $h_3^* = 0.625$  inches, is

$$R_3^* = 1.200 \text{ in} \quad (4.90)$$

The above shows that counterweights of the same mass but with two different angles will produce the identical maximum shaking force.

ii. Input Link Counterweights

The following shows the detailed determination of the input link counterweight parameters corresponding to the output link parameters of equations (4.87) and (4.88) and only gives the results for the input link counterweight design which corresponds to angle  $\theta_{32}^*$  as given by equation (4.89). Because of these two output link counterweight design possibilities, additional subscripts are introduced where appropriate. The computational sequence indicated in Section D.3 is followed.

- a. Angle  $\beta_1$  becomes, according to equations (4.47), (4.56), (4.57), (4.87) and (4.88):

$$\begin{aligned}\beta_1 &= \tan^{-1} \frac{Q_3^{\circ} + m_3^* r_3^* \sin \theta_{31}^*}{P_3^{\circ} + m_3^* r_3^* \cos \theta_{31}^*} \\ &= \tan^{-1} \frac{2.755 \times 10^{-4} + 24.880 \times 10^{-4} \sin(134.168)}{30.913 \times 10^{-4} + 24.880 \times 10^{-4} \cos(134.168)} \\ &= 56.613 \text{ deg} \quad (4.91)\end{aligned}$$

- b. The angle of rotation  $\psi_1$  is then obtained by way of equations (4.48) and (4.91):

$$\begin{aligned}\psi_1 &= \beta_1 - \beta^0 = 56.597 - 5.093 \\ &= 51.520 \text{ deg} = .89919 \text{ rad} \quad (4.92)\end{aligned}$$

where  $\beta^0$  is given by equation (4.61).

- c. The vector  $\overline{D^0C_1}$  is found with the help of equations (4.49), (4.68), (4.75), (4.76) and (4.92):

$$\begin{aligned}\overline{D^0C_1} &= \mu D^0C_S e^{i(\zeta + \psi_1)} = .795 \times 4.848 e^{(-.65690 + .89919)i} \\ &= 3.854 e^{.24229 i} \quad (4.93)\end{aligned}$$

- d. With the above, the vector  $\overline{OC_1}$  may be determined with equations (4.50) and (4.74):

$$OC_1 = 8.899 \quad (4.94)$$

$$\text{and} \quad \delta_1 = 2.714 \text{ deg} = .04737 \text{ rad} \quad (4.95)$$

- e. The input counterweight parameters become, according to equations (4.52) and (4.53):

$$(m_1^* r_1^*)_1 = \frac{|\overline{OC_1}|}{\phi_1^2} = \frac{8.899}{2741.557} = 32.460 \times 10^{-4} \text{ lb-sec}^2 \quad (4.96)$$

$$\text{and} \quad \theta_{11}^* = \delta_1 + \pi = 182.714 \text{ deg} \quad (4.97)$$

The corresponding circular counterweight radius is again found by way of equation (4.70) and with  $h_1^* = 0.625$  inches:

$$(R_1^*)_1 = 1.311 \text{ in} \quad (4.98)$$

When the output link counterweight of angle  $\theta_{32}^* = 236.090$  degrees is chosen, one obtains the following:

$$\beta_2 = -46.427 \text{ deg} \quad (4.99)$$

$$\psi_2 = -51.520 \text{ deg} \quad (4.100)$$

With the above:

$$(R_1^*)_2 = 1.198 \text{ in} \quad (4.101)$$

and  $\theta_{12}^* = 140.064 \text{ deg} \quad (4.102)$

c. Counterweight Design Flexibility And Its Influence On Various Mechanism Reactions

Figure 4.5 represents a graph of associated output link counterweight parameters  $R_3^*$  and  $\theta_3^*$  for the full design range. The counterweight thickness of 0.625 inches is maintained throughout. In addition, this graph shows input link counterweight parameters  $R_1^*$  and  $\theta_1^*$  for selected output link counterweight configurations. For purposes of

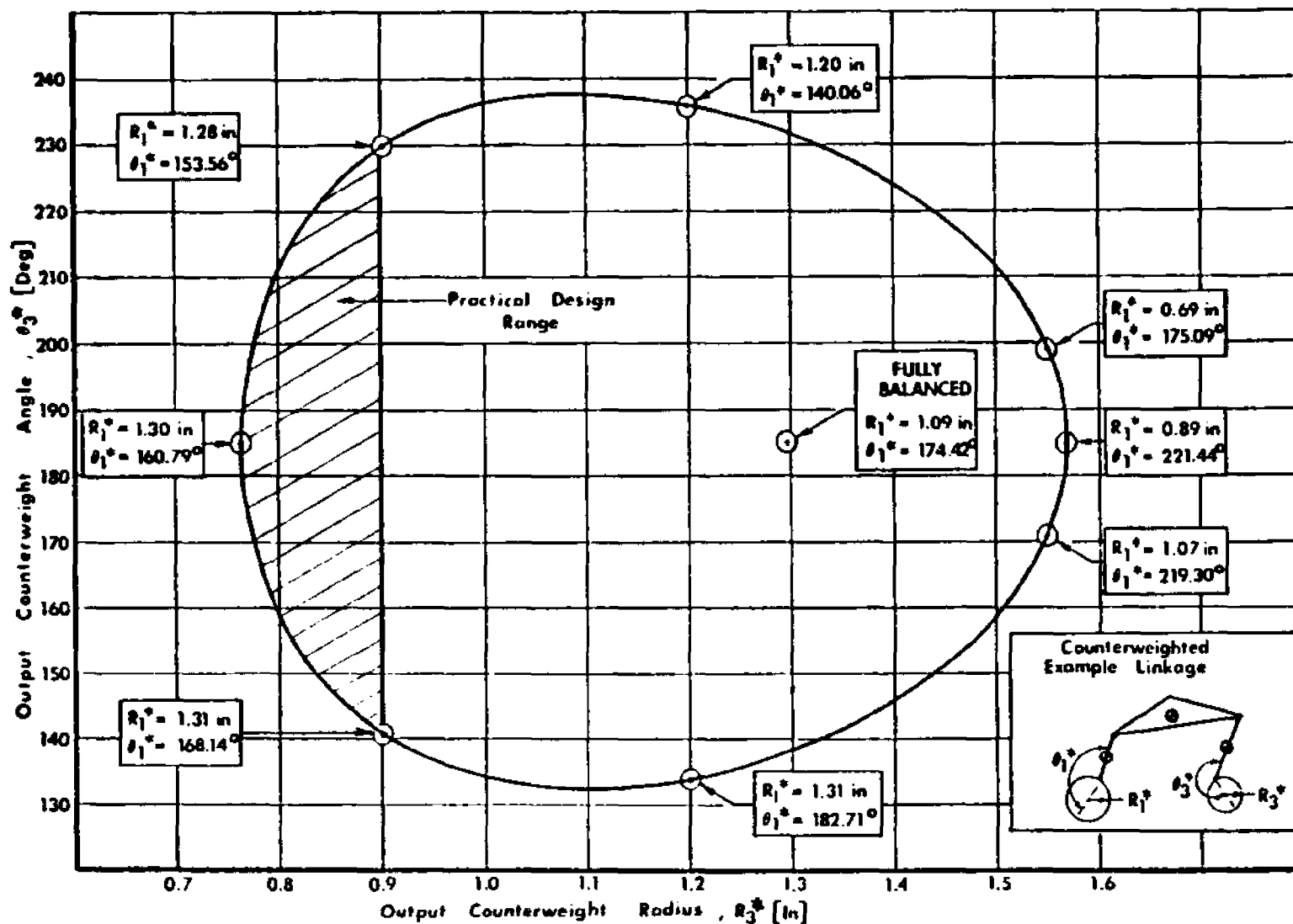


FIG. 4.5 RANGE OF OUTPUT LINK COUNTERWEIGHT PARAMETERS AND CERTAIN CORRESPONDING INPUT LINK COUNTERWEIGHT PARAMETERS FOR A 50 PERCENT REDUCTION IN MAXIMUM SHAKING FORCE [Counterweight Thickness = 0.625 in.]

comparison, the counterweight parameters of a fully force balanced mechanism are also indicated.

To gain perspective concerning the usefulness of this design flexibility, one must also consider the associated variations in the mechanism reactions. Table 4.2 lists the absolute maximum values of all the bearing forces, the input moment and the shaking moment (taken with respect to the midpoint between the ground pivots) for the counterweight configurations of Figure 4.5 and compares them with those of both the unbalanced and the fully balanced mechanism<sup>1</sup>. The table shows that the smallest increases of the maximum dynamic reactions are, for the most part, associated with the minimum mass-distance product of the theoretical design range.

If one considers increases in these reactions of as much as 20 to 30 percent above those of the unbalanced mechanism as an acceptable trade-off for a 50 percent reduction of the maximum shaking force, that portion of the curve in Figure 4.5 which lies to the left of the vertical line at  $R_3^* = .90$  inches represents a practical design range. Within this practical range, the output link counterweight angles may be varied between 140 and 230 degrees

---

<sup>1</sup> Expressions for these reactions are given in [75].

Table 4.2: Influence of Partial Balancing ( $\gamma=0.5$ ) on Various Forces and Moments

Percentage Reduction in Maximum Shaking Force	Input Counterweight Parameters (1)		Output Counterweight Parameters (1)		Maximum Bearing Force				Maximum Input Moment	Maximum Shaking Moment (2)	
	$R_1^*$ (in)	$\theta_1^*$ (deg)	$R_3^*$ (in)	$\theta_3^*$ (deg)	$ F_{41} $ (lb)	$ F_{21} $ (lb)	$ F_{23} $ (lb)	$ F_{43} $ (lb)	$ M_{41} $ (in-lb)	$ M_{M/G} $ (in-lb)	
0 Unbalanced ( $F_{M/G}$ ) <sub>MAX</sub> = 25.00 lb	-	-	-	-	52.12	50.74	40.38	39.27	38.72	90.90	
100 Fully Balanced (3) ( $F_{M/G}$ ) <sub>MAX</sub> = 0 lb	1.09	174.42	1.29	185.09	78.52	82.09	71.23	78.52	64.84	95.45	
50 Partially Balanced ( $F_{M/G}$ ) <sub>MAX</sub> = 12.50 lb	Practical Design Range	1.30	160.79	.76	185.09	49.05	54.47	44.00	43.73	41.83	94.39
		1.31	168.14	.90	140.59	51.75	58.13	47.58	42.91	44.88	84.31
		1.28	153.56	.90	229.60	53.78	58.13	47.58	52.13	44.88	110.59
		1.31	182.71	1.20	134.17	66.69	74.08	63.30	54.39	58.17	72.05
		1.20	140.06	1.20	236.02	71.91	74.08	63.30	76.92	58.17	140.72
		1.07	219.30	1.55	171.06	112.70	115.70	104.64	114.73	92.96	87.25
		.69	175.09	1.55	199.13	115.83	115.70	104.64	127.28	92.86	136.55
.89	221.44	1.57	185.09	118.16	119.20	108.13	126.05	95.77	111.64		

- (1) Steel counterweights, 0.625 inches thick (This is 2.5 times link thickness).  
 (2) Shaking moment is taken with respect to midpoint between ground bearings.  
 (3) Fully balanced by the Method of Linearly Independent Vectors[8].

while the associated output link counterweight radii remain considerably smaller than those needed for full force balancing. The resulting input link counterweights are somewhat larger than those of the fully balanced linkage.

5. Results For 75 Percent Reduction In Maximum Shaking Force By General Solution

Table 4.3 lists counterweight parameters and maximum dynamic reactions, again corresponding to a constant input speed of 500 rpm, for the extrema of the theoretical design range of a 75 percent reduction of the maximum shaking force by way of the general solution. In addition, the results for the unbalanced mechanism and the fully balanced mechanism are shown together with the limiting values of the 50 percent reductions, discussed in the previous section.

The smallest increases of most of the dynamic reactions are again associated with the smallest possible output link counterweight, i.e. the minima of the design range.

(Table 4.3 will also serve as a basis for certain comparisons presented in the following section on simultaneous optimization of dynamic reactions of a four-bar linkage.)

Table 4.3: Maximum Dynamic Reactions For Extrema Of Design Ranges Corresponding To 50 And 75 Percent Reductions Of Maximum Shaking Force

Percentage Reduction in Maximum Shaking Force	Counterweight Parameters (1)				Maximum Bearing Forces				Maximum Input Moment	Maximum Shaking Moment(2)
	$R_1^*$ (in)	$\theta_1^*$ (deg)	$R_3^*$ (in)	$\theta_3^*$ (deg)	$ F_{41} $ (lb)	$ F_{21} $ (lb)	$ F_{23} $ (lb)	$ F_{43} $ (lb)	$ M_{41} $ (in-lb)	$ M_{43} $ (in-lb)
0 Unbalanced ( $F_M/G$ ) <sub>MAX</sub> = 25.00 lb	-	-	-	-	52.12	50.74	40.38	39.27	38.72	90.90
100 Fully Balanced (3) ( $F_M/G$ ) <sub>MAX</sub> = 0	1.09	174.42	1.29	185.09	78.52	82.09	71.23	78.52	64.84	95.45
50 ( $F_M/G$ ) <sub>MAX</sub> = 12.50 lb (Minimum $R_3^*$ )	1.30	160.79	.76	185.09	49.05	54.47	44.00	43.73	41.83	94.39
50 ( $F_M/G$ ) <sub>MAX</sub> = 12.50 lb (Maximum $R_3^*$ )	.89	221.44	1.57	185.09	118.16	119.20	108.13	126.05	95.77	111.64
75 ( $F_M/G$ ) <sub>MAX</sub> = 6.25 lb (Minimum $R_3^*$ )	1.20	165.88	1.09	185.09	62.16	66.68	55.99	58.90	52.01	92.84
75 ( $F_M/G$ ) <sub>MAX</sub> = 6.25 lb (Maximum $R_3^*$ )	.98	190.51	1.44	185.09	97.35	99.67	88.69	101.17	79.49	102.43

(1) Steel counterweights .625 inches thick (This is 2.5 times the link thickness.)

(2) Shaking moment is taken with respect to midpoint between ground bearings.

(3) Fully balanced by the Method of Linearly Independent Vectors[8].

## V. SIMULTANEOUS OPTIMIZATION OF DYNAMIC REACTIONS OF A FOUR-BAR LINKAGE WITH PRESCRIBED MAXIMUM SHAKING FORCE

### A. Introduction

The following section introduces a technique which makes it possible to simultaneously minimize the maximum dynamic reactions of a constant speed four-bar linkage while maintaining the ability to prescribe the maximum shaking force. The general reduction of the values of these reactions when compared to those obtained by the method of the previous section is based on the introduction of a coupler counterweight in addition to those located on the input and output links. The resulting increase in the number of design variables is reflected in what has now been called the general equipollent circle constraint equation, which makes it possible to prescribe the maximum shaking force. The simultaneous optimum reduction of such dynamic reactions as the bearing forces, the input moment and the shaking moment now becomes a function of the proper combination of the coupler and output link counterweight parameters.

To this end, an optimization procedure was devised which allows for the determination of these counterweight

parameters. This procedure satisfies the general equipollent circle constraint equation while it imposes constraints on the maximum dynamic reactions. The latter inequality constraints are controlled by a minimization parameter  $z$  which serves as the objective function of the optimization.

The following first gives the form of the new general equipollent circle constraint equation and then describes the formulation of the optimization as well as its adaptation to the Harwell Augmented Lagrangian program. Subsequently, the design procedure for this type of partial force balancing, which also includes the determination of the input link counterweight parameters, is outlined. This procedure is incorporated into program OPTIMIZE, which represents the adaptation of the Harwell code. (Program OPTIMIZE is listed and explained, together with a sample run, in Appendix G.)

The design procedure has been applied to a 50 and a 75 percent reduction in the maximum shaking force. It was found that the reduction in the dynamic reactions due to the simultaneous optimization became most pronounced for the larger reduction in the maximum shaking force.

This new three-counterweight method is also adapted to a fully force balanced mechanism. The associated reductions in the dynamic reactions, when compared to those of the two-

counterweight Method of Linearly Independent Vectors, was found to be especially gratifying.

Finally, the optimization procedure was modified for an input moment minimization of a fully force balanced mechanism. The constraints on all dynamic reactions, with the exception of that for the input moment, were removed. Again, a comparison of the resulting maximum input moment with that associated with the Method of Linearly Independent Vectors shows a considerable reduction. In addition, even though unconstrained, all other reactions were either considerably smaller or, at worst, remained substantially the same as those obtained by the above two-counterweight method of full force balancing.

## B. General Equipollent Circle Constraint Equation

Equation (4.32) in Section IV, which is an expanded form of the equipollent circle constraint equation (4.35), shows that a prescribed maximum shaking force can be maintained as long as the following relationship is satisfied:

$$(P_3)^2 + (Q_3)^2 = (\mu B^0)^2 \quad (5.1)$$

where

$$P_3 = m_3 p_3 + \frac{a_3}{a_2} m_2 p_2 \quad (5.2)$$

$$Q_3 = m_3 q_3 + \frac{a_3}{a_2} m_2 q_2 \quad (5.3)$$

If one desires to make changes in the mass distribution of the coupler link in addition to that of the output link, equation (5.1) must be modified to become the following general equipollent circle constraint equation:

$$(P_3^* + P_3^0)^2 + (Q_3^* + Q_3^0)^2 = (\mu B^0)^2 \quad (5.4)$$

where

$$P_3^* = m_3^* p_3^* + \frac{a_3}{a_2} m_2^* p_2^* \quad (5.5)$$

$$Q_3^* = m_3^* q_3^* + \frac{a_3}{a_2} m_2^* q_2^* \quad (5.6)$$

$$P_3^0 = m_3^0 p_3^0 + \frac{a_3}{a_2} m_2^0 p_2^0 \quad (5.7)$$

$$Q_3^0 = m_3^0 q_3^0 + \frac{a_3}{a_2} m_2^0 q_2^0 \quad (5.8)$$

(See also equation (A.25).)

In order to be able to optimize mechanism reactions, a specific counterweight configuration has to be adopted. For the present work, circular counterweights which are tangent to their pivots will be used. (See Figure 5.2) Equations (5.5) and (5.6) then become:

$$P_3^* = \rho_3^* \pi h_3^* (R_3^*)^3 \cos \theta_3^* + \frac{a_3}{a_2} \rho_2^* \pi h_2^* (R_2^*)^3 \cos \theta_2^* \quad (5.9)$$

$$\text{and } Q_3^* = \rho_3^* \pi h_3^* (R_3^*)^3 \sin \theta_3^* + \frac{a_3}{a_2} \rho_2^* \pi h_2^* (R_2^*)^3 \sin \theta_2^* \quad (5.10)$$

where

$R_j^*$  = counterweight radius

$\theta_j^*$  = counterweight angle

$\rho_j^*$  = density of counterweight

$h_j^*$  = thickness of counterweight

### C. Formulation Of Optimization Problem

The basic objective of the optimization consists of choosing the variables  $R_2^*$ ,  $\theta_2^*$ ,  $R_3^*$  and  $\theta_3^*$  such that the maximum values of all bearing forces, the input moment and the shaking moment are simultaneously minimized while holding the maximum shaking force to a prescribed value by way of the general equipollent circle constraint equation. The magnitudes of the input link counterweight parameters depend entirely on the choice of the coupler and output link counterweight parameters and are attained in a manner similar to that shown in Section IV. (These values, of course, are necessary to compute the mechanism reactions.)

The optimization method is formulated in the following way:

$$\text{minimize } z \quad (5.11)$$

subject to the equality constraints of the general equipollent circle constraint equation (5.4) as well as the following inequality constraints:

$$W_1 \left[ \frac{(F_{41})^2 - (F_{41}^o)^2}{(F_{41}^o)^2} \right]_{\text{MAX}} \leq z \quad (5.12)$$

$$W_2 \left[ \frac{(F_{12})^2 - (F_{12}^o)^2}{(F_{12}^o)^2} \right]_{\text{MAX}} \leq z \quad (5.13)$$

$$W_3 \left[ \frac{(F_{23})^2 - (F_{23}^o)^2}{(F_{23}^o)^2} \right]_{\text{MAX}} \leq z \quad (5.14)$$

$$W_4 \left[ \frac{(F_{34})^2 - (F_{34}^o)^2}{(F_{34}^o)^2} \right]_{\text{MAX}} \leq z \quad (5.15)$$

$$W_5 \left[ \frac{(M_{M/G})^2 - (M_{M/G}^o)^2}{(M_{M/G}^o)^2} \right]_{\text{MAX}} \leq z \quad (5.16)$$

$$W_6 \left[ \frac{(M_{41})^2 - (M_{41}^o)^2}{(M_{41}^o)^2} \right]_{\text{MAX}} \leq z \quad (5.17)$$

- where  $F_{41}$  = bearing force between ground link and input link  
 $F_{12}$  = bearing force between input link and coupler link  
 $F_{23}$  = bearing force between coupler link and output link  
 $F_{34}$  = bearing force between output link and ground link  
 $M_{M/G}$  = shaking moment taken with respect to midpoint  
between ground pivots  $A_0$  and  $A_3$   
 $M_{41}$  = input moment  
 $W_j$  = weighting factors for each reaction, ( $j=1,2,\dots,6$ )

The usual notation is used whereby a zero superscript corresponds to the unbalanced linkage while the absence of a superscript represents the balanced linkage. (See Appendix A.3)

#### D. Computational Sequence Of Optimization Procedure

The following outlines computational procedures for partial as well as full force balancing which are used in program OPTIMIZE (see Appendix G).

##### 1. Determination Of Counterweight Parameters For Partial Force Balancing

To determine all mechanism reactions, each iteration of the optimization procedure requires a complete counterweight design. The following shows the necessary computational sequence. It is different from those used previously because of the changes in the mass distribution of the coupler link:

1. As in Section IV-B, from the dimensions of the unbalanced mechanism as well as for a given input speed and reduction factor  $\eta$ , the parameters  $R_S$ ,  $C_{Sx}$ ,  $C_{Sy}$ ,  $\delta_S$  and  $R_{MAX}^0$  are first obtained. Subsequently, the proportionality factor  $\mu$  is found according to equation (4.10).
2. The value of  $B = \mu B^0$  is then computed with the help of the parameters of the unbalanced linkage for use in equation (5.4).

3. A set of output link and coupler counterweight parameters  $R_2^*$ ,  $\theta_2^*$ ,  $R_3^*$  and  $\theta_3^*$ , which satisfy the constraint equation (5.4), is chosen. (The thickness  $h^*$  and density  $\rho^*$  are prescribed.)
4. To devise a method for determining the input link counterweight parameters, one must consider the changes in the shaking force hodograph as indicated by equation (4.3), i.e.

$$\bar{F}_{M/G} e^{-i\phi_1} = AK_1 e^{i\alpha} + BK_3 e^{i(\gamma_3 + \beta - \phi_1)} \quad (5.18)$$

In the previously shown flexible counterweight design (see Section IV-D), only the parameters  $B$  and  $\beta$  are different from  $B^{\circ}$  and  $\beta^{\circ}$ , respectively. The added change in the coupler link configuration also results in changes in the magnitudes of the parameters  $A^{\circ}$  and  $\alpha^{\circ}$  to  $A$  and  $\alpha$ . To illustrate how this difference reflects itself in the shaking force hodograph, it is useful to review Figure 4.3 which shows the effects of the changes in the parameters  $B$  and  $\beta$  only. Figure 5.1 indicates that, for the present case, there must not only be a rotation of the line  $D^{\circ}C$  through the angle  $\psi$ , but there must also be

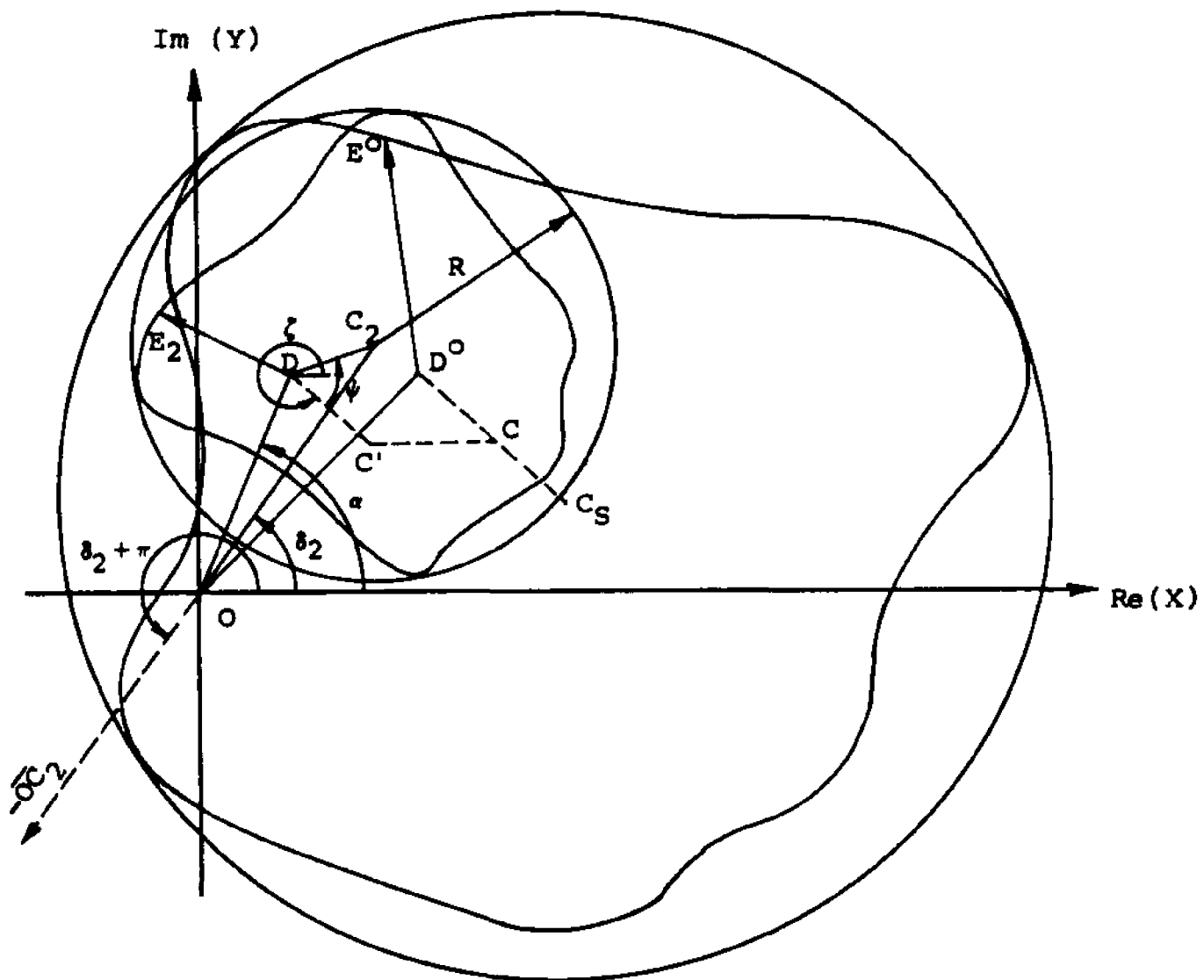


FIGURE 5.1: ORIGINAL AND REDUCED SHAKING  
 FORCE HODOGRAPH RESULTING FROM  
 THREE-COUNTERWEIGHT OPTIMIZATION  
 METHOD

a shift of point  $D^0$  to point  $D$ . This shift is due to the changes in  $A$  and  $\alpha$ . The input link counterweight is finally determined with the help of the vector  $\overline{OC}_2$  at the angle  $\delta_2$ . It may be noted that for the same reduction in shaking force, the vector  $\overline{DC}_2$  is identical in magnitude and direction to the vector  $\overline{D^0C_1}$  of the flexible method of Section IV-D. As a consequence of the above, the computation for the input link counterweight proceeds as follows:

- a. The angle  $\beta$  is obtained with the help of equation (4.16), i.e.

$$\beta = \tan^{-1} \frac{Q_3}{P_3} \quad (5.19)$$

where

$$P_3 = P_3^0 + \rho_3^* \pi h_3^* (R_3^*)^3 \cos \theta_3^* + \frac{a_3}{a_2} \rho_2^* \pi h_2^* (R_2^*)^3 \cos \theta_2^*$$

$$Q_3 = Q_3^0 + \rho_3^* \pi h_3^* (R_3^*)^3 \sin \theta_3^* + \frac{a_3}{a_2} \rho_2^* \pi h_2^* (R_2^*)^3 \sin \theta_2^*$$

(See equations (5.9), (5.10), (A.33), (A.34), (A.41) and (A.42).)

b. The angle of rotation  $\psi$  is then found from

$$\psi = \beta - \beta^{\circ} \quad (5.20)$$

where

$$\beta^{\circ} = \tan^{-1} \frac{Q_3^{\circ}}{P_3^{\circ}}$$

(See equations (4.2), (4.34).)

c. The vector  $\overline{DC}_2 = BK_3 e^{i(\gamma_3 + \beta - \phi_1)}$  is found with the help of equations (4.27) and (4.49):

$$\overline{DC}_2 = \overline{D^{\circ}C}_1 = \mu D^{\circ}C_S e^{i(\zeta + \psi)} \quad (5.21)$$

where

$$D^{\circ}C_S e^{i\zeta} = \sqrt{(C_{Sx})^2 + (C_{Sy})^2} e^{i\theta_S} - A^{\circ}K_1 e^{i\alpha^{\circ}}$$

and

$$\zeta = \tan^{-1} \frac{D^{\circ}C_{Sy}}{D^{\circ}C_{Sx}}$$

(See equations (4.2), (4.7), (4.10), (5.20).)

d. The vector  $\overline{OD}$  is obtained by way of:

$$\overline{OD} = AK_1 e^{i\alpha} \quad (5.22)$$

where

$$A = \left\{ \left( P_1^0 + \rho_2^* \pi h_2^* (R_2^*)^2 a_1 - \frac{a_1}{a_2} \rho_2^* \pi h_2^* (R_2^*)^3 \cos \theta_2^* \right)^2 + \left( Q_1^0 - \frac{a_1}{a_2} \rho_2^* \pi h_2^* (R_2^*)^3 \sin \theta_2^* \right)^2 \right\}^{\frac{1}{2}}$$

$$\alpha = \tan^{-1} \frac{OD_Y}{OD_X}$$

(See equations (A.31) and (A.32).)

- e. With the above, the vector  $\overline{OC}_2$ , which determines the input link counterweight, is found from:

$$OC_2 e^{i\delta_2} = ODe^{i\alpha} + DC_2 e^{i(\zeta + \psi)} \quad (5.23)$$

where  $\delta_2 = \tan^{-1} \frac{OC_{2Y}}{OC_{2X}}$

- f. Finally, since  $K_1 = \dot{\phi}_1^2$ , the force of the input link counterweight must equal:

$$m_1^* r_1^* \dot{\phi}_1^2 e^{i\theta_1^*} = -OC_2 e^{i\delta_2} = OC_2 e^{i(\delta_2 + \pi)} \quad (5.24)$$

This leads to the design equations:

$$m_1^* r_1^* = \frac{|\overline{OC}_2|}{\dot{\phi}_1^2} \quad (5.25)$$

and  $\theta_1^* = \delta_2 + \pi \quad (5.26)$

2. Determination Of Counterweight Parameters  
For Full Force Balancing

Just as for partial force balancing, each iteration of the optimization procedure for full force force balancing requires a complete counterweight design. The computational procedure given below represents a simplification of the partial force balancing procedure, since now the radius of the circumscribing circle vanishes:

- a. For full force balancing, the proportionality factor  $\mu$  in equations (5.1) and (5.4) is set equal to zero.
- b. A set of coupler and output link counterweight parameters  $R_2^*$ ,  $\theta_2^*$ ,  $R_3^*$  and  $\theta_3^*$  which satisfy this revised equipollent circle constraint equation is now chosen. (Again, the thickness  $h^*$  and density  $\rho^*$  are prescribed.)
- c. To devise a method<sup>1</sup> for determining the input link

---

<sup>1</sup>The present method for designing the input link counterweight was chosen because it is used in the existing computer program. With the mass of the coupler known, the identical counterweight design may be obtained with the help of equation (8) of [8].

counterweight parameters  $R_1^*$  and  $\theta_1^*$ , one considers the shaking force hodograph equation (4.3), which now has been reduced to:

$$\overline{F}_{M/G} e^{-i\phi_1} = AK_1 e^{i\alpha} \quad (5.27)$$

This, of course, indicates that the hodograph has been reduced to a single constant vector whose negative furnishes the input link counterweight. This vector corresponds to the vector  $\overline{OD}$  at angle  $\alpha$  in Figure 5.1.

- d. The quantities  $A$  and  $\alpha$  of equation (5.27) are now obtained with the help of equation (5.22):

$$A = \left\{ \left( P_1^0 + \rho_2^* h_2^* (R_2^*)^2 a_1 - \frac{a_1}{a_2} \rho_2^* h_2^* (R_2^*)^3 \cos \theta_2^* \right)^2 + \left( Q_1^0 - \frac{a_1}{a_2} \rho_2^* h_2^* (R_2^*)^3 \sin \theta_2^* \right)^2 \right\}^{\frac{1}{2}}$$

$$\alpha = \tan^{-1} \frac{OD_Y}{OD_X}$$

- e. Since  $K_1 = \dot{\phi}_1^2$ , the force of the input link counterweight is obtained, in a manner parallel to that represented by equation (5.24), from

$$m_1^* r_1^* \ddot{\phi}_1^2 e^{i\theta_1^*} = -ODe^{i\alpha} = ODe^{i(\alpha + \pi)}$$

The counterweight design equations become:

$$m_1^* r_1^* = \frac{|OD|}{\ddot{\phi}_1^2}$$

and 
$$\theta_1^* = \alpha + \pi$$

It is to be noted that the magnitude of the counterweight mass-distance product  $m_1^* r_1^*$  is equal to the quantity  $A$  in equation (5.27).

The above method also furnishes the correct answer even if the input link does not rotate at constant speed. Since the total mechanism center of mass is stationary in a fully balanced mechanism, the net force by the mechanism on the ground vanishes regardless of input speed. This may be shown in terms of the present method of derivation by considering the form of equation (5.27) when  $\ddot{\phi}_1 \neq 0$ . According to equation (A.12), equation (5.27) becomes:

$$\bar{F}_{M/G} e^{-i\gamma_1} = AK_1 e^{i\alpha}$$

Again, the quantity  $A$  in the above is identical with that in equation (5.27), even though one deals with a vector of variable length (and constant direction). If a counterweight whose mass-distance product equals the magnitude of  $A$  is added, the shaking force is reduced to zero.

### 3. Determination Of Optimum Mechanism Reactions

Once the optimum counterweight parameters  $R_i^*$  and  $\theta_i^*$  ( $i=1,2,3$ ) have been obtained, the associated maximum mechanism reactions are obtained with the help of program FMAX which is listed in Appendix F.2.

## E. Examples

The present section gives the results of several groups of optimization runs and discusses their significance in the light of previously shown methods of limiting the maximum shaking force. The example mechanism is the same as that used in the previous section, with the exception that now an additional coupler counterweight is introduced (see Figure 5.2 and Table 4.1). As before, both the original mechanism and all counterweights are assumed to be made of steel and the mechanism speed is taken to be 500 rpm.

The following groups of optimizations are involved:

1. Reduction Of 50 And 75 Percent In The Maximum Shaking Force

Optimized dynamic reactions were obtained both for a 50 percent and a 75 percent reduction in the maximum shaking force. The weighting factors  $W_1$  to  $W_6$ , associated with the constraint equations (5.12)-(5.17), were set equal to unity (see discussion below). The optimum counterweight parameters were obtained with the help of program OPTIMIZE. Appendix G shows the details of the optimization associated with the 50 percent reduction of the maximum shaking force. Program FMAX was subsequently used to obtain the maximum dynamic

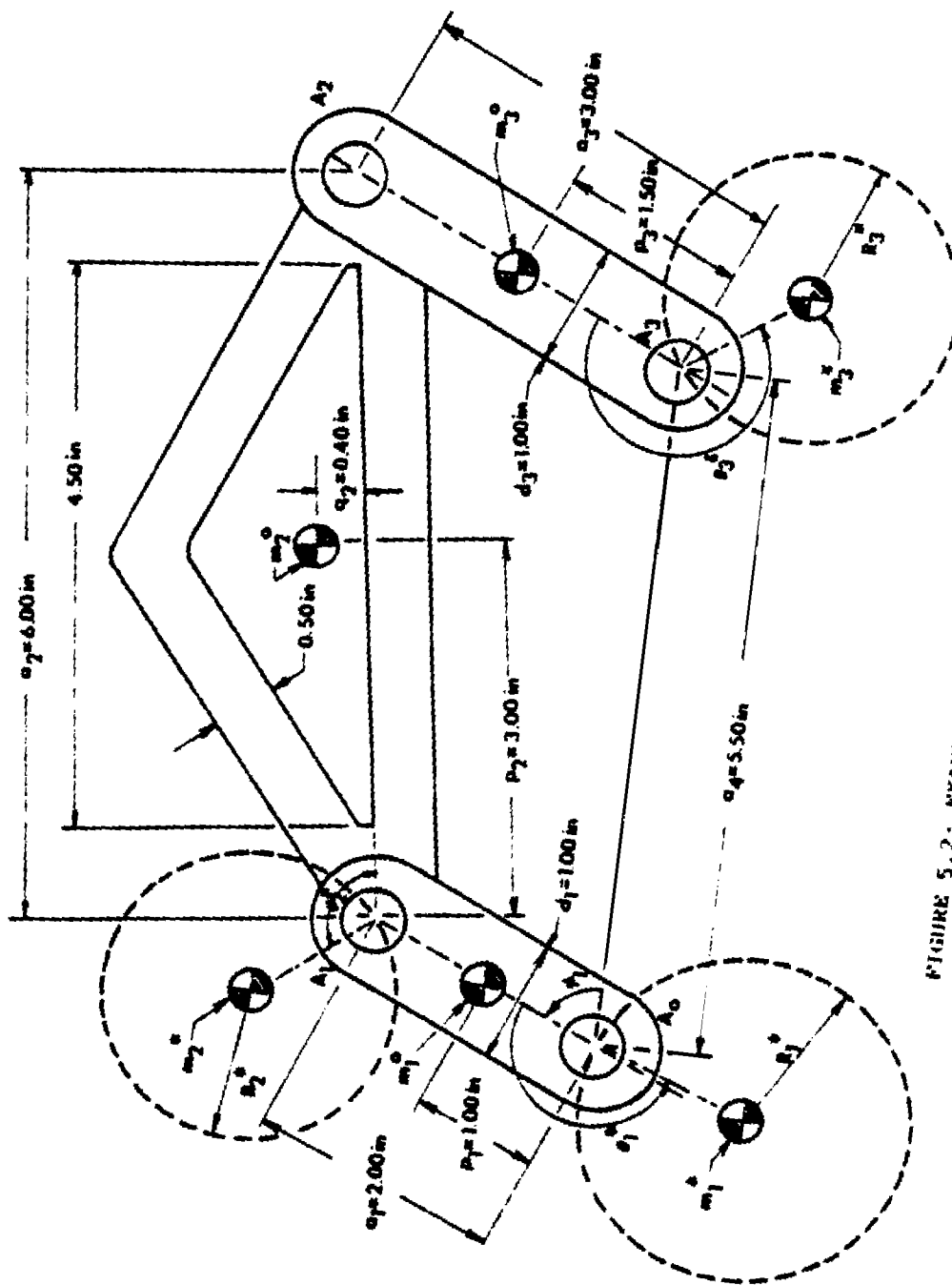


FIGURE 5.2: EXAMPLE FOUR-BAR LINKAGE WITH THREE COUNTERWEIGHTS

reactions associated with the counterweight parameters of program OPTIMIZE serving as the input.

## 2. Full Force Balance

The optimum dynamic reactions were also obtained for a fully force balanced mechanism employing three counterweights. The methods of optimization are identical to those described above.

## 3. Input Moment Optimization For A Fully Force Balanced Mechanism

An input moment optimization for a fully balanced mechanism was also performed. Appendix H, which outlines a modification of program OPTIMIZE, was used for this purpose. In order to minimize only the maximum input moment  $M_{41}$ , the constraint equations for all other dynamic reactions were removed from the program. This is equivalent to letting  $W_6=1$  and  $W_1=W_2=W_3=W_4=W_5=0$ .

## 4. Results Of Optimizations And Conclusions

Table 5.1 gives the results of the various optimizations. The three sets of optimized counterweight parameters, the four maximum bearing forces, the maximum input moment, and the maximum shaking moment are listed together with the minimization

Table 5.1: Comparison of Maximum Dynamic Reactions of Unbalanced, Balanced and Optimized Example Mechanism

Run	Percentage Reduction in Maximum Shaking Force	Quantity Optimized	Counterweight Parameters <sup>(1)</sup>			Maximum Bearing Forces				Maximum Input Moment $IM_{4I}$ (in-lb)	Maximum Shaking Moment <sup>(2)</sup> $IM_{M/G}$ (in-lb)	Optimization Parameter $z$ (lb <sup>2</sup> )
			$R_1^*$ (in)	$R_2^*$ (in)	$R_3^*$ (in)	$IP_{4I}$	$IP_{2I}$	$IP_{2J}$	$IP_{4J}$			
			$\theta_1^*$ (deg)	$\theta_2^*$ (deg)	$\theta_3^*$ (deg)	(lb)	(lb)	(lb)	(lb)			
1	0 Unbalanced $(F_{M/G})_{MAX}=25.00$ lb	None	-	-	-	52.12	50.74	40.38	39.27	38.72	90.90	-
2	50 $(F_{M/G})_{MAX}=12.50$ lb	Best Two- Cwt Case <sup>(5)</sup>	1.30 160.79	-	0.76 185.09	49.05	54.47	44.00	43.73	41.83	94.39	-
3	50 $(F_{M/G})_{MAX}=12.50$ lb	All Reactions	1.65 172.57	1.07 230.99	0.42 170.95	40.08	55.07	40.30	39.12	33.42	92.57	0.178
4	75 $(F_{M/G})_{MAX}=6.25$ lb	Best Two- Cwt Case <sup>(5)</sup>	1.20 165.88	-	1.09 185.09	62.16	66.68	55.99	58.90	52.01	92.84	-
5	75 $(F_{M/G})_{MAX}=6.25$ lb	All Reactions	1.81 179.10	1.37 214.67	0.71 153.29	41.44	62.29	45.30	43.00	38.53	91.72	0.507
6	100 Fully Balanced <sup>(3)</sup> $(F_{M/G})_{MAX}=0$ lb	None	1.09 174.42	-	1.29 185.09	78.52	82.09	71.23	78.52	64.84	95.45	-
7	100 $(F_{M/G})_{MAX}=0$ lb	All Reactions	1.88 182.50	1.48 202.92	0.92 146.43	49.10	72.68	53.23	49.10	51.19	92.40	1.052
8	100 $(F_{M/G})_{MAX}=0$ lb	Input Moment Only	1.86 187.10	1.49 236.17	1.19 135.63	55.82	79.70	64.43	55.82	44.03	75.40	0.293 <sup>(4)</sup>

(1) Steel counterweights, 0.625 inches thick. (This is 2.5 times the link thickness.)

(2) Shaking moment is taken with respect to midpoint between ground bearings.

(3) Fully balanced by the two-counterweight Method of Linearly Independent Vectors [ 8 ].

(4) Applies only to input moment constraint.

(5) Using the method of Section IV with minimum radius output link counterweight. (See Table 4.3)

parameter  $z$  for each of the optimization groupings discussed above. For purposes of comparison, similar data are given for the unbalanced mechanism, as well as a mechanism which has been fully balanced by the two-counterweight Method of Linearly Independent Vectors. In addition, the results associated with the minimum radius output link counterweight for the 50 percent and the 75 percent reductions in the maximum shaking force by the method of Section IV are reproduced from Table 4.3.

The following conclusions may be drawn:

- a. The optimizations associated with the 50 percent and the 75 percent reductions in the maximum shaking force are of interest from two points of view. First, it may be seen that when the values of the maximum dynamic reactions of the new optimization technique are compared to those of the minimum radius output link counterweight method of the previous section, it becomes clear that the value of the present optimization method increases as the prescribed reduction in the maximum shaking force increases. While run 3 of Table 5.1 shows some improvement in the maximum reactions over those of run 2, a

comparison of runs 4 and 5 clearly shows the advantages of the present optimization method. For this latter case, the majority of the dynamic reactions are from approximately 19 to 33 percent smaller than those obtained from the two-counterweight method.

Secondly, when comparing runs 3 and 5 with run 1, which gives the maximum dynamic reactions of the unbalanced mechanism, one finds decreases as well as suprisingly small increases in many of these reactions.

- b. The present three-counterweight optimization is especially effective when applied to the fully force balanced mechanism. Comparison with the two-counterweight method (see runs 6 and 7) shows a substantial decrease in all reactions, with the exception of the shaking moment, which remains essentially unchanged. This most advantageous result is obtained at the cost of the additional coupler counterweight as well as an increase in the size of the input counterweight. (This is associated with some decrease in the size of the output link counterweight.)

- c. The input moment optimization of the fully force balanced mechanism also shows favorable results when compared to the mechanism balanced by the Method of Linearly Independent Vectors (see runs 6 and 8). The maximum input moment is decreased by approximately 32 percent. In addition, all other reactions are either considerably decreased or, at worst, remain substantially the same.

While only a limited effort in this direction has been made, it has been found that the outcome of the various optimizations cannot be greatly influenced by modifying the weighting factors of the controlling constraint equations.

If desired, this controlling expression may be found by substituting the maximum reactions into the appropriate constraint equations (5.12)-(5.17) and by determining that result which is closest to the governing optimization parameter  $z$ . For example, in the optimization associated with the 50 percent reduction in maximum shaking force (see run 3 in Table 5.1), the constraint equations (5.12) and (5.13), pertaining to forces  $F_{41}$  and  $F_{21}$ , respectively, furnish the following values:

$$w_1 \left[ \frac{(F_{41})^2 - (F_{41}^o)^2}{(F_{41}^o)^2} \right] = (1) \left[ \frac{(40.08)^2 - (52.12)^2}{(52.12)^2} \right] = -.41$$

and

$$w_2 \left[ \frac{(F_{21})^2 - (F_{21}^o)^2}{(F_{21}^o)^2} \right] = (1) \left[ \frac{(55.07)^2 - (50.74)^2}{(50.74)^2} \right] = .18$$

Clearly, the second value is closest to  $z=.178$  and therefore, the constraint on the force  $F_{21}$  controls.

## VI. APPENDICES

## APPENDIX A

SHAKING FORCE EXPRESSIONS FOR A FOUR-BAR LINKAGE  
WITH GENERAL LINK MASS DISTRIBUTION

For the purpose of this work it is sometimes advantageous to use the general shaking force expressions as functions of the link angles  $\phi_1$ ,  $\phi_2$  and  $\phi_3$ , while at other times it is more desirable to have them as functions of  $\phi_1$  and  $\phi_3$  only (see Figure A.1). Both approaches are outlined below and expressions, both in exponential and Cartesian component form, are given. Finally, the previously introduced notation  $[8]$ , which allows the distinction between the mass parameters of balanced and unbalanced mechanism, is reviewed.

1. Shaking Force Expression in Terms of  $\phi_1$ ,  $\phi_2$  and  $\phi_3$ a. Exponential Form

The mass-distance product associated with the center of mass trajectory of the four-bar linkage shown in Figure A.1 may be expressed as follows  $[8]$ :

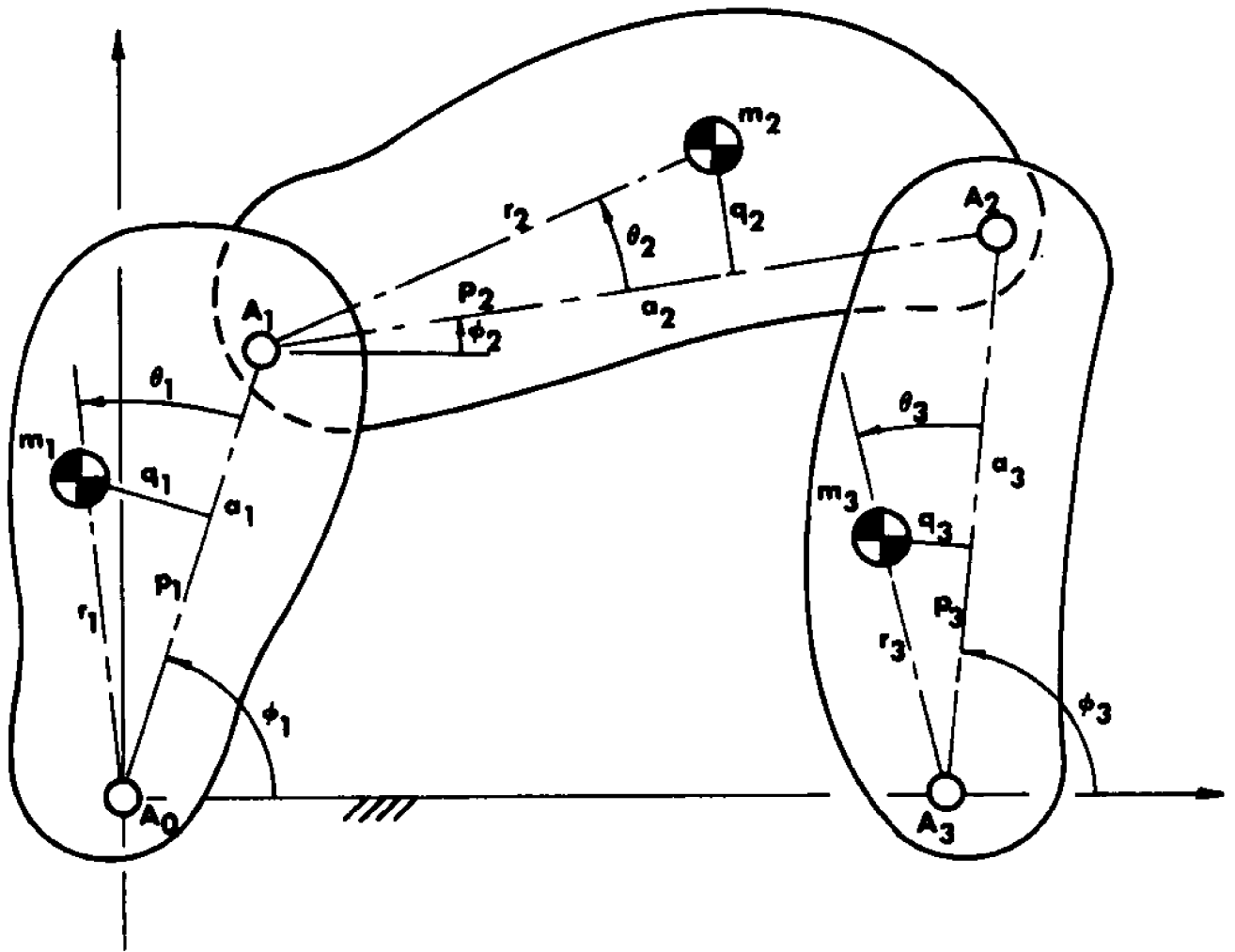


FIG. A.1 GENERAL FOUR-BAR LINKAGE

$$M\bar{F}_s = (m_1 r_1 e^{i\theta_1} + m_2 a_1) e^{i\phi_1} + m_2 r_2 e^{i\theta_2} e^{i\phi_2} + m_3 r_3 e^{i\theta_3} e^{i\phi_3} + m_3 a_4 \quad (\text{A.1})$$

Since the shaking force  $\bar{F}_{M/G}$  is equal to the sum of the D'Alembert forces of the individual links, it may be obtained by double differentiation of the above and the subsequent change of sign of the resulting expression:

$$\bar{F}_{M/G} = -M\ddot{\bar{F}}_s = \left[ m_1 (p_1 + iq_1) + m_2 a_1 \right] K_1 e^{i\gamma_1} + m_2 (p_2 + iq_2) K_2 e^{i\gamma_2} + m_3 (p_3 + iq_3) K_3 e^{i\gamma_3} \quad (\text{A.2})$$

where

$$\left. \begin{aligned} p_j &= r_j \cos \theta_j \\ q_j &= r_j \sin \theta_j \\ \gamma_j &= \phi_j - \phi_j' \\ \phi_j' &= \tan^{-1} \frac{\ddot{\phi}_j}{\dot{\phi}_j^2} \\ K_j &= \sqrt{\dot{\phi}_j^4 + \ddot{\phi}_j^2} \end{aligned} \right\} j = (1, 2, 3) \quad (\text{A.3})$$

### b. Cartesian Component Form

Transformation of equation (A.2) yields the following X and Y components of the shaking force:

$$\begin{aligned}
F_{M/G_X} &= (K_1 \cos \gamma_1) m_1 p_1 - (K_1 \sin \gamma_1) m_1 q_1 + (K_2 \cos \gamma_2) m_2 p_2 \\
&\quad - (K_2 \sin \gamma_2) m_2 q_2 + (K_3 \cos \gamma_3) m_3 p_3 - (K_3 \sin \gamma_3) m_3 q_3 \\
&\quad + m_2 a_1 K_1 \cos \gamma_1
\end{aligned} \tag{A.4}$$

$$\begin{aligned}
\text{and } F_{M/G_Y} &= (K_1 \sin \gamma_1) m_1 p_1 + (K_1 \cos \gamma_1) m_1 q_1 + (K_2 \sin \gamma_2) m_2 p_2 \\
&\quad + (K_2 \cos \gamma_2) m_2 q_2 + (K_3 \sin \gamma_3) m_3 p_3 + (K_3 \cos \gamma_3) m_3 q_3 \\
&\quad + m_2 a_1 K_1 \sin \gamma_1
\end{aligned} \tag{A.5}$$

## 2. Shaking Force Expression in Terms of $\phi_1$ and $\phi_3$

### a. Exponential Form

When the loop equation is used to express the angle  $\phi_2$  in terms of  $\phi_1$  and  $\phi_3$  [8], the expression for the mass-distance product associated with the center of mass trajectory becomes<sup>1</sup>:

$$\begin{aligned}
M\bar{r}_s &= \left[ (m_1 p_1 + m_2 a_1 - \frac{a_1}{a_2} m_2 p_2) + i(m_1 q_1 - \frac{a_1}{a_2} m_2 q_2) \right] e^{i\phi_1} \\
&\quad + \left[ (m_3 p_3 + \frac{a_3}{a_2} m_2 p_2) + i(m_3 q_3 + \frac{a_3}{a_2} m_2 q_2) \right] e^{i\phi_3} \\
&\quad + \left[ (m_3 a_4 + \frac{a_4}{a_2} m_2 p_2) + i \frac{a_4}{a_2} m_2 q_2 \right]
\end{aligned} \tag{A.6}$$

---

<sup>1</sup> Equation (A.6) can also be expressed in terms of other combinations of individual crank angles  $\phi_1$ , such as  $\phi_1$  and  $\phi_2$  or  $\phi_2$  and  $\phi_3$ .

Double differentiation of the above and change of sign again furnishes an expression for the shaking force  $\bar{F}_{M/G}$  :

$$\bar{F}_{M/G} = (P_1 + iQ_1)K_1 e^{i\gamma_1} + (P_3 + iQ_3)K_3 e^{i\gamma_3} \quad (A.7)$$

where the following "general mass-distance products" are defined:

$$P_1 = m_1 p_1 + m_2 a_1 - \frac{a_1}{a_2} m_2 p_2 \quad (A.8)$$

$$Q_1 = m_1 q_1 - \frac{a_1}{a_2} m_2 q_2 \quad (A.9)$$

$$P_3 = m_3 p_3 + \frac{a_3}{a_2} m_2 p_2 \quad (A.10)$$

$$Q_3 = m_3 q_3 + \frac{a_3}{a_2} m_2 q_2 \quad (A.11)$$

The  $K_j$  and  $\gamma_j$  terms are identical with those of equation (A.3) (now  $j = 1, 3$ ).

Under certain circumstances it proves useful to modify equation (A.7) further, i.e.

$$\bar{F}_{M/G} = AK_1 e^{i(\gamma_1 + \alpha)} + BK_3 e^{i(\gamma_3 + \beta)} \quad (A.12)$$

where  $A = \sqrt{(P_1)^2 + (Q_1)^2}$  (A.13)

$$\alpha = \tan^{-1} \frac{Q_1}{P_1} \quad (A.14)$$

$$B = \sqrt{(P_3)^2 + (Q_3)^2} \quad (A.15)$$

$$\beta = \tan^{-1} \frac{Q_3}{P_3} \quad (A.16)$$

### b. Cartesian Component Form

Transformation of equation (A.7) gives the following X and Y components of the shaking force:

$$F_{M/G_X} = (K_1 \cos \gamma_1) P_1 - (K_1 \sin \gamma_1) Q_1 + (K_3 \cos \gamma_3) P_3 - (K_3 \sin \gamma_3) Q_3 \quad (\text{A.17})$$

and  $F_{M/G_Y} = (K_1 \sin \gamma_1) P_1 + (K_1 \cos \gamma_1) Q_1 + (K_3 \sin \gamma_3) P_3 + (K_3 \cos \gamma_3) Q_3 \quad (\text{A.18})$

### 3. Notation Allowing Distinction Between Balanced and Unbalanced Mechanisms

In order to distinguish between the parameters of the links of balanced and unbalanced mechanisms as well as those of counterweights, the following notation is used:

- a) the superscript zero refers to parameters of the unbalanced mechanism
- b) the superscript asterisk refers to counterweight parameters
- c) the absence of any superscript refers to parameters of a balanced linkage.

Accordingly, the distances to the various centers of

mass, as shown in Figure A.2, and their corresponding angles are given by:

$$r_j^{\circ} = \sqrt{(p_j^{\circ})^2 + (q_j^{\circ})^2} \quad (A.19)$$

$$\theta_j^{\circ} = \tan^{-1} \frac{q_j^{\circ}}{p_j^{\circ}} \quad (A.20)$$

$$r_j^* = \sqrt{(p_j^*)^2 + (q_j^*)^2} \quad (A.21)$$

$$\theta_j^* = \tan^{-1} \frac{q_j^*}{p_j^*} \quad (A.22)$$

$$r_j = \sqrt{p_j^2 + q_j^2} \quad (A.23)$$

$$\theta_j = \tan^{-1} \frac{q_j}{p_j} \quad (A.24)$$

The mass-distance products for a balanced linkage become:

$$m_j p_j = m_j^{\circ} p_j^{\circ} + m_j^* p_j^* \quad (j = 1, 2, 3) \quad (A.25)$$

$$m_j q_j = m_j^{\circ} q_j^{\circ} + m_j^* q_j^*$$

When equation (A.12) represents an unbalanced mechanism, it becomes:

$$\bar{F}_{M/G} = A^{\circ} K_1 e^{i(\gamma_1 + \alpha^{\circ})} + B^{\circ} K_3 e^{i(\gamma_3 + \beta^{\circ})} \quad (A.26)$$

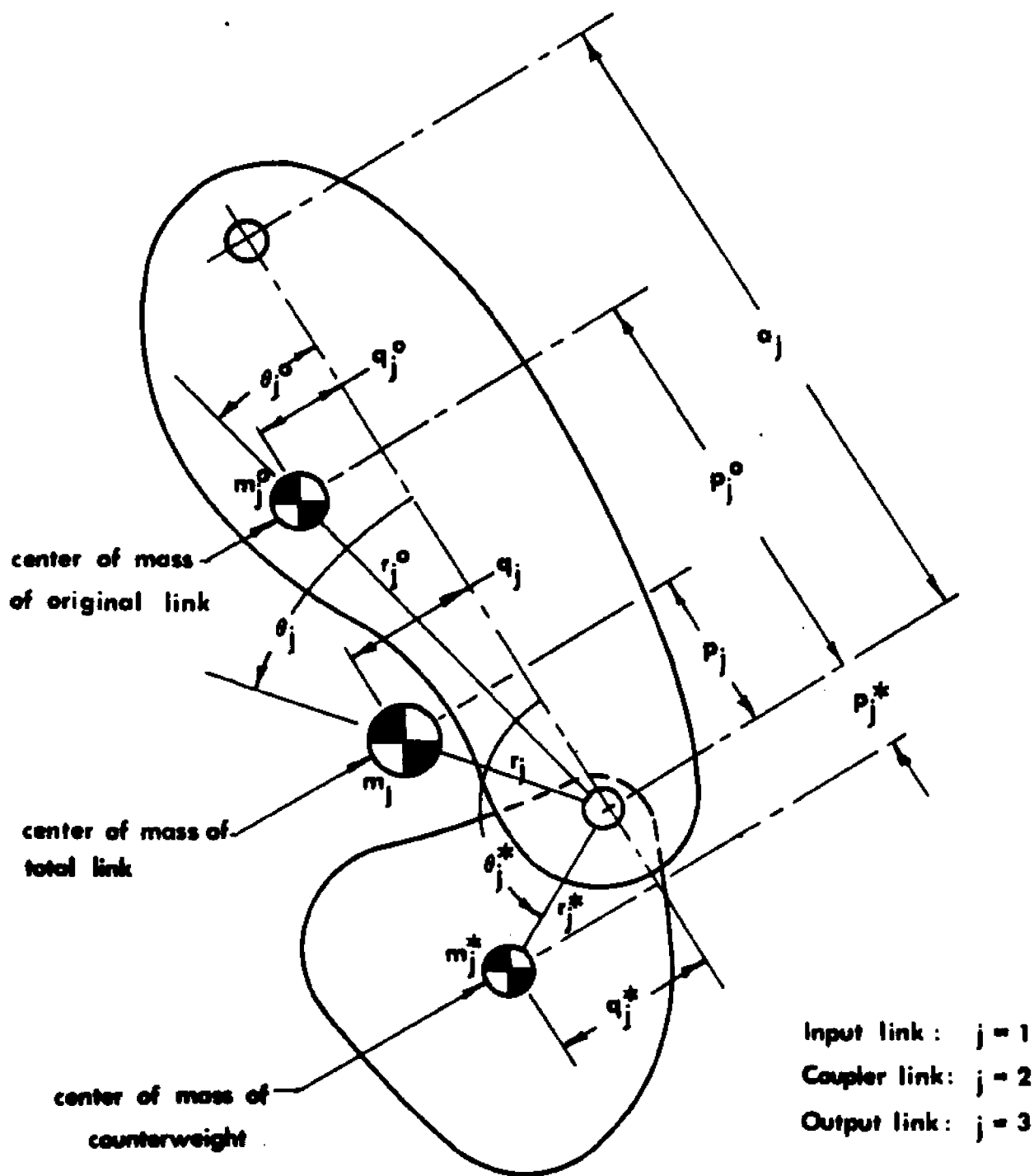


FIG. A.2 NOMENCLATURE ASSOCIATED WITH LINKS AND COUNTERWEIGHTS

where  $A^{\circ} = \sqrt{(P_1^{\circ})^2 + (Q_1^{\circ})^2}$  (A.27)

$$\alpha^{\circ} = \tan^{-1} \frac{Q_1^{\circ}}{P_1^{\circ}} \quad (\text{A.28})$$

$$B^{\circ} = \sqrt{(P_3^{\circ})^2 + (Q_3^{\circ})^2} \quad (\text{A.29})$$

$$\beta^{\circ} = \tan^{-1} \frac{Q_3^{\circ}}{P_3^{\circ}} \quad (\text{A.30})$$

and  $P_1^{\circ} = m_1^{\circ} p_1^{\circ} + m_2^{\circ} a_1 - \frac{a_1}{a_2} m_2^{\circ} p_2^{\circ}$  (A.31)

$$Q_1^{\circ} = m_1^{\circ} q_1^{\circ} - \frac{a_1}{a_2} m_2^{\circ} q_2^{\circ} \quad (\text{A.32})$$

$$P_3^{\circ} = m_3^{\circ} p_3^{\circ} + \frac{a_3}{a_2} m_2^{\circ} p_2^{\circ} \quad (\text{A.33})$$

$$Q_3^{\circ} = m_3^{\circ} q_3^{\circ} + \frac{a_3}{a_2} m_2^{\circ} q_2^{\circ} \quad (\text{A.34})$$

When equation (A.12) describes the shaking force of a mechanism with counterweights on links 1 and 3, the general mass-distance products become:

$$P_1 = m_1^* p_1^* + P_1^{\circ} \quad (\text{A.35})$$

$$Q_1 = m_1^* q_1^* + Q_1^{\circ} \quad (\text{A.36})$$

$$P_3 = m_3^* p_3^* + P_3^{\circ} \quad (\text{A.37})$$

$$Q_3 = m_3^* q_3^* + Q_3^{\circ} \quad (\text{A.38})$$

Finally, when counterweights are attached to all three moving links, the general mass-distance products become:

$$P_1 = P_1^0 + P_1^* \quad (\text{A.39})$$

$$Q_1 = Q_1^0 + Q_1^* \quad (\text{A.40})$$

$$P_3 = P_3^0 + P_3^* \quad (\text{A.41})$$

$$Q_3 = Q_3^0 + Q_3^* \quad (\text{A.42})$$

where

$$P_1^* = m_1^* p_1^* + m_2^* a_1 - \frac{a_1}{a_2} m_2^* p_2^* \quad (\text{A.43})$$

$$Q_1^* = m_1^* q_1^* - \frac{a_1}{a_2} m_2^* q_2^* \quad (\text{A.44})$$

$$P_3^* = m_3^* p_3^* + \frac{a_3}{a_2} m_2^* p_2^* \quad (\text{A.45})$$

$$Q_3^* = m_3^* q_3^* + \frac{a_3}{a_2} m_2^* q_2^* \quad (\text{A.46})$$

## APPENDIX B

ON THE NUMBER OF MASS-DISTANCE PARAMETERS  
OF A FOUR-BAR LINKAGE WHICH MAY BE DETERMINED  
WITH THE HELP OF THE SHAKING FORCE COMPONENTS

When the investigation concerning a force balancing machine for four-bar linkages was first started, it was felt desirable to determine the actual values of the individual link mass-distance products  $m_j p_j$  and  $m_j q_j$  ( $j=1,2,3$ ) in order to be able to modify them, by whatever force balancing method chosen, in the direction of full force balance.

It was subsequently found that this is not possible because the resulting set of shaking force expressions, which have to be based on the repeated use of equations (A.4) and (A.5), produce a singular coefficient matrix due to the linear dependence of certain coefficients.

The present approach resulted once this linear dependence was removed with the help of the component loop equations. In this formulation, the repeated use of equations (A.17) and (A.18) allows for the determination of the general mass-distance products  $P_j$  and  $Q_j$  ( $j=1,3$ ) from a resulting nonsingular matrix.

The following illustrates the above in detail.

1. Proof Of Singularity Of Matrix Originally Proposed For Solution Of Individual Link Mass-Distance Products

If it were possible to solve for the six  $m_j p_j$  and  $m_j q_j$  terms, a set of six simultaneous equations would have to be generated by writing the two shaking force component equations (A.4) and (A.5) for three different positions of the input crank. For each of these three sets of expressions, the associated shaking force components, together with the applicable kinematic quantities as well as the mass  $m_2$ , would have to be available.

To demonstrate that the solution matrix of such a set of component shaking force equations is singular, consider the only available loop equation [ 8 ] for the given mechanism:

$$a_1 e^{i\phi_1} + a_2 e^{i\phi_2} - a_3 e^{i\phi_3} - a_4 e^{i\phi_4} = 0 \quad (\text{B.1})$$

Double differentiation of the above leads to:

$$K_2 e^{i\gamma_2} = - \frac{a_1}{a_2} K_1 e^{i\gamma_1} + \frac{a_3}{a_2} K_3 e^{i\gamma_3} \quad (\text{B.2})$$

Equating real and imaginary parts, one obtains the following constraint equations:

$$K_2 \cos \gamma_2 = - \frac{a_1}{a_2} K_1 \cos \gamma_1 + \frac{a_3}{a_2} K_3 \cos \gamma_3 \quad (\text{B.3})$$

$$K_2 \sin \gamma_2 = - \frac{a_1}{a_2} K_1 \sin \gamma_1 + \frac{a_3}{a_2} K_3 \sin \gamma_3 \quad (\text{B.4})$$

If these relationships are now substituted into the component expressions (A.4) and (A.5), one obtains:

$$\begin{aligned}
 & (K_1 \cos \gamma_1) m_1 p_1 - (K_1 \sin \gamma_1) m_1 q_1 + \left( -\frac{a_1}{a_2} K_1 \cos \gamma_1 + \frac{a_3}{a_2} K_3 \cos \gamma_3 \right) m_2 p_2 \\
 & - \left( -\frac{a_1}{a_2} K_1 \sin \gamma_1 + \frac{a_3}{a_2} K_3 \sin \gamma_3 \right) m_2 q_2 + (K_3 \cos \gamma_3) m_3 p_3 - (K_3 \sin \gamma_3) m_3 q_3 \\
 & = F_{M/G_X} - m_2 K_1 a_1 \cos \gamma_1 \quad (B.5)
 \end{aligned}$$

and

$$\begin{aligned}
 & (K_1 \sin \gamma_1) m_1 p_1 + (K_1 \cos \gamma_1) m_1 q_1 + \left( -\frac{a_1}{a_2} K_1 \sin \gamma_1 + \frac{a_3}{a_2} K_3 \sin \gamma_3 \right) m_2 p_2 \\
 & + \left( -\frac{a_1}{a_2} K_1 \cos \gamma_1 + \frac{a_3}{a_2} K_3 \cos \gamma_3 \right) m_2 q_2 + (K_3 \sin \gamma_3) m_3 p_3 + (K_3 \cos \gamma_3) m_3 q_3 \\
 & = F_{M/G_Y} - m_2 K_1 a_1 \sin \gamma_1 \quad (B.6)
 \end{aligned}$$

It may now be seen that the coefficients of  $m_2 p_2$  and  $m_2 q_2$  in each of the above expressions are linear combinations of the coefficients of the remaining terms.

This linear dependence will cause the resulting 6 x 6 matrix, obtained by writing equations (B.5) and (B.6) for three positions of the input angle  $\phi_1$  and needed for the solution of the six  $m_j p_j$  and  $m_j q_j$  parameters, to be singular.

## 2. Proof Of Nonsingularity Of Balancing Equation Matrix Used To Solve For General Mass-Distance Products

When the linear dependence of terms in equations (B.5) and (B.6) is removed with the help of the component loop equations (B.3) and (B.4), equations (A.17) and (A.18) result, i.e.

$$F_{M/G_X} = (K_1 \cos \gamma_1)P_1 - (K_1 \sin \gamma_1)Q_1 \\ + (K_3 \cos \gamma_3)P_3 - (K_3 \sin \gamma_3)Q_3 \quad (B.7)$$

$$\text{and } F_{M/G_Y} = (K_1 \sin \gamma_1)P_1 + (K_1 \cos \gamma_1)Q_1 \\ + (K_3 \sin \gamma_3)P_3 + (K_3 \cos \gamma_3)Q_3 \quad (B.8)$$

The linear independence of terms in each expression is assured since there are no further mechanism loop equations. Furthermore, both expressions are linearly independent of each other since they represent the orthogonal components of a single vector.

In order to solve for the four  $P_j$  and  $Q_j$  parameters, two sets of shaking force component equations of type (B.7) and (B.8) are now written for two mechanism positions<sup>1</sup>. In matrix form this becomes:

---

<sup>1</sup>Of course, all kinematic values and shaking force components must be known from experimentation for these two positions.

$$\begin{bmatrix}
 K_{11} \cos \gamma_{11} & -K_{11} \sin \gamma_{11} & K_{31} \cos \gamma_{31} & -K_{31} \sin \gamma_{31} \\
 K_{11} \sin \gamma_{11} & K_{11} \cos \gamma_{11} & K_{31} \sin \gamma_{31} & K_{31} \cos \gamma_{31} \\
 K_{12} \cos \gamma_{12} & -K_{12} \sin \gamma_{12} & K_{32} \cos \gamma_{32} & -K_{32} \sin \gamma_{32} \\
 K_{12} \sin \gamma_{12} & K_{12} \cos \gamma_{12} & K_{32} \sin \gamma_{32} & K_{32} \cos \gamma_{32}
 \end{bmatrix}
 \begin{bmatrix}
 P_1 \\
 Q_1 \\
 P_3 \\
 Q_3
 \end{bmatrix}
 =
 \begin{bmatrix}
 F_M/G_{X1} \\
 F_M/G_{Y1} \\
 F_M/G_{X2} \\
 F_M/G_{Y2}
 \end{bmatrix}
 \quad (B.9)$$

The second subscripts in these terms indicate at which position the quantity is evaluated.

Each of the four row vectors of the coefficient matrix is linearly independent as long as no pairs of links produce identical kinematic terms for the two chosen positions of the mechanism. Thus, the matrix has rank four and may be solved uniquely for the four general mass-distance products. (The only known exception to this is the parallel-bar linkage in which the first and third terms as well as the second and fourth terms of equations (B.7) and (B.8) will be identical.)

## APPENDIX C

DESCRIPTION OF AUGMENTED LAGRANGIAN OPTIMIZATION PROGRAM  
AND APPLICATION TO MINIMAX BALANCING OPTIMIZATION

This appendix deals with the Augmented Lagrangian program which is used in various parts of this dissertation.

Section 1 briefly outlines the theory which forms the basis of this optimization method. Section 2 describes the associated computer program and details the manner in which it is used. Section 3 shows the minimax solution of the overdetermined system of balancing equations as an example.

1. Theory Of Optimization Method

The optimization program is based upon the minimization of the Augmented Lagrangian type of penalty function:

$$\Phi(\bar{x}, \bar{\sigma}, \bar{\theta}) = F(\bar{x}) + \frac{1}{2} \sum_1 \sigma_i \left( c_i(\bar{x}) - \theta_i \right)^2 \quad (\text{C.1})$$

In the above,  $F(\bar{x}) = F(x_1, x_2, \dots, x_n)$  is the function to be minimized, which may be subject to the equality constraints

$$c_i(\bar{x}) = 0 \quad (i = 1, 2, \dots, k), \quad k \leq n, \quad (\text{C.2})$$

as well as the inequality constraints

$$c_i(\bar{x}) \geq 0 \quad (i = k+1, \dots, m). \quad (\text{C.3})$$

The optimization variables are represented by  $x_i$  ( $i = 1, 2, \dots, n$ ). The negative subscript following the penalty terms implies that a specific term of this type only then becomes active when the associated constraint is violated.

In each inner iteration, with fixed values of the parameters  $\bar{\sigma}$  and  $\bar{\theta}$ , the function  $\Phi(\bar{x}, \bar{\sigma}, \bar{\theta})$  is then minimized by the variable metric method of Davidon, Fletcher and Powell [21]. Outer iterations vary the values of the parameters  $\bar{\sigma}$  and  $\bar{\theta}$  such that the sequence of minima  $\bar{x}_{\sigma, \theta}$  tends to the solution of the constrained problem.

## 2. Description Of Computer Program

The core of the computer program consists of the five subroutines VF01AD, VF01ZD, MC11AD, VA09AD and VE04AD<sup>1</sup>. In addition, the user must supply a main program and an additional subroutine VF01BD. The latter serves to define the specific objective function  $F(\bar{x})$  and the associated constraints  $c_i(\bar{x})$  together with the derivatives of the objective function and the constraints with respect to all the variables involved.

The following gives sequential instructions for the

---

<sup>1</sup>All subroutines are written in Fortran with double precision arithmetic.

formulation of the main program and the subroutine VF01BD. The core program is reproduced in conjunction with the example in Section 3 of this appendix.

a. Main Program

The main program begins with the following COMMON statements which define the array sizes for the constraints C and their derivatives GC (the latter is only necessary if any of the derivatives are constant):

```
COMMON/VF01ED/C(3M)
COMMON/VF01FD/GC(N,M).
```

Subsequently, the following arguments are defined:

- N - An integer, set to the number of variables  $n$  ( $N \geq 2$ )
- M - An integer, set to the total number of constraints  $m$  ( $M \geq 1$ )
- K - An integer, set to the total number of equality constraints  $k$
- X - A real array of  $N$  elements representing the initial estimate of the solution set. (This estimate need not be feasible, i.e. satisfy the constraints.) After the first iteration, VF01AD returns the solution  $\bar{x}$  in X.

- AKMIN - A real number in which the relative error tolerance required in the constraint residuals must be set. (For example,  $AKMIN = 1 \times 10^{-3}$  indicates that no further outer iterations will take place if the largest scaled constraint residual changes by less than  $1 \times 10^{-3}$ . (See below.))
- EPS - A real array of N elements in which the tolerances for the unconstrained minimizations must be set (i.e. if all the variables do not change by more than these values in the successive inner iterations, this inner iteration is terminated).  $EPS(I)$  should be set so that  $EPS(I)/X(I) \approx AKMIN$ .
- DFN - A real number in which the likely reduction in  $F(\bar{x})$  from its initial value as obtained from X must be set. Since DFN is used only in the first iteration, an order of magnitude estimate suffices.
- MAXFN - An integer in which the maximum number of calls of VF01BD (the user supplied subroutine) on any one unconstrained minimization, i.e. inner iteration, must be set. The number 500 has proven to be reasonable for this purpose.

- IPR1 - An integer controlling the frequency of the printing of the outer iterations. Printing occurs every IPR1 outer iterations except for details of increases to the  $\sigma_1$  which are always printed. No printing at all occurs (except for diagnostics) if IPR1=0.
- IPR2 - An integer controlling the frequency of the printing of the inner iterations. Its use is similar to that of IPR1.
- IW - An integer giving the amount of storage available in COMMON/VF01LD/W(IW). Set to 2500 unless the restrictions that  $N \leq 25$  and  $M \leq 50$  are violated.
- MODE - An integer controlling the mode of operation of VF01AD. A usual setting is MODE=1. (See specification sheet for Harwell Subroutine Library.)

Next, the constraint scale factors, also designated  $C(1), C(2), \dots, C(M)$ , are set by substituting the initial approximations of  $x_1$  into the constraint equations and using the absolute values of the results.

If any of the constraints are linear functions of any of the variables, their derivatives with respect to these

variables, i.e. the resulting constants, must be given by way of the array  $GC(N,M)$ , where  $N$  represents the variable number and  $M$  stands for the constraint number.

Finally, the subroutine is called by:

```
CALL VF01AD(N,M,K,X,EPS,AKMIN,DFN,MAXFN,IPR1,IPR2,IW,MODE).
```

b. Subroutine VF01BD

This subroutine starts by way of:

```
SUBROUTINE VF01BD(N,M,X)
REAL X(N)
COMMON/VF01CD/F
COMMON/VF01DD/G(2N)
COMMON/VF01ED/C(3M)
COMMON/VF01FD/GC(N,M)
```

where  $F$  is the objective function  $F(\bar{x})$  in terms of variables  $x$

$G$  represents the derivatives of the objective function with respect to the variables

$C$  represents the constraints

$GC$  represents the derivatives of the nonlinear constraints with respect to the variables.

For use of derivatives of linear constraints, see previous section.

The subroutine must now define the terms listed below. Data as well as expressions required to obtain these terms may be introduced where convenient.

$$F = F(x_1, x_2, \dots, x_n)$$

$$G = G(1), G(2), \dots, G(N) = \frac{\partial F}{\partial x_1}, \frac{\partial F}{\partial x_2}, \dots, \frac{\partial F}{\partial x_n}$$

$C = C(1), C(2), \dots, C(M)$ . (These constraints must be given such that the resulting expression is equal to or greater than zero. For an example, see Section 3b.)

$$GC = GC(1,1), GC(1,2), \dots, GC(N,M) = \frac{\partial C(1)}{\partial x_1}, \frac{\partial C(2)}{\partial x_1}, \dots, \frac{\partial C(M)}{\partial x_n}$$

### 3. Example: Minimax Solution Of Overdetermined System Of Balancing Equations

The following shows how the computer program is adapted to the minimax solution of the overdetermined system of balancing equations according to the formulation given by equations (3.2) and (3.3). Section 3a shows how the various parameters are defined in the main program according to Section 2a above. Subsequently, a listing of the actual routine is given. Section 3b gives the applicable subroutine

VF01BD. Again, the listing of the final program is preceded by a detailed discussion. This subroutine is also used to call on subprograms FOURIE and MOTION which furnish certain kinematic terms of the mechanism. Section 3c shows the Augmented Lagrangian subroutines VF01AD, VF01ZD, MC11AD, VA09AD and VE04AD. Section 4d gives the most important parts of the output of the program and interprets the results.

a. Main Program

The main program, which is listed at the end of this section, begins with comment cards which are designed to serve as additional explanations. These are followed by the COMMON statement which defines the array size for the constraint C. The following variables are then defined:

N = 5; stands for the five variables  $P_1$ ,  $Q_1$ ,  $P_3$ ,  $Q_3$  and the objective function z.

M = 144; stands for the number of constraints, representing the square of the difference of the two shaking force components evaluated every 5 degrees between 0 and 355 degrees.

K = 0, since there are no equality constraints.

X(1) to X(5), the starting point estimates of the variables, are made 0.5 and  $1 \times 10^{-3}$  since previous experience has shown these values to be of this order of magnitude. (Such accurate estimates are not necessary. They only serve to decrease the number of iterations.)

With AKMIN chosen arbitrarily to be  $1 \times 10^{-3}$ , EPS(1) to EPS(5) result from X(1) to X(5).

DFN is chosen to be smaller than  $X(1) = 0.5$ , i.e it is made 0.4.

MAXFN = 500, as discussed earlier.

IPR1 = 1, to print every outer iteration.

IPR2 = 1, to print every inner iteration.

IW = 10,000, since there are more than 50 constraints.

MODE = 1, as indicated earlier.

Subsequently, a DO loop is set up to set the scale factors C(I) for all 144 constraints equal to 0.3. These are estimates of the magnitudes of the constraints when evaluated with the starting point values of the variables.

Since there are no linear constraints, the derivatives GC(N,M) do not enter this routine.

## MAIN

```

0001 C THIS PROGRAM WILL CHOOSE THE VALUES OF THE GENERAL MASS DISTANCE
0002 C PRODUCTS P1,P2,P3 AND Q3 WHICH WILL RESULT IN THE BEST MINIMAX FIT
0003 C OF THE COMPUTED SHAKING FORCE CURVES IN THE X AND Y DIRECTIONS TO
0004 C A KNOWN EXPERIMENTAL CURVE. THIS WILL BE ACCOMPLISHED BY THE
0005 C USE OF THE AUGMENTED LAGRANGIAN OPTIMIZATION ROUTINE.
0006 C THE VARIABLES FOR THIS PROBLEM ARE
0007 C X(1) = F = FUNCTION TO BE MINIMIZED
0008 C X(2) = P1
0009 C X(3) = P2
0010 C X(4) = P3
0011 C X(5) = Q3
0012 C
0013 C THE CONSTRAINTS ARE
0014 C C(1) * X(1) - FSK(1) - FSK(1)*Q2
0015 C C(1)*Q2 + X(1) - FSK(1) - FSK(1)*Q2, I=1,2,.....,72
0016 C IMPLICIT REAL*8(A-H,O-Z)
0017 C COMMON/FOLED/C(1432)
0018 C REAL*8 (F5),EPS(5)
0019 C V = 5
0020 C W = 144
0021 C K=0
0022 C P1=3.14159300
0023 C THE STARTING POINT IS ESTIMATED TO BE
0024 C X(1)=0.500
0025 C X(2)=1.00-3
0026 C X(3)=1.00-3
0027 C X(4)=1.00-3
0028 C X(5)=1.00-3
0029 C AKM(1)=10-3
0030 C EP5(1)=3.50-3
0031 C EP5(2)=1.00-3
0032 C EP5(3)=1.00-6
0033 C EP5(4)=1.00-5
0034 C EP5(5)=1.00-6
0035 C DFN=.407
0036 C MAXF=530
0037 C IPR1=1
0038 C IPR2=1
0039 C SET I=10000, IF MORE STORAGE IS REQUIRED, VFDIAD WILL
0040 C STOP AND WAIT FOR NEW REQUIREMENT.
0041 C I=10000)
0042 C MODE=1
0043 C THE CONSTRAINT SCALE FACTORS ARE ALL ESTIMATED TO BE 0.3
0044 C DO 10 I=1,144
0045 C C(1)=-.3000
0046 C CALL VFDIAD(V,W,K,X,EP5,AKM(I),DFN,MAXFN,IPR1,IPR2,I,,MODE)
0047 C STOP
0048 C END

```

- b. Subroutine VF01BD (See program, followed by subroutines FOURIE and MOTION, at the end of this section.)

After allocating storage for the various subscripted variables, the subroutine VF01BD starts with the COMMON statements indicated in Section 2a. The subsequent steps are:

1.  $F = X(1)$ , i.e. the objective function  $z$  is declared as the variable  $x_1$  (see equation (3.2)).
2.  $G(1) = 1$ , represents the derivative  $\frac{\partial F}{\partial x_1}$ . Since all other derivatives of  $F$  vanish, they must be set equal to zero (i.e.,  $G(2)$  to  $G(5) = 0$ ).
3.  $A1$  to  $A4$  represent the link dimensions of links 1 to 4.
4.  $DELPHI = 5$ , stands for the 5 degree increments of the input angle  $\phi_1$ .
5.  $P_1, Q_1, P_3$  and  $Q_3$  are defined as the remaining variables  $x_2, x_3, x_4$  and  $x_5$ .
6.  $FEX(1)$  to  $FEY(72)$  are the 144 experimentally obtained shaking force components at 5 degree intervals from 0 to 355 degrees. (See Table 3.3)

7. A DO loop is set up to compute the constraints (see equation (3.3)) as well as their derivatives. Since the constraints must be set up such that they are equal to or larger than zero, the constraints of the type

$$(F_{CX} - F_{EX})^2 \leq z \quad (C.4)$$

or  $(F_{CY} - F_{EY})^2 \leq z$  (see equation (C.3)), (C.5)

become

$$C(I) = z - (F_{CX} - F_{EX})^2 \quad (C.6)$$

or  $C(I) = z - (F_{CY} - F_{EY})^2$  (C.7)

The derivatives of the constraints are derivatives with respect to the variables  $z, P_1, Q_1, P_3, Q_3$ , i.e.  $x_1, x_2, x_3, x_4, x_5$ , respectively. Both the constraints and their derivatives are obtained with the help of expressions for the computed shaking force components  $F_{CX}$  and  $F_{CY}$ . The following first shows how these specific 144 quantities are computed. Subsequently, the formulation of the constraint equations and their derivatives will be discussed:

i) Subroutine FOURIE starts from the experimentally obtained angular velocities, read in in terms of RPM, and converts these to a Fourier series in which the angular velocity  $\dot{\phi}_1$  is expressed in terms of the angle  $\phi_1$ . The associated angular accelerations are subsequently obtained from

$$\ddot{\phi}_1 = \frac{d\dot{\phi}_1}{d\phi_1} \cdot \dot{\phi}_1 \quad (C.8)$$

ii) Subroutine MOTION computes  $\phi_3$ ,  $\dot{\phi}_3$  and  $\ddot{\phi}_3$  as functions of  $\phi_1$ ,  $\dot{\phi}_1$  and  $\ddot{\phi}_1$ .

iii) The coefficients of the shaking force component expressions (see equations (A.3), (A.17) and (A.18)) are computed in the following manner:

$$\begin{aligned} \text{VAR1(I)} &= \text{KAY1(I)} \times \text{COS(GMA1(I))} \\ \text{VAR2(I)} &= \text{KAY1(I)} \times \text{SIN(GMA1(I))} \\ \text{VAR3(I)} &= \text{KAY3(I)} \times \text{COS(GMA3(I))} \\ \text{VAR4(I)} &= \text{KAY3(I)} \times \text{SIN(GMA3(I))} \\ \text{VAR5(I)} &= \text{KAY1(I)} \times \text{SIN(GMA1(I))} \\ \text{VAR6(I)} &= \text{KAY1(I)} \times \text{COS(GMA1(I))} \\ \text{VAR7(I)} &= \text{KAY3(I)} \times \text{SIN(GMA3(I))} \\ \text{VAR8(I)} &= \text{KAY3(I)} \times \text{COS(GMA3(I))} \end{aligned}$$

where

$$KAY1(I) = \sqrt{(\dot{\phi}_{1I})^4 + (\ddot{\phi}_{1I})^2}$$

$$KAY3(I) = \sqrt{(\dot{\phi}_{3I})^4 + (\ddot{\phi}_{3I})^2}$$

$$GMA1(I) = \phi_{1I} - \tan^{-1} \frac{\ddot{\phi}_{1I}}{(\dot{\phi}_{1I})^2}$$

$$GMA3(I) = \phi_{3I} - \tan^{-1} \frac{\ddot{\phi}_{3I}}{(\dot{\phi}_{3I})^2}$$

iv) The shaking force components  $F_{CX1}$  and  $F_{CY1}$  are evaluated in terms of  $P_1$ ,  $Q_1$ ,  $P_3$  and  $Q_3$ . These are given as:

$$F_{CX1} = P_1 \times VAR1(I) - Q_1 \times VAR2(I) + P_3 \times VAR3(I) - Q_3 \times VAR4(I)$$

$$F_{CY1} = P_1 \times VAR5(I) + Q_1 \times VAR6(I) + P_3 \times VAR7(I) + Q_3 \times VAR8(I)$$

v) The constraint equations are written in the form of equations (C.6) and (C.7), i.e.

$$C(I) = X(1) - (F_{CX1} - F_{EX1})^2$$

$$\text{and } C(I+72) = X(1) - (F_{CY1} - F_{EY1})^2$$

vi) Finally, differentiation of the constraints with

respect to the variables gives:

$$GC(1, I) = 1$$

$$GC(1, I+72) = 1$$

$$GC(2, I) = AA \times VAR1(I)$$

$$GC(2, I+72) = BB \times VAR5(I)$$

$$GC(3, I) = -AA \times VAR2(I)$$

$$GC(3, I+72) = BB \times VAR6(I)$$

$$GC(4, I) = AA \times VAR3(I)$$

$$GC(4, I+72) = BB \times VAR7(I)$$

$$GC(5, I) = -AA \times VAR4(I)$$

$$GC(5, I+72) = BB \times VAR8(I)$$

where

$$AA = -2(F_{CXi} - F_{EXi})$$

$$BB = -2(F_{CYi} - F_{EYi})$$

```

0001      SUBROUTINE VFOIND(N,M,K)
0002      IMPLICIT REAL*8(A-H,O-Z)
0003      REAL*8 X(5)
0004      INTEGER PM(3), PHE(3), DELPM
0005      REAL*8 KAY1(360),KAY3(360)
0006      DIMENSION DMAT(360),DMAT3(360),FCY(360),FCY3(360)
0007      DIMENSION VAR1(360),VAR2(360),VAR3(360),VAR4(360)
0008      DIMENSION VAR5(360),VAR6(360),VAR7(360),VAR8(360)
0009      DIMENSION PS1A(360),PS1V(360)
0010      DOUBLE PRECISION DCUS,DSIN,DCOST,DATAN2
0011      DOUBLE PRECISION FEY(72),FEY(72)
0012      COMMON/FOID0/F
0013      COMMON/FOID1/G(10)
0014      COMMON/FOID2/G(12)
0015      COMMON/FOID3/DC(15,144)
0016      F(*,14157300
0017      C   DEFINE OBJECTIVE FUNCTION
0018      F=K(1)
0019      C   G(11)=PARTIAL DERIVATIVES OF OBJECTIVE FUNCTION WITH
0020      C   RESPECT TO VARIABLES K(1) THRU K(5)
0021      G(11)=100
0022      G(21)=000
0023      G(31)=000
0024      G(41)=000
0025      G(51)=000
0026      C   THE LINK DIMENSIONS ARE
0027      A1=200
0028      A2=8.500
0029      A3=300
0030      A4=8.20400
0031      DELPM = 6
0032      C   DEFINE REMAINING VARIABLES
0033      P1 = X(2)
0034      P2 = X(3)
0035      P3 = X(4)
0036      P4 = X(5)
0037      C   THE EXPERIMENTAL CHANGING FORCE COMPONENTS, DETERMINED
0038      C   EVERY 5 DEGREES, ARE GIVEN AS FOLLOWS, WHERE THE
0039      C   FIRST VALUE CORRESPONDS TO THE READING AT 0 DEGREES
0040      C   AND THE SEVENTY SECOND VALUE TO THE READING AT 355 DEGREES.
0041      FEY(11) = .477
0042      FEY(12) = .487
0043      FEY(13) = .447
0044      FEY(14) = .394
0045      FEY(15) = .258
0046      FEY(16) = .202
0047      FEY(17) = .105
0048      FEY(18) = .060
0049      FEY(19) = .030
0050      FEY(20) = .007
0051      FEY(111) = -.003
0052      FEY(112) = -.015
0053      FEY(113) = -.026
0054      FEY(114) = -.027
0055      FEY(115) = -.031
0056      FEY(116) = -.034

```

0043	FEK(17)	■	-.035
0047	FEK(19)	■	-.034
0050	FEK(19)	■	-.031
0051	FEK(20)	■	-.029
0052	FEK(21)	■	-.023
0053	FEK(22)	■	-.027
0054	FEK(23)	■	-.024
0055	FEK(24)	■	-.023
0056	FEK(25)	■	-.020
0057	FEK(25)	■	-.015
0058	FEK(27)	■	-.012
0059	FEK(28)	■	-.012
0060	FEK(27)	■	-.015
0061	FEK(30)	■	-.017
0062	FEK(31)	■	-.019
0063	FEK(32)	■	-.021
0064	FEK(33)	■	-.024
0065	FEK(34)	■	-.027
0066	FEK(35)	■	-.030
0067	FEK(36)	■	-.031
0068	FEK(37)	■	-.032
0069	FEK(38)	■	-.033
0070	FEK(39)	■	-.037
0071	FEK(40)	■	-.039
0072	FEK(41)	■	-.033
0073	FEK(42)	■	-.032
0074	FEK(43)	■	-.030
0075	FEK(44)	■	-.041
0076	FEK(45)	■	-.045
0077	FEK(46)	■	-.051
0078	FEK(47)	■	-.053
0079	FEK(48)	■	-.056
0080	FEK(49)	■	-.051
0081	FEK(50)	■	-.063
0082	FEK(51)	■	-.072
0083	FEK(52)	■	-.077
0084	FEK(53)	■	-.084
0085	FEK(54)	■	-.091
0086	FEK(55)	■	-.096
0087	FEK(55)	■	-.101
0088	FEK(57)	■	-.113
0089	FEK(58)	■	-.119
0090	FEK(59)	■	-.126
0091	FEK(60)	■	-.134
0092	FEK(61)	■	-.143
0093	FEK(62)	■	-.147
0094	FEK(63)	■	-.150
0095	FEK(64)	■	-.144
0096	FEK(65)	■	-.123
0097	FEK(65)	■	-.110
0098	FEK(67)	■	-.081
0099	FEK(68)	■	-.032
0100	FEK(69)	■	.035
0101	FEK(70)	■	.122
0102	FEK(71)	■	.258
0103	FEK(72)	■	.356

0104	FEY(11)	* -.570
0105	FEY(2)	* -.590
0106	FEY(3)	* -.551
0107	FEY(4)	* -.463
0108	FEY(5)	* -.374
0109	FEY(6)	* -.282
0110	FEY(7)	* -.213
0111	FEY(8)	* -.173
0112	FEY(9)	* -.120
0113	FEY(10)	* -.087
0114	FEY(11)	* -.066
0115	FEY(12)	* -.054
0116	FEY(13)	* -.039
0117	FEY(14)	* -.029
0118	FEY(15)	* -.024
0119	FEY(16)	* -.019
0120	FEY(17)	* -.012
0121	FEY(18)	* -.009
0122	FEY(19)	* -.006
0123	FEY(20)	* 0.0
0124	FEY(21)	* .006
0125	FEY(22)	* .009
0126	FEY(23)	* .015
0127	FEY(24)	* .023
0128	FEY(25)	* .026
0129	FEY(26)	* .030
0130	FEY(27)	* .034
0131	FEY(28)	* .043
0132	FEY(29)	* .054
0133	FEY(30)	* .065
0134	FEY(31)	* .075
0135	FEY(32)	* .083
0136	FEY(33)	* .093
0137	FEY(34)	* .099
0138	FEY(35)	* .116
0139	FEY(36)	* .122
0140	FEY(37)	* .127
0141	FEY(38)	* .132
0142	FEY(39)	* .141
0143	FEY(40)	* .144
0144	FEY(41)	* .150
0145	FEY(42)	* .153
0146	FEY(43)	* .155
0147	FEY(44)	* .156
0148	FEY(45)	* .154
0149	FEY(46)	* .150
0150	FEY(47)	* .160
0151	FEY(48)	* .160
0152	FEY(49)	* .161
0153	FEY(50)	* .161
0154	FEY(51)	* .161
0155	FEY(52)	* .160
0156	FEY(53)	* .160
0157	FEY(54)	* .159
0158	FEY(55)	* .159
0159	FEY(56)	* .156

```

0160          FEY(57) = .155
0161          FEY(58) = .153
0162          FEY(59) = .150
0163          FEY(60) = .146
0164          FEY(61) = .144
0165          FEY(62) = .134
0166          FEY(63) = .129
0167          FEY(64) = .116
0168          FEY(65) = .096
0169          FEY(66) = .074
0170          FEY(67) = .044
0171          FEY(68) = -.023
0172          FEY(69) = -.111
0173          FEY(70) = -.206
0174          FEY(71) = -.345
0175          FEY(72) = -.452
0176          Z=PI/1.3702

C
0177          DO 120 PHID(1)=1,356,DELPHI
0178          PHID=PHID(1) - 1
0179          PHI=Z * PHID
0180          I = PHID/DELPHI + 1
C      THE ANGULAR VELOCITIES AND ACCELERATIONS ARE DETERMINED
C      IN SUBROUTINE FOURIE
0181          CALL FOURIE (I,PHIVEL,PHIACC)
C      THE KINEMATICS OF THE LINKAGE ARE DETERMINED IN
C      SUBROUTINE MOTION
0182          CALL MOTION (PHI, A1, A2, A3, A4, PSI, PHIVEL, PHIACC,
C      I
C      PSIV(I), PSIA(I))
0183          XAY1(I) = USQRT(PHIVEL**4 + PHIACC**2)
0184          XAY3(I) = USQRT(PSIV(I)**4 + PSIA(I)**2)
0185          GM1(I) = PHI - DATAN2(PHIACC,PHIVEL**2)
0186          GM3(I) = PSI - DATAN2(PSIV(I),PSIV(I)**2)
0187          VAR1(I) = XAY1(I)*DCOS(GM1(I))
0188          VAR2(I) = XAY1(I)*DSIN(GM1(I))
0189          VAR3(I) = XAY3(I)*DCOS(GM3(I))
0190          VAR4(I) = XAY3(I)*DSIN(GM3(I))
0191          VAR5(I) = XAY1(I)*DSIN(GM1(I))
0192          VAR6(I) = XAY1(I)*DCOS(GM1(I))
0193          VAR7(I) = XAY3(I)*DSIN(GM3(I))
0194          VAR8(I) = XAY3(I)*DCOS(GM3(I))
C      THE COMPUTED SHAKING FORCES ARE
0195          FCX(I) = P1*VAR1(I)-Q1*VAR2(I)+P3*VAR3(I)-Q3*VAR4(I)
0196          FCY(I) = P1*VAR5(I)+Q1*VAR6(I)+P3*VAR7(I)+Q3*VAR8(I)
C      THE CONSTRAINTS ARE
0197          C(1) = X(I) - (FCX(I) - FEY(I))**2
0198          C(1+72) = X(I) - (FCY(I) - FEY(I))**2
C      THE TERMS G(I,N) REPRESENT THE DERIVATIVES OF THE
C      * CONSTRAINTS WITH RESPECT TO THE N VARIABLES
0199          GC(1,1) = 100
0200          GC(1,1+72) = 100
0201          AA = -200*(FCX(I) - FEY(I))
0202          BB = -200*(FCY(I) - FEY(I))
0203          GC(2,1) = AA*VAR1(I)
0204          GC(2,1+72) = BB*VAR5(I)
0205          GC(3,1) = -AA*VAR2(I)

```

```
0205          GC(3,1+72) = 59*VAR6(1)
0207          GC(4,1) = 1A*VAR3(1)
0209          GC(4,1+72) = 8B*VAR7(1)
0207          GC(5,1) = -A1*VAR4(1)
0210          GC(5,1+72) = 8B*VAR8(1)
0211      120 CONTINUE
0212          RETURN
0213          END
```

```

0001      SUBROUTINE FOURIE (X,PHIVEL,PHIACC)
0002      (IMPLICIT REAL*8(A-Z)
C      PROGRAM TO TAKE DISCRETE EXPERIMENTAL READINGS OF RPM AND
C      CONVERT TO A CONTINUOUS CURVE OF ANGULAR VELOCITY AS A
C      FUNCTION OF THE INPUT LINK ANGLE. THIS FOURIER SERIES IS THEN
C      DIFFERENTIATED TO GIVE AN EXPRESSION FOR THE ANGULAR ACCELERATION
0003      INTEGER I,J,K
0004      DIMENSION PHI(72),PHID(72),A(36),B(36)
0005      DOUBLE PRECISION DCOS,DSIN
0006      DOUBLE PRECISION RPM(72)
C      INSERT DATA FROM AUTOMATED VELOCITY MEASUREMENT
0007      RPM(1) = 121.90
0008      RPM(2) = 123.56
0009      RPM(3) = 123.92
0010      RPM(4) = 123.78
0011      RPM(5) = 122.54
0012      RPM(6) = 121.71
0013      RPM(7) = 121.07
0014      RPM(8) = 120.24
0015      RPM(9) = 119.72
0016      RPM(10) = 119.13
0017      RPM(11) = 119.73
0018      RPM(12) = 119.34
0019      RPM(13) = 119.14
0020      RPM(14) = 117.75
0021      RPM(15) = 117.81
0022      RPM(16) = 117.71
0023      RPM(17) = 117.66
0024      RPM(18) = 117.62
0025      RPM(19) = 117.67
0026      RPM(20) = 117.69
0027      RPM(21) = 117.76
0028      RPM(22) = 117.85
0029      RPM(23) = 117.78
0030      RPM(24) = 119.13
0031      RPM(25) = 119.32
0032      RPM(26) = 119.52
0033      RPM(27) = 119.32
0034      RPM(28) = 119.12
0035      RPM(29) = 119.47
0036      RPM(30) = 119.35
0037      RPM(31) = 120.32
0038      RPM(32) = 120.33
0039      RPM(33) = 121.34
0040      RPM(34) = 121.44
0041      RPM(35) = 122.49
0042      RPM(36) = 123.10
0043      RPM(37) = 123.45
0044      RPM(38) = 123.93
0045      RPM(39) = 124.11
0046      RPM(40) = 124.32
0047      RPM(41) = 124.47
0048      RPM(42) = 124.55
0049      RPM(43) = 124.57
0050      RPM(44) = 124.51
0051      RPM(45) = 124.59

```

```

0052      RPM(46) = 124.30
0053      RPM(47) = 124.33
0054      RPM(48) = 124.29
0055      RPM(49) = 123.95
0056      RPM(50) = 123.56
0057      RPM(51) = 123.10
0058      RPM(52) = 122.56
0059      RPM(53) = 121.95
0060      RPM(54) = 121.17
0061      RPM(55) = 120.30
0062      RPM(56) = 117.43
0063      RPM(57) = 113.50
0064      RPM(58) = 117.32
0065      RPM(59) = 117.79
0066      RPM(60) = 115.26
0067      RPM(61) = 115.60
0068      RPM(62) = 114.75
0069      RPM(63) = 114.37
0070      RPM(64) = 113.75
0071      RPM(65) = 113.54
0072      RPM(66) = 113.60
0073      RPM(67) = 113.92
0074      RPM(68) = 114.49
0075      RPM(69) = 115.32
0076      RPM(70) = 115.50
0077      RPM(71) = 119.30
0078      RPM(72) = 120.35
0079      PI = 3.141592653589793
0080      Z = PI/1.502
0081      DELPHI = 5.00*Z
0082      PHI(1) = 0.00
0083      CO 10 I = 1.71
0084      PHI(I+1) = PHI(I) + DELPHI
0085      10 CONTINUE
0086      CO 20 I = 1.72
0087      PHID(I) = RPM(I)*200*PI/360
0088      20 CONTINUE
0089      SUMA0 = 000
0090      CO 30 I = 1.72
0091      SUMA0 = SUMA0 + PHID(I)
0092      30 CONTINUE
0093      A0 = (1.00/3.601)*SUMA0
0094      CO 40 N = 1.36
0095      SUMA1 = 000
0096      SUMA2 = 000
0097      CO 50 I = 1.72
0098      SUMA1 = SUMA1 + PHID(I)*COS(N*PHI(I))
0099      SUMA2 = SUMA2 + PHID(I)*SIN(N*PHI(I))
0100      50 CONTINUE
0101      A(1) = (1.00/3.601)*SUMA1
0102      B(1) = (1.00/3.601)*SUMA2
0103      40 CONTINUE
0104      F = 000
0105      CO 80 N = 1.36

```

```

0106      C   THE FOURIER SERIES OF THE ANGULAR VELOCITY IS
0107      F = F + A(N)*DCOS(N*PHI(K)) + B(N)*DSIN(N*PHI(K))
0108      90 CONTINUE
0109      PHIVEL = F + A0/2.00
0109      S=C00
0110      DO 21 N=1,36
0111      C   DIFFERENTIATING THE FOURIER SERIES OF THE ANGULAR VELOCITY WILL
0112      C   YIELD THE FOLLOWING EXPRESSION FOR THE ANGULAR ACCELERATION
0113      S=G + (-N*A(N))*DSIN(N*PHI(K)) + N*B(N)*DCOS(N*PHI(K))*PHI(DK)
0114      21 CONTINUE
0115      PHIACC = S
0116      RETURN
0117      END

```

```

0001      SUBROUTINE MOTION (PHI,A1,A2,A3,A4,PSI,PHIVEL,PHIACC,
          L
          PSIVEL,PSIACC)
C
C      THIS SUBROUTINE CALCULATES THE OUTPUT LINK ANGLE,
C      ANGULAR VELOCITY AND ANGULAR ACCELERATION AS FUNCTIONS OF
C      THE INPUT LINK ANGLE, ANGULAR VELOCITY AND ANGULAR ACCELERATION
C
0002      IMPLICIT REAL*8(A-H,O-Z)
0003      DOUBLE PRECISION DCOS, DSIN,DSQRT,DATAN2,DABS
0004      REAL*8 LAMBDA, LAMVEL, LAMACC
0005      PI=3.14157300
0006      TAUPI = 200*PI
0007      A = DSIN(PHI)
0008      B = DCOS(PHI) -A4/A1
0009      C = (A1*A1 - A2*A2 + A3*A3 + A4*A4)/(2.0*A1*A3) - A4* DCOS(PHI)/A3
0010      ROOT = DSQRT (A*A + B*B - C*C)
0011      PSI = 2.0 * DATAN2(A-ROOT, B*C)
0012      IF (PSI) 10,20,20
0013      10 PSI = PSI + TAUPI
0014      20 SA=DSIN(PHI)
0015      CA = DCOS (PHI)
0016      SB = DSIN(PSI)
0017      CB = DCOS (PSI)
0018      LAMBDA = DATAN2 (A3*SB-A1*SA,A3*CB+A4-A1*CA)
0019      IF (LAMBDA) 30,40,40
0020      30 LAMBDA = LAMBDA + 200*PI
0021      40 TAU1 = DSIN(PHI-LAMBDA)
0022      TAU3 = DSIN(PSI-LAMBDA)
C
C      CASE IN WHICH TAU3 GOES TO ZERO
0023      IF (DABS(TAU3)-10-3) 60,50,50
0024      50 TAU7 = DSIN(PHI-PSI)
0025      PSIVEL = PHIVEL*A1*TAU1/(A3*TAU3)
0026      LAMVEL = PHIVEL*A1*TAU7/(A2*TAU3)
0027      TAUDT1 = DCOS (PHI-LAMBDA) * (PHIVEL-LAMVEL)
0028      TAUDT3 = DCOS (PSI-LAMBDA) * (PSIVEL-LAMVEL)
0029      TAUDT7 = DCOS (PHI-PSI) * (PHIVEL-PSIVEL)
0030      PSIACC = PHIACC*PSIVEL/PHIVEL + PHIVEL*A1*(TAUDT1-TAUDT3*TAU1/
          L
          TAU3)/(A3*TAU3)
0031      LAMACC = PHIACC*LAMVEL/PHIVEL + PHIVEL*A1*(TAUDT7-TAUDT3*TAU7/
          L
          TAU3)/(A2*TAU3)
          L
0032      GO TO 999
0033      60 LAMVEL = 0.0
0034      LAMACC = 0.0
0035      PSIVEL = 0.0
0036      PSIACC = 0.0
0037      999 RETURN
0038      END

```

c. Augmented Lagrangian Subroutines

The following lists the Augmented Lagrangian subroutines VF01AD, VF01ZD, MC11AD, VA09AD and VE04AD for the convenience of the reader.

```

0001 SUBROUTINE VF01AD(N,N,K,X,SPS,AKM1,DFV,MAXF1,IPR1,IPR2,LM,"DDF")
0002 IMPLICIT REAL*8(A-H,J-Z)
0003 REAL*8 X(1),EPS(1)
0004 COMMON/VF01CD/F,N,K,L,IS,M,K,YU
0005 COMMON/VF01UD/J(17)
0006 COMMON/VF01ED/C(17)7)
0007 COMMON/VF01FD/GC(217)1
0008 COMMON/VF01SD/TL(317)1
0009 COMMON/VF01HD/GP(477)1
0010 COMMON/VF01IU/G2P(15)1
0011 COMMON/VF01UD/Y(479)1
0012 COMMON/VF01KD/W(1317)1
0013 COMMON/VF01LO/W(10000)1
0014 COMMON/VF01MO/ZZ(873)1
0015 COMMON/VF01VD/LT(879)1
0016 EXTENAL V=01ZD
0017 FORMAT(10I5)
0018 FORMAT(30I5,7I
0019 NU=MAX(25,N)
0020 IF(N.GT.50)NU=N
0021 IX=N
0022 ICS=M
0023 ICB=M+Y
0024 IS=M
0025 LL=IS+M
0026 IP=M
0027 LLT=M
0028 NN=N+1+1/2
0029 MM=M
0030 KL=M
0031 MVS=0
0032 AK=1060
0033 R=1D0
0034 MK=0
0035 CD 1 I=1,M
0036 C(ICS+1)=C(1)
0037 CALL VF01RJ(N,M,X)

```

C

```

0038 DF=DFV
0039 IF(DF.NE.LT+.0001)DF=0D85(DFV**2)
0040 IF(DF.NE.EQ.0D0)DF=F
0041 IF(DF.LE+.0001)DF=1D0
0042 DD 2 I=1,M
0043 CC=C(1)
0044 IF(1.GT.K)CC=0M/V(1)C(2+DD)1
0045 IF(1DABS(C(1)-ST.C(ICS+1))C(ICS+1)=D85(CC)
0046 CONTINUE
0047 IF(IPR1.EQ.0)GOTO6
0048 IF(MOD(MIN(I,PR1),N)=0)GOTO7
0049 PRINT 1792
0050 FORMAT(1E11Y TD VFOIA'///'CONSTRAIYF SCALE PARAMETERS ARE')
0051 PRINT 1001,(C(ICS+1),I=1,M)
0052 CONTINUE
0053 IF(MODEALY.01)GOTO5
0054 UD 3 I=1,M
0055 T(1S+1)=2D3*GF/C(ICS+1)**2

```

```

0056      T(I)=000
0057      CONTINUE
0058      MD=IABS(MODE)
0059      CONTINUE
0060      MINS=MINS+1
0061      DO 9 I=1,M
0062      W(I)=G2P(I)
0063      IF(IPR1.EQ.0)GOTO7
0064      IF(MD*MINS,(PR1).NE.0)GOTO7
0065      PRINT 1003,MINS
0066      FORMAT(//'OUTER ITERATION NUMBER IS',I3)
0067      CONTINUE
0068      PRINT 1004,(X(I),I=1,M)
0069      PRINT 1005
0070      FORMAT('OT-FTAI()')
0071      PRINT 1001,(T(I),I=1,M)
0072      PRINT 1006
0073      FORMAT('OS(GNA())')
0074      PRINT 1001,(T(S+1),I=1,M)
0075      CONTINUE
0076      CALL VAO9AJ(VF01ZD,N,X,PHI,GP,M,M,CF,EP5,MD,MAXFN,IPR2,(EXIT))
0077      CALL VF01B(N,M,X)
0078      MD=3
0079      AKK=000
0080      DO 10 I=1,M
0081      CC=C(I)
0082      IF(I.GT.K.AND.C(I).GE.(I))CC=DMINI(CC,000)
0083      T(I)=T(I)+I
0084      W(I)=DASS(CC)/C(IC5+1)
0085      IF(W(I).GT.AKK)AKK=W(I)
0086      CONTINUE
0087      IF(IPR1.EQ.0)GOTO16
0088      IF(MD*MINS,(PR1).NE.0)GOTO15
0089      PRINT 1007
0090      FORMAT('DEBIT FROM VAO9AD//OLAGRANDE MULTIPLIER ESTIMATES')
0091      PRINT 1001,(I),I=1,M)
0092      PRINT 1008
0093      FORMAT('LARGEST SCALED CONSTRAINT VIOLATION//
1' THIS ITERATION, BEST ITERATION')
0094      PRINT 1001,AKK,AK
0095      PRINT 1009
0096      FORMAT('CONSTRAINT RESIDUALS')
0097      PRINT 1001,(C(I),I=1,M)
0098      PRINT 1010
0099      FORMAT('SCALED CONSTRAINT VIOLATIONS')
0100      PRINT 1001,(W(I),I=1,M)
0101      CONTINUE
0102      IF(LEXTJ.EJ.0)JA,(EAT,EQ.)GOTO20
0103      IF(AKK.LE.AKMIN)GOTO20
0104      IF(AKK.GE.AK)GOTO11
0105      DO 15 I=1,M
0106      G2P(I)=W(I)
0107      DO 17 I=1,M
0108      IF(.GT.K.AND.V(I).EQ.000.AND.C(I).GT.000)GOTO17
0109      Z(I(I+1))=-I(I5+1)*C(I)
0110

```

```

0111      IF(I.GT.K.AND.ZZ(IP+1).LT.-T(I))ZZ(IP+1)=-T(I)
0112      17 CONTINUE
0113      IF(MINS.EQ.1)GOTO40
0114      GOTO18
0115      11 CONTINUE
0116      DO 14 I=1,N
0117      IF(W(I).LE.AK.DR.C(I)CB+1).SE.400*W(I)GOTO14
0118      DS=900*(IS+1)
0119      TIS+1)=1DI*TIS+1)
0120      IF(IPR.LE.0)PRINT 1011,I,T(IS+1)
0121      1011 FORMAT('SIGMA(',I3,') INCREASED TO ',D15.7)
0122      DO 12 J=1,N
0123      V(J)=GC(I)-1)*NU+J)
0124      CALL MC11A)(G2P,N,V,DS+V,N,N,DS)
0125      14 CONTINUE
0126      19 CONTINUE
0127      DO 13 I=1,N
0128      IF(DABS(X(I))-G(I)X+1)).GT.E*5(I)GOTO21
0129      13 CONTINUE
0130      PRINT 1013
0131      1013 FORMAT('REQUESTED ACCURACY NOT OBTAINED')
0132      20 CONTINUE
0133      IF(EXIT.EQ.0)PRINT 2000
0134      2000 FORMAT('MATRIX SET IN G2P BY USER IS NOT POSITIVE DEFINITE')
0135      IF(IPR.EQ.0)RETURN
0136      PRINT 1012
0137      1012 FORMAT('BEST SOLUTION OBTAINED'/OF,(3(I),I=1,N))
0138      PRINT 1001,F,1011,I=1,N)
0139      RETURN
0140      21 CONTINUE
0141      IF(AK.LT.AK)GOTO40
0142      DO 32 I=1,N
0143      V(I)=T(IL+1)
0144      GOTO70
0145      40 CONTINUE
0146      KK=0
0147      KK=0
0148      DO 41 I=1,N
0149      T(IL+1)=T(I)
0150      C(I)CB+1)*W(I)
0151      IF(I.GT.K.AND.T(IL+1).EQ.0).AND.C(I).GT.0)GOTO41
0152      KK=KK+1
0153      LT(IL+KK)=1
0154      GP(KK)=-1030
0155      IF(I.GT.K),PI(KK)=-T(IL+1)
0156      V(KK)=1030
0157      ZZ(KK)=-C(I)
0158      41 CONTINUE
0159      IF(KK.EQ.0)GOTO20
0160      DO 42 I=1,N
0161      42 G(I)X+1)=X(I)
0162      KKK=KK+PI(KK+1)/2
0163      I=MAX0(KK+NN,KK*KK)
0164      IF(I.LE.14)GOTO50
0165      PRINT 2001,I
0166      2001 FORMAT('INCREASE STORAGE IN COMMON/VARIABLES',I7,'ELEMENTS')

```

```

0167      RETURN
0168      50 CONTINUE
0169      II=I4-KKK
0170      DO 53 I=1, KK
0171      LI=LT(I,LT+1)
0172      DO 51 JJ=L,N
0173      51 X(JJ)=GC((L,I-1)*NU+JJ)
0174      CALL MC11B(W,N,X,X,N)
0175      DO 53 J=1,I
0176      LJ=LT(I,LT+J)
0177      Z=000
0178      DO 52 JJ=1,N
0179      52 Z=Z+X(JJ)*GC((LJ-1)*NU+JJ)
0180      II=II+1
0181      53 W(II)=Z
0182      JJ=I4-KKK
0183      II=0
0184      DO 55 I=1, KK
0185      DO 55 J=1, I
0186      JJ=JJ+1
0187      55 W((I+J)*NU+JJ)
0188      56 II=II+KK
0189      CALL VED4A(KK,W,KK,ZZ,GP,7,T,Z,LT, JJ,W)
0190      IF(IPR1.EQ.0)GOTO59
0191      IF(MOD(MING,IPR1).NE.0)GOTO59
0192      PRINT 1020, KK
0193      1020 FORMAT(14, ' ACTIVE CONSTRAINTS, NUMBERED')
0194      PRINT 1000, (LT(I,LT+I), I=1, KK)
0195      PRINT 1021
0196      1021 FORMAT('LAGRANGE MULTIPLIER CORRECTIONS FOR ACTIVE CONSTRAINTS')
0197      PRINT 1001, (T(II), I=1, KK)
0198      59 CONTINUE
0199      DO 60 I=1, 4
0200      60 V(II)*T(I,LT+1)
0201      DO 62 I=1, KK
0202      LI=LT(I,LT+1)
0203      V(LI)=V(LI)+T(II)
0204      Z=400*ABS(V(LI)-ZZ(IP+LI))/ZZ(IP+LI)
0205      IF(Z.LE.100)GOTO62
0206      US=(Z-100)*T(II+LI)
0207      T(II+LI)=Z+T(II+LI)
0208      IF(IPR1.NE.0)PRINT 1011, LI, T(II+LI)
0209      DO 61 J=1, N
0210      61 GP(J)=GC((L,I-1)*NU+JJ)
0211      CALL MC11A(GP,N,GP,DS,GP,N,N,DS)
0212      62 CONTINUE
0213      AK=8KK
0214      70 CONTINUE
0215      DO 71 I=1, 4
0216      71 T(II)=V(II)/T(II+1)
0217      DO 72 I=1, 4
0218      72 X(II)=G(I,X+1)
0219      DF=1050
0220      GOTO9
0221      END

```

```

0001 SUBROUTINE VFOI2D(N,X,PHI,IPHI)
0002 IMPLICIT REAL*8(A-H,O-Z)
0003 REAL*8 X(1),GPHI(1)
0004 COMMON/VFOI2D/F,M,X,IS,MK,IU
0005 COMMON/VFOI2D/S(10)
0006 COMMON/VFOIFD/G(1317)
0007 COMMON/VFOIFD/SC(2125)
0008 COMMON/VFOI2D/T(1317)
0009 IF(MK.E2.1)CALL VFOI90(N,X)
0010 MK=1
0011 PHI=300
0012 DO 10 I=1,N
0013   IN GPHI(I)=G(I)
0014   DO 12 J=1,M
0015     CC=C(I)-T(I)
0016     IF(I.GT.4)CC=OMI*H(CS,300)
0017     Y=T((S+I)*CC
0018     IF(Y.EQ.003)30T012
0019     PHI=PHI+Y*CC
0020   DO 11 J=L,I
0021     GPHI(J)=GPHI(J)+Y*CC((I-1)*NU+J)
0022   12 CONTINUE
0023   PHI=.500*P+I*F
0024   RETURN
0025   END

```

```

0001 SUBROUTINE MCLLAD(A,V,E,S;M,L,IMX,EP5)
0002 IMPLICIT REAL*9(A-H,O-Z)
0003 DIMENSION A(1),Z(1),M(1)
C UPDATE FACTORS GIVEN (Y A 3Y SIG=Z+ZTRAYSP7SE
A(1)=A(1)+SIS *Z(1)**2
IR=1
IF(A(1).GT.000)RETURN
A(1)=0.70
IR=0
RETURN
1 CONTINUE
NP=V+1
IF(SIG.GT.000)GOTO40
IF(SIG.EQ.000.OR.(R.EQ.0)RETURN
TI=100/SIG
1V=1
IF(V<=E)GOTO10
DO 7 I=1,N
IF(A(I).NE.000)FI=(TI+M(I))*Z/A(I)
7 I=A(I)+NP-I
GOTO20
10 CONTINUE
DO 11 I=1,N
M(I)=Z(I)
DO 15 I=L,N
IP=I+1
V=M(I)
IF(A(I).GT.000)GOTO12
M(I)=0.00
I=A(I)+NP-I
GOTO15
12 CONTINUE
TI=TI+V**2/A(I)
IF(TI.EQ.0)GOTO14
DO 13 J=1,P,N
I=A(J)+1
M(J)=M(J)-V*A(I)
13 M(J)=M(J)-V*A(I)
14 I=I+1
15 CONTINUE
20 CONTINUE
IF(TI.LE.0)GOTO21
IF(TI.GT.0)GOTO22
IF(V<=1)40,40,23
21 TI=0.00
IR=IR-1
GOTO23
22 FI=EPS/SIG
IF(EPS.EQ.000)IR=IR-1
23 CONTINUE
M=1
TIM=TI
DO 30 I=1,N
I=NP-I
IF(A(I).NE.000)TI=TI-M(I)**2/A(I)
0051
0052
0053
0054
0055

```

```

0056      W(I,J)=TI
0057      TI=TIM
0058      GOTD41
0059      CONTINUE
0060      M=M+1
0061      TIM=100/SEI
0062      CONTINUE
0063      IJ=1
0064      DO 66 I=1,N
0065      IP=I+1
0066      V=Z(I,I)
0067      IF(A(I,I).GT.0.001)GOTD53
0068      IF(I.R.GT.0.0R.SIG.LT.0.00.01.V.E3.000)GOTD52
0069      IR=I-IR
0070      A(I,I)=V**2/TIM
0071      IF(I.EQ.N)RETURN
0072      DO 51 J=IP,N
0073      IJ=IJ+1
0074      A(I,J)=Z(I,J)/V
0075      RETURN
0076      CONTINUE
0077      TI=TIM
0078      IJ=IJ+NP-1
0079      GOTD56
0080      CONTINUE
0081      AL=V/A(I,I)
0082      IF(M)54,54,55
0083      TI=TIM+V*AL
0084      GOTD56
0085      TI=4111
0086      CONTINUE
0087      R=TI/TIM
0088      A(IJ)=A(IJ)*R
0089      IF(R.E3.00)GOTD70
0090      IF(I.E3.N)GOTD70
0091      B=AL/PI
0092      IF(R.GT.40)GOTD62
0093      DO 51 J=IP,N
0094      IJ=IJ+1
0095      Z(I)=Z(I)-V*A(I,J)
0096      A(I,J)=A(I,J)+B*Z(I,J)
0097      GOTD54
0098      GM=TIM/PI
0099      DO 63 J=IP,N
0100      IJ=IJ+1
0101      Y=A(I,J)
0102      A(IJ)=B*Z(IJ)+Y*GM
0103      Z(IJ)=Z(IJ)-Y*Y
0104      CONTINUE
0105      TI=TI
0106      IJ=IJ+1
0107      CONTINUE
0108      TA=CONTINUE
0109      IF(IR.LT.0)IR=-IR
0110      RETURN

```

C FACTORIZE A MATRIX GIVEN IN A

```

0111      ENTRY 'C1130(A,N,IR)
0112      IR=N
0113      IF(N.GT.1)GOTO100
0114      IF(A(1).GT.000)RETURN
0115      A(1)=0.00
0116      IR=0
0117      RETURN
0118      100 CONTINUE
0119      NP=N+1
0120      II=1
0121      DO 104 I=2,N
0122      AA=A(II)
0123      VI=II*IP-1
0124      IF(AA.GT.000)GOTO101
0125      A(II)=0.00
0126      IR=IR+1
0127      II=II+1
0128      GOTO104
0129      101 CONTINUE
0130      IP=II+1
0131      II=II+1
0132      JK=II
0133      DO 103 IJ=IP,N
0134      V=A(IJ)/AA
0135      DO 102 IK=IJ,N
0136      A(IK)=A(IK)-A(IJ)*V
0137      JK=JK+1
0138      103 A(IJ)=V
0139      104 CONTINUE
0140      IF(A(II).GT.000)RETURN
0141      A(II)=0.00
0142      IR=IR+1
0143      RETURN
0144      C  MULTIPLY OUT THE FACTORS GIVEN IN A
0145      ENTRY 'C1130(A,N)
0146      NP=N+1
0147      II=NP/2
0148      DO 202 IJ=2,N
0149      JK=II
0150      VI=II-1
0151      II=II-1
0152      AA=A(II)
0153      IP=II+1
0154      IF(AA.GT.000)GOTO201
0155      DO 204 IJ=IP,N
0156      A(IJ)=0.00
0157      GOTO202
0158      201 CONTINUE
0159      DO 201 IJ=IP,N
0160      V=A(IJ)/AA
0161      DO 200 IK=IJ,N
0162      A(IK)=A(IK)+A(IJ)*V
0163      JK=JK+1
0164      200 A(IJ)=V
0165      202 CONTINUE

```



```

0220 I=NP-NIP
0221 IJ=IJ-NIP
0222 V=Z(I)/A(I)
0223 IP=I+1
0224 IJ=I
0225 DO 410 J=I+1,N
0226 I=I+1
0227 V=V-A(I)*Z(J)
0228 410 Z(I)=V
0229 RETURN

C COMPUTE THE INVERSE MATRIX FROM FACTORS GIVEN IN A
ENTRY MCLFD(A,N,IR)
IF(IR.LT.N)RETURN
A(I)=100/A(I)
IF(V.EQ.1)RETURN
NP=N+1
NI=N-1
I=2
DO 511 I=2,N
A(I)=-A(I)
IJ=I+1
IF(I.EQ.N)GOTO502
DO 501 I=I,N
K=I
JK=I
V=A(I)
DO 500 K=I,J
JK=J+NP-K
V=V+A(I)*A(JK)
500 IK=K+1
A(IJ)=-V
501 IJ=IJ+1
502 CONTINUE
A(IJ)=100/A(IJ)
I=IJ+1
AA=A(I)
IJ=I
I=I+1
NI=N-I
DO 511 J=2,I
V=A(I)*AA
K=I
K=IJ-IP+J
I=IJ-1
VIP=V*(+I)
DO 510 JK=I,I
A(JK)=A(JK)+V*A(IK)
510 IK=K+IP-JK
A(IJ)=V
511 IJ=IJ+NP-J
RETURN
END
0270

```

```

0001 SUBROUTINE/A09AD(FUNCT,N,X,F,G,H,M,GFN,EPS,MODE,MIXFN,PRINT,
      1  TEXT)
0002 IMPLICIT REAL*8 (A-T,D-Z)
0003 REAL*8 ((I),S(I),M(LI),M(LI),EPS(I))
0004 IF(IPRINT.NE.0)PRINT 1000
0005 FORMAT('ENTRY TO YA09AD'/)
0006 NY=N*(N+1)/2
0007 IS=N
0008 IGM=Y+Y
0009 IS=ISG
0010 TEXT=0
0011 IR=N
0012 IF(MODE.EQ.3)GOTO15
0013 IF(MODE.EQ.2)GOTO10
0014 JJ=NY+1
0015 ON 5 I=1,N
0016 GO 6 J=1,I
0017 JJ=J-1
0018 H(I,J)=0.00
0019 5 H(I,J)=1.00
0020 GOTO15
0021 CONTINUE
0022 CALL VC18JH,N,IR)
0023 IF(LT.'')RETURN
0024 CONTINUE
0025 Z=0
0026 ITN=0
0027 CALL FUNCT(N,X,F,G)
0028 (F)=1
0029 DF=DFN
0030 IF(DFN.EQ.000)DF=F-2
0031 IF(DFN.LT.000)DF=DA33(DF*FI)
0032 IF(DF.LE.000)DF=100
0033 CONTINUE
0034 IF(IPRINT.NE.0)GOTO21
0035 IF(MOD(ITN,IPRINT).NE.0)GOTO21
0036 PRINT 1001,(F),FV
0037 FORMAT(24I5)
0038 PRINT 1002,F
0039 FORMAT(5D5.16)
0040 PRINT 1002,(X(I),I=1,N)
0041 PRINT 1002,(S(I),I=1,N)
0042 CONTINUE
0043 ITN=ITN+1
0044 GO 22 I=1,I
0045 CALL MC1EJH,N,G,M,IR)
0046 GS=0.00
0047 ON 27 I=1,I
0048 M(S+I)=-G(I)
0049 GS=GS-G(I)+M(S+I)
0050 IF(GS.GE.0)GOTO22
0051 GS=GS
0052 ALPMA=-2.00*DF/GS
0053
0054
0055

```

```

0056      IF (ALPHA.GT.100) ALPHA=100
0057      DF=F
0058      TOT=0.00
0059      30 CONTINUE
0060      IEXIT=3
0061      IF ((FN.EQ.4)XFN) GOTD92
0062      ICON=0
0063      IEXIT=1
0064      DO 31 I=1,N
0065      Z=ALPHA*W(I5+1)
0066      IF (DABS(Z).GE.EPS(I)) ICON=1
0067      31 X(I)=X(I)+Z
0068      CALL FUNCTIN,X,FY,G)
0069      IFN=IFN+1
0070      GYS=0.00
0071      DO 32 I=1,N
0072      32 GYS=GYS+G(I)*W(I5+1)
0073      IF (FY.GT.F) GOTD40
0074      IF (DABS(GYS/GS0).LE..900) GOTD50
0075      IF (GYS.GT.000) GOTD40
0076      TOT=TOT+ALPHA
0077      Z=10.00
0078      IF (GS.LT.GYS) Z=GYS/(GS-GYS)
0079      IF (Z.GT.100) Z=1000
0080      ALPHA=ALPHA*Z
0081      F=FY
0082      GS=GYS
0083      GOTD30
0084      40 CONTINUE
0085      DO 41 I=1,N
0086      41 X(I)=X(I)-ALPHA*W(I5+1)
0087      IF (ICON.EQ.0) GOTD92
0088      Z=3.00*(F-FY)/ALPHA+GYS+GS
0089      ZZ=DSQRT(Z**2-GS*GYS)
0090      Z=100-(GYS+ZZ-Z)/(200*ZZ+GYS-GS)
0091      ALPHA=ALPHA*Z
0092      GOTD30
0093      50 CONTINUE
0094      ALPHA=TT+ALPHA
0095      F=FY
0096      IF (ICON.EQ.0) GOTD90
0097      DF=DF-F
0098      GSS=GYS-GSS
0099      DO 51 I=1,N
0100      W(I5+1)=G(I)
0101      51 G(I)=-W(I5+1)
0102      IF (GSS+ALPHA*GS0.GT.0.00) GOTD60
C  COMPLEMENTARY OFP FORMULA
0103      SIG=100/GSS
0104      IR=-IR
0105      CALL MCL1A)(H,N,G,SIG,W,IR,1,000)
0106      DO 52 I=1,N
0107      52 G(I)=W(I5+1)-W(I5+1)
0108      SIG=100/(ALPHA*GSS)
0109      IR=-IR
0110      CALL MCL1A)(H,N,G,SIG,W,IR,0,000)

```

```

0111      GOTJ70
0112      60 CONTINUE
          C   UFP FORMULA
0113      ZZ=ALPHA/(DGS-ALPHA*GSD)
0114      SIG=-ZZ
0115      CALL MC11A)(M,N,G,SIG,W,IR,1,10-16)
0116      Z=DGS*ZZ-1.00
0117      DO 61 I=1,N
0118      61 G(I)=W(I*G+1)+Z*W(I*G+1)
0119      SIG=1.00/(ZZ*DGS**2)
0120      CALL MC11A)(M,N,G,SIG,W,IR,0,000)
0121      70 CONTINUE
0122      DO 71 I=1,N
0123      71 G(I)=W(I*G+1)
0124      GOTJ20
0125      92 CONTINUE
0126      DO 91 I=1,I
0127      91 G(I)=W(I*G+1)
0128      90 CONTINUE
0129      IF(I*PRINT.EQ.0)RETURN
0130      PRINT 1001,(TN,IFN,EXIT
0131      PRINT 1002,F
0132      PRINT 1002,(X(I),I=1,N)
0133      PRINT 1002,(G(I),I=1,N)
0134      RETURN
0135      END

```

```

0001 SUBROUTINE VEO4ADIN,A,IA,B,FL,BU,X,Z,LT,K,S)
0002 IMPLICIT REAL*8 (A-H,O-Z)
0003 DIMENSION A(IA,1),B(1),BL(1),BU(1),X(1),LT(1),S(1)
0004 IS=N
0005 IAS=N
0006 IV=1
0007 ICAC=N*N
0008 ID=ICAC
0009 UD 9 I=1,N
0010 9 S(I)=-P(I)
0011 DO 10 I=1,N
0012 X(I)=0.00
0013 LT(I)=I
0014 S(ICAC+1)=A(I,1)
0015 IF(DD-GE-3L(1),AND,DDO,LE,SU(I))GOTO10
0016 IF(DD-LT,3L(1))X(I)=BL(I)
0017 IF(DD-GT,3U(1))X(I)=BU(I)
0018 DO 12 J=1,I
0019 S(J)=G(I)+A(J,1)*X(I)
0020 IF(1.E3,N)GOTO10
0021 I=I+1
0022 DO 11 J=1,I,N
0023 I1=G(J)+A(I,1,J)*X(I)
0024 GO TO 19 CONTINUE
0025 K=0
0026 KI=1
0027 20 CONTINUE
0028 IOUT=0
0029 DEL=0.00
0030 DO 21 I=K,I,N
0031 LI=LI(I)
0032 IF(X(LI),EQ,BL(LI),AND,G(1),GE,0.00)GOTO21
0033 IF(X(LI),EQ,BU(LI),AND,G(1),LE,0.00)GOTO21
0034 IF(S(1),LT,DD)GOTO22
0035 Z=X(LI)-AL(LI)
0036 J=1
0037 GOTO23
0038 22 CONTINUE
0039 Z=BJ(LI)-X(LI)
0040 J=0
0041 23 CONTINUE
0042 IF(1/ICAC+1),LE,0.00)GOTO24
0043 BETA=DA3S(I)/2(ICAC+1)
0044 IF(BETA,GE,2)GOTO24
0045 Z=ZETA
0046 D=-500*Z*DA3S(I)
0047 J=1
0048 GOTO26
0049 24 CONTINUE
0050 D=Z*DA3S(I)-.500*Z*G(ICAC+1)
0051 26 CONTINUE
0052 IF(D,LT,-DEL)GOTO21
0053 DEL=D
0054 ALP=1=2
0055 IOUT=1
0056 I1=1

```

```

0057 IF(J.LT.0)I1Y=0
0058 LB=J
0059 21 CONTINUE
0060 IF(IJOUT.'IE.0)GOTO29
0061 27 CONTINUE
0062 Q=0.00
0063 DO 28 I=1,K
0064 L=LT(I)
0065 Q=Q+X(L)*G(I)-B(L)
0066 Q=-500*Q
0067 RETURN
0068 29 CONTINUE
0069 SIG=1.00
0070 IF(G(IOUT).GT.000)SIG=-1.00
0071 LIQJ=LI(IJOUT)
0072 LIIN=LIJUT
0073 25 CONTINUE
0074 SAS=SFICAC*IJOUT)
0075 IF(K.EQ.0)GOTO31
0076 DO 30 I=1,K
0077 G(IIS+I)=G(ID+I)*A(IJOUT,I)
0078 31 CONTINUE
0079 DO 37 I=K1,N
0080 LI=LT(I)
0081 IF(LI-LIQJ)32,37,33
0082 Z=A(LI,LIQJ)
0083 GOTO34
0084 33 Z=A(LIOUT,-I)
0085 34 CONTINUE
0086 IF(K.EQ.0)GOTO36
0087 DO 35 J=1,K
0088 Z=Z-A(I,J)*G(IIS+J)
0089 36 G(IIS+I)=Z
0090 37 CONTINUE
0091 G(IIS+IOUT)=SAS
0092 IF(K.EQ.0)GOTO42
0093 G(IIS+K)=A(IJOUT,K)
0094 IF(K.EQ.1)GOTO42
0095 I=K
0096 DO 41 I=2,K
0097 I=I-1
0098 Z=-A(IJOUT,I)
0099 I1=I+1
0100 DO 40 J=I1,K
0101 Z=Z-G(IIS+J)*A(I,J)
0102 41 G(IIS+I)=Z
0103 42 CONTINUE
0104 IF(SIG.GT.1.00)GOTO51
0105 DO 50 I=1,K
0106 G(IIS+I)=G(IIS+I)
0107 51 CONTINUE
0108 IF(K.EQ.0)GOTO62
0109 DO 61 I=1,K
0110 IF(G(IIS+I).EQ.000)GOTO61
0111 LI=LT(I)
0112 J=I

```

```

0113      Z=BL(LI)-X(LI)
0114      IF(G(I5+I).LT.000)GOTO60
0115      J=0
0116      Z=DU(LI)-X(LI)
0117      60 CONTINUE
0118      Z=Z/G(I5+I)
0119      IF(Z.GE.ALPHA)GOTO61
0120      ALPHA=Z
0121      LB=J
0122      IIN=I
0123      LIIN=LI
0124      61 CONTINUE
0125      62 CONTINUE
0126      X(LIOUT)=X(LIOUT)+SIS*ALPHA
0127      IF(K.EQ.0)GOTO71
0128      DO 73 I=1,K
0129      LI=LI(I)
0130      70 X(LI)=X(LI)+ALPHA*G(I5+I)
0131      71 CONTINUE
0132      DO 72 I=K1,N
0133      72 G(I)=G(I)+ALPHA*G(I5+I)
0134      IF(IIN.EQ.0)GOTO90
0135      X(LIIN)=AL(LIIN)
0136      IF(LB.EQ.0)X(LIIN)=DU(LIIN)
0137      IF(IIN.EQ.1)GOTO20
0138      K2=K-1
0139      SQ=G(I0+IIN)
0140      I1=IIN+1
0141      DO 90 I=I1,N
0142      80 G(IV+I)=A(I,IIN)
0143      IF(IIN.EQ.1)GOTO86
0144      I2=IIN+2
0145      S0=100/SQ
0146      DO 95 I=IIN,K2
0147      V=G(IV+I)
0148      VD=V/G(I0+I1)
0149      S1=S0+V*VD
0150      R=S1/S0
0151      G(I0+I)=G(I0+I1)+R
0152      BETA=VD/S1
0153      IF(R.GT.4.00)GOTO84
0154      DO 81 J=I2,N
0155      81 G(IV+J)=G(IV+J)-V*A(J,I1)
0156      IF(I1.GT.K2)GOTO83
0157      DO 82 J=I1,K2
0158      J1=J+1
0159      82 A(J,I)=A(J,I1)+BETA*G(IV+J1)
0160      83 CONTINUE
0161      A(K,I)=BETA
0162      DO 84 J=K1,N
0163      84 A(J,I)=A(J,I1)+BETA*G(IV+J)
0164      GOTO949
0165      841 CONTINUE
0166      IF(I1.GT.K2)GOTO843
0167      DO 842 J=I1,K2
0168      J1=J+1

```

```

0169      842 A(J,I)=3ETA*G(IV+J)+A(JI,I)/2
0170      843 CONTINUE
0171          A(K,I)=BETA
0172          DO 844 J=K1,N
0173      844 A(J,I)=3ETA*G(IV+J)+A(J,I)/2
0174          DO 845 J=I2,N
0175      845 G(IV+J)=G(IV+J)-V*A(J,I)
0176      847 CONTINUE
0177          LT(I)=LT(I1)
0178          S0=S1
0179          I1=I2
0190      85 I2=I2+1
0181          SG=1.00/S1
0182          LT(K)=L(I1)
0183          G(I2+K)=SG
0184          IF(I1N.EQ.1)GOTO851
0185          I1=I1-1
0186          DO 852 I=1,I1
0187          Z=A(I1,I)
0188          DO 853 J=I1,K2
0189      853 A(J,I)=A(J+1,I)
0190      852 A(K,I)=Z
0191      851 CONTINUE
0192      86 CONTINUE
0193          DO 87 I=K1,N
0194      87 G(IGAC+I)=G(IGAC+I)+SG*(G(I)/I)**2
0195          K1=K
0196          K=K2
0197          I1N=0
0198          ALPHA=1075
0199          SAS=G(IGAC+IOUT)
0200          IF(SAS.GT.0.0001ALPHA=DABS(G(IOUT))/SAS
0201          IF(G(IOUT).LT.0.001GOTO898
0202          J=1
0203          Z=X(LIOUT)-OL(LIOUT)
0204          GOTO899
0205      898 CONTINUE
0206          J=0
0207          Z=OL(LIOUT)-X(LIOUT)
0208      897 CONTINUE
0209          IF(Z.GE.ALPHA)GOTO25
0210          ALPHA=Z
0211          L9=J
0212          I1N=IOUT
0213          LIT9=LIOUT
0214          GOTO25
0215      90 CONTINUE
0216          K2=K1+1
0217          IF(SIG.EQ.100)GOTO91
0218          DO 901 I=K1,N
0219      901 G(IAS+I)=-G(IAS+I)
0220      91 CONTINUE
0221          IF(IOUT.EQ.K1)GOTO97
0222          LT(IOUT)=LT(K1)
0223          LT(K1)=LIOUT
0224          G(IAS+IOUT)=G(IAS+K1)

```

```

0225 G(IICAC+IOU)=G(IICAC+K1)
0226 G(IICAC+K1)=SAS
0227 G(IJUT)=G(K1)
0228 IF(K.EQ.0)GOTO93
0229 DO 92 I=1,K
0230 Z=A(K1,I)
0231 A(K1,I)=A(IJUT,I)
0232 A(IJUT,I)=Z
0233 CONTINUE
0234 IF(K2.EQ.IJUT)GOTO95
0235 I1=IJUT-1
0236 DO 94 I=K2,I1
0237 A(IJUT,I)=A(I1,K1)
0238 CONTINUE
0239 IF(IJUT.EQ.1)GOTO97
0240 I1=IJUT+1
0241 DO 95 I=I1,N
0242 A(I1,IJUT)=A(I1,K1)
0243 CONTINUE
0244 G(K1)=0.00
0245 K=K1
0246 IF(K.EQ.N)GOTO27
0247 DO 98 I=K2,N
0248 Z=G(IAS+1)/SAS
0249 A(I,K1)=Z
0250 G(IICAC+1)=G(IICAC+1)-Z+G(IAS+1)
0251 K1=K2
0252 GOTO20

C
0253 ENTRY VEO43D(N,A,I,J,K)
0254 IF(K.EQ.0)RETURN
0255 ID=N+1
0256 G(I+1)=100/G(ID+1)
0257 IF(K.EQ.1)RETURN
0258 N1=K-1
0259 DO 111 I=1,N1
0260 I1=I+1
0261 A(I1,I)=A(I1,I)
0262 IF(I.EQ.N1)GOTO102
0263 I1=I+2
0264 DO 101 J=I1,K
0265 Z=A(IJ,I)
0266 J1=J-1
0267 DO 100 L=I1,J1
0268 Z=Z+A(IJ,L)+A(L,I)
0269 A(IJ,I)=Z
0270 CONTINUE
0271 AA=100/G(I1)+1)
0272 J1=I1+AA
0273 DO 111 J=1,I
0274 Z=A(I1,J)+AA
0275 G(N+J)=G(N+J)+Z+A(I1,J)
0276 IF(I.EQ.1)GOTO111
0277 J1=J+1
0278 DO 110 L=J1,I
0279 A(L,J)=A(L,J)+A(I1,L)+Z

```

```
0290      III A(II,J)=Z  
0291      RETURN  
0292      END
```

d. Essential Elements Of Program Output

The output of the program contains a series of outer iterations each of which consists of a number of inner ones. Each outer iteration is made for a chosen set of the parameters  $\sigma$  and  $\theta$ , while the variables  $x_i$  are changed in each inner iteration. The following shows composites of the essential portions of the first and fourth (last) outer iteration and gives all necessary explanations. The listings of the  $\sigma$ 's, the  $\theta$ 's, the Lagrange multipliers, etc. are omitted.

i) First Outer Iteration

OUTER ITERATION NUMBER 1, 1

$\sigma$	$\theta$						
0.5016334259761779E 00							
0.50010011170011000E 00	0.4470110000000000E 00	1.931910100000000E 00	0.319974000000000E 00	1.297441100000000E 00			
0.7874028800000000E 00	1.1155767721447625E 01	0.5107594612044411E 02	-0.7002374077589440E 02	0.1331541110274773E 02			

•	•	•	•	•
•	•	•	•	•
•	•	•	•	•

$\sigma$	$\theta$						
0.5016334259761779E 00							
0.50010011170011000E 00	0.4470110000000000E 00	-1.9622605105661101E 00	0.101124100000000E 00	1.1074605460074377E 01			
0.7874028800000000E 00	1.1155767721447625E 01	0.37037465776305770E 01	-0.52160707633014440E 01	0.101050000000000E 01			

The above shows the first and last inner iteration associated with outer iteration number 1. The following explains the format of the inner iterations.

First line: The first number stands for the total number of previously completed inner iterations. The second number represents the number of times the subroutine VF01ZD has been called. (Only the last iteration has a third number in this line. It represents a code number for stopping the iteration.)

Second line: This number represents the current value of the applicable composite function  $\phi$  according to equation (C.1).

Third line: This line gives the current values of the variables  $z$ ,  $P_1$ ,  $Q_1$ ,  $P_3$  and  $Q_3$  (in the given order). In the first iteration, the initial values are reproduced. (It is to be recalled that the solution of the problem becomes better as the value of  $z$  decreases.)

Fourth line: These numbers represent the derivatives of the composite function  $\phi$  with respect to the variables in the order of their subscripts.

ii) Fourth (Last) Outer Iteration

Outer Iteration Number 4

```

      1
      1
0.214141941428774E+01
0.21552752717271130E+01 -0.57136273810292475E+01 0.13223213017293150E+02 0.2153925977425154E+01
0.2155 777.61447150E+01 -0.57136273810292475E+01 0.13223213017293150E+02 -0.57136273810292475E+01 0.2153925977425154E+01
      1
      2
0.21775218472257440E+01
0.21775218472257440E+01 -0.57136273810292475E+01 -0.57136273810292475E+01 0.13223213017293150E+02 0.2153925977425154E+01
-0.57136273810292475E+01 +0.57136273810292475E+01 0.13223213017293150E+02 -0.57136273810292475E+01 0.2153925977425154E+01
      1
      3
0.21775218472257440E+01
0.21547433136471470E+01 -0.57136273810292475E+01 -0.57136273810292475E+01 0.13223213017293150E+02 0.2153925977425154E+01
-0.57136273810292475E+01 +0.57136273810292475E+01 0.13223213017293150E+02 -0.57136273810292475E+01 0.2153925977425154E+01
      1
      4
0.21775218472257440E+01
0.21547433136471470E+01 -0.57136273810292475E+01 -0.57136273810292475E+01 0.13223213017293150E+02 0.2153925977425154E+01
-0.57136273810292475E+01 +0.57136273810292475E+01 0.13223213017293150E+02 -0.57136273810292475E+01 0.2153925977425154E+01

```

The last group of inner iterations in the above contains the results of the minimax optimization, i.e.

$$z = .0235 \text{ lb}^2$$

$$P_1 = -50.85 \times 10^{-5} \text{ lb-sec}^2$$

$$Q_1 = -57.56 \times 10^{-5} \text{ lb-sec}^2$$

$$P_3 = 181.98 \times 10^{-5} \text{ lb-sec}^2$$

$$Q_3 = 21.95 \times 10^{-5} \text{ lb-sec}^2$$

The computation was terminated at this point since no further significant decrease in the value of  $z$  was possible, i.e. the prescribed value of AKMIN was reached.

APPENDIX D  
APPLICATION OF AUGMENTED LAGRANGIAN OPTIMIZATION PROGRAM  
TO LEAST SQUARES BALANCING OPTIMIZATION

The present appendix shows how the Augmented Lagrangian program is adapted to the least squares solution of the overdetermined system of balancing equations<sup>1</sup>. (For formulation, see equation (3.4).) Section 1 first outlines how the various parameters must be defined in the main program according to Section 2a of Appendix C. Subsequently, a listing of the actual routine is shown. Section 2 gives the applicable subroutine VF01BD and discusses it. Section 3 contains the important parts of the output of the program and interprets the results.

1. Main Program

The main program, which is listed at the end of this section, begins with comment cards which are designed to serve as additional explanations. These are followed by the COMMON statements which define the array size for the constraints C and their derivatives GC. The following variables are then defined:

---

<sup>1</sup> Since the Harwell program requires constraints and the least squares optimization represents an unconstrained problem, it becomes necessary to introduce a dummy constraint. This constraint is chosen in such a way that it will never be violated.

$N = 4$ ; stands for the four variables  $P_1, Q_1, P_3$  and  $Q_3$ .

$M = 1$ ; refers to the single dummy constraint required for the program to operate. (See Section 2 below.)

$K = 0$ , since there are no equality constraints.

$X(1)$  to  $X(4)$ , the starting point estimates of the variables, are made  $1 \times 10^{-3}$  since previous experience has shown these values to be of this order of magnitude. (While accurate estimates are not required, they decrease the number of iterations.)

With  $AKMIN$  chosen arbitrarily to be  $1 \times 10^{-3}$ ,  $EPS(1)$  to  $EPS(4)$  result from  $X(1)$  to  $X(4)$ .

$DFN$  is estimated to be 0.4.

$MAXFN = 500$  (See Section 2a of Appendix C.)

$IPR1 = 1$ , to print every outer iteration.

$IPR2 = 1$ , to print every inner iteration.

$IW = 2500$ , since the restrictions that  $N \leq 25$  and  $M \leq 50$  are met.

$MODE = 1$  (See Section 2a of Appendix C.)

The scale factor  $C(1) = 10.001$  represents the magnitude of the constraint when evaluated at the starting point  $X(1) = 1 \times 10^{-3}$ .  $G(1,1)$  to  $G(4,1)$  represent the derivatives of the single linear dummy constraint with respect to the four variables  $X(1)$  to  $X(4)$ .

## MAIN

```

C THIS PROGRAM WILL CHOOSE THE VALUES OF THE GENERAL MASS DISTANCE
C PRODUCTS P1,P2,P3 AND Q3 WHICH WILL RESULT IN THE BEST LEAST SQUARES
C FIT OF THE COMPUTED SHAKING FORCE CURVES IN THE X AND Y DIRECTIONS
C TO A KNOWN EXPERIMENTAL CURVES. THIS WILL BE ACCOMPLISHED BY THE
C USE OF THE AUGMENTED LAGRANGIAN OPTIMIZATION ROUTINE.
C THE VARIABLES FOR THIS PROBLEM ARE
C     X(1) = P1
C     X(2) = P2
C     X(3) = P3
C     X(4) = Q3
C
C THE CONSTRAINT IS
C     C(1) = X(1) + 10      (DUMMY CONSTRAINT)
C
C001      (IMPLICIT REAL*8(A-H,O-Z))
C002      COMMON/VF01E)/C(1:50)
C003      COMMON/VF01FD)/C(25:50)
C004      REAL*8 X(4),EPS(4)
C005      N = 4
C006      M = 1
C007      K = 0
C008      P1=3.14159300
C009      C THE STARTING POINT IS ESTIMATED TO BE
C010      X(1)=1.00-3
C011      X(2)=1.00-3
C012      X(3)=1.00-3
C013      X(4)=1.00-3
C014      AKMIN=10-3
C015      EPS(1)=1.00-5
C016      EPS(2)=1.00-5
C017      EPS(3)=1.00-5
C018      EPS(4)=1.00-5
C019      DEFN=.400
C020      MAXFN=500
C021      IPR1=1
C022      IPR2=1
C023      IW=2500
C024      MODE=1
C025      C THE CONSTRAINT SCALE FACTOR IS
C026      C(1)=10.00100
C027      C THE DERIVATIVES OF THE LINEAR CONSTRAINT WITH RESPECT
C028      TO THE VARIABLES ARE
C029      GC(1,1) = 100
C030      GC(2,1) = 000
C031      GC(3,1) = 000
C032      GC(4,1) = 000
C033      CALL VF71AUFN,M,K,X,EPS,AKMIN,DEFN,MAXFN,IPR1,IPR2,IW,MODE)
C034      STOP
C035      END

```

2. Subroutine VF01BD (See program at the end of this section.)

After allocating storage for the various subscripted variables, the subroutine VF01BD starts with the COMMON statements indicated in Section 2b of Appendix C. The subsequent steps are:

- a. A1 to A4 represent the link dimensions of links 1 to 4.
- b. DELPHI = 5, stands for the 5 degree increments of the input angle  $\phi_1$ .
- c. P<sub>1</sub>, Q<sub>1</sub>, P<sub>3</sub> and Q<sub>3</sub> are variables x<sub>1</sub>, x<sub>2</sub>, x<sub>3</sub> and x<sub>4</sub>.
- d. FEX(1) to FEY(72) are the 144 experimentally obtained shaking force components at 5 degree intervals from 0 to 355 degrees. (See Table 3.3)
- e. The dummy constraint  $C(1) = X(1) + 10$  was chosen such that it never will become negative for the anticipated range of the variable X(1). (See equation (C.3).)
- f. SUMF, SUMX1 to SUMX4 represent the initialization of the objective function F and its derivatives.

g. A DO loop, encompassing the 72 positions of the mechanism, is set up to compute the objective function as well as its derivatives. The objective function becomes, according to equation (3.4):

$$F = \sum_{i=0}^{355} \left[ (F_{CX_i} - F_{EX_i})^2 + (F_{CY_i} - F_{EY_i})^2 \right] \quad (D.1)$$

The derivatives of F with respect to the four variables are given by:

$$\frac{\partial F}{\partial P_1} = \sum_{i=0}^{355} \left[ AA_x PFCX1 + BB_x PFCY1 \right] \quad (D.2)$$

$$\frac{\partial F}{\partial Q_1} = \sum_{i=0}^{355} \left[ AA_x PFCX2 + BB_x PFCY2 \right] \quad (D.3)$$

$$\frac{\partial F}{\partial P_3} = \sum_{i=0}^{355} \left[ AA_x PFCX3 + BB_x PFCY3 \right] \quad (D.4)$$

$$\frac{\partial F}{\partial Q_3} = \sum_{i=0}^{355} \left[ AA_x PFCX4 + BB_x PFCY4 \right] \quad (D.5)$$

where

$$AA = 2(F_{CX}(I) - F_{EX}(I))$$

$$BB = 2(F_{CY}(I) - F_{EY}(I))$$

$$\text{PFCX1} = m_1 ( \overset{\cdot\cdot}{\phi}_{1i} \cos\phi_{1i} + \overset{\cdot}{\phi}_{1i} \sin\phi_{1i} )$$

$$\text{PFCY1} = m_1 ( \overset{\cdot\cdot}{\phi}_{1i} \sin\phi_{1i} - \overset{\cdot}{\phi}_{1i} \cos\phi_{1i} )$$

$$\text{PFCX2} = -m_1 ( \overset{\cdot\cdot}{\phi}_{1i} \sin\phi_{1i} - \overset{\cdot}{\phi}_{1i} \cos\phi_{1i} )$$

$$\text{PFCY2} = m_1 ( \overset{\cdot\cdot}{\phi}_{1i} \cos\phi_{1i} + \overset{\cdot}{\phi}_{1i} \sin\phi_{1i} )$$

$$\text{PFCX3} = m_3 ( \overset{\cdot\cdot}{\phi}_{3i} \cos\phi_{3i} + \overset{\cdot}{\phi}_{3i} \sin\phi_{3i} )$$

$$\text{PFCY3} = -m_3 ( -\overset{\cdot\cdot}{\phi}_{3i} \sin\phi_{3i} + \overset{\cdot}{\phi}_{3i} \cos\phi_{3i} )$$

$$\text{PFCX4} = m_3 ( -\overset{\cdot\cdot}{\phi}_{3i} \sin\phi_{3i} + \overset{\cdot}{\phi}_{3i} \cos\phi_{3i} )$$

$$\text{PFCY4} = m_3 ( \overset{\cdot\cdot}{\phi}_{3i} \cos\phi_{3i} + \overset{\cdot}{\phi}_{3i} \sin\phi_{3i} )$$

All force and motion computations are identical to those in Section 3b of Appendix C.

```

0001      SUBROUTINE VFOLDIN,M,K)
0002      IMPLICIT REAL*8(A-H,O-Z)
0003      REAL*8 (14)
0004      INTEGER PHID, PHID1, DELPHI
0005      REAL*8 KAY1(360),KAY3(360)
0006      DIMENSION GM41(360),GM43(360),FCX(360),FCY(360)
0007      DIMENSION VAR1(360),VAR2(360),VAR3(360),VAR4(360)
0008      DIMENSION VAR5(360),VAR6(360),VAR7(360),VAR8(360)
0009      DIMENSION PFCX1(360),PFCX2(360),PFCX3(360),PFCY4(360)
0010      DIMENSION PFCY1(360),PFCY2(360),PFCY3(360),PFCY4(360)
0011      DIMENSION PSIA(360),PSIV(360)
0012      DOUBLE PRECISION DCOS,DSIN,DSUPP,DATAN2
0013      DOUBLE PRECISION FE1(72),FEY(72)
0014      COMMON/VFOLD/F
0015      COMMON/VFOLD/G(10)
0016      COMMON/VFOLD/G(150)
0017      COMMON/VFOLD/G(125,50)
0018      PI=3.14159100
0019      C      THE LINK DIMENSIONS ARE
0020      A1=200
0021      A2=3.900
0022      A3=300
0023      A4=9.00400
0024      C
0025      C      DELPHI = 5
0026      C      DEFINE VARIABLES
0027      P1 = X(1)
0028      Q1 = X(2)
0029      P3 = X(3)
0030      Q3 = X(4)
0031      C      THE EXPERIMENTAL SHAKING FORCE COMPONENTS, DETERMINED
0032      C      EVERY 5 DEGREES, ARE GIVEN AS FOLLOWS, WHERE THE
0033      C      FIRST VALUE CORRESPONDS TO THE READING AT 0 DEGREES
0034      C      AND THE SEVENTY SECOND VALUE TO THE READING AT 355 DEGREES.
0035      FE1(1) = .477
0036      FE1(2) = .480
0037      FE1(3) = .447
0038      FE1(4) = .384
0039      FE1(5) = .253
0040      FE1(6) = .202
0041      FE1(7) = .105
0042      FE1(8) = .060
0043      FE1(9) = .030
0044      FE1(10) = .007
0045      FE1(11) = -.003
0046      FE1(12) = -.015
0047      FE1(13) = -.026
0048      FE1(14) = -.029
0049      FE1(15) = -.031
0050      FE1(16) = -.034
0051      FE1(17) = -.035
0052      FE1(18) = -.034
0053      FE1(19) = -.031
0054      FE1(20) = -.029
0055      FE1(21) = -.028
0056      FE1(22) = -.027

```

0050	FEX(23)	* -.024
0051	FEX(24)	* -.023
0052	FEX(25)	* -.020
0053	FEX(26)	* -.015
0054	FEX(27)	* -.012
0055	FEX(28)	* -.012
0056	FEX(29)	* -.015
0057	FEX(30)	* -.017
0058	FEX(31)	* -.019
0059	FEX(32)	* -.021
0060	FEX(33)	* -.024
0061	FEX(34)	* -.027
0062	FEX(35)	* -.030
0063	FEX(36)	* -.031
0064	FEX(37)	* -.032
0065	FEX(38)	* -.033
0066	FEX(39)	* -.037
0067	FEX(40)	* -.038
0068	FEX(41)	* -.038
0069	FEX(42)	* -.038
0070	FEX(43)	* -.039
0071	FEX(44)	* -.041
0072	FEX(45)	* -.046
0073	FEX(46)	* -.051
0074	FEX(47)	* -.053
0075	FEX(48)	* -.056
0076	FEX(49)	* -.061
0077	FEX(50)	* -.063
0078	FEX(51)	* -.072
0079	FEX(52)	* -.077
0080	FEX(53)	* -.084
0081	FEX(54)	* -.091
0082	FEX(55)	* -.096
0083	FEX(56)	* -.101
0084	FEX(57)	* -.113
0085	FEX(58)	* -.119
0086	FEX(59)	* -.125
0087	FEX(60)	* -.134
0088	FEX(61)	* -.143
0089	FEX(62)	* -.147
0090	FEX(63)	* -.150
0091	FEX(64)	* -.144
0092	FEX(65)	* -.123
0093	FEX(66)	* -.110
0094	FEX(67)	* -.081
0095	FEX(68)	* -.032
0096	FEX(69)	* .035
0097	FEX(70)	* .122
0098	FEX(71)	* .259
0099	FEX(72)	* .356
0100	FEY(1)	* -.570
0101	FEY(2)	* -.590
0102	FEY(3)	* -.551
0103	FEY(4)	* -.468
0104	FEY(5)	* -.374
0105	FEY(6)	* -.282

C106	FEY(71)	* -.219
C107	FEY(8)	* -.173
C108	FEY(9)	* -.120
C109	FEY(10)	* -.087
C110	FEY(11)	* -.066
C111	FEY(12)	* -.054
C112	FEY(13)	* -.037
C113	FEY(14)	* -.029
C114	FEY(15)	* -.024
C115	FEY(16)	* -.019
C116	FEY(17)	* -.012
C117	FEY(18)	* -.009
C118	FEY(19)	* -.006
C119	FEY(20)	* 0.0
C120	FEY(21)	* .006
C121	FEY(22)	* .009
C122	FEY(23)	* .015
C123	FEY(24)	* .023
C124	FEY(25)	* .026
C125	FEY(26)	* .030
C126	FEY(27)	* .037
C127	FEY(28)	* .048
C128	FEY(29)	* .058
C129	FEY(30)	* .065
C130	FEY(31)	* .075
C131	FEY(32)	* .083
C132	FEY(33)	* .093
C133	FEY(34)	* .097
C134	FEY(35)	* .115
C135	FEY(36)	* .122
C136	FEY(37)	* .129
C137	FEY(38)	* .132
C138	FEY(39)	* .141
C139	FEY(40)	* .144
C140	FEY(41)	* .150
C141	FEY(42)	* .153
C142	FEY(43)	* .155
C143	FEY(44)	* .156
C144	FEY(45)	* .158
C145	FEY(46)	* .159
C146	FEY(47)	* .160
C147	FEY(48)	* .160
C148	FEY(49)	* .161
C149	FEY(50)	* .161
C150	FEY(51)	* .161
C151	FEY(52)	* .160
C152	FEY(53)	* .160
C153	FEY(54)	* .159
C154	FEY(55)	* .159
C155	FEY(56)	* .156
C156	FEY(57)	* .155
C157	FEY(58)	* .153
C158	FEY(59)	* .150
C159	FEY(60)	* .146
C160	FEY(61)	* .144
C161	FEY(62)	* .134

```

0162      FEY(63) = .127
0163      FEY(64) = .116
0164      FEY(65) = .096
0165      FEY(66) = .074
0166      FEY(67) = .044
0167      FEY(68) = -.023
0168      FEY(69) = -.111
0169      FEY(70) = -.206
0170      FEY(71) = -.345
0171      FEY(72) = -.458

C
C      THE CONSTRAINT IS
0172      C(1) = X(1) + 1000
C
0173      Z=PI/1.2002
C
0174      SUMF = 000
0175      SUMX1 = 000
0176      SUMX2 = 100
0177      SUMX3 = 000
0178      SUMX4 = 000
0179      CD 120 PHID1=1.356,DELPHI
0180      PHID=PHID1 - 1
0181      PHI=2 * PHID
0182      I = PHID/DELPHI + 1
C      THE ANGULAR VELOCITIES AND ACCELERATIONS ARE DETERMINED
C      IN SUBROUTINE FOURIE
0183      CALL FOURIE (I,PHIVEL,PHIACC)
C      THE KINEMATICS OF THE LINKAGE ARE DETERMINED IN
C      SUBROUTINE MOTION
0184      CALL MOTION (PHI,A1,A2,A3,A4,PSI,PHIVEL,PHIACC,
1          PSIVEL,PSIACC)
0185      KAY1(I) = DSORT(PHIVEL**4 + PHIACC**2)
0186      KAY3(I) = DSORT(PSIVEL(I)**4 + PSIACC(I)**2)
0187      GM1(I) = PHI - DATAN2(PHIACC,PHIVEL**2)
0188      GM3(I) = PSI - DATAN2(PSIACC,PSIVEL(I)**2)
0189      VAR1(I) = KAY1(I)*DCOS(GM1(I))
0190      VAR2(I) = KAY1(I)*DSIN(GM1(I))
0191      VAR3(I) = KAY3(I)*DCOS(GM3(I))
0192      VAR4(I) = KAY3(I)*DSIN(GM3(I))
0193      VAR5(I) = KAY1(I)*DCOS(GM1(I))
0194      VAR6(I) = KAY1(I)*DCOS(GM1(I))
0195      VAR7(I) = KAY3(I)*DSIN(GM3(I))
0196      VAR8(I) = KAY3(I)*DCOS(GM3(I))
C      THE COMPUTED SHAKING FORCES ARE
0197      FC(I) = P1*VAR1(I)-P1*VAR2(I)+P3*VAR3(I)-D3*VAR4(I)
0198      FCI(I) = P1*VAR5(I)+D1*VAR6(I)+P3*VAR7(I)+D3*VAR8(I)
C
0199      A4 = 200*(FC(I) - FEX(I))
0200      B3 = 200*(FCI(I) - FCI(I))
C
0201      SP = DSIN(PHI)
0202      CP = DCOS(PHI)
0203      SS = DSIN(PSI)
0204      CS = DCOS(PSI)
0205      PHI/2 = PHIVEL**2

```

```

0205      PSIV2 = (PSIV1)**2
C
0207      PFCX1(I) = M1*(PHIV2*CP + PHIACC*SP)
0208      PFCY1(I) = M1*(PHIV2*SP - PHIACC*CP)
0209      PFCX2(I) = -M1*(PHIV2*SP - PHIACC*CP)
0210      PFCY2(I) = M1*(PHIV2*CP + PHIACC*SP)
0211      PFCX3(I) = M3*(PSIV2*CS + PSIA(I)*SS)
0212      PFCY3(I) = -M3*(-PSIV2*SS + PSIA(I)*CS)
0213      PFCX4(I) = M3*(-PSIV2*SS + PSIA(I)*CS)
0214      PFCY4(I) = M3*(PSIV2*CS + PSIA(I)*SS)
C
0215      SUMF = SUMF + (FCX(I) - FCX(I))**2 + (FCY(I) - FCY(I))**2
0216      SUMX1 = SUMX1 + A1*PFCX1(I) + B1*PFCY1(I)
0217      SUMX2 = SUMX2 + A2*PFCX2(I) + B2*PFCY2(I)
0218      SUMX3 = SUMX3 + A3*PFCX3(I) + B3*PFCY3(I)
0219      SUMX4 = SUMX4 + A4*PFCX4(I) + B4*PFCY4(I)
0220      120 CONTINUE
C      THE SUM OF THE SQUARES IS
0221      F = SUMF
C      THE DERIVATIVES OF THE SUM OF THE SQUARES WITH RESPECT
C      TO THE VARIABLES ARE
0222      G(1) = SUMX1
0223      G(2) = SUMX2
0224      G(3) = SUMX3
0225      G(4) = SUMX4
C
0226      RETURN
0227      END

```



The number in the second line represents the current value of the composite function  $\phi$  according to equation (C.1) of Appendix C.

The third line gives the current values of  $P_1$ ,  $Q_1$ ,  $P_3$  and  $Q_3$ . In the first inner iteration the initial values are reproduced.

The fourth line shows the derivatives of the composite function with respect to the four variables.

The last group of inner iterations in the above furnishes the results of the optimization, i.e.

$$\begin{aligned}
 P_1 &= -56.25 \times 10^{-5} \text{ lb-sec}^2 \\
 Q_1 &= -51.81 \times 10^{-5} \text{ lb-sec}^2 \\
 P_3 &= 158.42 \times 10^{-5} \text{ lb-sec}^2 \\
 Q_3 &= 0.36 \times 10^{-5} \text{ lb-sec}^2
 \end{aligned}
 \tag{D.6}$$

The computation was terminated at this point since the value for AKMIN of  $1 \times 10^{-3}$  was reached and, with that, no significant further reduction in the composite function could be obtained.

## APPENDIX E

REVIEW OF A CHEBYSHEV-TYPE SINGLE COUNTERWEIGHT SHAKING  
FORCE OPTIMIZATION OF CONSTANT SPEED PLANAR LINKAGES

This appendix briefly reviews a Chebyshev-type minimization of the maximum shaking force of a constant input speed mechanism which is accomplished with the help of a single counterweight attached to the input link. This approach was first described by Ya. L. Gheronimus [25].

Figure E.1 shows the shaking force hodograph of such a mechanism as it appears when it is rotated by the negative of the angle corresponding to the instantaneous position of the input link.

If vector  $\overline{OD}$  represents what is before the above rotation a constant magnitude shaking force component which revolves with the constant angular velocity of the input link, it must be stationary in this figure. Vector  $\overline{DE}$ , which is due to a component of the shaking force which originally is of variable magnitude and rotates with an angular velocity different from that of the input link, actually traces out the hodograph.

Assume now that a counterweight is attached to the input link which produces a force equal in magnitude but

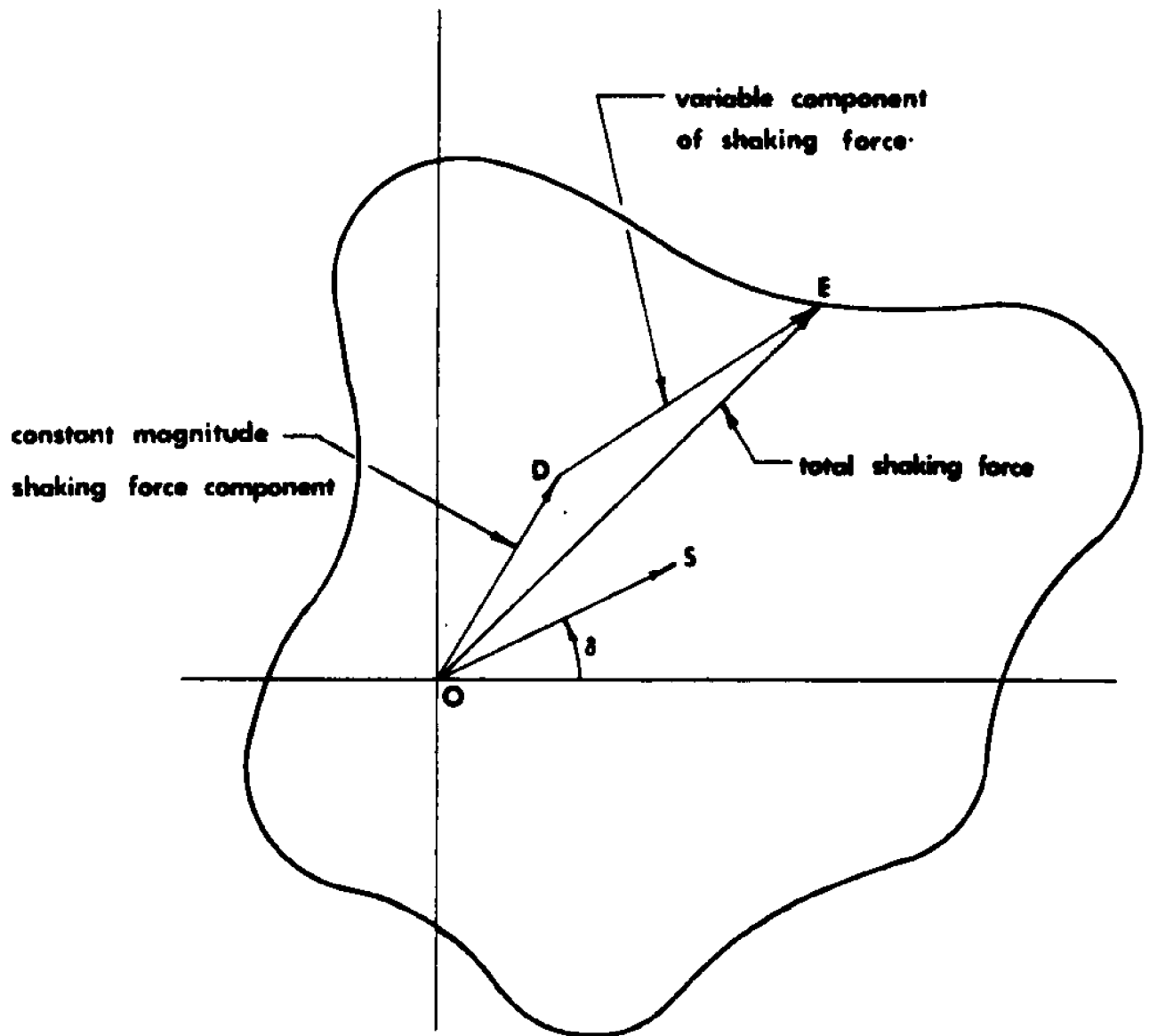


**FIG. E.1 SHAKING FORCE HODOGRAPH OF  
CONSTANT INPUT SPEED MECHANISM  
ROTATED BY NEGATIVE OF INPUT ANGLE**

opposite in direction to that represented by the arbitrary vector  $\overline{OS}$ , at angle  $\delta$ . Figure E.2 shows that this operation causes a shift of the hodograph with respect to the coordinate system such that point  $S$  of the hodograph now coincides with the origin  $O$ . If point  $S$  is appropriately chosen, a reduction of the maximum shaking force may be realized.

Ya. L. Gheronimus has shown that the maximum shaking force can be minimized if point  $S$  is chosen as the center  $C_S$  of the smallest circle which circumscribes the hodograph (see Figure E.3). The center of the circumscribing circle represents the Chebyshev, or best uniform, approximation to the given hodograph by a polynomial of degree zero, i.e. a constant. The maximum modulus of difference between the hodograph and its Chebyshev approximation is represented by the radius  $R_S$  of the smallest circumscribing circle.

When this point  $C_S$  is now moved to the origin in the manner indicated above, the resulting shaking force can never be larger than the force which is represented by the length of the radius  $R_S$  of the circumscribing circle.

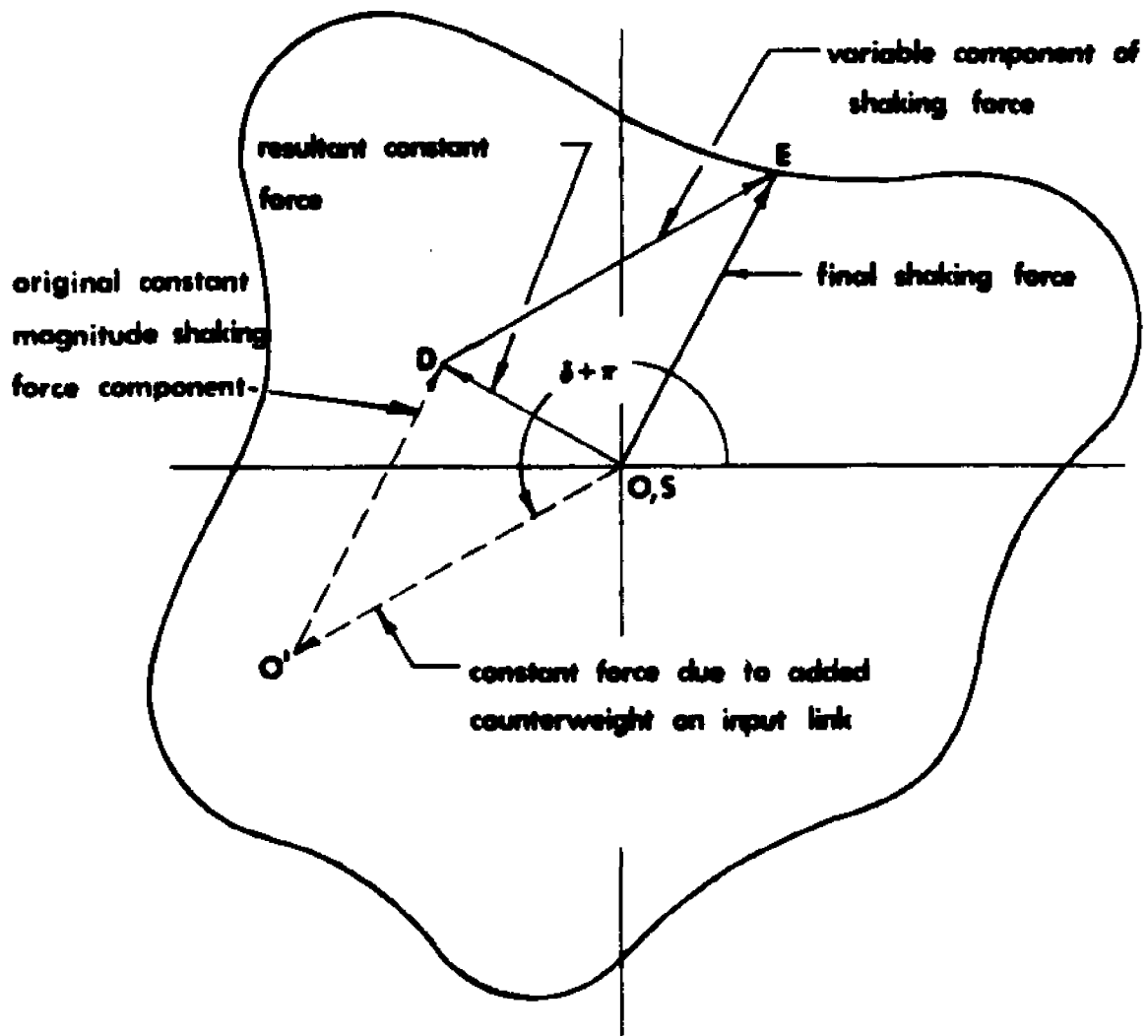


**FIG. E.2 SHAKING FORCE HODOGRAPH OF FIG. E.1 MODIFIED BY ADDITION OF INPUT LINK COUNTERWEIGHT**

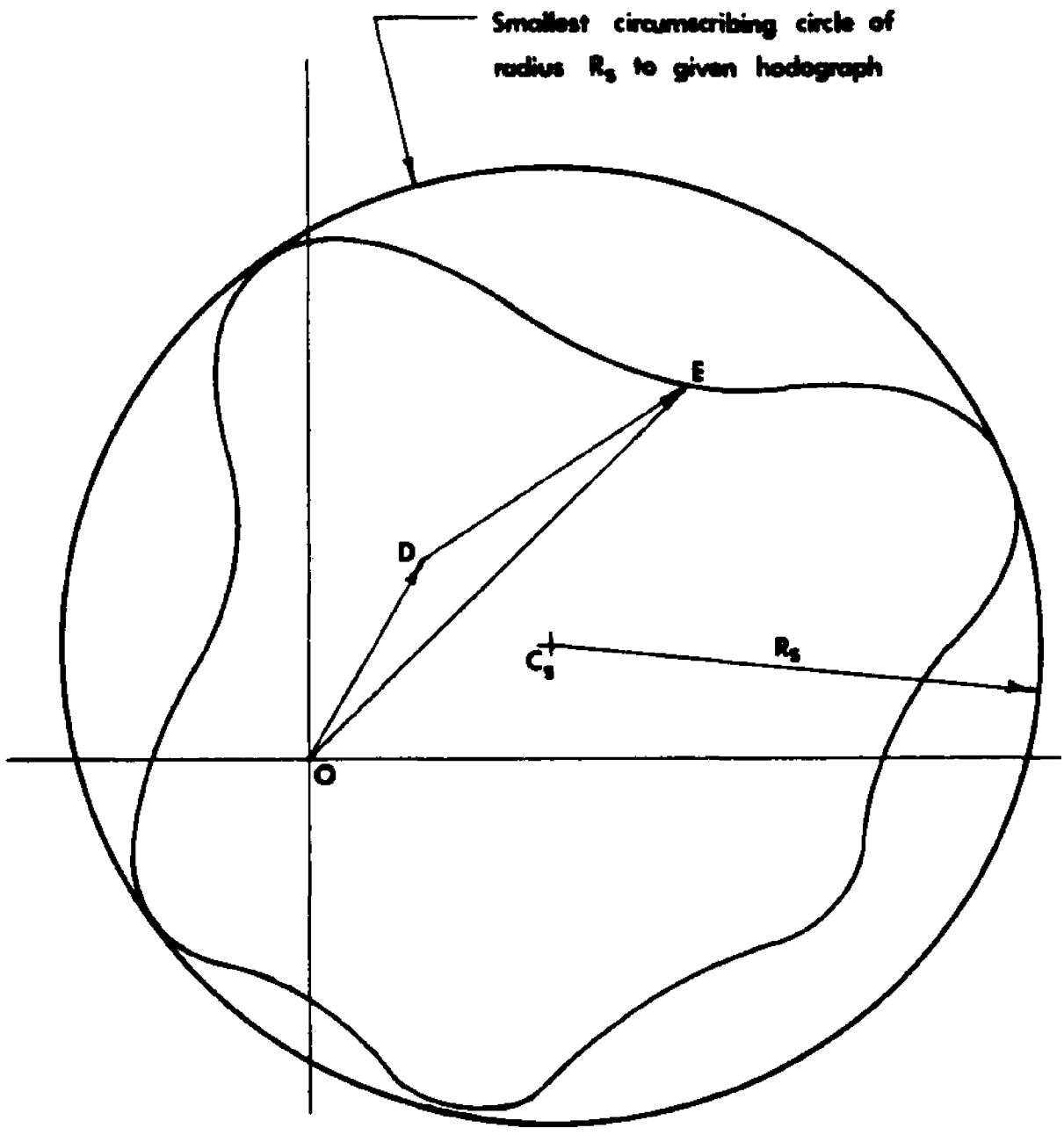


FIG. E.3 SMALLEST CIRCUMSCRIBING CIRCLE TO HODOGRAPH SHOWN IN FIG. E.1

## APPENDIX F

## COMPUTER PROGRAMS CIRCLE AND FMAX

This appendix gives the essential parts of program CIRCLE which represents an adaptation of the Harwell optimization code to the determination of the radius  $R_S$  and the coordinates  $C_{SX}$  and  $C_{SY}$  of the center of the smallest circumscribing circle to a given rotated shaking force hodograph. This program is based upon the formulation of equations (4.5) and (4.6). With the exception of the specific main program and subroutine VF01BD, the Harwell code is used as given in Appendix C.

In addition, the program FMAX, which finds the maximum values of all the reactions of a given mechanism, is shown. Outputs of programs CIRCLE and FMAX are required for the work of Appendix G.

1. Program CIRCLE: Determination Of Smallest Circumscribing Circle To A Given Shaking Force Hodograph

a. Main Program

The main program, which is listed at the end of this section, begins with the required COMMON statement which describes the array size for the constraints C. The

following variables are then defined:

$N = 3$ ; stands for the three variables  $X(1) = R_S'$ ,

$X(2) = C_{SX}'$  and  $X(3) = C_{SY}'$ .

$M = 360$ ; stands for the number of constraints.

(These constraints are formed by the use of equation (4.6)

at 1 degree intervals of the input angle  $\phi_1$ . See

subroutine VF01BD below.)

$K = 0$ , since there are no equality constraints.

$X(1)$ ,  $X(2)$  and  $X(3)$ , the starting point estimates of the variables, are made equal to 25, 6 and 1, respectively.

With  $AKMIN$  chosen arbitrarily to be  $1 \times 10^{-3}$ ,  $EPS(1)$  to  $EPS(3)$  result from  $X(1)$  to  $X(3)$ .

$DFN$  is estimated to be 10.

$MAXFN = 500$  (See Section 2a of Appendix C.)

$IPR1 = 1$ , to print every outer iteration.

$IPR2 = 1$ , to print every inner iteration.

$IW = 10000$ , since there are more than 50 constraints.

MODE = 1 (See Section 2a of Appendix C.)

Subsequently, a DO loop is set up to make the constraint scale factors, C(I), equal to 500 for all 360 constraints.

(See Appendix C.)

## MAIN

```

C THIS PROGRAM WILL CIRCUMSCRIBE A SHAKING FORCE HODOGRAPH
C ROTATED BY THE NEGATIVE OF THE INPUT ANGLE PHI
C WITH THE SMALLEST POSSIBLE CIRCLE.
C THE PROGRAM EXPANDS THE AUGMENTED LAGRANGIAN OPTIMIZATION
C ROUTINE TO HANDLE AS MANY AS 360 CONSTRAINTS
C THE VARIABLES FOR THIS PROBLEM ARE
C X(1) = RS = DISTANCE FROM TEST POINT TO POINTS ON HODOGRAPH
C X(2) = CSX = X COORDINATE OF TEST POINT
C X(3) = CSY = Y COORDINATE OF TEST POINT
C CSX AND CSY WILL REPRESENT THE CENTER OF THE CIRCUMSCRIBING
C CIRCLE AFTER THE OPTIMIZATION IS COMPLETE.
C
C THE CONSTRAINTS ARE
C C(I) = X(1)**2 - (FSXR(I) - X(2))**2 - (FSYR(I) - X(3))**2
C
C THE HODOGRAPH WILL BE APPROXIMATED BY DISCRETE POINTS
C TAKEN AT 1 DEGREE INTERVALS OF THE INPUT ANGLE PHI.
C THE STARTING POINT IS
C X(1)=25, X(2)=6, X(3)=1
0001 IMPLICIT REAL*8(A-H,O-Z)
0002 COMMON/VFOLEO/C(1080)
0003 REAL*8 X(3),EPS(3)
0004 N = 3
0005 M = 360
0006 K=0
0007 PI=3.14159300
C THE STARTING POINT IS ESTIMATED TO BE
0008 X(1)=2.501
0009 X(2)=6.000
0010 X(3)=1.000
C
0011 AKMIN=10-3
0012 EPS(1)=2.50-2
0013 EPS(2)=6.00-3
0014 EPS(3)=1.00-3
C
0015 OFN=101
0016 MAXFN=500
0017 IPR1=1
0018 IPR2=1
C SET IW=10000. IF MORE STORAGE IS REQUIRED, VFOLEO WILL
C STOP AND PRINT OUT NEW REQUIREMENT.
0019 IW=10000
0020 MODE=1
C THE CONSTRAINT SCALE FACTORS ARE ALL ESTIMATED TO BE 500
0021 DO 10 I=1,360
0022 10 C(I)=502
0023 CALL VFOLEOIN,M,K,X,EPS,AKMIN,OFN,MAXFN,IPR1,IPR2,IW,MODE)
0024 STOP
0025 END

```

- b. Subroutine VF01BD (See listing of program at the end of this section.)

After allocating storage for the various subscripted variables, subroutine VF01BD lists the COMMON statements described in Section 2a of Appendix C. The subsequent steps are:

1.  $F = X(1)$ , i.e. the objective function  $R_S'$  is declared as the variable  $x_1$ . (See equation (4.5).)
2.  $G(1) = 1$ , represents the derivative  $\frac{\partial F}{\partial x_1}$ .  
Since all other derivatives of  $F$  vanish, they must be set equal to zero (i.e.  $G(2)=G(3)=0$ ).
3.  $A1$  to  $A4$  represent the link dimensions of the sample mechanism of Section IV.E.
4.  $RPM = 500$ , stands for the constant input rpm.
5.  $PHIVEL$  converts  $RPM$  to the input angular velocity  $\dot{\phi}_1$ .
6.  $PHIACC = 0$ , represents the zero input link angular acceleration  $\ddot{\phi}_1$ .
7.  $DELPHI = 1$ , represents the 1 degree increments of the input link angle  $\phi_1$ .

8. The constant general mass-distance products are defined in P1, Q1, P3 and Q3 according to equations (4.54) to (4.57).

A DO loop is then set up to compute the constraints as well as their derivatives for each of the 360 positions of the mechanism. To this end, the shaking force components  $F_{SX}$  and  $F_{SY}$ , given in lines 50 and 51 of the program, must first be found.

The required kinematic values are supplied by way of subroutine MOTION (see Section 3b of Appendix C both for subroutine MOTION and the determination of  $F_{SX}$  and  $F_{SY}$ ).

The shaking force components are then rotated by the negative of the input angle  $\phi_1$ , according to equation (4.3), and one obtains:

$$F_{SX_R}(I) = F_{SX}(I)\cos\phi_1 + F_{SY}(I)\sin\phi_1 \quad (F.1)$$

$$F_{SY_R}(I) = -F_{SX}(I)\sin\phi_1 + F_{SY}(I)\cos\phi_1 \quad (F.2)$$

Finally, the constraint equation (4.6) and its derivatives with respect to the three variables are evaluated. Thus,

$$C(I) = (X_1)^2 - (F_{SX_R}(I) - X_2)^2 - (F_{SY_R}(I) - X_3)^2 \quad (F.3)$$

$$GC(1,I) = 2X_1 \quad (F.4)$$

$$GC(2,I) = 2(F_{SX_R}(I) - X_2) \quad (F.5)$$

$$GC(3,I) = 2(F_{SY_R}(I) - X_3) \quad (F.6)$$

```

0001      SUBROUTINE VFO1BD(N,M,X)
0002      IMPLICIT REAL*8(A-H,O-Z)
0003      REAL*8 X(3)
0004      INTEGER PHID, PHID1, DELPHI
0005      REAL*8 KAY1(360),KAY3(360)
0006      DIMENSION GMA1(360),GMA3(360),FSX(360),FSY(360)
0007      DIMENSION VAR1(360),VAR2(360),VAR3(360),VAR4(360)
0008      DIMENSION VAR5(360),VAR6(360),VAR7(360),VAR8(360)
0009      DIMENSION PSIA(360),PSIV(360),FSXR(360),FSYR(360)
0010      DOUBLE PRECISION DCOS,DSIN,DSQRT,DATAN2
0011      COMMON/VFO1CD/F
0012      COMMON/VFO1OD/G161
0013      COMMON/VFO1ED/C110B0)
0014      COMMON/VFO1FD/GC(3,360)
0015      PI=3.14159300
0016      C THE OBJECTIVE FUNCTION IS
0017      F=X(1)
0018      C G(I)=PARTIAL DERIVATIVES OF OBJECTIVE FUNCTION (FIX(1)) WITH
0019      C RESPECT TO VARIABLES X(1),X(2),X(3)
0020      G(1)=100
0021      G(2)=000
0022      G(3)=000
0023      C THE LINK DIMENSIONS ARE
0024      A1=200
0025      A2=600
0026      A3=300
0027      A4=5.500
0028      C THE ANGULAR VELOCITY IS
0029      RPM = 502
0030      Z=PI/1.3002
0031      PHIVEL=RPM*Z*600
0032      C THE ANGULAR ACCELERATION OF THE INPUT LINK IS
0033      PHIACC=000
0034      C THE ANGULAR INCREMENT FOR THE HODOGRAPH FORCES IS
0035      DELPHI = 1
0036      C THE GENERAL MASS-DISTANCE PRODUCTS ARE
0037      P1 = .1377720-2
0038      P2 = -.19366710-3
0039      P3 = .3099220-2
0040      P3 = .275470650-3
0041      C
0042      G(120,PHID)=1,360,DELPHI
0043      PHID=PHID1 - 1
0044      PHI=Z * PHID
0045      I = PHID/DELPHI + 1
0046      C THE KINEMATICS OF THE LINKAGE ARE DETERMINED IN
0047      C SUBROUTINE MOTION
0048      CALL MOTION (PHI,A1,A2,A3,A4,PSI,PHIVEL,PHIACC,
0049      I,PSIV(I),PSIA(I))
0050      KAY1(I) = DSQRT(PHIVEL**4 + PHIACC**2)
0051      KAY3(I) = DSQRT(PSIV(I)**4 + PSIA(I)**2)
0052      GMA1(I) = PHI - DATAN2(PHIACC,PHIVEL**2)
0053      GMA3(I) = PSI - DATAN2(PSIA(I),PSIV(I)**2)
0054      VAR1(I) = KAY1(I)*DCOS(GMA1(I))
0055      VAR2(I) = KAY1(I)*DSIN(GMA1(I))
0056      VAR3(I) = KAY3(I)*DCOS(GMA3(I))

```

```

0045      VAR4(I) = KAY3(I)*DSIN(GMA3(I))
0046      VAR5(I) = KAY1(I)*DSIN(GMA1(I))
0047      VAR6(I) = KAY1(I)*DCOS(GMA1(I))
0048      VAR7(I) = KAY3(I)*DSIN(GMA3(I))
0049      VAR8(I) = KAY3(I)*DCOS(GMA3(I))
      C THE SHAKING FORCES ARE
0050      FSX(I) = P1*VAR1(I)-Q1*VAR2(I)+P3*VAR3(I)-Q3*VAR4(I)
0051      FSY(I) = P1*VAR5(I)+Q1*VAR6(I)+P3*VAR7(I)+Q3*VAR8(I)
      C THE COMPONENTS OF THE SHAKING FORCE ROTATED BY THE NEGATIVE
      C OF THE INPUT ANGLE PHI ARE
0052      FSXR(I)=FSX(I)*DCOS(PHI) + FSY(I)*DSIN(PHI)
0053      FSYR(I)=-FSX(I)*DSIN(PHI) + FSY(I)*DCOS(PHI)
      C THE CONSTRAINTS ARE
0054      C(I) = (X(I))**2 - (FSXR(I) - X(2))**2 - (FSYR(I) - X(3))**2
      C THE DERIVATIVES OF THE CONSTRAINTS WITH RESPECT TO THE VARIABLES ARE
0055      GC(1,I) = 200*X(I)
0056      GC(2,I) = 200*(FSXR(I) - X(2))
0057      GC(3,I) = 200*(FSYR(I) - X(3))
0058      120 CONTINUE
0059      RETURN
0060      END

```

c. Essential Elements Of Program Output

The output format shown below is similar to that described in Section 3d of Appendix C. For this optimization, three outer iterations were required.

OUTER ITERATION NUMBER IS 1

```

-----
0      1
0.290000000000000000 C2
0.290000000000000000 C2  0.600000000000000000 01  0.100000000000000000 01
0.100000000000000000 01  0.0                                0.0
-----

```

```

      •
      •
      •

```

```

-----
13     23     1
0.15255706656822470 C2
0.14920486415677140 C2  0.89315658750766510 01 -0.33367080088616710 01
0.52749634140781110 C4 -0.43477863431320650 C4  0.10531633312126540 C4
-----

```

OUTER ITERATION NUMBER IS 3

```

-----
0      1
0.15835851727614230 C2
0.15829884040015580 C2  0.8977452524092560 01 -0.34566073040342180 01
0.74094556188739120 00 -0.11317110407828110 00  0.74453744090627700 01
-----
1      2
0.15801620644633070 C2
0.15743980865143670 C2  0.89633750502356850 01 -0.34841974976070650 01
0.85766978972432200 C1 -0.43209137791510810 C1  0.38879174659018260 C1
-----
2      3
0.15801011244315290 C2
0.15734146547757620 C2  0.89755503099812970 01 -0.34729575182740540 01
-0.16737533250817900 C3 -0.75433295809551500 C2  0.52712591029754190 C2
-----
3      4
0.15901001027578290 C2
0.15734273109447360 C2  0.89856917082630360 01 -0.34646686904177430 01
-0.93315460257641610 C3 -0.10730788385186310 C2  0.81725202592654220 C3
-----
4      5     1
0.15901000784353260 C2
0.15734431231227270 C2  0.8974637157024900 01 -0.34647600788965530 01
-0.43785818270244260 C4 -0.65226497824600570 C5  0.56372744323633130 C5
-----

```

Again, a set of four lines represent an inner iteration

where the first number in the first line stands for the total number of inner iterations within the given outer iteration. The second number in this line stands for the number of times the subroutine VF01ZD has been called upon.

The number in the second line represents the current value of the composite function  $\Phi$  according to equation (C.1).

The third line gives the current values of  $R_S'$ ,  $C_{SX}'$  and  $C_{SY}'$ . In the first iteration, the initial values are reproduced.

The fourth line shows the derivatives of the composite function with respect to the three variables.

The last group of inner iterations shown represents the final results, i.e.

$$R_S = 15.734 \quad (\text{lbs}) \quad (\text{F.7})$$

$$C_{SX} = 8.987 \quad (\text{lbs}) \quad (\text{F.8})$$

$$C_{SY} = -3.464 \quad (\text{lbs}) \quad (\text{F.9})$$

2. Program FMAX: Determination Of Maximum Bearing Forces, Shaking And Input Moments Of A Given Mechanism (See listing of program at the end of this section.)

This program, which is specifically written for the example mechanism of Section IV.E, first determines the X and Y components of the mechanism reactions with the help of the following subroutines:

MOTION: Finds the coupler and output link angles, angular velocities and angular accelerations. (See Appendix C for a listing of the program.)

KINMAT: Evaluates the positions, velocities and accelerations of the mass centers on the input, coupler and output links.

REACTS: Defines the X and Y components of each bearing force, the shaking force and the input moment as functions of the input angle  $\phi_1$ .

Programs KINMAT and REACTS are also reproduced below.

The absolute magnitudes of each of the reactions are then found for all 72 mechanism positions by way of:

$$F_{M/G(I)} = \left( [F_{SX(I)}]^2 + [F_{SY(I)}]^2 \right)^{\frac{1}{2}}$$

$$F_{41(I)} = \left( [F_{41X(I)}]^2 + [F_{41Y(I)}]^2 \right)^{\frac{1}{2}}$$

$$F_{43(I)} = \left( [F_{43X(I)}]^2 + [F_{43Y(I)}]^2 \right)^{\frac{1}{2}}$$

$$F_{21(I)} = \left( [F_{21X(I)}]^2 + [F_{21Y(I)}]^2 \right)^{\frac{1}{2}}$$

$$F_{23(I)} = \left( [F_{23X(I)}]^2 + [F_{23Y(I)}]^2 \right)^{\frac{1}{2}}$$

$$M_{M/G(I)} = \left( [2.75F_{41Y(I)} - 2.75F_{43Y(I)} - M_{41(I)}]^2 \right)^{\frac{1}{2}}$$

$$M_{41(I)} = \left( [M_{41(I)}]^2 \right)^{\frac{1}{2}}$$

The maximum values of each of the above is obtained by continuous comparison with the previously established largest value. The results are given by:

$$(F_{41})_{MAX} = 52.122 \quad \text{lbs} \quad (\text{F.10})$$

$$(F_{21})_{MAX} = 50.743 \quad \text{lbs} \quad (\text{F.11})$$

$$(F_{23})_{MAX} = 40.377 \quad \text{lbs} \quad (\text{F.12})$$

$$(F_{43})_{MAX} = 39.273 \quad \text{lbs} \quad (\text{F.13})$$

$$(M_{M/G})_{MAX} = 90.902 \quad \text{lb-in} \quad (\text{F.14})$$

$$(M_{41})_{MAX} = 38.720 \quad \text{lb-in} \quad (\text{F.15})$$

$$\text{and } (F_{M/G})_{MAX} = R^O_{MAX} = 25.004 \quad \text{lbs} \quad (\text{F.16})$$

MAIN

```

C THIS PROGRAM WILL FIND THE MAXIMUM ABSOLUTE VALUES OF THE
C BEARING REACTIONS, SHAKING MOMENT, INPUT MOMENT AND SHAKING
C FORCE FOR A GIVEN MECHANISM.
0001      IMPLICIT REAL*8(A-H,O-Z)
0002      INTEGER PHID, PHID1, DELPHI
0003      REAL*8 K2,K3,M1,M2,M3,LAMBDA,LAMB1(73),LAMB2(73)
0004      REAL*8 MMG(73),M41(73),M41A(73),MMGMAX,M41MAX
0005      DIMENSION F41X(73),F41Y(73),F21X(73),F21Y(73),F23X(73),
0006      F23Y(73),F43X(73),F43Y(73),F5X(73),F5Y(73)
0007      DIMENSION F43(73),F41(73),F21(73),F23(73)
0008      DIMENSION PSIV(73),PSIA(73),FMG(73)
0009      DIMENSION X1(73),Y1(73),X2(73),Y2(73),X3(73),Y3(73)
0010      DIMENSION VX1(73),VY1(73),VX2(73),VY2(73),VX3(73),VY3(73)
0011      DIMENSION AX1(73),AY1(73),AX2(73),AY2(73),AX3(73),AY3(73)
0012      DOUBLE PRECISION DCOS,DSIN,DSQRT,DATAN2
0013      PI=3.14159300
0014      Z = PI/1.802
C THE LINK DIMENSIONS ARE
0014      A1=200
0015      A2=600
0016      A3=300
0017      A4=5.500
C THE ANGULAR VELOCITY OF THE INPUT LINK IS
0018      RPM = 502
0019      PHIVEL = RPM*2*PI
C THE ANGULAR ACCELERATION OF THE INPUT LINK IS
0020      PHIACC = 000
C THE ANGULAR INCREMENT IS
0021      DELPHI = 5
C THE CENTER OF MASS LOCATIONS FOR EACH LINK ARE
0022      Z1 = 100
0023      Z1 = 000
0024      Z2 = 300
0025      Z2 = .40300
0026      Z3 = 1.500
0027      Z3 = 000
C THE RAOULI OF GYRATION OF COUPLER AND OUTPUT LINKS ARE
0028      K2 = 2.097000
0029      K3 = 1.574700
C THE LINK MASSES ARE
0030      M1 = 5.10420-4
0031      M2 = 13.57100-4
0032      M3 = 5.23780-4
C
0033      F41MAX = 000
0034      F21MAX = 000
0035      F23MAX = 000
0036      F43MAX = 000
0037      MMGMAX = 000
0038      M41MAX = 000
0039      FMGMAX = 000
0040      CO 120 PHID1=1.356,DELPHI
0041      PHID=PHID1 - 1
0042      PHI=2*PHID
0043      I = PHI/DELPHI * 1
0044      CALL MOTION(PHI,A1,A2,A3,A4,PSI,PHIVEL,PHIACC,PSIV(I),PSIA(I),

```

```

LAMBDA,LAMB(L),LAMB(L))
CALL KINMAT(PH),PHVEL,PHACC,PSI,PSIV(L),PSTAI(L),AI,AZ,A3,A4,
1 P1,Q1,P2,Q2,P3,Q3,X1(L),V1(L),X2(L),V2(L),X3(L),
2 V3(L),X4(L),V4(L),X5(L),V5(L),X6(L),V6(L),
3 AX(L),AV(L),AX2(L),AV2(L),AX3(L),AV3(L))
CALL REACTS(PH),PHVEL,PHACC,LAMBDA,LAMB(L),LAMB(L),PSI,PSIV(L),
1 PSTAI(L),AI,AZ,A3,A4,P1,Q1,P2,Q2,P3,Q3,K1,M1,M2,M3,
2 F4X(L),F4Y(L),F4Z(L),F21X(L),F21Y(L),F23X(L),F23Y(L),
3 F4X(L),F4Y(L),F4Z(L),F21X(L),F21Y(L),F23X(L),F23Y(L),
F41(L)=DSQR(F4X(L)*F4X(L)+F4Y(L)*F4Y(L))
F42(L)=DSQR(F4X(L)*F4X(L)+F4Z(L)*F4Z(L))
F43(L)=DSQR(F4Y(L)*F4Y(L)+F4Z(L)*F4Z(L))
F21(L)=DSQR(F21X(L)*F21X(L)+F21Y(L)*F21Y(L))
F23(L)=DSQR(F23X(L)*F23X(L)+F23Y(L)*F23Y(L))
MG(L)=DSQR(F21(L)*F21(L)+F23(L)*F23(L))
M4(L)=DSQR(M4(L)*M4(L))
TEST FOR MAXIMUM VALUES
C
IF (F41(L).GT.F41MAX)F41MAX=F41(L)
IF (F42(L).GT.F42MAX)F42MAX=F42(L)
IF (F43(L).GT.F43MAX)F43MAX=F43(L)
IF (F21(L).GT.F21MAX)F21MAX=F21(L)
IF (F23(L).GT.F23MAX)F23MAX=F23(L)
IF (MG(L).GT.MGMAX)MGMAX=MG(L)
IF (M4(L).GT.M4MAX)M4MAX=M4(L)
120 CONTINUE
WRITE (5,130)
130 FORMAT (5X,'F41MAX',9X,'F21MAX',9X,'F23MAX',9X,'F43MAX',7X,
'MGMAX',9X,'M4MAX',
)
WRITE (5,140) F41MAX,F21MAX,F23MAX,F43MAX,MGMAX,M4MAX
140 FORMAT (1,'6015.7)
WRITE (5,150)
150 FORMAT (1,'01.2X',THE MAXIMUM SHAKING FORCE IS!)
WRITE (5,160) F5MAX
160 FORMAT (1015.7)
STOP
END
CC71

```

```

0001 SUBROUTINE KINMAT (PHI,PHIVEL,PHIACC,PSI,PSIVEL,PSIACC,A1,A2,A3,
1      A4,P1,Q1,P2,Q2,P3,Q3,X1,Y1,X2,Y2,X3,Y3,VX1,VY1,VX2,VY2,
2      VX3,VY3,AX1,AY1,AX2,AY2,AX3,AY3)
C      CALCULATION OF X AND Y COMPONENTS OF POSITION, VELOCITY, AND
C      ACCELERATION OF ARBITRARY POINTS ON CRANK, COUPLER, AND OUTPUT
C      LINK OF A FOUR BAR LINKAGE.
C      GIVEN INPUT AND OUTPUT ANGLES, LINKAGE DIMENSIONS,
0002 IMPLICIT REAL*8(A-H,O-Z)
0003 DOUBLE PRECISION DCOS, DSIN, DSORT, DATAN2, DABS
0004 SA = DSIN (PHI)
0005 CA = DCOS (PHI)
0006 SB = DSIN (PSI)
0007 CB = DCOS (PSI)
0008 X1 = P1*CA - Q1*SA
0009 Y1 = P1*SA + Q1*CA
0010 VX1 = -Y1*PHIVEL
0011 VY1 = X1*PHIVEL
0012 AX1 = -Y1*PHIACC - VY1*PHIVEL
0013 AY1 = X1*PHIACC + VX1*PHIVEL
0014 TA = (A2 - P2) * A1/A2
0015 TB = Q2 * A1/A2
0016 TC = P2 * A3/A2
0017 TD = Q2 * A3/A2
0018 BPH = TA*CA + TB*SA
0019 BPS = TA*SA - TB*CA
0020 APS = TC*CB - TD*SB
0021 BPS = TC*SB + TD*CB
0022 X2 = BPH + APS + A4*P2/A2
0023 Y2 = BPS + BPS + A4*Q2/A2
0024 VX2 = -BPH*PHIVEL - BPS*PSIVEL
0025 VY2 = BPH*PHIVEL + BPS*PSIVEL
0026 AX2 = -BPH*PHIACC - BPH*PHIVEL**2 - BPS*PSIACC - APS*PSIVEL**2
0027 AY2 = BPH*PHIACC - BPH*PHIVEL**2 + APS*PSIACC - BPS*PSIVEL**2
0028 X3 = P3*CB - Q3*SB + A4
0029 Y3 = P3*SB + Q3*CB
0030 VX3 = -Y3*PSIVEL
0031 VY3 = X3*PSIVEL
0032 AX3 = -Y3*PSIACC - VY3*PSIVEL
0033 AY3 = X3*PSIACC + VX3*PSIVEL
0034 RETURN
0035 END

```

```

0001 SUBROUTINE REACTS(PHI,PHIVEL,PHIACC,LAMBDA,LAMVEL,LAMACC,PSI,
      1PSIVEL,PSIACC,A1,A2,A3,A4,P1,Q1,P2,Q2,P3,Q3,K2,K3,M1,M2,M3,F41X
      2,F41Y,F21X,F21Y,F23X,F23Y,F43X,F43Y,FSX,FSY,M41)
0002 IMPLICIT REAL*8(A-H,O-Z)
0003 DOUBLE PRECISION DCOS, DSIN,DSQRT,DATAN2,DABS
0004 REAL*8 LAMBDA,LAMVEL,M1,M2,M3,M4,LAMV2,I2,I3,LAMACC,K2,K3
0005 SP = DSIN(PHI)
0006 CP = DCOS(PHI)
0007 SL = DSIN(LAMBDA)
0008 CL = DCOS(LAMBDA)
0009 SS = DSIN(PSI)
0010 CS = DCOS(PSI)
0011 TAU1 = DSIN(PHI - LAMBDA)
0012 TAU11 = DCOS(PHI - LAMBDA)
0013 TAU3 = DSIN(PSI - LAMBDA)
0014 PHIV2 = PHIVEL*PHIVEL
0015 LAMV2 = LAMVEL*LAMVEL
0016 PSIV2 = PSIVEL*PSIVEL
0017 I2 = M2*I2*P2 + Q2*Q2 + K2*K2)
0018 I3 = M3*I3*P3 + Q3*Q3 + K3*K3)
0019 D2 = I2*LAMACC/(A2*TAU3)
0020 D3 = I3*PSIACC/(A3*TAU3)
0021 A2T3 = A2*TAU3
0022 F41X = -M2*A1*PHIV2*CP - M1*P1*PHIV2*CP + M1*Q1*PHIV2*SP
      1 - M2*P2*(LAMACC*SL + LAMV2*CL - A1*CS*PHIV2*TAU1/A2T3)
      2 - M2*Q2*(LAMACC*CL - LAMV2*SL + A1*CS*PHIV2*TAU11/A2T3)
      3 - D2*CS - D3*CL
0023 F41Y = -M2*A1*PHIV2*SP - M1*P1*PHIV2*SP - M1*Q1*PHIV2*CP
      1 + M2*P2*(LAMACC*CL - LAMV2*SL + A1*SS*PHIV2*TAU1/A2T3)
      2 - M2*Q2*(LAMACC*SL + LAMV2*CL + A1*SS*PHIV2*TAU11/A2T3)
      3 - D2*SS - D3*SL
0024 F21X = M2*A1*PHIV2*CP + M2*P2*(LAMACC*SL + LAMV2*CL - A1*CS
      1 *PHIV2*TAU1/A2T3) + M2*Q2*(LAMACC*CL - LAMV2*SL
      2 + A1*CS*PHIV2*TAU11/A2T3) + D2*CS + D3*CL
0025 F21Y = M2*A1*PHIV2*SP + M2*P2*(LAMACC*CL + LAMV2*SL - A1*SS
      1 *PHIV2*TAU1/A2T3) + M2*Q2*(LAMACC*SL + LAMV2*CL
      2 + A1*SS*PHIV2*TAU11/A2T3) + D2*SS + D3*SL
0026 F23X = M2*P2*A1*CS*PHIV2*TAU1/A2T3 - M2*Q2*A1*CS*PHIV2*TAU11/A2T3
      1 - D2*CS - D3*CL
0027 F23Y = M2*P2*A1*SS*PHIV2*TAU1/A2T3 - M2*Q2*A1*SS*PHIV2*TAU11/A2T3
      1 - D2*SS - D3*SL
0028 F43X = -M2*P2*A1*CS*PHIV2*TAU1/A2T3 + M2*Q2*A1*CS*PHIV2*TAU11/A2T3
      1 - M3*P3*(PSIACC*SS + PSIV2*CS) - M3*Q3*(PSIACC*CS - PSIV2
      2 *SS) + D2*CS + D3*CL
0029 F43Y = -M2*P2*A1*SS*PHIV2*TAU1/A2T3 + M2*Q2*A1*SS*PHIV2*TAU11/A2T3
      1 + M3*P3*(PSIACC*CS - PSIV2*SS) - M3*Q3*(PSIACC*SS + PSIV2
      2 *CS) + D2*SS + D3*SL
0030 FSX = -(F41X + F43X)
0031 FSY = -(F41Y + F43Y)
0032 M41 = M2*P2*(A1*(LAMACC*TAU11 + LAMV2*TAU1)
      1 - A1*A1*DSIN(PHI - PSI) *PHIV2*TAU1/A2T3)
      2 + M2*Q2*(A1*(LAMACC*TAU1 - LAMV2*TAU11)
      3 + A1*A1*DSIN(PHI - PSI) *PHIV2*TAU11/A2T3)
      4 + D2*A1*DSIN(PHI - PSI) *PHIV2*TAU11/A2T3
0033 RETURN
0034 END

```

Output from program FMAX:

F41MAX	F21MAX	F23MAX	F43MAX	MFGMAX	M41MAX
0.52122020 02	0.50743260 02	0.40376340 02	1.39273270 02	0.90901020 02	0.38720070 02
THE MAXIMUM SHAKING FORCE IS					
0.29003760 02					

## APPENDIX G

## COMPUTER PROGRAM OPTIMIZE

This appendix describes program OPTIMIZE which adapts the Harwell optimization code to the problem of simultaneously minimizing the maximum bearing forces, input moment and shaking moment associated with a prescribed maximum shaking force of a given four-bar linkage. This program is based on the formulation of equations (5.11) - (5.17) and follows the computational sequence outlined in Sections V-D-1 and V-D-2. The main program and the subroutine VF01BD, which are written for the sample mechanism of Section IV-E and a 50 percent reduction in the maximum shaking force<sup>1</sup>, are first described. Both of the above routines follow the outline of Appendix C which shows the use of the Harwell code. Subsequently, essential elements of the output of the program are given.

### 1. Main Program

The main program, which is listed at the end of this section, begins with COMMON statements which define the array size for the constraints C and their derivatives GC.

---

<sup>1</sup> Both the main program and the subroutine VF01BD may be easily adapted to other four-bar linkages and reductions in maximum shaking force, including full force balance.

The following variables are then defined:

$N = 5$ ; stands for the five variables  $X(1)=z$ ,  $X(2)=R_3^*$ ,  
 $X(3)=\theta_3^*$ ,  $X(4)=R_2^*$ , and  $X(5)=\theta_2^*$ .

$M = 439$ ; stands for the number of constraints. (See  
comment cards at beginning of program for definition  
of constraints.)

$K = 1$ ; refers to the single equality constraint as  
represented by the general equipollent circle equation.  
(See equation (5.4).)

$X(1)$  to  $X(5)$ , the starting point estimates of the  
variables, are made equal to 1, .705, 3.23, .559,  
and 3.23, respectively (a guess based on the two-  
counterweight method of Section IV).

With  $AKMIN$  chosen to be  $1 \times 10^{-4}$ ,  $EPS(1)$  to  $EPS(5)$   
result from  $X(1)$  to  $X(5)$ . (This value results in  
sufficiently close adherence to the equipollent circle  
equality constraint to insure an accurate prescribed  
maximum shaking force.)

$DFN$  is estimated to be 0.5.

MAXFN = 900 was specified, rather than the usual 500,  
because of the increased number of constraints.

IPR1 = 1, to print each outer iteration.

IPR2 = 1, to print each inner iteration.

IW = 10000; since there are more than 50 constraints.

MODE = 1

After setting scale factors for the constraints  
C(1) to C(7) equal to their starting point estimates, a  
DO loop is used to make the remaining 432 constraints  
equal to 0.5. (This again represents an arbitrary estimate.)  
Subsequently, all derivatives of constraints which result in  
a constant term are defined by the parameters GC(N,M). (See  
line 37 in Section 2.) Finally, the subroutine VF01AD is  
called.

## MAIN

```

C THIS PROGRAM OPTIMIZES THE MAXIMUM BEARING FORCES, MAXIMUM
C SHAKING MOMENT AND MAXIMUM INPUT MOMENT FOR A PRESCRIBED
C MAXIMUM SHAKING FORCE FOR A GIVEN FOUR-BAR LINKAGE.
C CIRCULAR COUNTERWEIGHTS, TANGENT TO PIVOT POINTS, ARE USED ON
C ALL MOVING LINKS. EACH REACTION IS EVALUATED AT FIVE DEGREE
C INCREMENTS OF THE INPUT LINK ANGLE.
C
C VARIABLES ARE X(1)=Z, X(2)=R3STAR=OUTPUT COUNTERWEIGHT
C RADIUS, X(3)=THETA3STAR=OUTPUT CWT. ANGLE, X(4)=R2STAR=
C COUPLER COUNTERWEIGHT RADIUS, X(5)=THETA2STAR=COUPLER CWT.
C ANGLE.
C
C THE CONSTRAINTS ARE
C C(1) = FOUR-PI-LEFT CIRCLE CONSTRAINT EQUATION
C C(2) = X(2) (RADIUS R3STAR GREATER THAN ZERO)
C C(3) = X(3) (ANGLE THETA3STAR GREATER THAN ZERO)
C C(4) = 2*PI - X(3) (ANGLE THETA3STAR LESS THAN 2*PI)
C C(5) = X(4) (RADIUS R2STAR GREATER THAN ZERO)
C C(6) = X(5) (ANGLE THETA2STAR GREATER THAN ZERO)
C C(7) = 2*PI - X(5) (ANGLE THETA2STAR LESS THAN 2*PI)
C C(8) - C(19) = INPUT GROUND BEARING CONSTRAINTS
C C(20) - C(31) = OUTPUT GROUND BEARING CONSTRAINTS
C C(32) - C(43) = INPUT-TO-COUPLER BEARING CONSTRAINTS
C C(44) - C(55) = COUPLER-TO-OUTPUT BEARING CONSTRAINTS
C C(56) - C(67) = SHAKING MOMENT CONSTRAINTS WITH RESPECT TO
C MIDPOINT BETWEEN GROUND PIVOTS
C C(68) - C(79) = INPUT MOMENT CONSTRAINTS
C (IMPLICIT REAL*9(A-H,O-Z))
C001 COMMON/VF01E0/C(1,31)
C002 COMMON/VF01F0/GC(15,43)
C003 REAL*9 X(5),EPS(5)
C004
C005 -----
C THE TOTAL NUMBER OF VARIABLES IS DESIGNATED BY N
C006 N=5
C THE TOTAL NUMBER OF CONSTRAINTS IS DESIGNATED BY M
C007 M=43
C THE TOTAL NUMBER OF EQUALITY CONSTRAINTS IS DESIGNATED BY K
C008 K=1
C THE STARTING POINT IS ESTIMATED TO BE
C009 X(1)=100
C010 X(2)=.70500
C011 X(3)=3.23000
C012 X(4)=.55900
C013 X(5)=3.23000
C014 AKM(1)=10-4
C015 EPS(1)=10-4
C016 EPS(2)=.7050-4
C017 EPS(3)=3.2300-4
C018 EPS(4)=.5570-4
C019 EPS(5)=3.2300-4
C
C020 DFN=0.900
C021 MAXFN=9.00
C022 IPR1=1
C023 IPR2=1
C SET IW=10000. IF MORE STORAGE IS REQUIRED, VF01AD WILL

```



2. Subroutine VF01BD (See listing of program at the end of this section.)

After allocating storage for the various subscripted variables, subroutine VF01BD lists the COMMON statements described in Section 2a of Appendix C. The subsequent steps satisfy program requirements and introduce necessary functions and input data:

1.  $F = X(1)$ ; the objective function  $z$  is declared as the variable  $X(1)$ . (See equation (5.11).)
2.  $G(1)$  to  $G(5)$ ; represent the derivatives of the objective function  $F$  with respect to the five variables  $X(1)$  to  $X(5)$ .
3.  $A1$  to  $A4$  represent the link dimensions of the sample mechanism as given in Table 4.1
4.  $RHO1ST$ ,  $RHO2ST$ , and  $RHO3ST$  represent the densities of the steel counterweights used on the input, coupler and output links. (All are made  $7.3316 \times 10^{-4}$  lb-sec<sup>2</sup>/in<sup>4</sup>.)
5.  $H1STAR$ ,  $H2STAR$ , and  $H3STAR$  define the counterweight thicknesses as 0.625 inches.

6.  $R_{MAX}^0 = 25.004$  lbs; this maximum shaking force of the unbalanced linkage is obtained with the help of program FMAX (See Appendix F.2)
7.  $R_S = 15.734$  lbs,  $C_{SX} = 8.987$  lbs,  $C_{SY} = -3.464$  lbs; the radius and coordinates of the center of the smallest circumscribing circle to the rotated shaking force hodograph are found with the help of program CIRCLE. (See Appendix F.1)
8.  $OC_S =$  magnitude of vector  $\overline{OC}_S$  (see equation (4.24)).
9. DELTAS = angle  $\delta_S$  of vector  $\overline{OC}_S$  (see equation (4.24)).
10. ETA = 0.5; defines reduction factor  $\eta$ .
11. MU; proportionality factor  $\mu$ , as given by equation (4.10).
12. RPM = 500; stands for the constant input rpm.
13. PHIVEL converts RPM to the input angular velocity  $\dot{\phi}_1$ .
14. PHIACC = 0, represents the zero input link angular acceleration  $\ddot{\phi}_1$ .
15. DELPHI = 5, represents the 5 degree increments of the input link angle  $\phi_1$ .

16.  $W_1$  to  $W_6$ , stand for the weighting factors of equations (5.12) to (5.17). They are set equal to unity.
17.  $(F_{41}^{\circ})_{MAX} = 52.12$  lbs,  $(F_{43}^{\circ})_{MAX} = 39.27$  lbs,  
 $(F_{21}^{\circ})_{MAX} = 50.74$  lbs,  $(F_{23}^{\circ})_{MAX} = 40.38$  lbs,  
 $(M_{M/G}^{\circ})_{MAX} = 90.90$  in-lbs, and  $(M_{41}^{\circ})_{MAX} = 38.72$  in-lbs  
 represent the maximum values of the reactions of the unbalanced linkage as found with the help of program FMAX (see Appendix F.2) and used in equations (5.12) - (5.17).
18. At this point, the masses, center of mass locations and the radii of gyration with respect to the centers of mass of the input, coupler and output links of the unbalanced mechanism are defined according to Table 4.1:

$$m_1^{\circ} = 5.1062 \times 10^{-4} \text{ lb-sec}^2/\text{in}$$

$$m_2^{\circ} = 13.6710 \times 10^{-4} \text{ lb-sec}^2/\text{in}$$

$$m_3^{\circ} = 6.9378 \times 10^{-4} \text{ lb-sec}^2/\text{in}$$

$$p_1^{\circ} = 1.0 \text{ in}$$

$$q_1^{\circ} = 0.0 \text{ in}$$

$$p_2^{\circ} = 3.0 \text{ in}$$

$$q_2^{\circ} = 0.403 \text{ in}$$

$$p_3^{\circ} = 1.5 \text{ in}$$

$$q_3^{\circ} = 0.0 \text{ in}$$

$$k_2^{\circ} = 2.0970 \text{ in}$$

$$k_3^{\circ} = 1.6747 \text{ in}$$

Subsequently, the following computations are made:

$$P_1^{\circ} = m_1^{\circ} p_1^{\circ} + m_2^{\circ} a_1 - \frac{a_1}{a_2} m_2^{\circ} p_2^{\circ} \quad (\text{See equation (A.31).})$$

$$Q_1^{\circ} = m_1^{\circ} q_1^{\circ} - \frac{a_1}{a_2} m_2^{\circ} q_2^{\circ} \quad (\text{See equation (A.32).})$$

$$P_3^{\circ} = m_3^{\circ} p_3^{\circ} + \frac{a_3}{a_2} m_2^{\circ} p_2^{\circ} \quad (\text{See equation (A.33).})$$

$$Q_3^{\circ} = m_3^{\circ} q_3^{\circ} + \frac{a_3}{a_2} m_2^{\circ} q_2^{\circ} \quad (\text{See equation (A.34).})$$

$$A^{\circ} = \sqrt{(P_1^{\circ})^2 + (Q_1^{\circ})^2} \quad (\text{See equation (A.26).})$$

$$\alpha^{\circ} = \tan^{-1} \frac{Q_1^{\circ}}{P_1^{\circ}} \quad (\text{See equation (A.27).})$$

$$B^{\circ} = \sqrt{(P_3^{\circ})^2 + (Q_3^{\circ})^2} \quad (\text{See equation (A.28).})$$

$$\beta^{\circ} = \tan^{-1} \frac{Q_3^{\circ}}{P_3^{\circ}} \quad (\text{See equation (A.29).})$$

19. The coupler counterweight, which is circular and tangent to point  $A_1$  (see Figure 5.2), has the following parameters:

$$m_2^* = \rho_2^* \pi h_2^* (R_2^*)^2$$

$$p_2^* = R_2^* \cos \theta_2^* \quad (\text{See Figure A.2})$$

$$q_2^* = R_2^* \sin \theta_2^* \quad (\text{See Figure A.2})$$

20. The parameters of the balanced coupler link are given by:

$$m_2 = m_2^{\circ} + m_2^*$$

$$p_2 = (m_2^{\circ} p_2^{\circ} + m_2^* p_2^*) / m_2 \quad (\text{See equation (A.25).})$$

$$q_2 = (m_2^{\circ} q_2^{\circ} + m_2^* q_2^*) / m_2 \quad (\text{See equation (A.25).})$$

21. The radius of gyration of link 2 with respect to its center of mass is defined as:

$$k_2 = \left[ (m_2^{\circ} \{ (p_2^{\circ})^2 + (q_2^{\circ})^2 + (k_2^{\circ})^2 \} + 1.5 m_2^* (R_2^*)^2) / m_2 - (p_2^2 + q_2^2) \right]^{1/2}$$

22. The output link counterweight, which is circular and tangent to point  $A_3$  (see Figure 5.2), has the parameters:

$$m_3^* = \rho_3^* \pi h_3^* (R_3^*)^2$$

$$p_3^* = R_3^* \cos \theta_3^*$$

$$q_3^* = R_3^* \sin \theta_3^*$$

23. The balanced output link parameters are given by:

$$m_3 = m_3^o + m_3^*$$

$$p_3 = (m_3^o p_3^o + m_3^* p_3^*) / m_3$$

$$q_3 = (m_3^o q_3^o + m_3^* q_3^*) / m_3$$

24. The radius of gyration of link 3 with respect to its center of mass is defined as:

$$k_3 = \left[ (m_3^o \{ (p_3^o)^2 + (q_3^o)^2 + (k_3^o)^2 \} + 1.5 m_3^* (R_3^*)^2) / m_3 - (p_3^2 + q_3^2) \right]^{1/2}$$

25. The parameters of the input link are now found according to the computational sequence outlined in Section V-D-1:

$$a. \quad \beta = \tan^{-1} \frac{m_3 q_3 + \frac{a_3}{a_2} m_2 q_2}{m_3 p_3 + \frac{a_3}{a_2} m_2 p_2} \quad (\text{See equation (5.19).})$$

b.  $\psi = \beta - \beta^{\circ}$  , where  $\psi$  equals the angle of rotation of the shaking force hodograph.

c. Vector  $\overline{D^{\circ}C_S}$  is found with the help of equation (4.27):

$$D^{\circ}C = \left[ (D^{\circ}C_{SX})^2 + (D^{\circ}C_{SY})^2 \right]^{\frac{1}{2}}$$

where

$$D^{\circ}C_{SX} = OC_S \cos \delta_S - A^{\circ} \phi_1^2 \cos \alpha^{\circ}$$

$$D^{\circ}C_{SY} = OC_S \sin \delta_S - A^{\circ} \phi_1^2 \sin \alpha^{\circ}$$

and angle  $\zeta$  is given by

$$\zeta = \tan^{-1} \frac{D^{\circ}C_{SY}}{D^{\circ}C_{SX}}$$

d. Vector  $\overline{DC_2}$  is then found by way of equation (5.22), i.e.

$$DC_2 = \left[ (DC_{2X})^2 + (DC_{2Y})^2 \right]^{\frac{1}{2}}$$

where

$$DC_{2X} = \mu D^{\circ}C_S \cos(\zeta + \psi)$$

$$DC_{2Y} = \mu D^{\circ}C_S \sin(\zeta + \psi)$$

e. The term  $A$  is found according to

equation (5.22):

$$A = (P_1^2 + Q_1^2)^{\frac{1}{2}}$$

$$\text{where } P_1 = m_1^0 p_1^0 + m_2 a_1 - \frac{a_1}{a_2} m_2 p_2$$

$$Q_1 = m_1^0 q_1^0 - \frac{a_1}{a_2} m_2 q_2$$

and the angle  $\alpha$  is given by

$$\alpha = \tan^{-1} \frac{Q_1}{P_1}$$

- f. The resulting location of the rotated center of the circumscribing circle is given by vector  $\overline{OC}_2$  at angle  $\delta_2$  (see equation (5.23)):

$$OC_2 = \left[ (OC_{2X})^2 + (OC_{2Y})^2 \right]^{\frac{1}{2}}$$

$$\text{where } OC_{2X} = A \phi_1^2 \cos \alpha + DC_2 \cos(\zeta + \psi)$$

$$OC_{2Y} = A \phi_1^2 \sin \alpha + DC_2 \sin(\zeta + \psi)$$

at angle

$$\delta_2 = \tan^{-1} \frac{OC_{2Y}}{OC_{2X}}$$

- g. The input counterweight radius and angle is then found with the help of equations (4.70),

(5.25) and (5.26):

$$R_1^* = \left[ \frac{OC_2}{\rho_1^* h_1^* \pi \dot{\phi}_1^2} \right]^{\frac{1}{3}}$$

$$\text{and } \theta_1^* = \delta_2 + \pi$$

26. The input counterweight parameters are given by:

$$m_1^* = \rho_1^* h_1^* \pi (R_1^*)^2$$

$$p_1^* = R_1^* \cos \theta_1^*$$

$$q_1^* = R_1^* \sin \theta_1^*$$

27. Finally, the input link parameters are given by:

$$m_1 = m_1^{\circ} + m_1^*$$

$$p_1 = (m_1^{\circ} p_1^{\circ} + m_1^* p_1^*) / m_1$$

$$q_1 = (m_1^{\circ} q_1^{\circ} + m_1^* q_1^*) / m_1$$

28. Constraints C(1) to C(7) are now set along with the derivatives of C(1) with respect to variables X(2) to X(5):

- a. C(1); general equipollent circle constraint equation (see equations (5.4), (5.9) and (5.10)).

- b.  $C(2) = X(2)$ ; the constraint on the output counterweight radius, i.e.  $R_3^* \geq 0$ .
  - c.  $C(3), C(4)$ ; the constraints on the output link counterweight angle, i.e.  $\theta_3^* \geq 0$  and  $2\pi - \theta_3^* \geq 0$ .
  - d.  $C(5) = X(3)$ ; the constraint on the coupler counterweight radius, i.e.  $R_2^* \geq 0$ .
  - e.  $C(6), C(7)$ ; the constraints on the coupler counterweight angle, i.e.  $\theta_2^* \geq 0$  and  $2\pi - \theta_2^* \geq 0$ .
  - f.  $GC(2,1)$  to  $GC(5,1)$ ; represent the partial derivatives of the equipollent circle constraint equation with respect to the variables  $X(2)$  to  $X(5)$ . (Note that  $GC(1,1)$ , the derivative of  $C(1)$  with respect to  $X(1)$ , is zero and is given in the main program because it is a constant.)
29. With all appropriate mechanism parameters now defined, a DO loop is set up to evaluate the remaining constraints and their derivatives. The mechanism reactions corresponding to each input angle  $\phi_1$  are first obtained by way of the following subroutines which are listed in Appendix F:

**MOTION:** evaluates coupler and output link angles, angular velocities and angular accelerations.

**KINMAT:** finds positions, velocities and accelerations of mass centers on input, coupler and output links.

**REACTS:** determines the X and Y components of each bearing force, the shaking moment as well as the input moment as functions of the input angle  $\phi_1$ .

30.  $SHAKM(I) = 2.75F_{41Y} - 2.75F_{43Y} - M_{41}$  ; defines the shaking moment  $M_{M/G}$  with respect to the midpoint between the ground bearings for the given configuration.

31.  $F_{41}(I) = (F_{41X}^2 + F_{41Y}^2)^{\frac{1}{2}}$  ; the absolute value of bearing force  $F_{41}$ .

32.  $F_{43}(I) = (F_{43X}^2 + F_{43Y}^2)^{\frac{1}{2}}$  ; the absolute value of bearing force  $F_{43}$ .

33.  $F_{21}(I) = (F_{21X}^2 + F_{21Y}^2)^{\frac{1}{2}}$  ; the absolute value of bearing force  $F_{21}$ .

34.  $F_{23}(I) = (F_{23X}^2 + F_{23Y}^2)^{\frac{1}{2}}$  ; the absolute value of bearing force  $F_{23}$ .

35. The constraints are now evaluated according to equations (5.12) - (5.17), where  $I = 1, 2, \dots, 72$ :

$$\begin{aligned}
 \text{a. } C(I + 7) &= X(1) - W1 \left[ \frac{(F_{41})^2 - (F_{41}^{\circ})^2}{(F_{41}^{\circ})^2} \right] \\
 \text{b. } C(I + 79) &= X(1) - W4 \left[ \frac{(F_{43})^2 - (F_{43}^{\circ})^2}{(F_{43}^{\circ})^2} \right] \\
 \text{c. } C(I + 151) &= X(1) - W2 \left[ \frac{(F_{21})^2 - (F_{21}^{\circ})^2}{(F_{21}^{\circ})^2} \right] \\
 \text{d. } C(I + 223) &= X(1) - W3 \left[ \frac{(F_{23})^2 - (F_{23}^{\circ})^2}{(F_{23}^{\circ})^2} \right] \\
 \text{e. } C(I + 295) &= X(1) - W5 \left[ \frac{(M_{M/G})^2 - (M_{M/G}^{\circ})^2}{(M_{M/G}^{\circ})^2} \right] \\
 \text{f. } C(I + 367) &= X(1) - W6 \left[ \frac{(M_{41})^2 - (M_{41}^{\circ})^2}{(M_{41}^{\circ})^2} \right]
 \end{aligned}$$

36. The following partial derivatives are then defined so that the derivatives of the constraints with respect to the five variables  $X(1)$  to  $X(5)$  may be found. (The subscript  $K$  is introduced here to distinguish between these variables.):

$$\left. \begin{aligned}
 \text{a. } PF43X(K) &= \frac{\partial F_{43X}}{\partial X_K} \\
 \text{b. } PF43Y(K) &= \frac{\partial F_{43Y}}{\partial X_K}
 \end{aligned} \right\} K = 2, 3, 4, 5$$

$$\begin{array}{ll}
 \text{c. } PF_{41X}(K) = \frac{\partial F_{41X}}{\partial X_K} & \left. \vphantom{\frac{\partial F_{41X}}{\partial X_K}} \right\} K = 2,4,5 \\
 \text{d. } PF_{41Y}(K) = \frac{\partial F_{41Y}}{\partial X_K} & \\
 \text{e. } PF_{21X}(K) = \frac{\partial F_{21X}}{\partial X_K} & \left. \vphantom{\frac{\partial F_{21X}}{\partial X_K}} \right\} K = 2,4,5 \\
 \text{f. } PF_{21Y}(K) = \frac{\partial F_{21Y}}{\partial X_K} & \\
 \text{g. } PF_{23X}(K) = \frac{\partial F_{23X}}{\partial X_K} & \left. \vphantom{\frac{\partial F_{23X}}{\partial X_K}} \right\} K = 2,4,5 \\
 \text{h. } PF_{23Y}(K) = \frac{\partial F_{23Y}}{\partial X_K} & \\
 \text{i. } PM_{41}(K) = \frac{\partial M_{41}}{\partial X_K} & , \quad K = 2,4,5 \\
 \text{j. } PSHAKM(K) = \frac{\partial M_{M/G}}{\partial X_K} & , \quad K = 2,3,4,5
 \end{array}$$

37. Finally,  $GC(N,M)$ , the partial derivatives of constraint  $M$  with respect to variable  $N$ , are found. Note that the partial derivatives of  $F_{41X}$ ,  $F_{41Y}$ ,  $F_{21X}$ ,  $F_{21Y}$ ,  $F_{23X}$ ,  $F_{23Y}$  and  $M_{41}$  with respect to  $X_3$  are zero. This is the reason

why  $GC(3, I+7)$ ,  $GC(3, I+151)$ ,  $GC(3, I+223)$  and  $GC(3, I+367)$  have been set equal to zero in the main program for  $I = 1, 2, \dots, 72$ :

$$a. \quad GC(K, I+7) = - \frac{2W_1}{(F_{41}^0)^2} \left( F_{41X} \frac{\partial F_{41X}}{\partial X_K} + F_{41Y} \frac{\partial F_{41Y}}{\partial X_K} \right), \quad K = 2, 4, 5$$

$$b. \quad GC(K, I+79) = - \frac{2W_4}{(F_{43}^0)^2} \left( F_{43X} \frac{\partial F_{43X}}{\partial X_K} + F_{43Y} \frac{\partial F_{43Y}}{\partial X_K} \right), \quad K = 2, 3, 4, 5$$

$$c. \quad GC(K, I+151) = - \frac{2W_2}{(F_{21}^0)^2} \left( F_{21X} \frac{\partial F_{21X}}{\partial X_K} + F_{21Y} \frac{\partial F_{21Y}}{\partial X_K} \right), \quad K = 2, 4, 5$$

$$d. \quad GC(K, I+223) = - \frac{2W_3}{(F_{23}^0)^2} \left( F_{23X} \frac{\partial F_{23X}}{\partial X_K} + F_{23Y} \frac{\partial F_{23Y}}{\partial X_K} \right), \quad K = 2, 4, 5$$

$$e. \quad GC(K, I+295) = - \frac{2W_5}{(M_{M/G}^0)^2} M_{M/G} \frac{\partial M_{M/G}}{\partial X_K}, \quad K = 2, 3, 4, 5$$

$$f. \quad GC(K, I+367) = - \frac{2W_6}{(M_{41}^0)^2} M_{41} \frac{\partial M_{41}}{\partial X_K}, \quad K = 2, 4, 5$$

```

0001      SUBROUTINE VF0100IN,M,XI
0002      IMPLICIT REAL*8(A-H,O-Z)
0003      REAL*8 X(5)
0004      INTEGER PHID, PHID1, DELPHI
0005      REAL*8 LAMU,K2,K3,M1,M2,M3,JJ,KK,LL,MM,LAMBDA,MU,MZERO
0006      REAL*8 M2ZL10,M3STAR,M3ZERO,M3STAR,M3STAR,K2ZERO,K3ZERO
0007      REAL*8 M41(73),M410,LAMV(73),LAMAI(73),LAMU(73),LAMV2(2,13)
0008      DIMENSION SHAKM(73)
0009      DIMENSION F41X(73),F41Y(73),F21X(73),F21Y(73),F23X(73),
0010      F23Y(73),F43X(73),F43Y(73),FSX(73),FSY(73)
0011      DIMENSION F43(73),F41(73),F21(73),F23(73)
0012      DIMENSION MS10(73),MS1V(73),PS1A(73)
0013      DIMENSION X1(73),Y1(73),X2(73),Y2(73),X3(73),Y3(73)
0014      DIMENSION VX1(73),VY1(73),VX2(73),VY2(73),VX3(73),VY3(73)
0015      DIMENSION AX1(73),AY1(73),AX2(73),AY2(73),AX3(73),AY3(73)
0016      DOUBLE PRECISION DCS,DSIN,DSORT,DATAN2
0017      COMMON/VF0100/F
0018      COMMON/VF0100/G(10)
0019      COMMON/VF0100/C(1317)
0020      COMMON/VF0100/GC(5,439)
0021      PI=3.14159300
0022      C THE OBJECTIVE FUNCTION IS
0023      F=X(1)
0024      C G(I)=PARTIAL DERIVATIVES OF OBJECTIVE FUNCTION (F(X(I))) WITH
0025      C RESPECT TO VARIABLES X(1),X(2),X(3),X(4) AND X(5)
0026      G(1)=100
0027      G(2)=000
0028      G(3)=000
0029      G(4)=000
0030      G(5)=000
0031      C THE LINK DIMENSIONS ARE
0032      L1=200
0033      L2=600
0034      L3=300
0035      L4=5.500
0036      C THE COUNTERWEIGHT DENSITIES AND THICKNESS FOR LINKS 1, 2 AND 3 ARE
0037      RHO1ST=7.3315060E-4
0038      RHO2ST=7.3316060E-4
0039      RHO3ST=7.3316060E-4
0040      M1STAR=.62500
0041      M2STAR=.62500
0042      M3STAR=.62500
0043      C THE MAXIMUM SHAKING FORCE FOR THE UNBALANCED LINKAGE IS
0044      FOMAK = .2500376002
0045      C THE RADIUS AND COORDINATES OF THE CENTER OF THE SMALLEST
0046      C CIRCUMSCRIBING CIRCLE TO THE ROTATED SHAKING FORCE HODDOGRAPH ARE
0047      RS = .1573443002
0048      CSY = .3947464001
0049      CSX = -.3464050001
0050      C THE MAGNITUDE OF VECTOR CCS IS
0051      CCS = DSORT(CSX**2 + CSY**2)
0052      C AT ANGLE
0053      DELTA5 = DATAN2(CSY,CSX)
0054      C THE REDUCTION FACTOR IS
0055      ETA = .500
0056      C THE PROPORTIONALITY FACTOR IS GIVEN BY

```

```

CC44      NU = ETS*RIJMAX/RS
C         THE ANGULAR VELOCITY OF THE INPUT LINK IS
0045      W=0.500
CC46      Z=PI/1.5002
CC47      PHI7LL=IP**Z*600
C         THE ANGULAR ACCELERATION OF THE INPUT LINK IS
0048      PHIACC=100
C         DELPHI=INCREMENT OF INPUT ANGLE PHI
0049      DELPHI=5
C SET WEIGHTING FACTORS FOR CONSTRAINTS
0050      W1= 100
0051      W2= 100
0052      W3= 100
0053      W4= 100
0054      W5= 100
0055      W6= 100
C         THE MAXIMUM VALUES OF REACTIONS FOR UNBALANCED LINKAGE ARE
0056      F410=.5212202002
0057      F41D=.3327327002
0058      F210=.5074326002
0059      F230=.4937654002
0060      SHAKMO=.0050192002
0061      M410=.3872007002
C
C OFFLINE INPUT TO SUBROUTINE USED TO DETERMINE MECHANISM REACTIONS
C P1,P2=X AND Y COMPONENTS OF CENTER OF MASS OF INPUT LINK
C P2,G2=X AND Y COMPONENTS OF CENTER OF MASS OF COUPLER LINK
C P3,G3=X AND Y COMPONENTS OF CENTER OF MASS OF OUTPUT LINK
C M1,M2,M3=MASS OF INPUT,COUPLER AND OUTPUT LINK, RESPECTIVELY
C K2,K3=RADIUS OF GYRATION OF COUPLER AND OUTPUT LINKS
C
C THE PARAMETERS OF THE UNBALANCED LINKAGE ARE
0062      M1ZERO=5.10620-4
0063      M2ZERO=13.67100-4
0064      M3ZERO=6.95730-4
0065      P10 = 100
0066      Q10 = 000
0067      P20=300
0068      Q20=.40300
0069      P30=1.500
0070      Q30 = 000
0071      K2ZERO = 2.7970
0072      K3ZERO= 1.67470
0073      PE10 = M1ZERO*P10 + M2ZERO*P1 - M1*M2ZERO*Q20/A2
0074      QU10 = M1ZERO*Q10 - M1*M2ZERO*Q20/A2
0075      P3ZERO = M3ZERO*P30 + M3*M2ZERO*Q20/A2
0076      Q3ZERO = M1ZERO*Q30 + M1*M2ZERO*Q20/A2
0077      AZERO = DSQRT(P10**2 + Q10**2)
0078      ALPHA0 = DATAN2(QU10,PE10)
0079      BZERO = DSQRT(P3ZERO**2 + Q3ZERO**2)
0080      PF40 = DATAN2(Q3ZERO,P3ZERO)
C
C THE COUPLER COUNTERWEIGHT PARAMETERS ARE
0081      M2STAR = RHO2ST*PI*M2STAR*(I41**2)
0082      P2STAR = X(4)*COS(X(5))

```

```

0083      Q2STAR = X14**2*DSIN(X15)
C
C      THE COUPLER LINK PARAMETERS ARE
0084      M2 = MZERO + M2STAR
0085      P2 = (MZERO*P20 + M2STAR*P2STAR)/M2
0086      Q2 = (MZERO*Q20 + M2STAR*Q2STAR)/M2
C      THE RADIUS OF GYRATION OF LINK 2 IS
0087      K2 = DSQRT((MZERO*(P20**2 + Q20**2 + M2ZERO**2) +
1          1.500*M2STAR*(X14**2))/M2 - (P2**2 + Q2**2))
C
C      THE OUTPUT LINK COUNTERWEIGHT PARAMETERS ARE
0088      M3STAR = M3STAR*(M3STAR*(X12**2)
0089      P3STAR = X12*DCOS(X13)
0090      Q3STAR = X12*DSIN(X13)
C
C      THE OUTPUT LINK PARAMETERS ARE THEN GIVEN BY
0091      M3 = MZERO + M3STAR
0092      P3 = (MZERO*P30 + M3STAR*P3STAR)/M3
0093      Q3 = (MZERO*Q30 + M3STAR*Q3STAR)/M3
C
C      THE RADIUS OF GYRATION OF THE OUTPUT LINK IS
0094      K3 = DSQRT((M3ZERO*(P30**2 + Q30**2 + M3ZERO**2)
1          + 1.500*M3STAR*(X12**2))/M3 - (P3**2 + Q3**2))
C
C      THE PARAMETERS OF THE INPUT CWT. MUST NOW BE FOUND WHICH WILL
C      RESULT IN THE PRESCRIBED MAXIMUM SHAKING FORCE.
C
C      ANGLE BETA0 IS GIVEN BY
C      THE ANGLE BETA IS FOUND BY WAY OF
0095      P3 = M3*P3 + (A3/A2)*M2*P2
0096      Q3 = M3*Q3 + (A3/A2)*M2*Q2
0097      BETA = DATAN2(Q3,P3)
C      THE ANGLE OF ROTATION PSI MAY NOW BE FOUND AS
0098      ROTPSI = BETA - BETA0
C      THE COMPONENTS OF VECTOR OC2 ARE
0099      OC2X = OC0*DCOS(DELTA1) - AZERO*(PHIVEL**2)*DCOS(ALPHA0)
0100      OC2Y = OC0*DSIN(DELTA1) - AZERO*(PHIVEL**2)*DSIN(ALPHA0)
C      THE MAGNITUDE OF OC2 MAY NOW BE FOUND AS
0101      OC2 = DSQRT(OC2X**2 + OC2Y**2)
C      AT ANGLE
0102      ZETA = DATAN2(OC2Y,OC2X)
C      THE COMPONENTS OF VECTOR OC2 MAY NOW BE FOUND
0103      OC2X = MU*OC2*DCOS(ZETA + ROTPSI)
0104      OC2Y = MU*OC2*DSIN(ZETA + ROTPSI)
C      THE MAGNITUDE OF OC2 IS
0105      OC2 = DSQRT(OC2X**2 + OC2Y**2)
C      DUE TO THE ADDITION OF A COUPLER COUNTERWEIGHT, THE TERM AZERO
C      BECOMES 3, WHICH IS FOUND BY WAY OF
0106      PE1 = M1ZERO*P10 + M2*A1 - (A1/A2)*M2*P2
0107      QU1 = M1ZERO*Q10 - (A1/A2)*M2*Q2
0108      3 = DSQRT(PE1**2 + QU1**2)
C      THE ANGLE ALPHA0 BECOMES ALPHA, WHERE
0109      ALPHA = DATAN2(QU1,PE1)
C
C      THE RESULTING LOCATION OF THE ROTATED CENTER OF THE CIRCUMSCRIBING
C      CIRCLE IS THEN GIVEN AS OC2 AT ANGLE DELTA2, WHERE

```

```

C110      DC2X = A*(PHLEVEL**2)*DCOS(ALPHA) +
          | DC2*DCOS(ZETA + ROTPSI)
C111      DC2Y = A*(PHLEVEL**2)*DSIN(ALPHA) +
          | DC2*DSIN(ZETA + ROTPSI)
C112      DC2 = DSQRT(DC2X**2 + DC2Y**2)
C113      DELTA2 = ATAN2(DC2Y,DC2X)
C          THE INPUT LINK CNT. RADIUS IS GIVEN BY
C114      R1STAR = (DC2/(H01STAR*H1STAR*PI*(PHLEVEL**2)))*(1.00/3.00)
C          AT ANGLE
C115      THIST = DELTA2 + PI
C
C          THE INPUT CNT. PARAMETERS ARE
C116      M1STAR = H01STAR*H1STAR*PI*(R1STAR**2)
C117      P1STAR = R1STAR*DCOS(THIST)
C118      Q1STAR = R1STAR*DSIN(THIST)
C
C          THE REQUIRED INPUT LINK PARAMETERS ARE
C119      M1 = M1ZERO + M1STAR
C120      P1 = (M1ZERO*P10 + M1STAR*P1STAR)/M1
C121      Q1 = (M1ZERO*Q10 + M1STAR*Q1STAR)/M1
C          CONSTRAINTS C111 TO C117 ARE NOW SET ALONG WITH THE
C          DERIVATIVES OF C111 WITH RESPECT TO VARIABLES X(2) TO X(5)
C
C111=EQUALITY CONSTRAINT (GENERAL EQUIPOLLENT CIRCLE CONSTR. EQ.)
C122      RPH2=RPH12STAR*PI*(H2STAR*(X(4)**3)
C123      RPH=RPH1STAR*PI*(H1STAR*(X(2)**3)
C124      C(1)=(RPH*DCOS(X(3)) + (A3/A2)*RPH2*DCOS(X(5)) + P3ZERO)**2
          | + (RPH*DSIN(X(3)) + (A3/A2)*RPH2*DSIN(X(5)) + Q3ZERO)**2
          | - (MU*BZERO)**2
C          C(2)=CONSTRAINT ON OUTPUT COUNTERWEIGHT RADIUS
C125      C(2)= X(2)
C          C(3),C(4)=CONSTRAINTS ON OUTPUT COUNTERWEIGHT ANGLE
C126      C(3)= X(3)
C127      C(4)= 200*PI - X(3)
C          C(5)=CONSTRAINT ON COUPLER COUNTERWEIGHT RADIUS
C128      C(5)= X(4)
C          C(6),C(7)=CONSTRAINTS ON COUPLER COUNTERWEIGHT ANGLE
C129      C(6)=X(5)
C130      C(7)=200*PI - X(5)
C          GC(R,S)=PARTIAL OF C(S) WITH RESPECT TO VARIABLE R
C131      GC(1,1)=RPH*DCOS(X(3)) + (A3/A2)*RPH2*DCOS(X(5)) + P3ZERO
C132      GC(1,2)=RPH*DSIN(X(3)) + (A3/A2)*RPH2*DSIN(X(5)) + Q3ZERO
C133      GC(2,1) = 600*GC(1,1)*RPH*DCOS(X(3))/X(2) +
          | 600*GC(1,2)*RPH*DSIN(X(3))/X(2)
C134      GC(3,1) = -200*GC(1,1)*RPH*DSIN(X(3)) +
          | 200*GC(1,2)*RPH*DCOS(X(3))
C135      GC(4,1) = 600*GC(1,1)*(A3/A2)*(RPH2*DCOS(X(5)))/X(4) +
          | 600*GC(1,2)*(A3/A2)*(RPH2*DSIN(X(5)))/X(4)
C136      GC(5,1) = -200*GC(1,1)*(A3/A2)*RPH2*DSIN(X(5)) +
          | 200*GC(1,2)*(A3/A2)*RPH2*DCOS(X(5))
C
C137      CO(120)PHI0=1.356,DELPHI
C138      PHID=PHI0 - 1
C139      PHI=2*PHI0
C140      I = PHI0/DELPHI + 1
C141      CALL MOTION(PHI,A1,A2,A3,A4,PSI,PHLEVEL,PHIACC,PSIV(I),PSTAR(I),

```



C THE PARTIAL OF F43X WITH RESPECT TO X(2) IS  
 C183 PF43X2 = -300\*RPH\*DCOS(X(3))\*CC/X(2)  
 1 = 300\*RPH\*DSIN(X(3))\*DD/X(2)  
 2 + 600\*RPH\*FF

C THE PARTIAL OF F43Y WITH RESPECT TO X(2) IS  
 C184 PF43Y2 = 300\*RPH\*DCOS(X(3))\*JJ/X(2)  
 1 = 300\*RPH\*DSIN(X(3))\*KK/X(2)  
 2 + 600\*RPH\*MM

C THE PARTIAL OF F43X AND F43Y WITH RESPECT TO X(3) ARE  
 C185 PF43X3 = RPH\*DSIN(X(3))\*CC - RPH\*DCOS(X(3))\*DD  
 C186 PF43Y3 = -RPH\*DSIN(X(3))\*JJ - RPH\*DCOS(X(3))\*KK

C THE PARTIAL OF F43X W/R TO X(4) AND X(5) ARE  
 C187 PF43X4 = -300\*(RPH2/X(4))\*DCOS(X(5))\*VV  
 1 + 300\*(RPH2/X(4))\*DSIN(X(5))\*WW  
 2 + 600\*(LAM4(1))\*CS/2T3)\*RPH2

C188 PF43X5 = RPH2\*DSIN(X(5))\*VV + RPH2\*DCOS(X(5))\*WW

C THE PARTIAL OF F43Y W/R TO X(4) AND X(5) ARE  
 C189 PF43Y4 = -300\*(RPH2/X(4))\*DCOS(X(5))\*XX  
 1 + 300\*(RPH2/X(4))\*DSIN(X(5))\*YY  
 2 + 600\*(LAM4(1))\*SS/2T3)\*RPH2

C190 PF43Y5 = RPH2\*DSIN(X(5))\*XX + RPH2\*DCOS(X(5))\*YY

C THE PARTIAL OF F41 W/R TO X(4) AND X(5) ARE  
 C191 PF41X4 = -200\*(RPH2/X(4))\*E1\*A1\*PHIV2\*CP  
 1 = 300\*(RPH2/X(4))\*DCOS(X(5))\*CC  
 2 = 300\*(RPH2/X(4))\*DSIN(X(5))\*RR  
 3 = 600\*(LAM4(1))\*CS/2T3)\*RPH2

C192 PF41X5 = RPH2\*DSIN(X(5))\*DD - RPH2\*DCOS(X(5))\*RR

C THE PARTIALS OF F41Y W/R TO X(4) AND X(5) ARE  
 C193 PF41Y4 = -200\*(RPH2/X(4))\*E2\*A1\*PHIV2\*SP  
 1 + 300\*(RPH2/X(4))\*DCOS(X(5))\*TT  
 2 = 300\*(RPH2/X(4))\*DSIN(X(5))\*LL  
 3 = 600\*(LAM4(1))\*SS/2T3)\*RPH2

C194 PF41Y5 = -RPH2\*DSIN(X(5))\*TT - RPH2\*DCOS(X(5))\*UU

C THE PARTIALS OF F21X AND F21Y W/R TO X(4) AND X(5) ARE  
 C195 PF21X4 = -PF41X4  
 C196 PF21X5 = -PF41X5  
 C197 PF21Y4 = -PF41Y4  
 C198 PF21Y5 = -PF41Y5

C THE PARTIALS OF F23X AND F23Y W/R TO X(4) AND X(5) ARE  
 C199 PF23X4 = -PF43X4  
 C200 PF23X5 = -PF43X5  
 C201 PF23Y4 = -PF43Y4  
 C202 PF23Y5 = -PF43Y5

C THE PARTIALS OF M41 ARE FOUND FROM (W/R TO X(4) AND X(5))  
 C203 AAA = A1\*(LAM4(1)\*TAU11 + LAMV2\*TAU11)  
 1 = -A1\*A1\*DSIN(PHI-PSI)\*PHIV2\*TAU1/2T3

C204 BBB = A1\*(LAM4(1)\*TAU11 - LAMV2\*TAU11)  
 1 = A1\*A1\*DSIN(PHI-PSI)\*PHIV2\*TAU11/2T3

C205 PM414 = 300\*(RPH2/X(4))\*DCOS(X(5))\*AAA  
 1 + 300\*(RPH2/X(4))\*DSIN(X(5))\*BBB  
 2 + 600\*(LAM4(1))\*A1\*DSIN(PHI-PSI)/2T3)\*RPH2

C206 MM415 = -RPH2\*DSIN(X(5))\*AAA + RPH2\*DCOS(X(5))\*3BB

C THE PARTIALS OF THE SHAKING MOMENT W/R TO X(4) AND X(5) ARE  
 C207 PSHKM4 = 2.7500\*PF41Y4 - 2.7500\*PF43Y4 - PM414  
 C208 PSHKM5 = 2.7500\*PF41Y5 - 2.7500\*PF43Y5 - PM415

C THE PARTIAL OF F41X WITH RESPECT TO X(2) IS

```

C209      PF41X2 = -6D0*RP*PF
C         THE PARTIAL OF F41Y WITH RESPECT TO X(2) IS
C210      PF41Y2 = -6D0*RP*MM
C         THE PARTIAL OF F21X WITH RESPECT TO X(2) IS
C211      PF21X2 = -PF41Y2
C         THE PARTIAL OF F21Y WITH RESPECT TO X(2) IS
C212      PF21Y2 = -PF41Y2
C         THE PARTIAL OF F23X WITH RESPECT TO X(2) IS
C213      PF23X2 = PF41X2
C         THE PARTIAL OF F23Y WITH RESPECT TO X(2) IS
C214      PF23Y2 = PF41Y2
C
C         THE PARTIALS OF F41X,F41Y,F21X,F21Y,F23X,F23Y AND M41
C         WITH RESPECT TO X(3) ARE ZERO. THEREFORE, GC(3,5)-GC(3,9),
C         GC(3,15)-GC(3,19),GC(3,25)-GC(3,29) AND GC(3,35)-GC(3,39)
C         ARE SET TO ZERO IN MAIN PROGRAM
C         THE PARTIAL OF M41 WITH RESPECT TO X(2) IS
C215      PM412 = 6D0*RP*PF*AI*TAU/CL
C         THE PARTIALS OF THE SHAKING MOMENT W/R TO X(2) AND X(3) ARE
C216      PSHKM2 = 2.75D0*PF41Y2 - 2.75D0*PF43Y2 - PM412
C217      PSHKM3 = -2.75D0*PF43Y3
C         NOW THE GRADIENTS MAY BE FOUND
C218      GC(2,1+71) = -2D0*W1*(F41X(1)*PF41Y2 + F41Y(1)*PF41Y2)/(F410)**2
C219      GC(4,1+71) = -2D0*W1*(F41X(1)*PF41X4 + F41Y(1)*PF41Y4)/(F410)**2
C220      GC(5,1+71) = -2D0*W1*(F41X(1)*PF41X5 + F41Y(1)*PF41Y5)/(F410)**2
C221      GC(2,1+73) = -2D0*W4*(F43X(1)*PF43X2 + F43Y(1)*PF43Y2)/(F430)**2
C222      GC(3,1+73) = -2D0*W4*(F43X(1)*PF43X3 + F43Y(1)*PF43Y3)/(F430)**2
C223      GC(4,1+73) = -2D0*W4*(F43X(1)*PF43X4 + F43Y(1)*PF43Y4)/(F430)**2
C224      GC(5,1+73) = -2D0*W4*(F43X(1)*PF43X5 + F43Y(1)*PF43Y5)/(F430)**2
C
C225      GC(2,1+151) = -2D0*W2*(F21X(1)*PF21X2 + F21Y(1)*PF21Y2)/(F210)**2
C226      GC(4,1+151) = -2D0*W2*(F21X(1)*PF21X4 + F21Y(1)*PF21Y4)/(F210)**2
C227      GC(5,1+151) = -2D0*W2*(F21X(1)*PF21X5 + F21Y(1)*PF21Y5)/(F210)**2
C228      GC(2,1+223) = -2D0*W3*(F23X(1)*PF23X2 + F23Y(1)*PF23Y2)/(F230)**2
C229      GC(4,1+223) = -2D0*W3*(F23X(1)*PF23X4 + F23Y(1)*PF23Y4)/(F230)**2
C230      GC(5,1+223) = -2D0*W3*(F23X(1)*PF23X5 + F23Y(1)*PF23Y5)/(F230)**2
C231      GC(2,1+275) = -2D0*W5*(SHAKM(1)*PSHKM2)/(SHAKM0)**2
C232      GC(3,1+275) = -2D0*W5*(SHAKM(1)*PSHKM3)/(SHAKM0)**2
C233      GC(4,1+275) = -2D0*W5*(SHAKM(1)*PSHKM4)/(SHAKM0)**2
C234      GC(5,1+275) = -2D0*W5*(SHAKM(1)*PSHKM5)/(SHAKM0)**2
C235      GC(2,1+367) = -2D0*W6*(M4(1)*PM412)/(M410)**2
C236      GC(4,1+367) = -2D0*W6*(M4(1)*PM414)/(M410)**2
C237      GC(5,1+367) = -2D0*W6*(M4(1)*PM415)/(M410)**2
C238      120 CONTINUE
C239      RETURN
C240      END

```



the subroutine VF01ZD has been called upon in the specific outer iteration.

The number in the second line represents the current value of the composite function  $\Phi$  according to equation (C.1).

The third line gives the current values of  $z$ ,  $R_3^*$ ,  $\theta_3^*$ ,  $R_2^*$ , and  $\theta_2^*$ . In the first iteration, the initial values are reproduced.

The fourth line shows the derivatives of the composite function with respect to the five variables.

The last group of inner iterations shown represents the final results, i.e.

$$z = 0.178 \text{ lb}^2 \quad (\text{G.1})$$

$$R_3^* = 0.42 \text{ in} \quad (\text{G.2})$$

$$\theta_3^* = 2.984 \text{ rad} = 170.95 \text{ deg} \quad (\text{G.3})$$

$$R_2^* = 1.07 \text{ in} \quad (\text{G.4})$$

$$\theta_2^* = 4.032 \text{ rad} = 230.99 \text{ deg} \quad (\text{G.5})$$

The computational sequence given in Section V-D-1 is then followed to determine the final input link counterweight

parameters (see equations (4.70), (5.19) - (5.26)):

$$R_1^* = 1.65 \text{ in} \quad (\text{G.6})$$

$$\theta_1^* = 3.012 \text{ rad} = 172.57 \text{ deg} \quad (\text{G.7})$$

APPENDIX H  
COMPUTER PROGRAM OPTM41

The present appendix shows how program OPTIMIZE is modified for the exclusive optimization of the maximum input moment  $M_{41}$  of a fully force balanced four-bar linkage. To this end, the constraints on the forces  $F_{41}$ ,  $F_{12}$ ,  $F_{23}$ ,  $F_{34}$  as well as on the moment  $M_{M/G}$  are removed. Thus, the number of variables remains the same as in program OPTIMIZE while the number of constraints is reduced from 439 to 79.

Only the modifications to the main program and subroutine VF01BD are detailed below. These are followed by the essential elements of the program output.

1. Main Program

The main program, which is listed at the end of this section, begins with COMMON statements which define the array size for the constraints  $C$  and their derivatives  $GC$ . The remainder of the program is identical to that given in Appendix G except for the following modifications:

$M = 79$ ; stands for the number of constraints. (See comment cards at beginning of program for definition of constraints. Note that only the input moment appears.)

$GC(1,I) = 1$  and  $GC(3,I) = 0$  for  $I = 8,9,\dots,79$ . These changes are a result of the fewer number of constraints.

## MAIN

```

C THIS PROGRAM OPTIMIZES THE MAXIMUM INPUT MOMENT FOR A PRESCRIBED
C MAXIMUM SHAKING FORCE FOR A GIVEN FOUR-BAR LINKAGE.
C CIRCULAR COUNTERWEIGHTS, TANGENT TO PIVOT POINTS, ARE USED ON
C ALL MOVING LINKS. THE INPUT MOMENT IS EVALUATED AT FIVE DEGREE
C INCREMENTS OF THE INPUT LINK ANGLE.
C
C VARIABLES ARE X(1)=Z, X(2)=R3STAR*OUTPUT COUNTERWEIGHT
C RADIUS, X(3)=R1STAR*OUTPUT CWT. ANGLE, X(4)=R2STAR*
C COUPLER COUNTERWEIGHT RADIUS, X(5)=R2STAR*COUPLER CWT.
C ANGLE.
C
C THE CONSTRAINTS ARE
C C(1) = EQUIVALENT CIRCLE CONSTRAINT EQUATION
C C(2) = X(2) (RADIUS R3STAR GREATER THAN ZERO)
C C(3) = X(3) (ANGLE THETA3STAR GREATER THAN ZERO)
C C(4) = 2*PI - X(3) (ANGLE THETA3STAR LESS THAN 2*PI)
C C(5) = X(5) (RADIUS R2STAR GREATER THAN ZERO)
C C(6) = X(5) (ANGLE THETA2STAR GREATER THAN ZERO)
C C(7) = 2*PI - X(5) (ANGLE THETA2STAR LESS THAN 2*PI)
C C(8)=C(7)* INPUT MOMENT CONSTRAINTS
C IMPLICIT REAL*8(A-H,O-Z)
0001 COMMON/FOURBAR/IC(237)
0002 COMMON/VEFOIFD/IC(15,79)
0003 REAL*8 X(5),EPS(5)
0004 PI=3.14159300
0005
C THE TOTAL NUMBER OF VARIABLES IS DESIGNATED BY N
0006 N=5
C THE TOTAL NUMBER OF CONSTRAINTS IS DESIGNATED BY M
0007 M=77
C THE TOTAL NUMBER OF EQUALITY CONSTRAINTS IS DESIGNATED BY K
0008 K=1
C THE STARTING POINT IS ESTIMATED TO BE
0009 X(1)=100
0010 X(2)=.70500
0011 X(3)=3.23000
0012 X(4)=.55900
0013 X(5)=3.23000
0014 ARPT=17-4
0015 EPS(1)=10-4
0016 EPS(2)=.7050-4
0017 EPS(3)=3.2300-4
0018 EPS(4)=.5590-4
0019 EPS(5)=3.2300-4
C
0020 OFN=0.500
0021 MAXFN=700
0022 IPR1=1
0023 IPR2=1
C SET IW=10000. IF MORE STORAGE IS REQUIRED, VIOLAD WILL
C STOP AND PRINT OUT NEW REQUIREMENT
0024 IW=10000
0025 MONE=1
C THE CONSTRAINT SCALE FACTORS ARE SET AS FOLLOWS
0026 C(1)=10-6
0027 C(2)=.70500
0028 C(3)=3.23000

```

0029	C(4)=3.100
0030	C(5)=3.55000
0031	C(6)=3.27000
0032	C(7)=3.100
0033	C(10)=9.79
0034	10 C(11)=5.00
C THE DERIVATIVES OF LINEAR CONSTRAINTS ARE	
0035	GC(1,1)=0.00
0036	GC(1,2)=0.00
0037	GC(2,2)=1.00
0038	GC(3,2)=0.00
0039	GC(4,2)=0.00
0040	GC(5,2)=0.00
0041	GC(2,3)=0.00
0042	GC(2,3)=0.00
0043	GC(3,3)=1.00
0044	GC(4,3)=0.00
0045	GC(5,3)=0.00
0046	GC(1,4)=0.00
0047	GC(2,4)=0.00
0048	GC(3,4)=-1.00
0049	GC(4,4)=0.00
0050	GC(5,4)=0.00
0051	GC(1,5)=0.00
0052	GC(2,5)=0.00
0053	GC(3,5)=0.00
0054	GC(4,5)=1.00
0055	GC(5,5)=0.00
0056	GC(1,6)=0.00
0057	GC(2,6)=0.00
0058	GC(3,6)=0.00
0059	GC(4,6)=0.00
0060	GC(5,6)=1.00
0061	GC(1,7)=0.00
0062	GC(2,7)=0.00
0063	GC(3,7)=0.00
0064	GC(4,7)=0.00
0065	GC(5,7)=-1.00
0066	CO 11 I=9.79
0067	11 GC(11,I)=1.00
0068	CO 12 I=3.79
0069	12 GC(13,I)=0.00
0070	CALL VFG(AJIN,M,K,X,EPS,&KM%DEFN,MAXFN,(PR1,(PR2,(W,MODE)
0071	STOP
0072	END

2. Subroutine VF01BD (See listing at end of this section.)

After redefining the COMMON statements, the following modifications are made to the subroutine detailed in

Appendix G:

a.  $ETA = 0$ ; defines the reduction factor  $\eta$  associated with full force balance.

b.  $W6 = 1$ ; only the weighting factor associated with the constraint on the input moment  $M_{41}$  need be defined.

c.  $(M_{41}^0)_{MAX} = 38.72$ ; the maximum bearing reactions and shaking moment are not needed.

d.  $SHAKM(I)$ ,  $F_{41}(I)$ ,  $F_{43}(I)$ ,  $F_{21}(I)$  and  $F_{23}(I)$  are not required.

e.  $C(I + 7) = X(1) - W6 \left[ \frac{(M_{41})^2 - (M_{41}^0)^2}{(M_{41}^0)^2} \right]$ ,  $I = 1, 2, \dots, 72$ .

The input moment constraints are designated as  $C(8) - C(79)$ . All higher numbered constraints are eliminated.

f. All partial derivatives which do not involve  $M_{41}$  are eliminated. This leaves

$$PM_{41}(K) = \frac{\partial M_{41}}{\partial X_K}, \quad K = 2, 4, 5$$

- g. Finally, the derivatives of the constraints dealing with the input moment are defined as:

$$GC(K, I+7) = - \frac{2W6}{(M_{41}^0)^2} M_{41} \frac{\partial M_{41}}{\partial X_K} , \quad K = 2, 4, 5$$

All other derivatives are deleted.

```

0001      SUBROUTINE VF01DD(N,M,X)
0002      IMPLICIT REAL*8 (A-H,O-Z)
0003      REAL*8 X(5)
0004      INTEGER PHID, PIID1, DELPHI
0005      REAL*8 LAMDA,K2,K3,M1,M2,M3,LAMDA4,MU,MZERO
0006      REAL*8 M2ZERO,M2STAR,M3ZERO,M3STAR,M1STAR,K2ZERO,K3ZERO
0007      REAL*8 M41(73),M410,LAMV1(73),LAMV1(73),LAMV1(73),LAMV2(12,13)
0008      DIMENSION F41X(73),F41Y(73),F21X(73),F21Y(73),F23X(73),
0009      F23Y(73),F43X(73),F43Y(73),FSX(73),FSY(73)
0010      DIMENSION F43(73),F41(73),F21(73),F23(73)
0011      DIMENSION PSI0(73),PSI1(73),PSI4(73)
0012      DIMENSION X1(73),Y1(73),X2(73),Y2(73),X3(73),Y3(73)
0013      DIMENSION VX1(73),VY1(73),VX2(73),VY2(73),VX3(73),VY3(73)
0014      DIMENSION AX1(73),AY1(73),AX2(73),AY2(73),AX3(73),AY3(73)
0015      DOUBLE PRECISION DCS,DSIN,DCOS,DATA2
0016      COMMON/VF01CD/F
0017      COMMON/VF01OD/G110)
0018      COMMON/VF01ED/C1237)
0019      COMMON/VF01FD/GC15,79)
0020      PI=3.141592653589793
0021      C THE OBJECTIVE FUNCTION IS
0022      F=X11)
0023      C C11)=PARTIAL DERIVATIVES OF OBJECTIVE FUNCTION (F(X11)) WITH
0024      C RESPECT TO VARIABLES X(1),X(2),X(3),X(4) AND X(5)
0025      G11=100
0026      C12=007
0027      G13=000
0028      C14=00.0)
0029      G15=000
0030      C THE LINK DIMENSIONS ARE
0031      A1=200
0032      A2=600
0033      A3=300
0034      A4=5.50)
0035      C THE COUNTERWEIGHT DENSITIES AND THICKNESS FOR LINKS 1, 2 AND 3 ARE
0036      RHO1ST=7.3316060E-4
0037      RHO2ST=7.3316060E-4
0038      RHO3ST=7.3316060E-4
0039      F1STAR=.62500
0040      F2STAR=.62500
0041      F3STAR=.62500
0042      C THE MAXIMUM STARTING FORCE FOR THE UNBALANCED LINKAGE IS
0043      F2MAX = .2500376002
0044      C THE RADIUS AND COORDINATES OF THE CENTER OF THE SMALLEST
0045      C CIRCUMSCRIBING CIRCLE TO THE ROTATED SHAKING FORCE HODOGRAPH ARE
0046      RS = .15733463002
0047      CSX = .4987464001
0048      CSY = -.3464060001
0049      C THE MAGNITUDE OF VECTOR DCS IS
0050      DCS = DSQRT(CSX**2 + CSY**2)
0051      C AT ANGLE
0052      DELTA5 = DATA2/DCS,051)
0053      C THE REDUCTION FACTOR IS
0054      ET4 = 000
0055      C THE PROPORTIONALITY FACTOR IS GIVEN BY
0056      MU = ET4*RM1MAX/RS

```

```

C THE ANGULAR VELOCITY OF THE INPUT LINK IS
0044 RPH=0.503
CC45 Z=PI/1.5002
0046 PHIVEL=CPH*Z*600
C THE ANGULAR ACCELERATION OF THE INPUT LINK IS
0047 PHIACC=100
C DELPHI=INCREMENT OF INPUT ANGLE PHI
0048 DELPHI=5
C SET WEIGHTING FACTOR FOR CONSTRAINTS
0049 W6=100
C THE MAXIMUM VALUE OF INPUT MOMENT FOR UNBALANCED LINKAGE IS
0050 M410=.3572007002
C
C DEFINE INPUT TO SUBROUTINE USED TO DETERMINE MECHANISM REACTIONS
C P1,Q1=X AND Y COMPONENTS OF CENTER OF MASS OF INPUT LINK
C P2,Q2=X AND Y COMPONENTS OF CENTER OF MASS OF COUPLER LINK
C P3,Q3=X AND Y COMPONENTS OF CENTER OF MASS OF OUTPUT LINK
C M1,M2,M3=MASS OF INPUT, COUPLER AND OUTPUT LINKS, RESPECTIVELY
C K2,K3=RADIUS OF GYRATION OF COUPLER AND OUTPUT LINKS
C
C THE PARAMETERS OF THE UNBALANCED LINKAGE ARE
0051 M1ZERO=5.17620E-4
0052 M2ZERO=11.77100E-4
0053 M3ZERO=0.793740E-4
CC54 P10 = 1.03
0055 Q10 = 0.00
CC56 P20=300
0057 Q20=.40100
0058 P30=1.500
0059 Q30 = 0.00
CC60 K2ZERO = 2.09700
CC61 K3ZERO = 1.676700
CC62 PE10 = M1ZERO*P10 + M2ZERO*P1 - A1*M2ZERO*P20/A2
CC63 Q110 = M1ZERO*Q10 + A1*M2ZERO*Q20/A2
CC64 P3ZERO = M1ZERO*P30 + A3*M2ZERO*P20/A2
CC65 Q3ZERO = M3ZERO*Q30 + A3*M2ZERO*Q20/A2
CC66 AZERO = DSQRT(PE10**2 + Q110**2)
CC67 ALP10 = DATAN2(Q110,PE10)
CC68 BZERO = DSQRT(P3ZERO**2 + Q3ZERO**2)
CC69 BETA0 = DATAN2(Q3ZERO,P3ZERO)
C
C THE COUPLER COUNTERWEIGHT PARAMETERS ARE
C
0070 M2STAR = RHO2STAR*PI*R2STAR*XC14**2
0071 P2STAR = X14*DCOS(X15)
0072 Q2STAR = X14*DSIN(X15)
C
C THE COUPLER LINK PARAMETERS ARE
0073 M2 = M2ZERO + M2STAR
CC74 P2 = (M2ZERO*P20 + M2STAR*P2STAR)/M2
0075 Q2 = (M2ZERO*Q20 + M2STAR*Q2STAR)/M2
C THE RADIUS OF GYRATION OF LINK 2 IS
0076 K2 = DSQRT((M2ZERO*(P20**2 + Q20**2 + K2ZERO**2) +
1.0500*M2STAR*(X14**2)/M2 - (P2**2 + Q2**2))
C
C THE OUTPUT LINK COUNTERWEIGHT PARAMETERS ARE

```

```

0077 M3STAR=0.0035*PI*M3STAR*(X(2)**2)
0078 P3STAR=X(2)*DCOS(X(2))
0079 G3STAR=X(2)*DSIN(X(2))
C
C THE OUTPUT LINK PARAMETERS ARE THEN GIVEN BY
0080 M3 = M3ZERO + M3STAR
0081 P3 = (M3ZERO)*P30 + M3STAR*G3STAR/M3
0082 G3 = (M3ZERO)*G30 + M3STAR*G3STAR/M3
C
C THE RADIUS OF GYRATION OF THE OUTPUT LINK IS
0083 R3 = DSQRT((M3ZERO*IP30**2 + G30**2 + M3ZERO**2)
      + 1.500*M3STAR*(X(2)**2)/M3 - (P3**2 + G3**2))
C
C THE PARAMETERS OF THE INPUT CWT. MUST NOW BE FOUND WHICH WILL
C RESULT IN THE PRESCRIBED MAXIMUM SHAKING FORCE.
C
C THE ANGLE ZETA IS FOUND BY WAY OF
0084 PE3 = M3*P3 + (A3/A2)*M2*P2
0085 Q3 = M3*G3 + (A3/A2)*M2*G2
0086 BETA = DATAN2(Q3,PE3)
C THE ANGLE OF ROTATION PSI MAY NOW BE FOUND AS
0087 ROTPSI = BETA - BETA0
C THE COMPONENTS OF VECTOR DCCS ARE
0088 DCCSX = DCS*DCOS(DELTA2)*AZERO*(PHIVEL**2)*DCOS(ALPHA0)
0089 DCCSY = DCS*DSIN(DELTA2)*AZERO*(PHIVEL**2)*DSIN(ALPHA0)
C THE MAGNITUDE OF DCCS MAY NOW BE FOUND AS
0090 DCCS = DSQRT(DCCSX**2 + DCCSY**2)
C AT ANGLE
0091 ZETA = DATAN2(DCCSY,DCCSX)
C THE COMPONENTS OF VECTOR DCC2 MAY NOW BE FOUND
0092 CC2X = A0*DCCS*DCOS(ZETA + ROTPSI)
0093 CC2Y = A0*DCCS*DSIN(ZETA + ROTPSI)
C THE MAGNITUDE OF DCC2 IS
0094 DCC2 = DSQRT(CC2X**2 + CC2Y**2)
C DUE TO THE ADDITION OF A COUPLER COUNTERWEIGHT, THE TERM AZERO
C BECOMES A1, WHICH IS FOUND BY WAY OF
0095 PE1 = M1ZERO*P10 + M2*A1 - (A1/A2)*M2*P2
0096 Q1 = M1ZERO*G10 + M2*A1
0097 S = DSQRT(PE1**2 + Q1**2)
C THE ANGLE ALPHA0 BECOMES ALPHA1, WHERE
0098 ALPHA = DATAN2(Q1,PE1)
C
C THE RESULTING LOCATION OF THE ROTATED CENTER OF THE CIRCUMSCRIBING
C CIRCLE IS THEN GIVEN AS DCC2 AT ANGLE DELTA2, WHERE
0099 CC2X = A*(PHIVEL**2)*DCOS(ALPHA) +
      DCC2*DCOS(ZETA + ROTPSI)
0100 CC2Y = A*(PHIVEL**2)*DSIN(ALPHA) +
      DCC2*DSIN(ZETA + ROTPSI)
0101 DCC2 = DSQRT(CC2X**2 + CC2Y**2)
0102 DELTA2 = DATAN2(CC2Y,CC2X)
C THE INPUT LINK CWT. RADIUS IS GIVEN BY
0103 R1STAR = (DCC2/1.0015)*M1STAR*(PHIVEL**2)**0.75*(1.00/3.00)
C AT ANGLE
0104 TH1ST = DELTA2 + PI
C
C THE INPUT CWT. PARAMETERS ARE

```

```

0105 M1STAR = R1*01ST*M1STAR*PI*(R1STAR**2)
0106 M1STAR = M1STAR*DCOS(M1ST)
0107 M1STAR = R1STAR*DSIN(M1ST)
C
C THE REQUIRED INPUT LINK PARAMETERS ARE
0108 M1 = M1ZERO + M1STAR
0109 M2 = (M1ZERO*P1) + M1STAR*(M1STAR)/M1
0110 C1 = (M1ZERO*Q1) + M1STAR*(M1STAR)/M1
C
C CONSTRAINTS C111 TO C171 ARE NOW SET ALONG WITH THE
C DERIVATIVES OF C111 WITH RESPECT TO VARIABLES X(2) TO X(5)
C
C C111=EQUALITY CONSTRAINT (GENERAL EQUIPOLLENT CIRCLE CONSTR. EQ.)
0111 RPH2=RH12ST*PI*M1STAR*(X(4)**3)
0112 RPH=RPH1ST*PI*M1STAR*(X(2)**3)
0113 C111=(RPH*DCOS(X(3)) + (A3/A2)*RPH2*DCOS(X(5)) + P3ZERO)**2
1 = (RPH*DSIN(X(3)) + (A3/A2)*RPH2*DSIN(X(5)) + Q3ZERO)**2
2 = (MU*Q3ZERO)**2
C
C C(2)=CONSTRAINT ON OUTPUT COUNTERWEIGHT RADIUS
0114 C(2) = X(2)
C
C C(3),C(4)=CONSTRAINTS ON OUTPUT COUNTERWEIGHT ANGLE
0115 C(3) = X(3)
0116 C(4) = 200*PI - X(3)
C
C C(5)=CONSTRAINT ON COUPLER COUNTERWEIGHT RADIUS
0117 C(5) = X(4)
C
C C(6),C(7)=CONSTRAINTS ON COUPLER COUNTERWEIGHT ANGLE
0118 C(6) = X(5)
0119 C(7) = 200*PI - X(5)
C
C GC(1,1)=DERIVATIVE OF C111 WITH RESPECT TO VARIABLE R
0120 GC(1,1) = RPH*DCOS(X(3)) + (A3/A2)*RPH2*DCOS(X(5)) + P3ZERO
0121 GC(1,2) = RPH*DSIN(X(3)) + (A3/A2)*RPH2*DSIN(X(5)) + Q3ZERO
0122 GC(2,1) = 200*DC(1,1)*RPH*DCOS(X(3))/X(2) +
1 200*DC(1,2)*RPH*DSIN(X(3))/X(2)
0123 GC(3,1) = -200*DC(1,1)*RPH*DSIN(X(3)) +
1 200*GC(1,1)*RPH*DCOS(X(3))
0124 GC(4,1) = 600*GC(1,1)*(A3/A2)*RPH2*DCOS(X(5))/X(4) +
1 600*GC(1,2)*(A3/A2)*RPH2*DSIN(X(5))/X(4)
0125 GC(5,1) = -200*GC(1,1)*(A3/A2)*RPH2*DSIN(X(5)) +
1 200*GC(1,2)*(A3/A2)*RPH2*DCOS(X(5))
C
0126 DO 120 PHID1=1,35,DELPHI
0127 PHID=PHID1 - 1
0128 PHI=2*PHID
0129 I = PHI/DELPHI + 1
0130 CALL MOTION(PHI,A1,A2,A3,A4,PSI,PHI,VEL,PHI,ACC,PSI,VEL(I),PSI,ACC(I),
1 LAMBDA,LAMBDA(I),LAMBDA(I))
0131 CALL KINMAT(PHI,PHI,VEL,PHI,ACC,PSI,PSI,VEL(I),PSI,ACC(I),A1,A2,A3,A4,
1 P1,P2,P3,P4,X(1),Y(1),X(2),Y(2),X(3),Y(3),
2 Y3(I),V41(I),V41(I),X2(I),Y2(I),X3(I),Y3(I),
3 X1(I),Y1(I),X2(I),Y2(I),X3(I),Y3(I))
0132 CALL RECTST(PHI,PHI,VEL,PHI,ACC,LAMBDA,LAMBDA(I),LAMBDA(I),PSI,PSI,VEL(I),
1 PSI,ACC(I),A1,A2,A3,A4,P1,P2,P3,P4,K2,K3,M1,M2,M3,
2 F41X(I),F41Y(I),F21X(I),F21Y(I),F23X(I),F23Y(I),
3 F43X(I),F43Y(I),F5X(I),F5Y(I),M4(I))
C
C INPUT MOMENT CONSTRAINTS MAY NOW BE SET
0133 C(1+7)*X(1) = W0*(M4(I))**2 - (M*G)**2/(M4(I))**2

```

```

C
C LEFTHE PARTIAL DERIVATIVES CC(1,5), RPH2(1,6), S=CONSTANT
C NUMBER
C
C DEFINE PARAMETERS NECESSARY TO FIND PARTIAL DERIVATIVES
0134 CL = DCOS(LAMBDA)
0135 TAU1 = DSIN(PHI - LAMBDA)
0136 TAU2 = DCOS(PHI - LAMBDA)
0137 TAU3 = DSIN(PHI - LAMBDA)
0138 PH1/2 = PHIVEL*PHIVEL
0139 LAMV2 = (LAMV(1))**2
0140 A2T3 = A2*TAU3
0141 FF = (PSIA(1)*CL)/(A3*TAU3)
C THE PARTIAL OF M41 WITH RESPECT TO X(2) IS
0142 PM412 = 600*RPH*FF*A1*TAU1/CL
C THE PARTIALS OF M41 WITH RESPECT TO X(4) AND X(5) ARE FOUND FROM
0143 AAA = A1*(LAMV(1)*TAU1 + LAMV2*TAU1)
1 AAA = A1*A1*DSIN(PHI-PSI)*PHIV2*TAU1/A2T3
0144 BBB = A1*(LAMV(1)*TAU1 - LAMV2*TAU1)
1 AAA = A1*A1*DSIN(PHI-PSI)*PHIV2*TAU1/1732T3
0145 PM414 = 300*(RPH2/X(4))*DCOS(X(5))*AAA
1 PM414 = 300*(RPH2/X(4))*DSIN(X(5))*BBB
2 PM415 = -RPH2*DSIN(X(5))*AAA + RPH2*DCOS(X(5))*BBB
0146 C THE GRADIENTS MAY NOW BE FOUND
0147 CC(2,1+7) = -200*W6*(M41(1)+PM412)/M41(1)**2
0148 CC(4,1+7) = -200*W6*(M41(1)+PM414)/M41(1)**2
0149 CC(5,1+7) = -200*W6*(M41(1)+PM415)/M41(1)**2
0150 120 CONTINUE
0151 RETURN
0152 END

```



The last group of inner iterations shown represents the final results, i.e.

$$z = 0.293 \text{ lb}^2 \quad (\text{H.1})$$

$$R_3^* = 1.19 \text{ in} \quad (\text{H.2})$$

$$\theta_3^* = 2.367 \text{ rad} = 135.63 \text{ deg} \quad (\text{H.3})$$

$$R_2^* = 1.49 \text{ in} \quad (\text{H.4})$$

$$\theta_2^* = 4.122 \text{ rad} = 236.17 \text{ deg} \quad (\text{H.5})$$

Again, the corresponding final input link counterweight parameters are found with the help of equations (4.70) and (5.19)-(5.26):

$$R_1^* = 1.86 \text{ in} \quad (\text{H.6})$$

$$\theta_1^* = 3.266 \text{ rad} = 187.10 \text{ deg} \quad (\text{H.7})$$

## APPENDIX I

## KINEMATIC EQUATIONS OF A FOUR-BAR LINKAGE

The present appendix reproduces a collection of kinematic equations for the four-bar linkage shown in Figure 2.1 [ 4 ] .

1. Link Angles

$$\phi_3 = 2 \tan^{-1} \left( \frac{A \pm \sqrt{A^2 + B^2 - C^2}}{B + C} \right) \quad (\text{I.1})$$

where

$$\left. \begin{aligned} A &= \sin \phi_1 \\ B &= \cos \phi_1 - \frac{v}{\lambda} \\ C &= \frac{\lambda^2 + \mu^2 + v^2 - 1}{2\mu\lambda} - \frac{v}{\mu} \cos \phi_1 \\ \lambda &= \frac{a_1}{a_2} \\ \mu &= \frac{a_3}{a_2} \\ v &= \frac{a_4}{a_2} \end{aligned} \right\} \quad (\text{I.2})$$

$$\phi_2 = \tan^{-1} \left( \frac{\lambda \sin \phi_1 - \mu \sin \phi_3}{\lambda \cos \phi_1 - \mu \cos \phi_3 - v} \right) \quad (\text{I.3})$$

## 2. Link Angular Velocities

$$\dot{\phi}_2 = \frac{\lambda}{r_3} \sin(\phi_1 - \phi_3) \dot{\phi}_1 \quad (\text{I.4})$$

$$\dot{\phi}_3 = \frac{\lambda r_1}{\mu r_3} \dot{\phi}_1 \quad (\text{I.5})$$

where

$$\left. \begin{aligned} r_1 &= \mu \sin(\phi_1 - \phi_3) + \nu \sin \phi_1 \\ r_3 &= \lambda \sin(\phi_1 - \phi_3) + \nu \sin \phi_3 \end{aligned} \right\} \quad (\text{I.6})$$

## 3. Link Angular Accelerations

$$\ddot{\phi}_2 = \left( \frac{\dot{\phi}_2}{\dot{\phi}_1} \right) \ddot{\phi}_1 + \frac{\nu \lambda}{r_3^2} [\cos(\phi_1 - \phi_3) \dot{\phi}_1 \sin \phi_3 - \dot{\phi}_3 \sin \phi_1] \dot{\phi}_1 \quad (\text{I.7})$$

$$\begin{aligned} \ddot{\phi}_3 &= \left( \frac{\dot{\phi}_3}{\dot{\phi}_1} \right) \ddot{\phi}_1 + \frac{\lambda}{r_3} \cos(\phi_1 - \phi_3) (\dot{\phi}_1 - \dot{\phi}_3)^2 \\ &\quad + \frac{\nu}{\mu r_3} (\lambda \dot{\phi}_1^2 \cos \phi_1 - \mu \dot{\phi}_3^2 \cos \phi_3) \end{aligned} \quad (\text{I.8})$$

VII. REFERENCES

1. M. Y. M. Afifi, "Reducing Frame Vibrations", Engineering, 212 (1), Jan. 1972, pp.30-32.
2. C. E. Benedict and D. Tesar, "Optimal Torque Balance for a Complex Stamping and Indexing Machine", ASME Paper No. 70-MECH-82, Mechanisms Conference, Columbus, Ohio, Nov. 1970.
3. C. E. Benedict, G. K. Matthew and D. Tesar, "Torque Balancing of Machines by Sub-Unit Cam Systems", Paper No. 15, Proceedings, Second Appl. Mechanisms Conference, Oklahoma State University, Oct. 1971.
4. R. S. Berkof, "On the Optimization of Mass Distribution in Mechanisms", Ph.D. Dissertation, The City University of New York, University Microfilms, No. 19-19052, Ann Arbor, Michigan, 1969.
5. R. S. Berkof, "Balancing Concepts and the Four-Bar Linkage", Paper No. 9, Proceedings, Third Appl. Mechanisms Conference, Oklahoma State University, Nov. 1973.
6. R. S. Berkof, "Complete Force and Moment Balancing of Inline Four-Bar Linkages", Mechanism and Machine Theory, Vol. 8 (3) 1973, pp. 397-410.
7. R. S. Berkof, "On the Input Torque in Mechanisms", Fourth World Congress on the Theory of Machines and Mechanisms, Newcastle Upon Tyne, G.B., The Institution of Mechanical Engineers, 1975, pp. 151-156.
8. R. S. Berkof and G. G. Lowen, "A New Method for Completely Force Balancing Simple Linkages", Trans. ASME, Journal of Engineering for Industry, Series B, Vol. 91, No. 1, Feb. 1969, pp. 21-26.
9. R. S. Berkof and G. G. Lowen, "Theory of Shaking Moment Optimization of Force Balanced Four-Bar Linkages", Journal of Engineering for Industry, Trans. ASME, Series B, Vol. 93, Feb. 1971, pp. 53-60.

10. R. S. Berkof, G. G. Lowen and F. R. Tepper, "Balancing of Linkages", The Shock and Vibration Digest, Vol. 9, No. 6, June 1977.
11. A. P. Bessenov, "Balancing a Planar Mechanism with Variable Mass Links", ASME Paper No. 68-MECH-67, Mechanisms Conf., Atlanta, Georgia, Oct. 1968.
12. W. G. Bickley and R. S. H. G. Thompson, "Matrices - Their Meaning and Manipulation", Van Nostrand Rheinhold Co., New York, N. Y.
13. F. Y. Chen, "Isomomental Ellipsoids and the Distribution of Shaking Moments in Spatial Mechanisms", ASME Paper No. 74-DET-28, Mechanisms Conf., New York, N.Y., Oct. 1974.
14. F. L. Conte, G. R. George, R. W. Mayne and J. P. Sadler, "Optimum Mechanism Design Combining Kinematic and Dynamic Force Considerations", Journal of Engineering for Industry, Trans. ASME, Series B, Vol. 97, 1975.
15. G. B. Dantzig, "Linear Programming and Extensions", 1963.
16. W. C. Davidson, "Variable Metric Method for Minimization", A. E. C Research and Development Report ANL-5990, 1959.
17. T. H. Davies, "The Kinematics and Design of Linkages, Balancing Mechanisms and Machines", Machine Design Engineering, March 1968, pp. 40-51.
18. H. Dresig and P. Jacobi, "Vollstandiger Tragheitskraftausgleich von Ebenen Koppelgetrieben durch Anbringung eines Zweischlags", (Complete Inertia Force Balancing of Planar Linkages by Way of the Addition of a Link Dyad), Maschinenbautechnik, Vol. 23 (1), 1974, pp. 5-8.
19. H. Dresig and S. Schonfeld, "Tragheitskraftausgleich fur Ebene Koppelgetriebe", (Inertia-Force Balance for Planar Linkages), Wess. Z. der T. U. Dresden, Vol. 23 (5), 1971, pp. 1341-1349.
20. Yu. Epshtein and L. I. Shteinvolf, "The Optimum Shape for Rotating Counterweights", (Russian), Trudy Inst. Mash., Teor. Mash. i Mekh., Vol. 15, No. 57, 1955, pp. 47-60.

21. R. Fletcher and M. J. D. Powell, "A Rapidly Convergent Descent Method for Minimization", Computer J., 1963, Vol. 6, pp. 163-168.
22. F. Freudenstein, "Quasi Lumped-Parameter Analysis of Dynamical Systems", Paper No. 27, Proceedings, Third Appl. Mechanisms Conference, Oklahoma State University, Nov. 1973.
23. T. T. Gappoev, "Balancing the Inertial Load of a Plane Mechanism", Mashinostroenie, No. 8, 1967, pp. 5-8.
24. Ya. L. Gheronimus, "On the Application of Chebyshev's Methods to the Problem of Balancing of Mechanisms", (Russian), OGIZ, Gostekhizdat, Moscow-Leningrad, 1948, 148 pp.
25. Ya. L. Gheronimus, "On the Application of Chebyshev's Methods to the Problem of Balancing of Mechanisms", (Selected excerpts translated from 19), Journal of Mechanisms, Vol. 3, No. 4, 1968, pp. 235-281.
26. P. J. Gierse, "Ein Beitrag zur Bestimmung der Lagerbelastungen und Bewegungsgesetze ebener Gelenk- und Kurvengetriebe", (A Contribution Towards the Determination of Bearing Forces and Laws of Motion of Planar Linkage and Cam Mechanisms), Dissertation, Rhein.-Westf. Technische Hochschule Aachen, 1966.
27. D. Goldfarb, "A Family of Variable Metric Methods Derived by Variational Means", Math. of Comp., 1970, Vol. 24, pp. 23-26.
28. V. Heron, "The Vibrationless Engine", Automobile Engineer, Vol. 60 (9), August 1970, pp. 340-341.
29. F. R. Hertrich, "How to Balance High-Speed Mechanisms with Minimum Inertia Counterweights", Machine Design, Vol. 35, No. 6, March 14, 1963, pp. 160-164.
30. M. R. Hestenes, "Multiplier and Gradient Methods", J. of Optimization Theory and Application, Vol. 4, 1969, pp. 303-320.
31. R. Hill, "Super-Smooth Superbike", Popular Science, March 1973, pp. 101 and 153.

32. B. A. Hockey, "The Method of Dynamically Similar Systems Applied to the Distribution of Mass in Spatial Mechanisms", Journal of Mechanisms, Vol. 5, 1970, pp. 169-180.
33. B. A. Hockey, "An Improved Technique for Reducing the Fluctuations of Kinetic Energy in Plane Mechanisms", Journal of Mechanisms, Vol. 6 (4), 1971, pp. 405-418.
34. B. A. Hockey, "The Minimization of the Fluctuation of Input-Shaft Torque in Plane Mechanisms", Mechanism and Machine Theory, Vol. 3 (3), 1972, pp. 335-346.
35. K. Ishida, "Fundamental Researches on a Perfectly Balanced Rotation Reciprocation Mechanism, Report No. 1: Basic Theories of This Mechanism and Basic Constitution", Bull. JSME Vol. 17, No. 103, Jan. 1974, pp. 132-140.
36. K. Ishida and T. Matsuda, "Theories and Experiments on Perfectly Balanced, Vibrationless, Geared Devices to Convert Linear Reciprocating Motion to Rotary Motion or Vice Versa", ASME Paper No. 72-PTG-12, Mechanisms Conf. and Int. Symp. on Gearing Transmissions, San Francisco, California, Oct. 1972.
37. K. Ishida, T. Matsuda, S. Nagata and Y. Oshitani, "Fundamental Researches on a Perfectly Balanced Rotation Reciprocation Mechanism, Report No. 2: Vibration on an Eccentric Geared Device of a Crankshaft Planetary Motion System and a Dynamic Balancing Machine", Bull. JSME Vol. 17, No. 103, Jan. 1974, pp. 141-148.
38. K. Ishida, T. Matsuda, S. Shinmura and Y. Oshitani, "Fundamental Researches on a Perfectly Balanced Rotation Reciprocation Mechanism, Report No. 3: Structural Analysis on Vibrationless Geared Devices of a Crankshaft Rotary Motion System and Their Vibration and Friction Loss", Bull. JSME, Vol. 17, No. 108, June 1974, pp. 818-828.
39. K. Ishida and T. Matsuda, "Inertia Force and Moment Balancing of Rotation Reciprocating Mechanisms", ASME Paper No. 74-DET-57, Mechanisms Conf., New York, N. Y., Oct. 1974.

40. P. Jacobi, "Vollständiger Tragheitskraftausgleich bei Mehrgliedrigen Koppelgetrieben", (Complete Inertia Balancing of Multiple Linked Mechanisms), Maschinenbautechnik, Vol. 18, No. 11, 1969, pp. 605-606.
41. P. Jacobi and J. Volmer, "Bestimmung von Optimalen Koppelgetrieben nach dem Hauptkriterium Kräfte und Momente am Gestell", (Determination of the Most Advantageous Linkages According to the Main Criterion "Forces and Moments Acting on the Frame"), Proceedings, Third World Congress for the Theory of Machines, Kupari, Yugoslavia, Vol. D, Paper D-8, Sept. 1971, pp. 105-118.
42. P. Jacobi and W. Rose, "Experimentelle Untersuchungen Dynamisch Ausgeglicherer Ebener Koppelgetriebe", (Experimental Investigations of Dynamically Balanced Planar Linkages), Maschinenbautechnik, Vol. 21, No. 8, Aug. 1972, pp. 354-358.
43. G. Jungk, "Experimentelles Verfahren zur Ermittlung von Dynamischen Massenkraften", (An Experimental Method for the Determination of Dynamic Forces in Machines), Proceedings, "Dynamik und Getriebetechnik", Dresden GDR 1973, Vol. B, Paper No. 19, VEB Buchverlag, Leipzig, 1973.
44. R. E. Kaufman and G. N. Sandor, "Complete Force Balancing of Spatial Linkages", Journal of Engineering for Industry, Trans. ASME, Vol. 93, Ser B, May 1971, pp. 620-626.
45. H. Koch, "Auswertalgorithmus zur Bestimmung der Dynamischen Maschinenkräfte aus den Messwerten", (Evaluation Algorithm for the Determination of Dynamic Forces in Machines from Test Data), Proceedings, "Dynamik und Getriebetechnik", Dresden GDR 1973, Vol. B, Paper No. 19, VEB Fachbuchverlag Leipzig, 1973.
46. P. Kulitzscher, "Leistungsausgleich von Koppelgetrieben durch Veränderung von Massenverteilung oder Zusatzkoppelgetriebe", (Performance Compensation of Linkages by Way of Redistribution of Mass or Linkage Addition), Maschinenbautechnik, Vol. 19 (11), 1970, pp. 562-568.
47. B. O. Lavery and D. E. Henshaw, "The Dynamic Balancing of Murray's Cycloidal Drive", Mech. and Chem. Engr., Trans. I. E. Aust., Vol. MCB, No. 1, May 1972, pp. 97-99.

48. P. A. Lebedev, "Equilibrium of Inertia Forces in a Spatial Four-Bar Linkage", Third World Congress for the Theory of Machines, Kupari, Yugoslavia, Vol. F, Paper F-12, Sept. 1971, pp. 161-174.
49. G. G. Lowen and R. S. Berkof, "Survey of Investigations into the Balancing of Linkages", Journal of Mechanisms, Vol. 3, No. 4, 1968, pp. 221-231.  
(Plus 11 translations of Russian and German articles.)
50. G. G. Lowen and R. S. Berkof, "Determination of Force Balanced Four-Bar Linkages with Optimum Shaking Moment Characteristics", Journal of Engineering for Industry, Trans. ASME, Series B, Vol. 93, No. 1, Feb. 1971, pp. 39-46.
51. G. G. Lowen, F. R. Tepper and R. S. Berkof, "The Quantitative Influence of Complete Force Balancing on the Forces and Moments of Certain Families of Four-Bar Linkages", Mechanism and Machine Theory, Vol. 9, No. 3/4, 1974, pp. 299-323 and Vol. 10, No. 4, 1975, pp. 361-363 (Erratum).
52. G. G. Lowen and F. R. Tepper, "Flexibility in Counterweight Design for Partial Balancing of Four-Bar Linkages: Theory of Equipollent Circles". Contribution to Festschrift in honor of 70th birthday of Academician I. I. Artobolevskii, 1975.
53. J. W. McLernon and C. W. Phelps, "Balancing the Chevrolet V-8 Engine", General Motors Engineering Journal, Vol. 7, No. 3, pp. 14-20, 1962.
54. C. Offt, "Experimentelle Untersuchungen an Koppelgetrieben mit Leistungsausgleich", (Experimental Investigations on Linkages with Performance Compensation), Mechanism and Machine Theory, Vol. 9 (2), 1974, pp. 239-246.
55. K. Ogawa and H. Funabashi, "On the Balancing of the Fluctuating Input Torques Caused by Inertia Forces in the Crank-and-Rocker Mechanism", Journal of Engineering for Industry, Trans. ASME, Series B, Vol. 91, No. 1, Feb. 1969, pp. 97-102.

56. T. Pantelic and A. Sekulic, "Application of Bessel's Functions in Balancing of Inertial Forces of Planar Linkages", (Yugoslavian), Proceedings, Third World Congress for the Theory of Machines and Mechanisms, Kupari, Yugoslavia, Vol. B, Paper No. B-11, Sept. 1971, pp. 127-140.
57. B. Paul, "A Unified Criterion for the Degree of Constraint of Plane Kinematic Chains", Journal of Applied Mechanics, Trans. ASME, Vol. 82, Series E, No. 4, March 1960, pp. 196-200.
58. Z. Popov, "Possibilities for the Improvement of the Dynamics of the Loom", Proceedings, Third World Congress for the Theory of Machines and Mechanisms, Kupari, Yugoslavia, Vol. B, Paper No. B-14, Sept. 1971, pp. 167-180.
59. B. Porter and D. J. Sanger, "Synthesis of Dynamically Optimal Four-Bar Linkages", Mechanisms 1972, Proceedings of Conference, Institution of Mechanical Engineers, Paper C69/72, Sept. 1972, pp. 24-28.
60. M. J. D. Powell, "A Method for Nonlinear Constraints in Minimization Problems", Optimization, R. Fletcher, ed., Acad. Press, London, 1969, pp. 283-298.
61. R. T. Rockafeller, "New Applications of Duality in Nonlinear Programming", Symposium on Math. Programming, The Hague, 1970.
62. W. Rose, "Kraftmessungen in Drehgelenken mit Hilfe Piezo-Elektrischer Zwei-Komponenten - Kraftmesseinrichtungen", (Force Measurements in Pin Joints with Piezoelectric Two-Component Force Gages), Maschinenbautechnik, Vol. 21, No. 8, Aug. 1972, pp. 365-368.
63. J. P. Sadler and R. W. Mayne, "Balancing of Mechanisms by Nonlinear Programming", Paper No. 29, Proceedings, Third Appl. Mechanisms Conf., Oklahoma State University, Nov. 1973.
64. J. P. Sadler, "Balancing of Six-Bar Linkages by Nonlinear Programming", Proceedings, Fourth World Congress on the Theory of Machines and Mechanisms, Newcastle upon Tyne, G. B. 1975, The Inst. of Mech. Eng., pp. 139-144.

65. S. Schonfeld, "Dynamische Synthese Ebener Koppelgetriebe mit dem Programmsystem KOGGOP", (Dynamic Synthesis of Planar Linkages with the Program KOGGOP), Maschinebau-technik, Vol. 23, No. 3, 1974, pp. 119-124.
66. S. Schonfeld and H. Dresig, "Der Dynamische Ausgleich von Ebenen Koppelgetrieben und seine Rechentechnische Behandlung als Optimierungsproblem", (Dynamic Balancing of Planar Linkages and its Computer Treatment as an Optimization Problem), Wiss. Z. d. Techn. Hochsch. Karl-Marx-Statd, Vol. 14, No. 2, 1972, pp. 289-308.
67. V. A. Shchepetilnikov, "The Balancing of Bar Mechanisms with Unsymmetrical Links", Mechanism and Machine Theory, Vol. 10, No. 6, 1975, pp. 461-466.
68. A. A. Sherwood and B. A. Hockey, "The Optimization of Mass Distribution in Mechanisms Using Dynamically Similar Systems", Journal of Mechanisms, 4 (3), 1969, pp. 243-260.
69. Ye. A. Shorokh, "Design of Counterweights for Unloading the Main Supports of a Crankshaft", (Russian), Izv. Vyssh. Ucheb. Zaved. - Mashinostroenie, Vol. 3, 1969, pp. 74-79.
70. M. R. Smith, "Linkage Design: Dr. Smith Studies Ways to Minimize Inertia", Eng. Materials and Design, Dec. 1973, pp. 23-25.
71. M. R. Smith, "Optimal Balancing of Planar Multi-Bar Linkages", Proceedings, Fourth World Congress on the Theory of Machines and Mechanisms, Newcastle upon Tyne, G. B., 1975, The Inst. of Mech. Eng., pp. 145-149.
72. F. H. Speckhart and D. Wright, "Balancing Slider-Crank Mechanisms", ASME Paper No. 75-DE-32, Design Engineering Conference, New York, N. Y., April 1975.
73. E. N. Stevensen Jr., "Balancing of Machines", Journal of Engineering for Industry, Trans. ASME, Series B, Vol. 95, No. 2, May 1973, pp. 650-656.
74. D. Stundel, "Der Einfluss der Mechanismengeometrie auf die Reibungsverluste in den Gelenken", (The Influence of the Geometry of Linkages on the Friction Losses in Joints), Feingeratetechnik, Vol. 23, No. 1, 1974, pp. 7-11.

75. F. R. Tepper, "Contributions to the Theory of Mechanism Balancing", Ph.D. Dissertation, The City University of New York, University Microfilms, No. 72-24162, Ann Arbor, Michigan, 1972.
76. F. R. Tepper and G. G. Lowen, "General Theorems Concerning Full Force Balancing of Planar Linkages by Internal Mass Redistribution", Journal of Engineering for Industry, Trans. ASME, Series B, Vol. 94, No. 3, Aug. 1972, pp. 789-796.
77. F. R. Tepper and G. G. Lowen, "On the Distribution of the RMS Shaking Moment of Unbalanced Planar Mechanisms: Theory of Isomomental Ellipses", Journal of Engineering for Industry, Trans. ASME, Series B, Vol. 95, No. 3, Aug. 1973, pp. 665-671.
78. F. R. Tepper and G. G. Lowen, "Two General Rules for Full Force Balancing of Planar Linkages", Paper No. 10, Proceedings, Third Appl. Mechanisms Conference, Oklahoma State University, Nov. 1973.
79. F. R. Tepper and G. G. Lowen, "A New Criterion for Evaluating the RMS Shaking Moment in Unbalanced Planar Mechanisms", Paper No. 11, Proceedings, Third Appl. Mechanisms Conf., Oklahoma State University, Nov. 1973.
80. F. R. Tepper and G. G. Lowen, "Shaking Force Optimization of Four-Bar Linkage With Adjustable Constraints on Ground Bearing Forces", Journal of Engineering for Industry, Trans. ASME, Series B, Vol. 97, No. 2, May 1975, pp. 643-651.
81. J. T. Tinsley and W. L. Carson, "Reduction of Shaking Forces in a Slider-Crank Mechanism", ASME Paper No. 70-MECH-73, Mechanisms Conf., Columbus, Ohio, Nov. 1970.
82. K. D. Urion, "Linkage Mechanism Matches the Path and Velocity of a Rotating Machine", Paper No. 8, Proceedings, Second Appl. Mechanisms Conf., Oklahoma State Univ., Oct. 1971.
83. K. Weiss and R. G. Fenton, "Minimum Inertia Balance Weight", Mech. and Chem. Eng. Trans. I. E. Aust., Vol MCB, No. 1, May 1972, pp. 93-96.
84. S. I. Zuhovitskiy and L. I. Avdeyeva, "Linear and Convex Programming", W. B. Saunders and Co., Phila., Pa., 1966.